

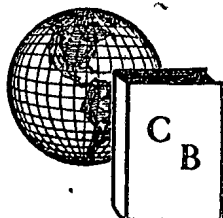
# Атомная энергия

Number 1, 1956

The Soviet Journal of

# ATOMIC ENERGY

IN ENGLISH TRANSLATION



## CONSULTANTS BUREAU, INC.

227 WEST 17TH STREET, NEW YORK 11, N. Y.

## SOVIET JOURNAL OF ATOMIC ENERGY

NUMBER 1, 1956

## CONTENTS

	Page	Russ. Page
1. Atomic Energy - In the Service of Peace! . . . . .	1	3
2. A Gas-Cooled Heavy Water Power Reactor. <u>A. I. Alikhanov, V. V. Vladimirovskii, P. A. Petrov and P. I. Khristenko</u> . . . . .	3	5
3. The Reactor of the USSR Academy of Sciences Atomic Power Station. <u>D. I. Blokhintsev, N. A. Dollezhal and A. K. Krasin</u> . . . . .	7	10
4. The Physical and Thermal Calculations for the USSR Academy of Sciences Atomic Power Station Reactor. <u>D. I. Blokhintsev, M. E. Minashin and Yu. A. Sergeev</u> . . . . .	21	24
5. A Study of the Iodide Process of Refining Zirconium. <u>V. S. Emel'yanov, N. D. Bystrov and A. I. Evstyukhin</u> . . . . .	43	43
6. Energy Levels of $\text{Pu}^{238}$ and $\text{Pu}^{239}$ Nuclei. <u>S. A. Baranov and K. N. Shlyagin</u> . . . . .	51	52
7. Measurement of Fast-Neutron Spectra by Time of Flight. <u>G. F. Bogdanov, A. A. Kurashov, B. V. Rybakov, V. A. Sidorov</u> . . . . .	67	66
8. Principles of Acceleration of Charged Particles. <u>V. A. Veksler</u> . . . . .	77	75
9. Methods of Uranium Prospecting. <u>V. G. Melkov</u> . . . . .	85	83
10. Isotopes in the Study of the Pathogenesis of Metabolic Diseases. <u>D. E. Grodzenskii</u> . . . . .	93	91
11. Conference on the Physics of Nuclear Fission. . . . .	101	99
12. An Exhibition On the Uses of Atomic Energy for Peaceful Purposes. . . . .	105	102
13. Construction of the First Atomic Power Station in England . . . . .	109	106
14. Projected Dual Cycle Boiling Water Reactor . . . . .	115	110
15. The Atomic Submarine "Nautilus" . . . . .	117	111
16. Design of a Portable Power Reactor. . . . .	119	113
17. Atomic Batteries . . . . .	121	115
18. On Work Conducted in the U. S. A. Toward the Realization of a Controlled Thermonuclear Reaction . . . . .	125	117
19. Discovery of the Antiproton . . . . .	127	119
20. Experimental Portable Equipment for the Irradiation of Potatoes . . . . .	129	120
21. A Physical Method for Separating Uranium From Fission Fragments . . . . .	131	121
22. Bibliography . . . . .	133	123

**ATOMNAYA ENERGIYA**

**Academy of Sciences of the USSR**

Number 1, 1956

**EDITORIAL BOARD**

**A. I. Alikhanov, A. A. Bochvar, V. I. Veksler,  
A. P. Vinogradov, N. A. Vlasov (Acting Editor in Chief),  
V. F. Kalinin, G. V. Kurdyumov  
A. V. Lebedinsky, I. I. Novikov (Editor in Chief),  
V. V. Semenov (Executive Secretary), V. S. Fursov.**

---

**The Soviet Journal**

**of**

**ATOMIC ENERGY**

**IN ENGLISH TRANSLATION**

**Copyright, 1956**

**CONSULTANTS BUREAU, INC.**

**227 West 17th Street**

**New York 11, N. Y.**

Printed in the **United States**

**Annual Subscription \$ 75.00  
Single Issue \$ 20.00**

**Note: The sale of photostatic copies of any portion of this copyright translation is expressly prohibited by the copyright owners. A complete copy of any article in the issue may be purchased from the publisher for \$12.50.**

## ATOMIC ENERGY - IN THE SERVICE OF PEACE!

The discovery of a method for the liberation and practical utilization of the energy within the nucleus of the atom is the greatest achievement of modern science.

"The summit of the modern stage in the development of science and technology is the discovery of methods of obtaining and utilizing the energy within the atom. We are standing on the threshold of a new scientific, technological and industrial revolution exceeding by far in significance the industrial revolution resulting from the discovery of steam and electric power" (N. A. Bulganin).

From the time when the fission of uranium by neutrons was first demonstrated until the world's first practical atomic power plant was placed in operation in the U.S.S.R. on June 27, 1954, thus marking the beginning of the use of atomic power, there was a lapse of 15 years. During those years atomic energy brought into being an entirely new and extensive branch of science and technology and became a powerful factor in the development of productive capacity.

The creative work of scientists and engineers has produced atomic power plants - new powerful sources of energy - which generate electrical energy by burning "nuclear fuel". Practical atomic energy power plants are now being constructed in various parts of the world. Practical proof has also been given of the possibility of using atomic energy in transportation.

Atomic technology enables us to prepare artificially a large number of different radioactive isotopes. The utilization of these isotopes as "tracers" has led to the creation of extremely precise methods for the investigation of the most widely diversified phenomena and processes.

Powerful sources of penetrating radiation have made it possible to develop new methods of inspecting metals for flaws through the use of gamma rays and to develop a large number of diversified and improved methods for the technological control and automatic regulation of the processes of production. Radioactive fission products and ionizing radiation are beginning to be used extensively to sterilize pharmaceutical products and medical instruments, for the preservation of food products, to stimulate chemical processes, etc.

In medicine radioactive isotopes and ionizing radiation are being employed with great success for the diagnosis of various illnesses and the cure of malignant growths. In agriculture radioactive isotopes and radiation have led to the clarification of many important problems concerning the nutrition and artificial feeding of plants and have at the same time provided the means of combatting insects which are harmful to crops.

The Soviet Union lays great stress on the peaceful uses of atomic energy. The advances of the U.S.S.R. in this field are well known. These were shown especially clearly at the International Conference on the Peaceful Uses of Atomic Energy at Geneva during August 1955.

The wide experience gained in the U.S.S.R. in connection with atomic power plants has made possible a substantially increased use of atomic energy for peaceful purposes in the sixth Five Year Plan and, in



particular, the development of atomic power as one of the new supplementary aids in the universal electrification of our national economy.

The directives of the 20th Congress of the Communist Party of the Soviet Union concerning the sixth Five Year Plan aimed:

"To expand considerably during the sixth five year period the use of atomic energy for peaceful purposes. To construct from 1956 to 1960 atomic power plants with a total capacity of 2 to 2.5 million kilowatts. To erect atomic power plants primarily in regions which lack their own fuel supply. To expand work leading to the use of atomic energy for transportation. To build an icebreaker with an atomic engine. To expand in every way possible the work being done on the widest possible utilization of radioactive products in industry, agriculture and medicine, and in particular for controlling the quality of materials; to control the processes of production and to regulate these processes automatically; and also for the diagnosis and cure of various diseases. To make wider application of tracer atoms in scientific research. To expand considerably the production of dosimetric and radiation monitoring instruments and control devices."

In connection with the wide utilization of atomic energy great importance attaches to the exchange of experience between scientists and engineers and to broad knowledge of the achievements of our own and of foreign science and technology in the field of the peaceful uses of atomic energy.

The Soviet Union is anxious to share its experience in the peaceful use of atomic energy. It is known that the U.S.S.R. is giving scientific and technological assistance to, and exchanging information with, a number of countries. In the future the scientific and technological relations of the U.S.S.R. with other countries will be greatly extended and strengthened.

This new Soviet Journal of Atomic Energy will play an important part in the exchange of scientific and technological experience and information on the peaceful uses of atomic energy.

The journal will print original and review articles by Soviet and foreign authors on nuclear physics (research reactors, elementary particle accelerators, experimental methods in atomic laboratories); atomic power (power reactors and atomic power plants, metallurgy and the technology of fuels and construction materials for reactors, heat transfer problems, the chemistry of processes involving nuclear fuels, the economics of atomic power); atomic raw materials (methods and technology of prospecting, mining and initial processing); applications of radioactive isotopes (in industry, agriculture, science and medicine); radiation protection (equipment of radioactive laboratories, control and measuring instruments and automation in atomic industry, personnel monitoring and protection against radiation, the decontamination and utilization of radioactive waste products) and other problems.

The editors of the Soviet Journal of Atomic Energy invite scientists and engineers working in the field of the peaceful utilization of atomic energy, both in the U.S.S.R. and abroad, to submit the results of their investigations for publication. The editors call upon scientists and engineers to intensify their efforts to extend the peaceful uses of atomic energy for the sake of the prosperity and happiness of mankind, and against the military use of atomic energy which threatens mankind with terrible disaster.

Atomic energy - in the service of peace!

## A GAS-COOLED HEAVY WATER POWER REACTOR\*

A. I. Alikhanov, V. V. Vladimirov, P. A. Petrov and P. I. Khristenko

Nuclear reactors in which heavy water is used as a moderator have a comparatively high neutron multiplication factor since the losses in heavy water are small. This makes it possible to use natural uranium as fuel and to attain a sufficiently large burn-up of  $U^{235}$  without recourse to chemical or metallurgical processing of the fuel. In power reactors this circumstance in turn lowers the cost of the fuel needed to produce electric power. The large reactivity of heavy water reactors permits considerable enlargement of the surface of the fuel elements, since in these reactors it is possible to deviate considerably from the geometrical arrangement of the uranium that would result in the maximum multiplication factor and, in addition, to use in the core a fairly large amount of construction materials and materials needed to shield the uranium surface. The large surface area of the fuel elements permits an increase of the specific heat load of the uranium. These characteristics lead us to expect that heavy water reactors will prove to be sufficiently economical for utilization in atomic power plants.

However the high cost of heavy water requires that the reactor be designed with a view to using a small quantity of heavy water with minimum losses.

Although our first design required a large quantity of heavy water and was therefore unsatisfactory, we must still spend some time discussing it.

In this reactor the heavy water served simultaneously as moderator and coolant. It was used at a pressure of 25 atmospheres. Only aluminum alloys were used as construction materials in the core. The fuel elements were clad in pure aluminum. Steam was generated in the steam generators heated by the heavy water and fed to steam turbines.

It is known that the thermal power of a nuclear reactor depends to a considerable extent on the maximum attainable temperature of the fuel elements. In a heavy water reactor this temperature is determined by the properties of the material used as protective cladding of the fuel elements. On the basis of a number of experiments the maximum temperature for aluminum jackets was taken as  $230^{\circ}\text{C}$ .

At the maximum temperature of the jacket surface the heat removal increases as the temperature of the coolant in the process channels is lowered. With identical flow of the coolant the quantity of heat transmitted by the fuel elements is proportional to the difference between the temperatures of the cladding surface and of the coolant. When the average temperature of the coolant in the pipes is reduced its temperature at the reactor outlet is also reduced. The lower this temperature is the lower the efficiency of the power plant becomes for the conversion of heat from the reactor into electrical energy. Thus by raising the coolant temperature closer to the permissible limit attainable for the surface of the cladding we improve the efficiency of the power plant even while reducing the thermal power of the reactor. The electric power of an atomic power station is the product of these two quantities — the thermal power of the reactor and the efficiency of the electric power plant. Since one of these two factors increases as the other decreases we may expect to establish a maximum of electric power. This maximum does indeed exist. At a maximum temperature of  $230^{\circ}\text{C}$  for the cladding surface of the cans of the fuel elements this maximum corresponds to a pressure of 2.5 atmospheres pressure of saturated steam. At the

\* Report at the Fourth Annual Conference on the Use of Atomic Energy in Industry in New York, October 27, 1955 (there are a few additions to the text).

pressure of 2.5 atmospheres the efficiency of the power plant consisting of steam generators and steam turbines and condensers does not exceed 14%.

If by some means we should succeed in raising the maximum permissible temperature limit of the surface of the fuel elements there would be a corresponding rise of the optimal steam pressure in the secondary circuit. Thus, for example, if the maximum temperature of protective jackets made of zirconium is taken to be about 300° C the optimal saturated steam pressure rises to approximately 5 atmospheres. There is a corresponding increase by a factor of 1.5 in the thermal power of the plant. These examples show that the efficiency of nuclear power plants is determined in the final analysis by the choice of materials. The low efficiency of uranium cooling by ordinary or heavy water can be explained by the difficulty of selecting a satisfactory heat- and corrosion-resistant material that is a poor neutron absorber.

The question arises as to whether electric power plants of such low efficiencies can be economically justified.

For the ordinary thermal power plant the answer would have to be in the negative. There is a reciprocal relationship between the fuel cost of one kilowatt hour of electric power and the efficiency of an electric power plant. Of course at the high fuel cost which is peculiar to thermal electric power stations the cost of electric power depends strongly on the efficiency. Consequently thermal electric power plants of low efficiency are unprofitable.

The cost of constructing atomic power plants and their operating costs are considerably higher than for thermal electric power stations. Therefore atomic plants can successfully compete with coal-fueled plants only if the fuel cost per kilowatt hour is small. When the fuel cost is small it is profitable to have an efficiency that is lower within reasonable limits and obtain the highest power for the same capital expenditure and operating costs.

How can we reduce to a minimum the fuel cost per kilowatt hour of electric power from nuclear energy?

In the ideal case of a reactor whose multiplication factor for the fissionable material is greater than one, the fuel cost of the electric power may be considered practically zero. In the case of the usual reactors it is possible to achieve low fuel costs only through the use of natural uranium as fuel with large burn-up of  $U^{235}$ . It is just this that can be accomplished more easily with a heavy water reactor than with other types.

However, in order to enable atomic power plants to compete with coal-fueled plants it is insufficient to reduce only the fuel costs. A second cost factor must also be reduced, whose magnitude depends primarily on the capacity of the power plant. For this purpose it is possible to use an old and well-known method -- an increase of the capacity both of the power plant itself and of its basic units. In an atomic power plant this means that we must first endeavor to increase the power of the reactor. Of course this refers not so much to the total thermal power as to the maximum electric capacity in the above sense. The construction costs and operating expenses increase more slowly than the rated capacity. Therefore the larger the power plant the cheaper the electric power. In atomic power plants this relationship is even more marked.

Thus we have arrived at the conclusion that it is most expedient to employ only natural uranium, achieve large  $U^{235}$  burn-up and obtain the maximum electric power possible with a certain decrease in efficiency.

It must be admitted that the economic aspect of atomic electric power plants is unique. It is evident that some time must pass before power engineers will become accustomed to it.

We shall now return to our first design for a heavy water power reactor. In building it we aimed at high power and large  $U^{235}$  burn-up, although this was done at the expense of obtaining low steam pressure and comparatively low efficiency.

To be sure, we attained the maximum economy for the heavy water used in the first circuit. The quantity was slightly more than 1 ton per megawatt of electric power. Only about 40% of the heavy water was within the core of the reactor while the remainder was outside. We could not be satisfied with this and began to seek means of utilizing the heavy water more economically.

For this we had to give up use of heavy water as a coolant, e.g., we could utilize the heavy water only as a moderator and use ordinary water to remove the heat from the fuel elements. This would then be similar to the Canadian NRX reactor and would differ from the latter only through the higher water pressure in the process tubes. But this method would not result in any important decrease of the quantity of heavy water per unit of electric capacity, since with the same core volume as in the case of the heavy water cooled reactor the power of the reactor cooled by ordinary water would be about one half lower. The introduction of ordinary water and of an additional amount of aluminum into the core would make it necessary to increase the spacing between the channels, i.e., to decrease the number of channels and thus reduce the power of the reactor. Moreover the design of the channels in this reactor is not entirely satisfactory; the channel is not immersed in the heavy water and, consequently, there is no additional cooling of its outer surface. In emergencies this additional cooling might be necessary.

We therefore dropped this design and decided to use a gas coolant while leaving the channels immersed in heavy water.

The gas-cooled heavy water reactor has the following important advantages.

First, it is possible to reduce the quantity of heavy water in the system to 0.2-0.4 tons per megawatt, 66 - 75% less than that for reactors in which the heavy water serves both as moderator and coolant. This also considerably simplifies the operational treatment of the heavy water and eliminates losses during the unloading of the fuel elements.

Second, the use of a gas, especially in combination with a heavy water moderator, makes it possible to raise considerably the steam parameters of the second circuit. And this in turn enables us to increase the efficiency of the plant and to use turbogenerators of greater capacity. Instead of low pressure equipment it is possible to utilize more modern medium pressure equipment. In view of the fact that the process channels are immersed in heavy water and thus are sufficiently cooled on the outside, they may be made of aluminum alloys (the gas temperature at the channel outlet reaches 500° C).

The fuel elements in the form of thin long wires or sheets of natural uranium are covered with a protective cladding of light metal which can withstand a maximum temperature of 550° C.

Under this condition an increase of the steam parameters is advantageous. Generally speaking reactors of this type can bring the steam pressure up to 90 atmospheres at 470° C. For the first plants more conservative figures were decided upon: the turbine steam pressure is 29 atmospheres at 400° C.

Carbon dioxide gas at 40 - 60 atmospheres was used as coolant. The expenditure of energy for gas circulation comprised about 15% of the power of the plant.

For improved utilization of low potential heat a two-stage power cycle was chosen. In the low pressure stage, which comprises not more than 20% of the total power, saturated steam at 2 atmospheres was used.

Figure 1 is a diagram of the reactor and Figure 2 is a diagram of a process channel.

The reactor has a steel shell rated to withstand 60 atmospheres, which contains the Avialite tank penetrated by the process channels, and which is filled with the heavy water moderator. The channels contain the sets of fuel elements which are suspended from removable plugs in the upper shield. As can be seen from Figure 2 the space above the heavy water level connects with the space inside the steel shell for equalization of pressures. The set of fuel elements is in an Avialite shielding tube. Between the shielding tube and the process tube there is a narrow annular space for the passage of the gas which cools the shielding tube. At the outlet this gas is mixed with the gas issuing from the fuel elements heated to 430° C. After mixing, the gas reaches the steam generators at 420° C. The passage of cool gas through the gap between the shielding tube and the process tube ensures a low temperature of the tube walls. The temperature of the shielding tube does not exceed the value permissible for several aluminum alloys when the strength requirements are not set forth in advance.

The Soviet Union plans to construct an atomic power station of this type with a capacity of 100 - 200 megawatts.

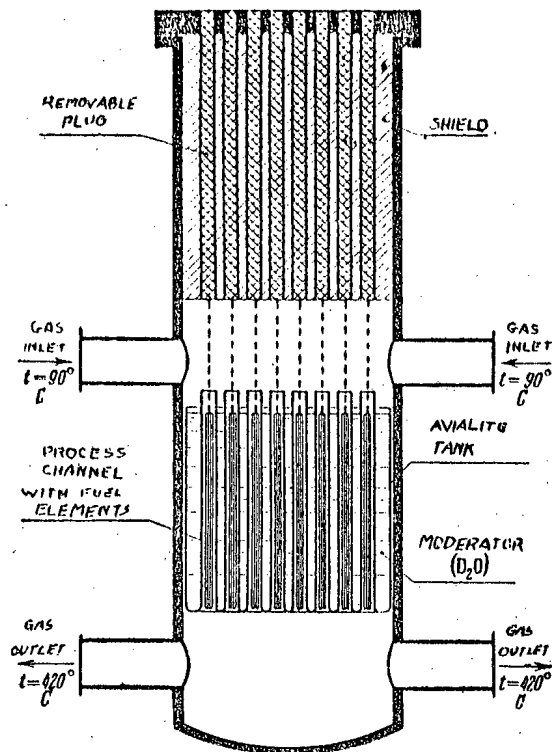


Fig. 1. Diagram of reactor.

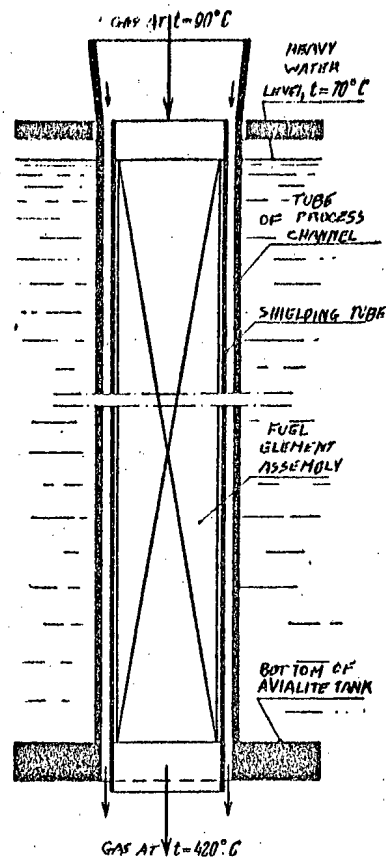


Fig. 2. Diagram of process channel.

It is believed that such atomic electric power plants will be able to produce electric power at the same price as a coal-burning plant. In our cost calculations we arbitrarily set the value of spent nuclear fuel at zero. Then the fuel cost per kilowatt hour will not exceed 20-30%. However this figure will be still lower if spent nuclear fuel is used for recycling.

Another possible way of reducing the quantity of heavy water in the heat removal system involves the use of steam to remove heat. Therefore we also designed a boiling heavy water homogeneous reactor. This type of reactor does not require expensive uranium fuel elements.

The design of the boiling heavy water homogeneous reactor was discussed at the International Conference on the Peaceful Uses of Atomic Energy held in Geneva during August 1955. The U.S.S.R. plans to construct the first reactor of this type during the next five years.

## THE REACTOR OF THE USSR ACADEMY OF SCIENCES ATOMIC POWER STATION\*

D. I. Blokhintsev, N. A. Dollezhal and A. K. Krasin

### Fundamental Aspects

At the beginning of the practical work directed towards the construction in the Soviet Union of an atomic power plant on an experimental industrial scale a large group of scientists and engineers had already become fully acquainted with the technological processes involved in the production of fissionable materials, thus making it possible to proceed with the search for methods of utilizing these materials most intelligently for peaceful purposes. The problem was to design and construct a small atomic power plant on a semi-industrial scale which would enable engineers and physicists in a comparatively short time to evaluate the operation of the nuclear reactor under the new conditions, which differ from previous conditions principally in the higher temperatures involved.

The design, construction and operation of such an electric power plant would provide the experience required for the subsequent building of atomic power plants on a much larger scale.

The thermal capacity of the power plant reactor was set at 30,000 kilowatts, sufficient to produce 5000 kilowatts of electric power.

When the work of designing the reactor began, our ideas as to the type of the first power reactor were not definite. It was decided to use thermal neutrons in the first power station reactor since only for such reactors had enough experience been accumulated, as well as sufficiently complete information regarding the physical constants of the materials.

As moderator it was decided to use graphite which, as is well-known, possesses a number of positive qualities: it is a weak neutron absorber; it is easily machined; through large-scale production it is comparatively easy to attain a density of  $1.65 - 1.70 \text{ g/cm}^3$  thus ensuring an acceptable neutron slowing down length; objects made of graphite possess good mechanical strength and may even be used to some extent as construction materials; moreover, in an inert gas atmosphere at  $500 - 600^\circ \text{C}$  graphite is sufficiently stable, as was proved by special experiments, etc. Finally, through extrapolation of experimental data we were able to assume that at high temperatures the change of the properties of graphite subjected to neutron bombardment would not be sufficient to endanger the operation of the reactor.

All these considerations indicated that among the different possible types of reactors which can be utilized to produce electrical energy, graphite-moderated reactors will occupy an important position.

As coolant it is possible to use carbon dioxide gas, nitrogen, air, helium, water, sodium, bismuth-lead, etc.

We chose ordinary distilled water, which has a number of advantages over other coolants:

---

\* The authors consider it necessary to mention that in the construction of the atomic power plant a large number of physicists and engineers participated, many of whom made creative contributions during the erection of this unique plant.

- a) The utilization of very pure distilled water facilitates the design of biological shielding since the water passing through the reactor does not acquire a significant amount of residual activity.
- b) Ordinary light water is cheap.
- c) Compared with other types of coolant it is least dangerous for the operating personnel.
- d) In designing the units of the heat-transfer circuit (pumps, piping and other equipment) it is possible to use the experience already acquired in ordinary fields of technology.
- e) Water makes it possible to attain such a high level of heat removal that the quantity of construction materials in the active zone (core) of the reactor can be reduced to a minimum. This latter circumstance in turn increases the economy of the reactor.
- f) Since water is a weak absorber of neutrons the presence of a certain amount of water in the core of a graphite-moderated reactor does not affect the neutron balance unfavorably.

On the negative side the use of water as coolant in a nuclear power plant requires high pressures for the purpose of heating the water to a high temperature. This means that in accordance with the design parameters of the atomic power plant it would be necessary to circulate the water at a pressure of 100 atmospheres.

Pressurized ordinary water may be used as coolant in two ways:

- 1) The pressure is borne by the overall jacket of the reactor (pressure vessel variant), or
- 2) The reactor casing is relieved of the high pressure and the coolant flows through tubes (operating channels) which penetrate the core of the reactor (tubular variant).

The second variant was selected for the atomic power plant. The following considerations were in favor of this variant. The presence of construction materials in the core is of course undesirable but the pressure vessel variant requires the shielding of the uranium elements from the water in any event. The use of pure aluminum or pure zirconium as shielding materials at a coolant temperature of about 280° C is excluded as well, because of the mechanical and corrosion properties of these materials. To be sure, it is possible to use zirconium alloys but alloying inevitably makes the metal inferior with respect to neutron capture. The presence in the core of the thin-walled steel tubes for the fuel elements, in the tubular design, worsens the neutron balance to only an insignificant degree in the chosen type of reactor.

The pressure vessel variant compared with the tubular variant complicates considerably the operation of channel replacement, including the experimental channels, which was undesirable for the first plant.

Finally, an argument in favor of the tubular variant was the fact that in the future when larger reactors of this type were to be constructed (that is, graphite-moderated) the use of the pressure vessel variant would be entirely eliminated, whereas an experimental reactor should be as much as possible a prototype of future power reactors.

The tubular variant may in turn be constructed in several ways differing in the form of the uranium fuel elements.

Figure 1 shows schematically the three types of fuel elements: a) tubular, b) rod, c) with bilateral cooling. In the atomic power reactor tubular uranium fuel elements were used.

The basic structural part of this type of element is a thin-walled steel tube. The uranium which is in exterior contact with this tube is provided with an anti-fragment shield.

The tubular elements possess the following positive characteristics:

- 1. The pressure-bearing steel tube of the uranium fuel element is at the same time a construction element of the operating channel.
- 2. With a suitable tube diameter allowing for the required heat transfer surface the thickness of the tube walls may be reduced to a minimum.
- 3. The tube also protects the uranium from contact with the water. The anti-fragment shield of the uranium is relieved of pressure so that its thickness is determined only by the technological possibilities of tube manufacture and by the technology of the preparation of fuel elements.

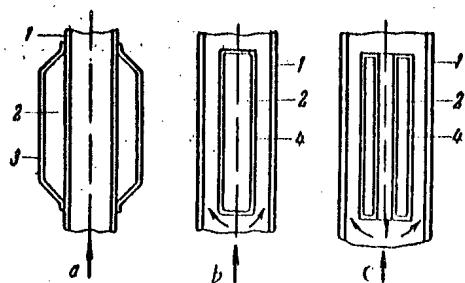


Figure 1. Diagram of three types of fuel elements: tubular (a), rod (b) and with bilateral cooling (c). 1) Tube bearing pressure, 2) uranium, 3) anti-fragment shielding, 4) shielding protecting uranium from interaction with water.

4. The strength of the tube which is under pressure eliminates the possibility that it will be warped due to a change of shape of the uranium parts in the neutron field; this ensures a continuous and stable flow of the coolant through the uranium fuel element.

5. In case of an accidental rupture of the fuel element tube the water will flow out and no radioactive fission products will enter the coolant loop, and since the tubes are of small diameter the quantity of escaping water will be small. In addition the operating channels containing the tubes can be supplied with automatic cutoff devices. Therefore the rupture of a tube under pressure presents no danger.

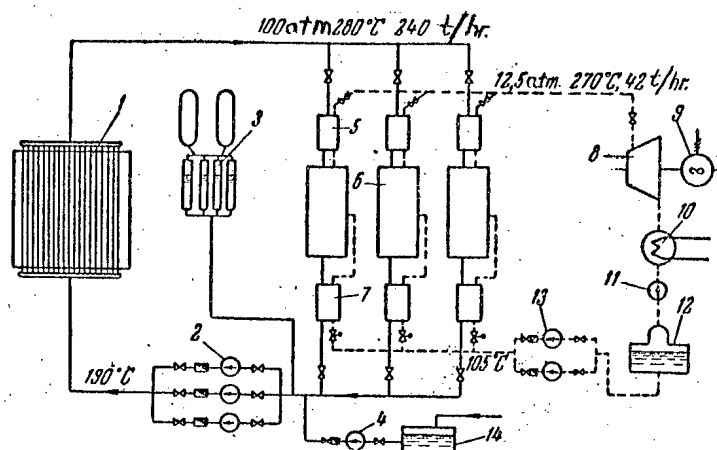


Figure 2. Thermal flow sheet of the electric power station.

1) Reactor, 2) circulating pumps, 3) volume compensators, 4) feed pump of first circuit, 5) steam superheater, 6) evaporator, 7) pre-heater, 8) turbine, 9) generator, 10) condenser, 11) condensate pump, 12) deaerator, 13) second circuit circulating pumps, 14) auxiliary water tank.

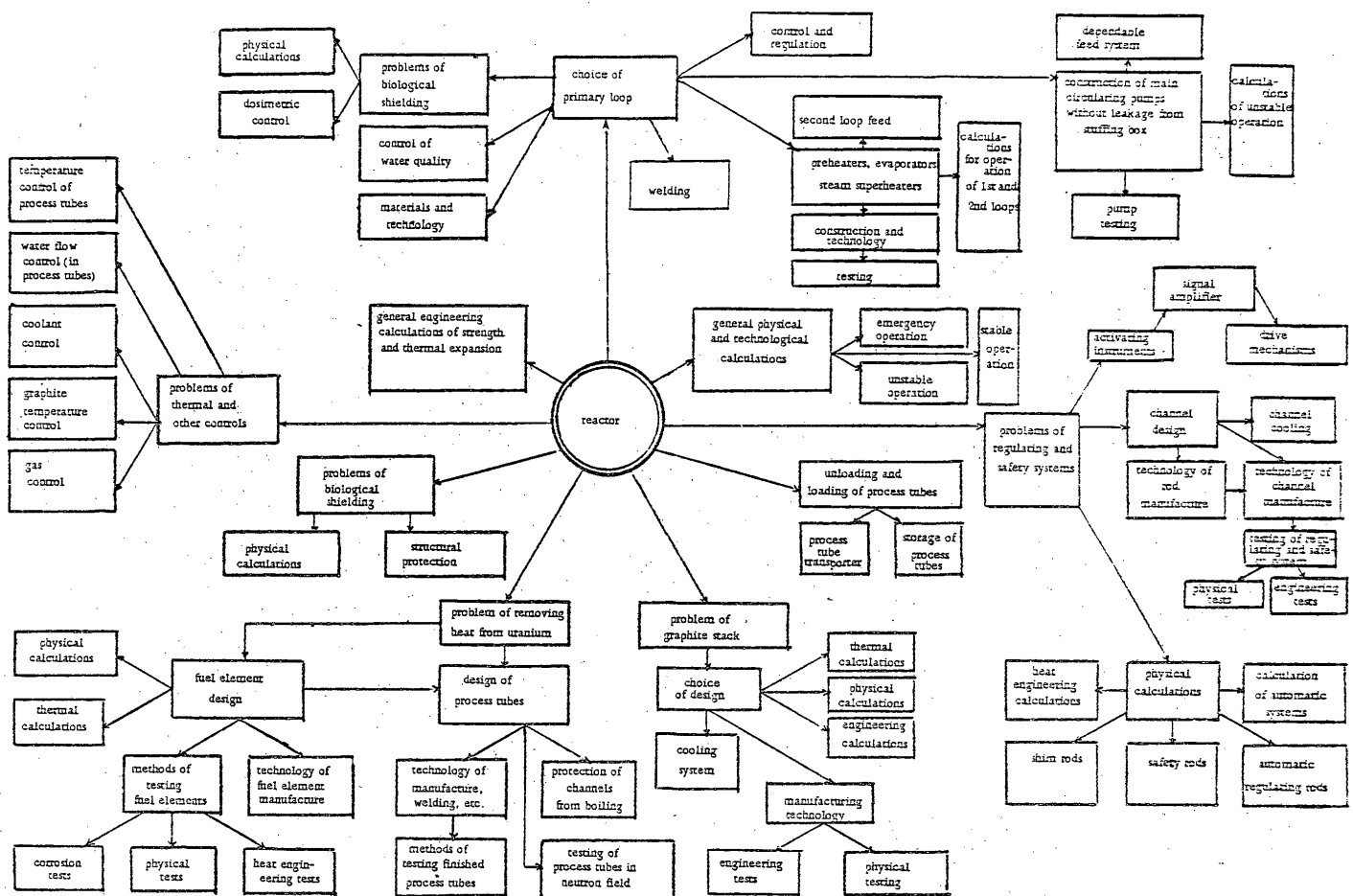
As was shown by experience in operating the power station the use in this type of reactor of very long tubes containing a large number of welded seams does not decrease the dependability of the plant operation under the present stage of development of the technology of production of fuel elements and operating channels.

The pressure of 100 atmospheres was a compromise between the desire to have both a high coolant temperature and the lowest possible neutron absorption rate of the construction materials. It was decided to make the tubes of the fuel elements of austenitic stainless steel of the IX18H9T type. The outside diameter of the tubes was 9 mm and the wall thickness 0.4 mm. The anti-fragment sheathing was 0.2 mm thick and was made of the same kind of steel.

The IX18H9T steel was chosen because of its good corrosion resisting properties and high tensile strength and particularly because experiment has shown that austenitic steels are sufficiently stable against neutrons.

The amount of uranium in the reactor could be changed depending on the operating period and the number of operating channels in the core. On the other hand, with a given amount of uranium the amount





of enrichment could lead to different operating periods. Thermal power of 30,000 kilowatts, since it was decided to use thermal loads of the order of  $2 \cdot 10^6$  kcal/m<sup>2</sup> hour, was provided by approximately 120 operating channels in the core. The design of the channels permitted the loading of different amounts of uranium.

It was decided that the first operating period would last 100 days. This period was sufficient for a thorough test of the fuel elements and required only moderate enrichment of a small quantity of uranium.

Thus with the given channel design and period of operation the quantity of uranium loaded into the reactor was 550 kg. It was calculated that this amount of uranium would have to be enriched 5%, i.e., it would have to contain 27.5 kg of U<sup>235</sup>.

The thermal scheme of the atomic electric power station consists of two circuits (Figure 2). The primary circuit includes the reactor, steam generators, circulating and feed pumps and a few auxiliary devices. The secondary circuit includes the secondary side of the steam generators, a turbo-generator, feed pumps and a few auxiliary devices. The inclusion of the turbine in the secondary circuit prevents radioactive contamination and makes it possible to operate the turbine under normal conditions.

The temperature of the water at the reactor outlet was given as 280° C. This made it possible to obtain either superheated steam at comparatively low pressure or saturated steam at a higher pressure. In the atomic power station an already available turbine was used which operated with steam at 12.5 atmospheres and about 270° C, thus determining the thermal parameters of the secondary circuit.

It must be noted that the choice of materials and of concrete values of the individual quantities was based on an evaluation of a large volume of experimental and theoretical study produced by many agencies engaged in the work of constructing the USSR Academy of Sciences atomic power station.

Some idea of the scope of the problems to be solved is given by the scheme shown in Figure 3.

### Design of the Reactor

The structural nucleus of the reactor, a vertical section of which is shown in Figure 4, consists of a cylindrical graphite stack 3 m in diameter and 4.6 m high. The central portion of the stack contains 157 vertical holes 65 mm in diameter which form a regular triangular lattice in a plane, with 120 mm spacing. Operating channels containing uranium fuel elements were put into these holes. The central portion of the uranium stack, which is the reactor core, is surrounded by a graphite reflector built of sector-shaped blocks. The stack is enclosed in a steel jacket which is welded to the lower steel plate. The latter rests on a supporting ring set up on jacks upon a reinforced concrete foundation. The foundation and steel plate are cooled by water flowing through coils.

The stack is covered on top by a heavy cast iron plate with openings that correspond exactly to the holes in the reactor stack. The weight of this plate is distributed through jacks on a ring-shaped support attached to the inner wall of the lateral water shield. The reactor jacket is connected to the plate by a thermal expansion compensator. With the lower and upper plates the jacket forms a hermetically sealed volume which is filled with an inert gas during operation of the reactor.

The cast iron plate together with the upper part of the graphite stack serve at the same time as a biological shield of the reactor from above. On its sides the reactor is surrounded by an annular reservoir filled with water. The layer of water in the reservoir is 100 cm thick and is a component of the lateral biological shield. Coils containing a flow of cold water are used to remove the heat generated in the water shield. The entire reactor and its water shield are placed in a concrete-lined pit. The walls, which are 3 m thick, serve as the outer layer of the biological shield. Above the cast iron plate are located the pipes which conduct the flow of water to and from each operating channel. Here is also located the outlet header from which water heated in the reactor is piped to the steam generators.

The concrete pit containing the reactor is shielded on top by a cast iron cover. This cover serves as a shield against radiation from the water, which is highly radioactive on leaving the reactor. The inlet header is located in a different place and is shielded by a lighter cast iron cover.

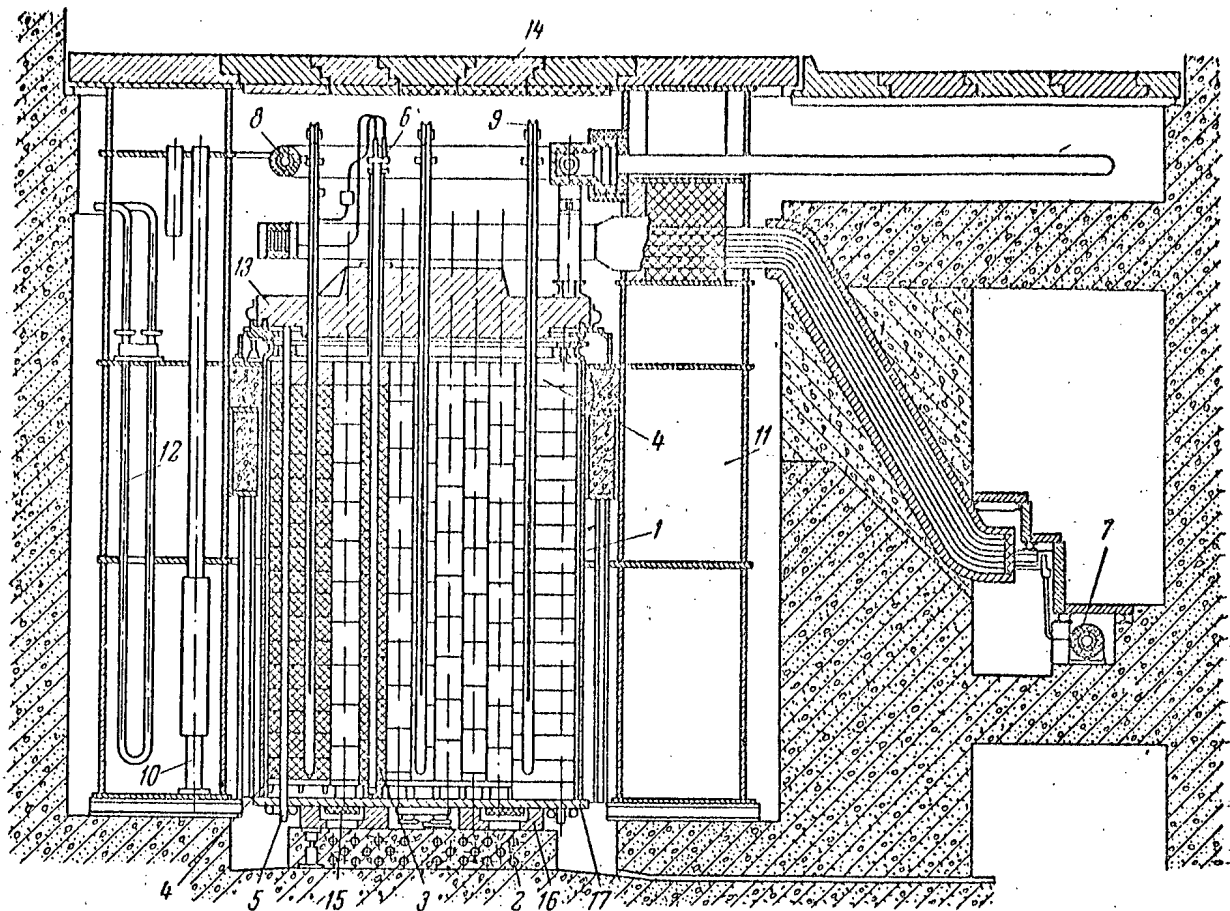


Figure 4. Vertical section of the reactor.

1) Jacket, 2) reactor foundation cooling tubes, 3) graphite channel sleeves, 4) graphite reflector blocks, 5) reflector cooling tube, 6) fuel channel, 7) inlet header, 8) outlet header, 9) regulating rod, 10) tube of ionization chamber, 11) water shield, 12) cooling coils of water shield, 13) cast iron plate, 14) cast iron cover, 15) cooling of steel plate, 16) supporting ring, 17) steel plate.

The water shield contains 12 vertical tubes in which ionization chambers are placed at the level of the core. The upper part of the reactor is shown in Figure 5 with the cover removed.

As was stated above there are altogether 157 holes in the reactor stack of which 128 are used as operating channels with the remainder designed for control rods and auxiliary purposes.

Figure 6 is a schematic drawing of a process (operating) channel with the water supply and removal route. The operating channel is a long 65 mm cylinder made up of separate graphite sleeves with five longitudinal holes through which the tubes of the elements pass. Water entering through the head flows down through the central tube cooling the graphite of the cell containing the channel and returning to the top through four tubes. The uranium is placed in the lower part of the channel outside these four tubes, i.e., the water flows inside four fuel elements with an active portion of 1700 mm length. The active zone (core) whose diameter is 1500 mm and height 1700 mm comprises 128 process channels. The heat flow in the most intensely operating fuel elements reaches  $1.8 \cdot 10^6$  kcal/m<sup>2</sup> hour.

Fuel elements of various designs were subjected to prolonged testing in standpipes where their heat output was simulated through electric heating. The best types were tested in the water "loop" of the RFT.

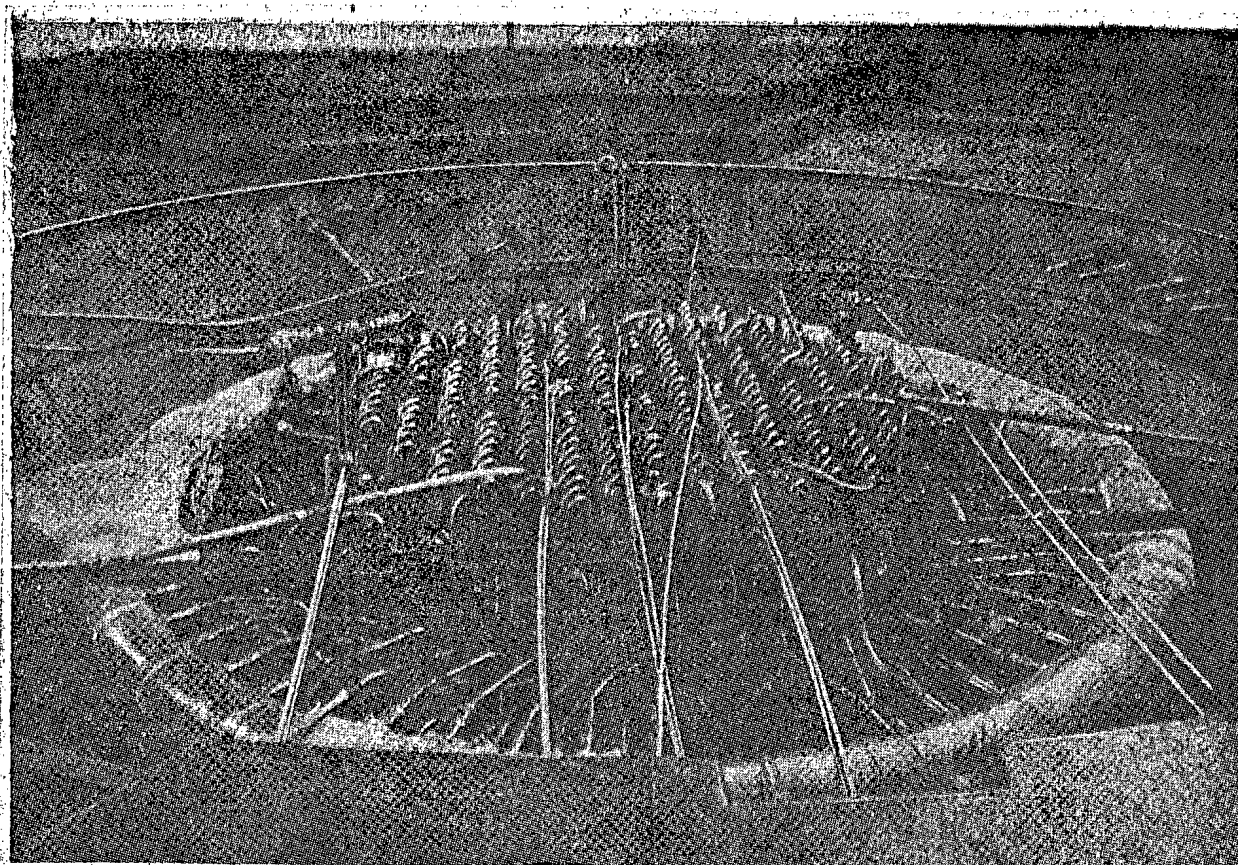


Figure 5. Upper part of the reactor with cast iron cover removed.

experimental reactor which was built especially for physical and heat engineering experiments connected with the development of power reactors. The experiments carried out on this "loop" enabled us not only to check the heat transfer properties but also to determine the stability of the various fuel elements under operating conditions.

Water from the inlet header before entering the operating channel passes successively through a throttle which controls the water flow, a cutoff valve and a regulating valve. At the outlet the water passes through a second valve and a non-return valve. A resistance thermometer is mounted on the housing of the non-return valve for the purpose of measuring the water temperature at the operating channel outlet.

The cutoff and the non-return valve would in case of rupture of any tube of the channels almost completely block the flow of water through the channel. By the use of valves it is possible to regulate the water flow and to cut off a channel from the headers during changes, for example.

The reactor is regulated by boron carbide rods. There are 24 control rods altogether, divided into three groups: rods for automatic regulation of the reactor power, shim rods and scram rods. The position of the control rods is shown in Figure 7. Since the control rods give off a considerable quantity of heat due to neutron absorption the control rod channels are water cooled. The cooling water is supplied under a pressure of 5 atmospheres and is heated in the channels from 30° C to 60 – 80° C.

The reactor power is controlled by means of 12 ionization chambers with solid boron coating. The regulating and safety scheme of the reactor is shown in Figure 8. The ionization chambers are divided into three groups which activate the mirror galvanometers; and actuate the servomotors and the emergency safeguards according to the level and rate of change of the power.

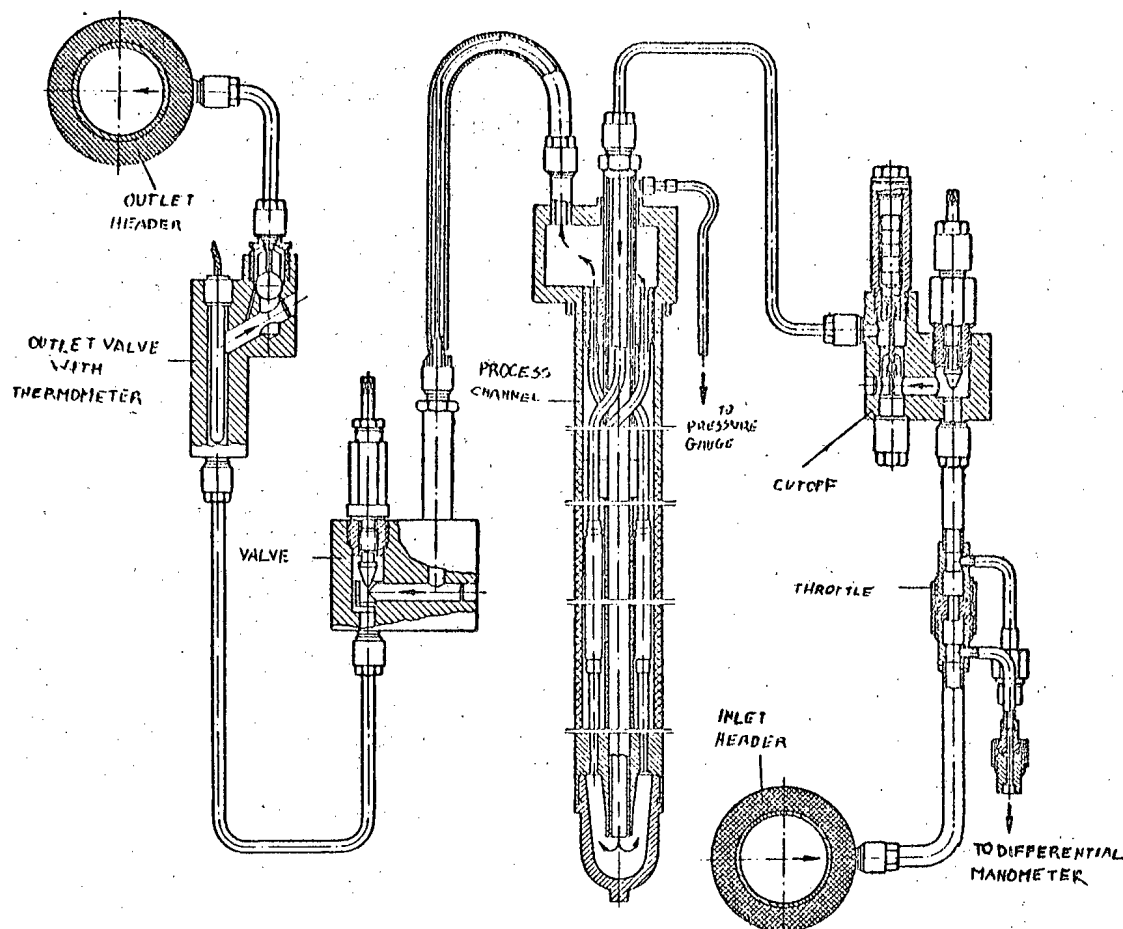


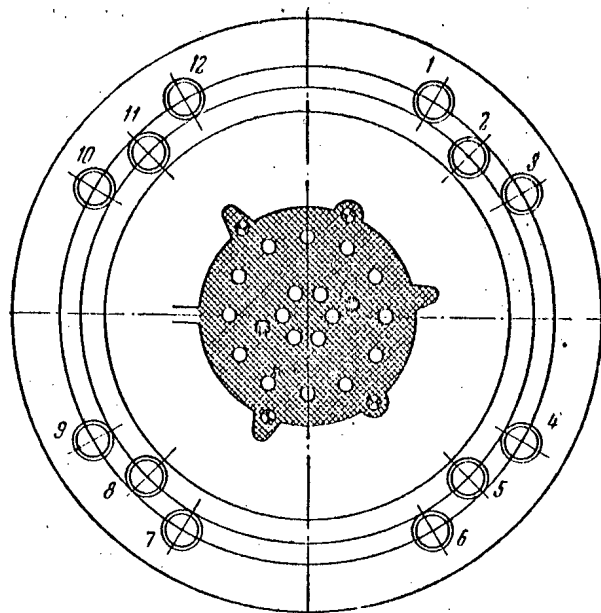
Figure 6. Process channel circuit of the reactor.

During the operation of the reactor about 7% of the thermal power is evolved in the graphite moderator. The heat is removed from the moderator through the process channels and the control and safety channels. In spite of the relatively high thermal conductivity of graphite the spaces which serve to compensate the thermal expansion of the graphite and facilitate the removal of the channels produce heating of the pile. The temperature of the graphite in the core is measured in two channels of the reactor by conventional chromelalumel thermocouples. Each of these channels contains three thermocouples which measure the graphite temperature at different heights in the core.

The reactor of the atomic power station is also equipped to produce radioactive isotopes, to study the effect of reactor radiations on various materials and for other experimental investigations. Figure 9 shows the arrangement of the experimental channels, one of which reaches to the center of the core while the others penetrate the side reflector as far as the edge of the core. Three channels are water cooled. These channels enable us to study the behavior of various materials at different temperatures in neutron fluxes up to  $8 \cdot 10^{13}$  neutrons/cm<sup>2</sup> sec.

The samples to be irradiated are placed in special containers and are inserted into the irradiation zone through the channels, after which they are withdrawn and placed in shielded containers or storage channels. Figure 10 shows the act of unloading an irradiated sample.

There are four channels which serve to extract neutron and gamma ray beams, of which the vertical channel passes through the center of the reactor. The remaining three channels are horizontal. At the outlet of two channels the neutron fluxes reach  $10^9$  neutrons/cm<sup>2</sup> sec; the others reach  $10^7$  neutrons/cm<sup>2</sup> sec.



- ⊗ 4 channels for automatic regulating rods
- 18 channels for manual regulation
- ⊗ 2 channels of SES (slow emergency shielding).

Figure 7. Distribution of ionization chambers (IC) and channels of regulating and shielding system (RSS).

2 and 8) IC of first range of automatic regulation; 1, 4, 7, and 10) IC of second range of automatic regulation; 5) IC of first range of safety amplifier; 11) IC of first range of power recorder; 3 and 9) IC of second range of safety amplifier; 6 and 12) IC of second range of safety amplifier.

through the neutron flux by means of the ionization chambers with solid boron coating. These chambers are connected with galvanometers of  $10^{-8}$  ampere sensitivity and with the measuring systems of the automatic regulating and safety rods. These systems and the electronic and electromechanical equipment maintain qualitative regulation of the chain reaction. The automatic regulating rods maintain the power of the reactor at a given level in the range from 3 kw to 36,000 kw. The accuracy of regulation is  $\pm 1.5\%$ . Besides the galvanometers the power is controlled initially within 2 - 3% by the quantity of heat removed from the reactor through the operating and regulating channels. The reactivity is determined by the depth of the absorbing rods in the core.

The rods are calibrated periodically, i.e., the relation between the position of the rods and the reactivity is established in absolute units since during the operation of the reactor the reactivity equivalent of the rods is attenuated with time. The operating personnel regularly keeps a record of the reactivity expressed in centimeters.

It is known that the relationship between the rod position and the reactivity is not linear; therefore it is convenient throughout the entire range of rod motion to reduce the sensitivity of the rod in the nonlinear portion to its equivalent in the linear portion. Then the position of the rod expressed in centimeters is related to the absolute reactivity by some constant factor.

For stability and safe operation of the reactor it is absolutely necessary to control the pressure in the first circuit and the water temperature at the outlet of each operating channel. A drop in pressure in the

For studies using thermal neutrons a graphite thermal column adjacent to the reflector is used. The column contains spaced inserts which permit a change of instruments and irradiated materials without interrupting the operation of the reactor. The thermal neutron flux in the column reaches about  $10^9$  neutrons/cm<sup>2</sup> sec.

### Control of Reactor Operation

In order to ensure continuous and dependable control of the operation of the reactor and the power plant as a whole all of the equipment was supplied with the necessary control and measuring instruments and with emergency and warning signals. The control and measuring apparatus may be divided into two main groups. The first group includes the instruments for the control and regulation of the reactor; the second group contains the control and measuring instruments of the thermal power equipment of the power station.

The principal factors which must be controlled are:

- a) For the reactor: the power; reactivity; pressure and equality of gas in the stack; temperature of the graphite; flow and temperature of water for the auxiliary cooling systems.
- b) For the operating (process) channels: water temperature at the exit of each channel; water flow in each channel and appearance of moisture in the graphite stack around each channel.

The power of the reactor is monitored

Declassified and Approved For Release 2013/04/03 : CIA-RDP10-02196R000100090001-4

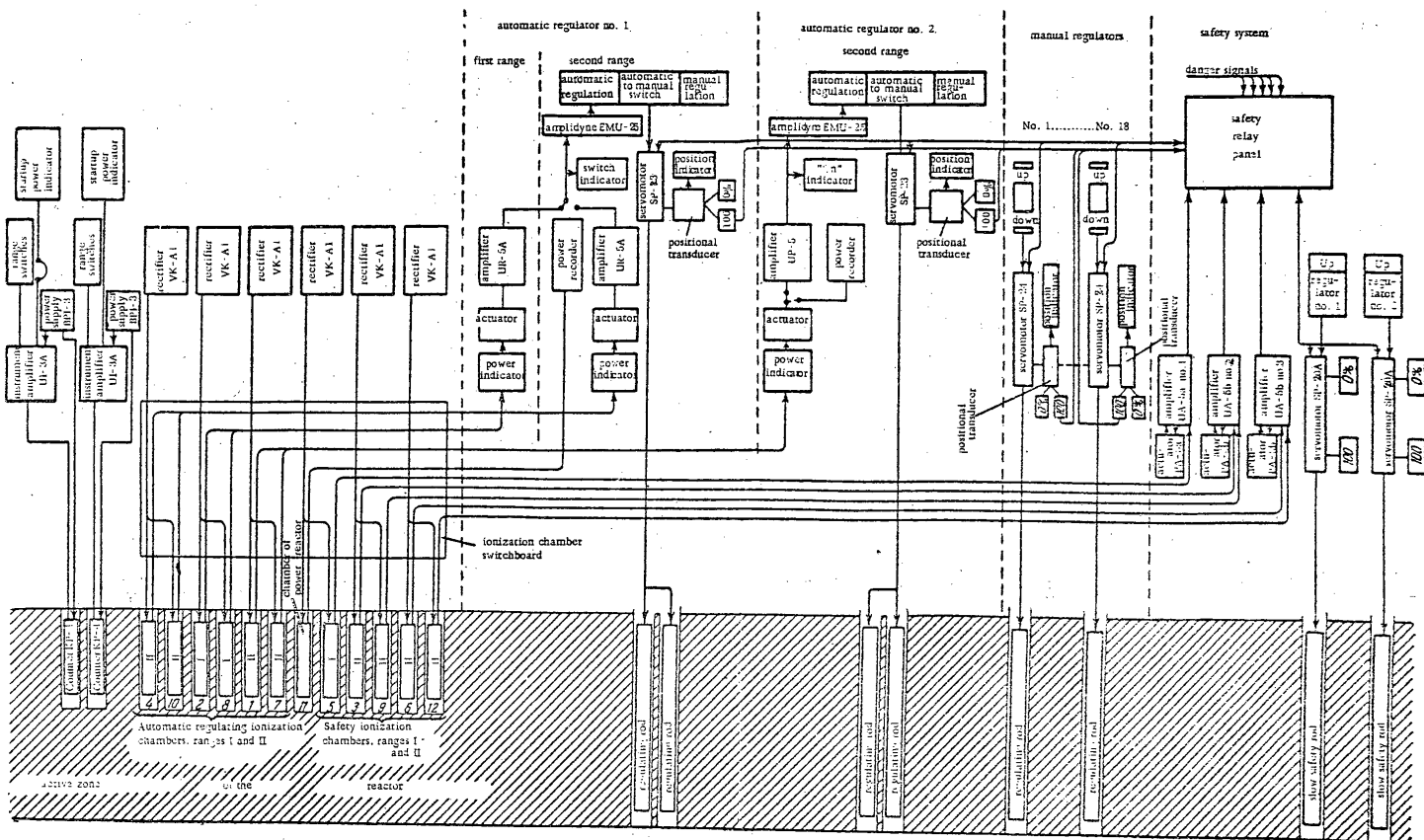


Figure 8. Regulating and safety scheme of the reactor.

Declassified and Approved For Release 2013/04/03 : CIA-RDP10-02196R000100090001-4



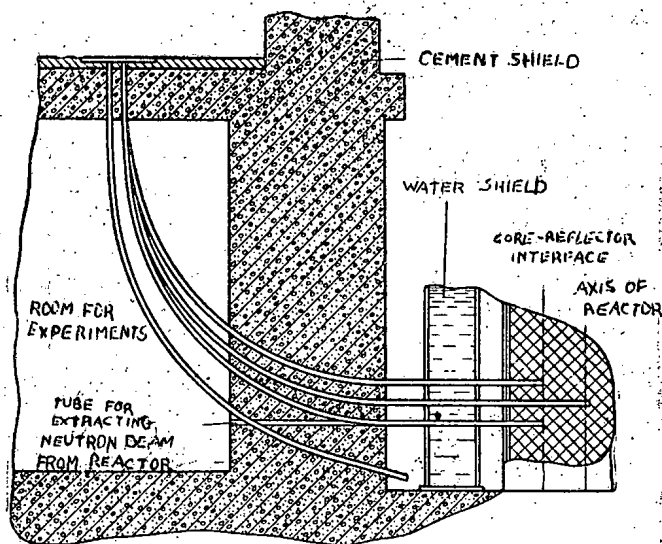


Figure 9. Arrangement of experimental channels (side view with channels completely exposed).

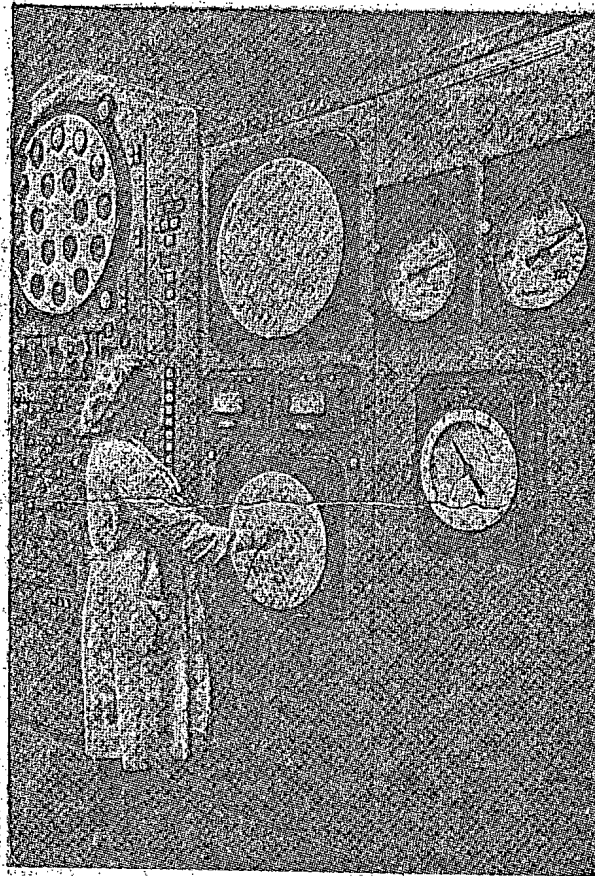


Figure 11. Measurement of water temperature in an operating channel.

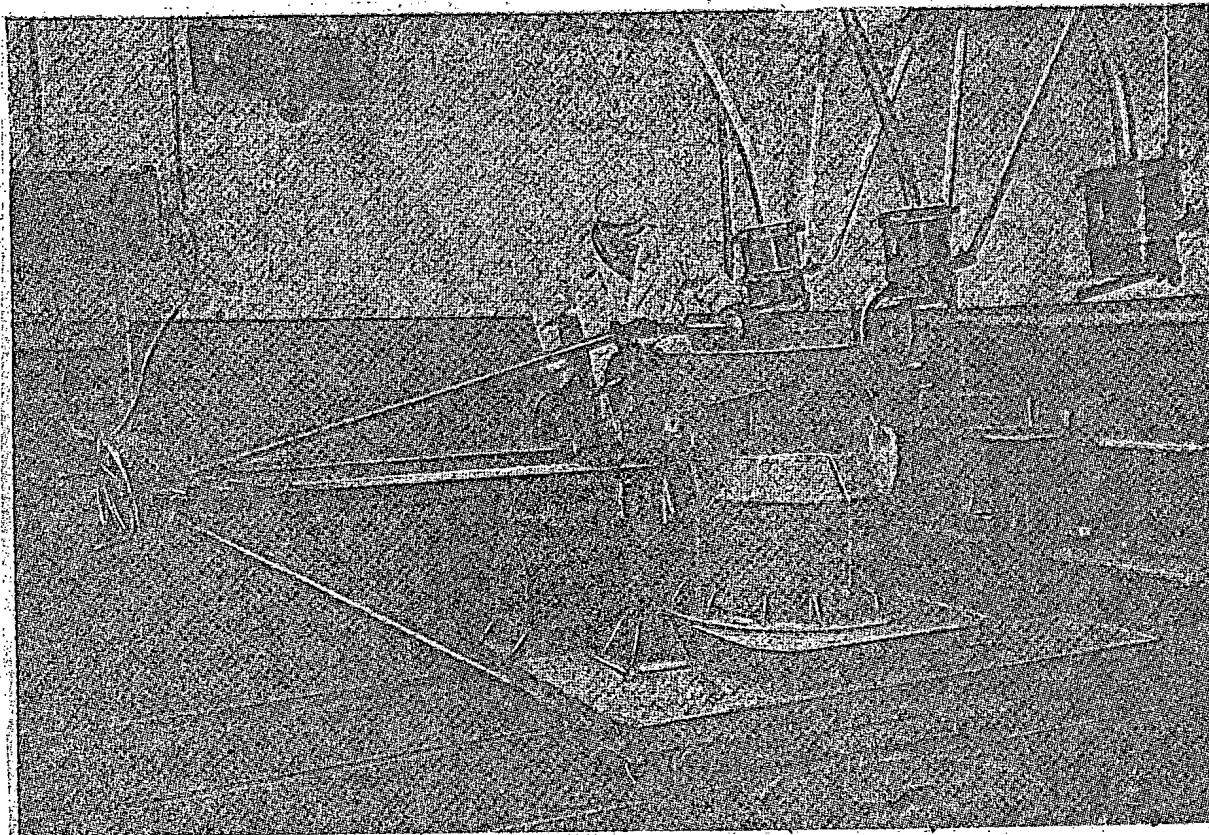


Figure 10. Unloading of irradiated object from reactor.



first circuit may result in boiling of the water in the operating channels. This in turn could cause melting of the fuel elements since their thermal load is large. Therefore a constant watch is kept over the water pressure, water level in the volume compensators, drainage and feed of the primary circuit, and temperature and flow of water in the operating channels.

The water temperature at the outlet of the operating channels is monitored by an automatic relay system which alternately connects the channel thermometers to the measuring system which is set for a given temperature. The time of a complete cycle of thermometer switching is 20 seconds. If the water temperature in any channel exceeds the set value a light flashes immediately to inform the engineer on duty of the number of that channel.

For exact measurement of the water temperature at a channel outlet provision was made for connecting the channel thermometer to an instrument. Figure 11 shows a measurement of the water temperature of an operating channel being taken.

The instruments which measure the pressure in the circuit and the water flow in the channels are provided with signaling devices which are connected to the warning system and which in case of a large deviation of pressure or flow from the fixed value will automatically shut down the reactor.

In the primary circuit a measurement is also taken of the total water flow and the mean temperature of the water at the reactor inlet and outlet. The stability of these variables is very important for the operation of the reactor. The magnitude and stability of the set water temperature at the reactor inlet reflect the normal operation of the steam power plant; the water temperature at the outlet determines the quality of the steam fed to the turbine.

In the secondary circuit measurements are taken of the quantity and quality of the steam fed to the turbine. Set values of the steam variables corresponding to a given level of reactor power are provided by automatic regulation of water feed and by the maintenance of a constant water level in the evaporators. The water-chemical control of the operation of the evaporator is conducted exactly as in conventional electric power plants; the quality of water and steam is controlled by the salt content.

The reactor's emergency system provides twenty different emergency signals caused, for example, by an increase of reactor power by 20% over the established level, increased rate of reactor speedup (100% in 1 sec.), simultaneous voltage loss (6 kv) in two sources, water pressure drop in the first circuit, etc.

The control of the plant and supervision of the operation of the basic equipment is concentrated at the central control room which is depicted in Figure 12. The control console is shown at the center of the foreground. To the left of the desk are the instruments for control and regulation of the physical processes in the reactor, on the right side is the control of the thermal power equipment. The middle control panel holds the indicators of the positions of the compensating rods and the annunciator of the warning and emergency light signal system. The adjoining right and left panels hold the instruments which indicate the water flow in the first circuit, the water temperature in the channels, the steam variables, etc.

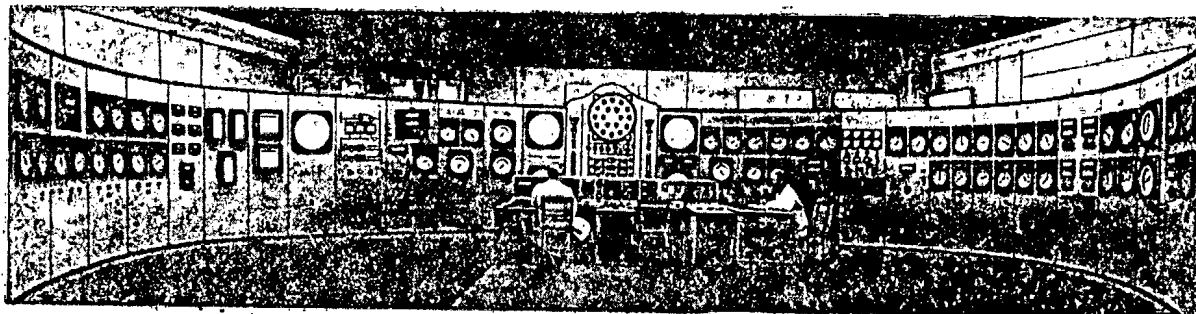


Figure 12. Control room of the atomic power station (control console in foreground).

One of the features of the operation of an atomic power plant is the need for constant dosimetric control of the rooms of the station, supervision of the activation of water in the primary and secondary circuits, the activation of the gas in and around the reactor and the activation of dumped water. Such control together with the biological shielding of the reactor ensures the safety of the operating personnel.

The overall dosimetric control system provides for measurement of gamma ray intensity in rooms in which radioactivity appears or may appear. The activation of the air is also monitored. If the gamma radiation in any room exceeds the permissible level (1.8 micro-roentgens/sec) or the activation of the air exceeds the permissible norm the attendant at the central dosimetric panel is warned by light and sound signals. These signals also are given in the room where the radioactivity has increased.

#### SUMMARY

The atomic power plant of the USSR Academy of Sciences was set in operation on June 27, 1954. During the time of its operation not a single fuel element has gone out of order. There has been a rupture of an operating channel tube from which no dangerous consequences resulted. The emergency shielding of the reactor proved to be fully adequate. There have been stoppages of primary feeding of the circulating pumps but the emergency shielding fulfilled its purpose.

Generalizations drawn from our experience are the basis for the following conclusions which will be useful for further developments in the construction of power reactors:

1. The dependable operation of the atomic power plant has shown that the technical principles upon which it is based are correct.
2. The biological shielding of the operating personnel and of the surrounding inhabited area have been fully reliable.
3. The fuel elements have shown extremely high strength. 120 elements were tested for durability and degree of uranium "burning" beyond the design figures. The fuel elements were tested for a prolonged period at a thermal output of about  $1.5 \cdot 10^6$  kcal/m<sup>2</sup> hr during which the "burning" of the U<sup>235</sup> reached 10 kg per ton.
4. The operation of the station provided a large amount of information which will be useful in drawing conclusions regarding the operation of individual units and instruments.
5. The successful operation of the station and its economic prospects are a guarantee of the further successful development of atomic power.

In Geneva during August 1955 at the International Conference on the Peaceful Uses of Atomic Energy special attention was paid to the problem of constructing nuclear reactors for electric power. A large number of reports on this problem were presented by various countries.

Some of these reports presented only theoretical views on the construction and development of power reactors, while others reported on reactors being built, already built or already in operation.

Because of the quantity of reports on reactors and the large number of details regarding them the proceedings of the Conference are of great interest, especially because at the present time evidently no one thinks that the construction of nuclear reactors for electric power is unprofitable.

The great interest shown by engineers of different countries in these matters is evidenced by the large number of articles in foreign journals which discuss different types and designs of reactors.

One of the reports at the Geneva Conference, presented by a group of American specialists [2] describes the plan of an American nuclear power plant with a graphite-water reactor. This reactor essentially repeats the principles used in the first USSR Academy of Sciences nuclear power plant. As tubing material for the cooling water under 140 atmospheres and passing through the reactor core the American design calls for zirconium alloys. Slightly enriched uranium will be used as fuel.

The designers believe that a plant of this type may be profitable even at the present time.

The same conclusion is reached in a review by G. Ford [3], one of England's leading specialists in the field of nuclear energy. For comparative profitableness and prospects he places the graphite-water reactor first among all other possible variations of nuclear power station reactors.

The authors of the present article believe that a graphite-water reactor with slightly enriched uranium, based on the structural units and elements tested in work on the first USSR Academy of Sciences nuclear power station, possesses important advantages and can be used in a large industrial nuclear power plant.

#### LITERATURE CITED

[1] D. I. Blokhintsev and N. A. Nikolaev, The First USSR Atomic Power Station and the Development of Nuclear Power. Report of the Soviet Delegation at the International Conference on the Peaceful Uses of Atomic Energy. USSR Academy of Sciences Press, 1955.

[2] R. K. Andersen, A graphite-moderated nuclear power plant design, Report No. 492 at the Geneva Conference on the Peaceful Uses of Atomic Energy, 1955.

[3] G. W. K. Ford, Engineering, 180, No. 4680, 490 - 500 (1955).

PHYSICAL AND THERMAL CALCULATIONS FOR THE USSR ACADEMY OF SCIENCES  
ATOMIC POWER STATION REACTOR

D. I. Blokhintsev, M. E. Minashin and Yu. A. Sergeev

INTRODUCTION

The basic principles of physical and thermal reactor calculations are already well known. But the knowledge of these principles is still insufficient for exact calculations on reactors since a reactor is a very complicated structure all of whose characteristics can only with great difficulty be represented in any theoretical calculation. The main problem is therefore the estimation of the errors which result from the inevitable simplifications used in the calculation itself as well as because of the inaccuracy of the initial physical constants. It is precisely these circumstances which make the calculation for an actual reactor a very difficult problem which must be checked at all principal points by separate experiments.

It must also be kept in mind that we are not referring to any single calculation but rather to a considerable number of successive calculations. At first only crude provisional calculations are made which correspond to the preliminary design stage. Thereafter as the designing and technological work progress new calculations are carried out essentially for the purpose of checking on the values chosen by the designers. The acceptability of any solution is determined by the aggregate of linked results of the physical, thermal and other calculations.

As initial parameters for the nuclear power plant reactor only two could be considered as fixed: the net electric power output of the plant (5000 kw) and the period of operation of the reactor without additional loading of uranium (the run) which was fixed initially at about 100 days. Another requirement was that the enrichment of the uranium with  $U^{235}$  should be as low as possible for the reactor type to be used and especially for the type of fuel elements (FE).

The physical calculations involved the exact determination of the reactor dimensions corresponding to the uranium load (with the desired enrichment) and the structural data. At the same time it was necessary to calculate the amount of uranium (above the critical mass) required for the reactor operation, the regulating and safety rods, the radioactivity and the size of the biological shielding. The heat source and temperature distributions in the various components of the reactor design also entered into both the physical and thermal calculations.

Finally, it was necessary to consider unstable modes of operation of the reactor allowing for all possible kinds of accidents.

This large amount of calculation was performed by the simplest methods and particular applications were controlled by separate calculations based on more exact methods.

The present article describes the basic results of the physical and thermal calculations for the APS (atomic power station) reactor. The numerical data refer to the actually realized type of loading and uranium enrichment.

These results were obtained by utilizing the following basic reactor characteristics:

1. Thermal power of reactor	$30 \cdot 10^3$ kw
2. Core diameter	154 cm
3. Core height	170 cm
4. Lateral reflector thickness	80 cm
5. Thickness of end reflectors	60 cm
6. Lattice	rhombic
7. Lattice spacing	12 cm
8. Number of operating channels	128
9. Number of cells of regulating and safety rod channels	20
of which: shim rods	18
safety rods	2
10. Number of automatic regulating rods (in reflector)	2
11. Number of cells with channels for physical experiments	1
12. Moderator in core and reflectors	graphite ( $\gamma = 1.67$ g/cm <sup>3</sup> ) and coolant in channels
13. Coolant— ordinary distilled water at 100 atmospheres pressure	$t_{in} = 190^\circ \text{C}; t_{out} = 275^\circ \text{C}$
14. Uranium load	560 kg
15. Uranium enrichment	5%
16. Uranium concentration (for operating conditions)	$\frac{C}{U} = 171; \quad \frac{H}{U} = 4.2$
17. Power production per ton of uranium (average)	$53.5 \cdot 10^3$ kw/ton
18. Run	75 days

In order to avoid uncertainty in the interpretation of the results of the calculations, the table gives the numbers of the equations used in this article.

The calculations are based on the Fermi age theory, which is very well explained in the literature [1].

### PHYSICAL CALCULATIONS

In working out a method of performing the APS reactor calculations the authors endeavored to reduce the labor as much as possible. We know that exact methods of calculation, which often are a means of checking simplified methods, cannot guarantee the correctness of absolute results since the initial data used in both the approximate and more accurate calculations are obtained with an experimental error which at times exceeds the error of the calculational methods. When the work of designing the APS reactor was started certain initial data were not known from experiment. There were no reliable means of calculating the temperature of the neutron gas, the energy distribution of resonance capture in  $U^{238}$ , etc; even at the present time these quantities are more frequently taken from experimental measurements. Experimental methods of determining the absorption and multiplication of epithermal neutrons above thermal energies as a rule give summations of these quantities over the entire epithermal region. Among such quantities are, for example, the resonance absorption and fission integrals  $\left( \int \sigma_a \frac{dE}{E}, \int \sigma_f \frac{dE}{E} \right)$ , the probability of resonance neutron absorption in  $U^{238}$  ( $1 - \phi$ ), and the square of the slowing-down length ( $\tau$ ). The absence of data showing the energy dependence of these quantities decreases to a considerable degree the value of attempts to employ mathematical methods which would observe such dependence rigorously. (In the general case the mutual screening of elements (especially  $U^{235}$  and  $U^{238}$ ) may be important, which doubtless exists in resonance neutron absorption) If this is to be taken into consideration it is necessary to know in detail the variation of the cross sections, which when the designing of the APS reactor began was far from being known for all elements.

Finally, we must dwell especially on one important circumstance which introduces a certain amount of indeterminacy into the calculation of variation of neutron density for  $E < 1$  ev. This applies mostly to heterogeneous reactors with a geometrically complicated distribution of materials possessing different moderating

properties and temperatures and is associated with insufficient knowledge of the slowing-down mechanism at energies below 1 ev. In this energy range the binding energy of atoms in molecules and crystals cannot be considered insignificant compared with neutron energies; consequently the model of neutron scattering by free nuclei is incorrect. The absence of data on neutron interaction with bound nuclei also affects calculations of the thermal neutron distribution in the reactor lattice and in the end causes some uncertainty in calculations of the capture mean free path and diffusion length of thermal neutrons ( $\lambda_a$  and  $L_T^2$ ) as well as the thermal neutron yield ( $\Theta$ ).

It should be noted however that if the reactor is sufficiently large an error in the determination of  $L_T^2$  has little effect on the critical size. Moreover, for heterogeneous reactors the variation of neutron density in a lattice cell may be unimportant if most of the mass of the absorbers (steel tubes, water coolant, etc.) is concentrated in the immediate vicinity of the uranium, i.e., if the same neutron flux enters these materials as the uranium.

In general it must be said that the method of calculation described here can be applied only in case of weak capture (as we have assumed, for a capture mean free path ( $\lambda_a$ ) two or more times longer than the lattice spacing) and unthorough heterogeneity of distribution of materials with different moderating ability (including different crystal structure).

As can be seen from the basic characteristics as well as from the results of the calculation the APS reactor satisfies all these requirements.

For these reasons in solving problems involving physical calculations we used predominantly the simple two-group method of the age approximation. The accuracy of the results obtained by this method was checked in some cases by the single-group method (neutron distribution in the reactor) as well as by the use of solutions of the kinetic equations (check of the age approximation, calculation of the square of the slowing-down length).

The use of the two-group method in many problems requiring a determination of the reactivity is justified also by the fact that this method is used only to estimate the efficiency of the reflectors (for more details see below). This means that if the increase in the critical size of the core resulting from the imaginary removal of the reflectors is small compared with the size of the core ( $< 15 - 20\%$ ), a mistake of 30% in determining the effective contributions of the reflectors will not materially affect the calculation of the multiplication factor for a core of such dimensions.

After these remarks we proceed to the calculation for the APS reactor, noting that the ratio of the concentrations of the moderator and fissionable materials in our case was such that neutron capture in the epithermal (intermediate) energy range is a considerable factor in the overall neutron economy ( $\sim 22\%$ , including capture in  $U^{238}$ ).

For not very strong absorption the slowing-down equation, neglecting resonance capture in  $U^{238}$ \*, is

$$\Delta q - \frac{q}{L^2(E)} = \frac{\partial q}{\partial x}, \quad (1)^{**}$$

where  $q$  is the slowing-down density, i.e., the number of neutrons per  $\text{cm}^3$  intersecting the energy level  $E$  in 1 sec.:

$$L^2(E) = \frac{\lambda_a(E) \lambda_n(E)}{3}, \quad (2)$$

$\lambda_a(E)$  is the path traversed by a neutron before capture;  $\lambda_n(E)$  is the mean free neutron path.

\* We shall allow for resonance capture in  $U^{238}$  through the resonance escape probability  $\phi$  which was measured experimentally for the lattice.

\*\* For calculation on the APS reactor in Equations (1), (7) and thereafter we used averaged values of  $\lambda_n$  and  $L^2$  for a heterogeneous lattice. The methods of averaging these quantities are analogous to those described in reference [1].

In Eq. (1)  $\tau(E)$  - the square of the slowing-down length - is determined by

$$\tau(E) = \int_E^\infty \left\{ \frac{\lambda_s^0(E_0)}{3} + \int_E^{E_0} \frac{\lambda_s(E') \lambda_{tr}(E')}{3E'} \frac{dE'}{E'} \right\} S(E_0) dE_0, \quad (3)$$

where  $S(E_0)$  is the energy spectrum of the generated neutrons. In the calculations  $S(E_0)$  was expressed by

$$S(E_0) = 0.484 e^{-E_0} \operatorname{sh} \sqrt{2E_0}.$$

The initial condition for  $q(r, \tau)$  is:

$$q(r, 0) = \left[ \frac{\Phi}{\lambda_a} \Theta \nu_f \right]_\tau + \int_0^{\tau_T} q^\nu(E) \Theta(E) \varphi(E) \mu(E) \frac{d\tau}{L^2(E)}. \quad (4)$$

Here the following notation has been used:

$$\nu = \frac{\lambda_a}{\lambda_f} \nu_f, \quad (5)$$

where  $\lambda_f$  is the neutron mean free path before fission capture;  $\nu_f$  is the average number of neutrons generated in one fission of the isotopes  $U^{235}$ ,  $Pu^{239}$  or  $Pu^{241}$ ;  $\mu$  is the fast fission factor of  $U^{238}$  (for  $E > 1.3$  Mev);  $\Phi$  is the kinetic thermal neutron flux:  $\Phi = n v(E_T)$ .

(Here and in the following the subscript "T" refers to thermal energies.)

$\Theta$  is the probability of neutron capture in fissioning isotopes (thermal utilization):

$$\Theta = \frac{\int \Phi \Sigma_a^f dv}{\int \Phi \Sigma_a dv}. \quad (6)$$

The integration in Eq. (6) is extended over the entire volume of the lattice cell of a process channel.

$\Sigma_a^f$  is the macroscopic capture cross section of the fissionable isotopes  $U^{235}$ ,  $Pu^{239}$  and  $Pu^{241}$ ;  $\Sigma_a$  is the neutron absorption cross section of all elements in the lattice with the exception of the regulating rod materials\*;  $n v(r)$  is the neutron flux at the point (r) of the process cell. For our case this flux is determined by the solution of the neutron diffusion equation;  $\Theta(E)$  is a quantity which is analogous to (6) and is calculated for epithermal neutrons with energy E.

The thermal neutron equation has the usual form

$$\Delta \Phi - \frac{\Phi}{L_T^2} + \frac{3\varphi}{\lambda_n} q(\tau_T) = 0. \quad (7)$$

The set of equations (1), (4) and (7) is solved exactly only for a reactor without reflectors. \*\*

\* Absorption by the regulating rods in these calculations was allowed for by an appropriate decrease of the multiplication factor  $\Delta k$ . Therefore strictly speaking Eq. (11) holds good for our determination of the quantities contained in it only at a time when all absorbing rods are removed from the reactor (i.e., at the beginning of a run). At any other time of operation the corresponding relation will be

$$\Delta k^* + (1 + x^2 L_T^2) e^{x^2 \tau_T} = \frac{[\nu \mu \Theta \varphi]_\tau e^{-\int_0^{\tau_T} \frac{d\tau'}{L^2}}}{1 - \mu \int_0^{\tau_T} \nu \Theta \varphi e^{-\left(x^2 \tau + \int_0^{\tau} \frac{d\tau'}{L^2}\right)} \frac{d\tau}{L^2}}.$$

\*\* In general even for a reactor without reflectors the solution of this system of equations is fairly complicated since the boundary conditions (the position of the extrapolated boundary) depend on the energy. However we are concerned with reactors whose dimensions are considerably greater than the extrapolation distances.

The APS, which has reflectors, can be calculated as though it were "bare", with a certain amount of error, by replacing the true dimensions of the core with equivalent dimensions which should obviously be greater than the true dimensions by an amount to be determined by the effect of the reflector. This quantity is known as the effective augmentation due to the reflector.

For a cylindrical reactor without reflectors and with radius  $R_{ex}$  and height  $H_{ex}$  the solution of (1) is

$$q(r, \tau) = q_0(r) e^{-\kappa^2 \tau} e^{-\int_0^\tau \frac{d\tau'}{L^2}}, \quad (8)$$

where

$$q_0 = \frac{\left[ \frac{\Phi}{\lambda_n} \Theta_{\nu\mu} \right]_\tau}{1 - \int_0^{\tau_T} \mu \nu \Theta \exp \left[ -\left( \kappa^2 \tau + \int_0^\tau \frac{d\tau'}{L^2} \right) \right] \frac{d\tau}{L^2}}, \quad (9)$$

$$\kappa^2 = \left( \frac{\pi}{H_{ex}} \right)^2 + \left( \frac{\xi_0}{R_{ex}} \right)^2; \quad \xi_0 = 2.405. \quad (10)$$

Substituting in (7) the expression for  $q(E)$  with  $\tau = \tau_T$  we obtain the following equation for the determination of the critical size ( $R_{ex}$  or  $H_{ex}$ ):

$$(1 + \kappa^2 L_T^2) e^{\kappa^2 \tau_T} = \frac{[\mu \nu \Theta]_\tau \exp \left[ -\int_0^{\tau_T} \frac{d\tau'}{L^2} \right]}{1 - \int_0^{\tau_T} \mu \nu \Theta \exp \left[ -\left( \kappa^2 \tau + \int_0^\tau \frac{d\tau'}{L^2} \right) \right] \frac{d\tau}{L^2}}. \quad (11)$$

The product  $[\mu \nu \Theta]_\tau$  is usually called the infinite multiplication factor of thermal neutrons ( $k_{\infty}$ ).

The right hand side of (11) can be regarded as the multiplication factor in the core taking into consideration the reactions in the intermediate energy region, i.e.,

$$k_{\infty}^* = k_{\infty} \mu_{inter} \quad (12)$$

where  $\mu_{inter}$  is the multiplication factor for intermediate neutrons:

$$\mu_{inter} = \frac{\exp \left[ -\int_0^{\tau_T} \frac{d\tau}{L^2} \right]}{1 - \int_0^{\tau_T} \mu \nu \Theta \exp \left[ -\left( \kappa^2 \tau + \int_0^\tau \frac{d\tau'}{L^2} \right) \right] \frac{d\tau}{L^2}}. \quad (13)$$

With this notation the critical size equation assumes the usual simple form

$$(1 + \kappa^2 L_T^2) e^{\kappa^2 \tau_T} = k_{\infty}^*. \quad (14)$$

In these calculations as the upper boundary of the thermal region we took an energy below which the slowing down spectrum becomes Maxwellian.\*

\* Thus we assume a priori that at the operating temperature of the reactor the slow neutrons are in thermal equilibrium with the medium in which they are diffusing. In actuality this is not so much a result of neutron slowing down for  $E < 1$  ev as of strong absorption in the vicinity of  $E = 0$  (see [2], [3]).  $T_0$  for the reactor at  $t = 20^\circ \text{C}$  is given the experimental value  $T_0 = 420^\circ \text{K}$ .



The boundary energy value between these two spectra ( $E_b$ ) can be obtained approximately from the continuity of the kinetic neutron currents at the boundary:

$$\frac{q(E_b)\varphi}{E_b \xi \Sigma_s(E_b)} = \frac{2}{\sqrt{\pi}} \frac{Nv(E_b)}{E_0^{3/2}} e^{-\frac{E_b}{E_0}} E_b^{1/2} \quad (15)$$

where  $v$  is the neutron velocity at  $E = E_b$ ;  $N$  is the thermal neutron density (neutrons/cm<sup>3</sup>); and  $E_0 = kT_0$  ( $T_0$  is the temperature of the neutron gas in °K).

The quantity  $q(E_b)$  can be normalized from the conditions of the balance so that the number of neutrons crossing the boundary  $E_b$  between the thermal and slowing-down regions would be equal to the number of neutrons absorbed or escaping from the reactor in the thermal region, i.e.,

$$q(E_b)\varphi = \int_0^{E_b} \frac{2}{\sqrt{\pi}} \frac{Nv(E)\Sigma_a(E)}{E_0^{3/2}} \times e^{-\frac{E}{E_0}} E^{1/2} (1 + \kappa^2 L_T^2) dE. \quad (16)$$

Using the  $\frac{1}{v}$  law for the cross section  $\Sigma_a(E)$  in the thermal region, that is,

$$\Sigma_a(E) = \Sigma_a(E_0) \frac{v(E_0)}{v(E)},$$

we obtain in this case:

$$q(E_b)\varphi = Nv(E_0)\Sigma_a(E_0)(1 + \kappa^2 L_T^2).$$

Substituting the expression for  $q(E_b)\varphi$  in (15) we obtain the following equation determining  $E_b$ :

$$\alpha^{3/2} e^{-\alpha} = \frac{\Sigma_a(E_0) \sqrt{\frac{\pi}{4}} (1 + \kappa^2 L_T^2)}{\xi \Sigma_s(E_b)}, \quad (17)$$

where

$$\alpha = \frac{E_b}{E_0}.$$

### Two-Group Method of Calculating Extrapolated Reflector Boundaries

In order to make it possible to utilize (1) to (14) it is necessary to calculate the values of the equivalent reflector boundary extrapolations, i.e., to represent the reactor with reflectors as an equivalent "bare" reactor with the same lattice and identical reactivity.

As has already been mentioned the simplest means of evaluating the extrapolations is the two-group method, which divides all the neutrons into two groups: the slowing-down and the thermal groups. By this method the slowing-down equation (1) with the aid of

$$q(r, \tau) = j(r, \tau) e^{-\int_0^\tau \frac{d\tau'}{L^2}} \quad (18)$$

becomes

$$\Delta j = \frac{\partial f}{\partial \tau}; \quad (19)$$

with the initial condition

$$j(r, 0) = \frac{\Phi}{\lambda_a} \cdot \frac{k_{\infty}^*}{\varphi e^{-\kappa^2 \tau}}, \quad (20)$$

where

$$e_T = \int_0^{\tau_T} \frac{d\tau}{L^2} \quad (21)$$

Then Equation (19) is replaced by the approximation

$$\Delta j(\tau_T) = \frac{j(\tau_T) - j(0)}{\tau_T} \quad (22)$$

This replacement does not lead to errors only for large reactor dimensions, namely when  $\kappa^2 \tau_T \ll 1$ .

(22) is used only to calculate the reflector efficiency; however, this procedure may be extended to smaller reactors (see errors on page 28).

This calculation is carried out on the basis of the solution of (22), (20) and (7) for a concrete geometrical reactor shape with appropriate conditions at the core-reflector interface.

The boundary conditions are, as usual, the equality of the kinetic [ $\Phi$  and  $nv(E)$ ] and diffusion currents  $\left( \frac{\lambda_n}{3} \frac{d\Phi}{dN} \text{ and } \frac{\lambda_n}{3} \frac{d nv(E)}{dN} \right)$ , where  $N$  is the normal to the interface). It is important to choose correctly the energy at which the currents

$$nv(E) \text{ and } \frac{\lambda_n}{3} \cdot \frac{d nv(E)}{dN}$$

are matched.

Our calculations show that for reactors in which absorption in the epithermal region does not exceed 15–20% the most suitable energy is 1 ev, which makes the procedure valid practically up to  $E \approx 10^4$  ev. This is due to the fact that for the majority of elements the scattering cross sections determining the continuity coefficients are constant for these energies. The slowing down density can be approximated by the law

$$nv(E) = \frac{\text{const}}{\xi \Sigma_s E}$$

It follows that in the indicated energy region is contained the main portion of the slowing down neutrons.

Reactors in actual practice have as a rule both end and side reflectors. For such complicated geometrical shapes even simplified equations such as (22) can only be solved numerically. Therefore we have used the so-called arbitrary separation of variables, which means that a real reactor is represented either as a reactor without end reflectors or as a reactor without side reflectors (Figure 1). For such reactors equations (22) and (7) can be solved exactly.

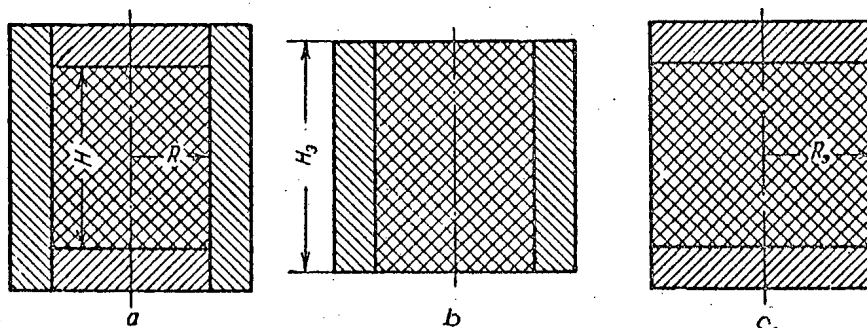


Figure 1. Calculated reactor types.

a) Real reactor; b) equivalent reactor with side reflector; c) equivalent reactor with end reflector.

Thus, for example, in calculating the effective side extrapolation distance the reactor is assumed not to have end reflectors but its height is not taken to be the actual height of the core  $H$  but, instead  $H_{ex}$  which is obtained from

$$H_{ex} = H + \delta_{up} + \delta_1 \quad (23)$$

where  $\delta_{up}$  is the extrapolation distance added to the height of the core in the assumed absence of an upper end reflector and  $\delta_1$  is the same for the lower end.

For  $H \approx 2R$  the accuracy of  $H_{ex}$  does not strongly affect the size of the lateral extrapolation distance and is therefore acceptable as a preliminary rough estimate.

In the calculation of  $\delta_{up}$  and  $\delta_1$  the reactor is assumed to lack a side reflector and its radius is assumed to equal  $R_{ex}$ :

$$R_{ex} = R + \delta_{side} \quad (24)$$

By the method of successive approximations  $\delta_{up}$ ,  $\delta_1$  and  $\delta_{side}$  can be made more accurate. Two approximations are usually sufficient since the  $\delta$  are only weakly dependent (for  $x^2 \tau_T \ll 1$ ) on dimensions and consequently on  $k_{\infty}^*$ .

The size of the error in the multiplication factor which results from the inexact determination of  $\delta = R_{ex} - R$  can be shown by using the example of a spherical reactor with reflector. The replacement of this reactor with an equivalent reactor without reflector requires increasing the radius of the core by  $\delta$ . We assume an error of 30% in  $\delta$  and that  $\delta$  itself is given  $\frac{\delta}{R_{ex}} \approx 0.2$ ; then the absolute error will be  $\Delta R = |\Delta \delta|$  and the relative error

$$\frac{\Delta R}{R} \approx \frac{|\Delta \delta|}{\delta} \cdot \frac{\delta}{R} = 0.3 \cdot 0.2 \left(1 - \frac{\delta}{R}\right) < 0.06.$$

For a spherical reactor we can easily obtain from (14) the following relation between  $R$  and  $k_{\infty}^*$ :

$$\frac{k_{\infty}^* - 1}{L_T^2 + \tau_T} \approx \left(\frac{\pi}{R}\right)^2.$$

Hence

$$\frac{\Delta k_{\infty}^*}{k_{\infty}^*} = \frac{|\Delta R|}{R} \left(1 - \frac{1}{k_{\infty}^*}\right).$$

In our case  $\frac{\Delta k_{\infty}^*}{k_{\infty}^*} \leq 0.06 \left(1 - \frac{1}{k_{\infty}^*}\right)$ . For  $k_{\infty}^* = 1.25$  we have  $\frac{\Delta k_{\infty}^*}{k_{\infty}^*} \leq 0.06 \cdot 0.2 = 0.012$ .

For  $k_{\infty}^* = 1.03$ , we have  $\frac{\Delta k_{\infty}^*}{k_{\infty}^*} \leq 0.06 \cdot 0.028 = 0.0017$ .

This example shows that even for a small reactor ( $k_{\infty}^* = 1.25$ ) crude errors in  $\delta$  lead to errors in the multiplication factor of the order of 1-2%, whereas an error of 1% in the initial value of  $\delta$  leads to an error in  $k_{\infty}^* \sim 1.5-2\%$ , i.e., as a result of inaccuracy in one of the initial parameters we have the same order of error.

Sets of equations such as (7) and (22) for the core and reflector can be solved for the geometrical reactor shapes in which we are interested. The solution can be obtained as a universal critical size equation which fits many different combinations of core and reflectors; the geometrical distinctions are represented in this equation by four coefficients.

The determination of the critical size of a reactor or the finding of another critical parameter subject to given dimensions (not only in the two-group but in any approximation) reduces to the solution of a transcendental equation which can be solved in one way or another by the method of successive approximations. The use of a simple general equation reduces considerably the time required for calculations.

The heat source distribution in the APS reactor was also obtained from the solution of the two-group equations: for the longitudinal direction with end reflectors and without side reflector; for the radial direction the reverse.\*

### Intermediate Neutron Absorption in the Calculation of the Isotope Ratio

The isotope ratio of the active material of the fuel elements after prolonged operation at a given power is calculated by solving the differential equations describing the change in density of the isotopes ( $U^{235}$ ,  $Pu^{239}$ ,  $Pu^{240}$ ,  $Pu^{241}$ , etc.). These equations have a comparatively simple solution for a purely thermal reactor, and thus in the APS reactor, which is essentially thermal, it is convenient to use the thermal reactor equations with corrections for intermediate neutron absorption.

The number of neutrons captured by element  $i$  is the sum of the captures in the thermal region  $\Phi \Sigma_{aT}^i$  and in the epithermal region:

$$\int_{E_0}^{E_\infty} n v(E) \Sigma_a^i(E) dE = \int_{E_b}^{E_\infty} \frac{q(E) \varphi(E)}{\xi \Sigma_s(E)} \Sigma_a^i(E) \frac{dE}{E}.$$

The total number captured in the  $i$ th element is

$$\Phi \Sigma_{aT}^i + \int_{E_b}^{E_\infty} \frac{q(E) \varphi(E)}{\xi \Sigma_s(E)} \Sigma_a^i(E) \frac{dE}{E},$$

where  $E_\infty$  is the energy above which neutron capture due to slowing down becomes unimportant.

For a reactor without reflector  $q \sim \Phi$ ; therefore it is convenient to introduce the neutron absorption cross section:

$$\Sigma_{a\text{eff}}^i = \Sigma_{aT}^i + \frac{q_0}{\Phi} \int_{E_b}^{E_\infty} \frac{\varphi(E) e^{-\kappa(E) - \kappa^2 \tau(E)}}{\xi \Sigma_s(E)} \Sigma_a^i(E) \frac{dE}{E}. \quad (25)$$

In using this expression to determine the isotope ratio we assumed that the neutron energy distribution in the reactor does not change essentially during a run, i.e.,  $\Sigma_{a\text{eff}}^i$  is practically constant. In this case the isotope ratio formulas obtained for a thermal reactor do not change formally and have physical meaning if instead of  $\Sigma_{aT}^i$  we substitute  $\Sigma_{a\text{eff}}^i$ .

If the run is so long that there is considerable change of density of  $U^{235}$  and  $\Sigma_{a\text{eff}}^i$  cannot be considered constant, the set of linear equations determining the rate of change of nuclear density is transformed in general into a set of nonlinear equations which must be solved by numerical integration. However, even in this case the run can be divided into a sufficient number of intervals so that the set of equations can be considered linear within each interval.

\* See Figures 1b and 1c; for  $R_{\text{ex}}$  and  $H_{\text{ex}}$  see the table on page 30.

TABLE I

Basic Calculated Data of the APS Reactor

No.	Quantity	Designation in text	Source or formula	Values obtained	
				At start	At end of operating period
1	Multiplication factor: for $T_0 = 420^\circ \text{K}$ ..... for $T_0 = 700^\circ \text{K}$ .....	$k_{\infty}^*$ $k_{\infty}$	(12) (12)	1.394 1.372	— 1.254
2	Resonance escape probability in $\text{U}^{238}$ : for $T_0 = 420^\circ \text{K}$ ..... for $T_0 = 700^\circ \text{K}$ .....	$\varphi$ $\varphi$	exper. est.	0.92 0.908	0.92 0.908
3	Number of secondary neutrons in the thermal energy region: for $T_0 = 420^\circ \text{K}$ ..... for $T_0 = 700^\circ \text{K}$ .....	$\nu$ $\nu$	[5] [5]	2.08 2.08	— 2.06
4	Boundary between slowing-down and thermal spectra (ev): for $T_0 = 420^\circ \text{K}$ ..... for $T_0 = 700^\circ \text{K}$ .....	$E_b$ $E_b$	(17) (17)	0.2 0.35	— 0.35
5	Square of slowing-down length in core ( $\text{cm}^2$ ): for $T_0 = 420^\circ \text{K}$ ..... for $T_0 = 700^\circ \text{K}$ .....	$\tau_T$ $\tau_T$	[2] [2]	254 260	— —
6	Square of diffusion length of thermal neutrons in core ( $\text{cm}^2$ ): for $T_0 = 420^\circ \text{K}$ ..... for $T_0 = 700^\circ \text{K}$ .....	$L_T^2$ $L_T^2$	(2) (2)	70 92	— 89
7	Core dimensions (cm)	$R \times H$	constr.	$77 \times 170$	—
8	Size of equivalent reactor without reflector (cm): for $T_0 = 420^\circ \text{K}$ ..... for $T_0 = 700^\circ \text{K}$ .....	$R_{eq} \times H_{eq}$ $R_{eq} \times H_{eq}$	(23.24) (23.24)	$113 \times 216$ $113 \times 222$	— $113 \times 222$
9	Critical value of multiplication factor: for $T_0 = 420^\circ \text{K}$ ..... for $T_0 = 700^\circ \text{K}$ .....	$k_{\infty}^*$ $k_{\infty}^*$	(14) (14)	1.245 1.256	— 1.254
10	Temperature effect	$\Delta k_t$	(27)	0.028	0.028
11	Reactivity decrease due to $\text{Xe}^{135}$ poisoning	$\Delta k_{\text{pois.}}$	(28)	0.037	0.037
12	Reactivity for depletion and "slagging"	$\Delta k_{\text{res.}}$	(30)	0.057	—
13	Critical mass (number of fuel-bearing channels) $t = 20^\circ \text{C}$	—	calc.	59	—
14	Reactivity equivalent of one rod of inner ring	—	calc.	0.012	—
15	Reactivity equivalent of one rod of outer ring	—	calc.	0.007	—
16	Reactivity equivalent of two safety rods	—	calc.	0.02	—

Note: The values given in this table (and the neutron balance) were obtained by V. I. Orekhov and V. N. Sharapov with consideration of new data on the relation  $\nu(E)/\nu_T$  in the intermediate energy region [5].

### Reactivity and Regulating Rods

As mentioned above the neutron multiplication factor varies with time. This change results from the "burn-up" of  $U^{235}$  due both to fission and transformation into  $U^{238}$ . At the same time there is formation and partial "burn-up" of  $Pu^{239}$ ,  $Pu^{240}$  and  $Pu^{241}$ .

Out of each fissioning nucleus of  $U^{235}$ ,  $Pu^{239}$  and  $Pu^{241}$  two new nuclei are formed which are customarily called fission products. Fission products are as a rule radioactive and thus give rise to series of radioactive transformations. Moreover they possess appreciable neutron absorption cross sections in both the thermal and epithermal regions.

The appearance of these additional "poisonous" absorbers as well as the loss of  $U^{235}$  sooner or later leads to a reduction of the multiplication factor, since the newly formed  $Pu^{239}$  or  $Pu^{241}$  nuclei can compensate the capture by poisons only for a limited time and only when for each burned-up  $U^{235}$  nucleus very close to one nucleus of  $Pu^{239}$  or  $Pu^{241}$  is formed.

We shall not here touch on the conditions for the breeding of fuel, but only note that one of the most important prerequisites for substantial breeding is the absence of any considerable amount of capture by poisons or of neutron leakage.

To satisfy these conditions the reactor must be large ( $\kappa^2 \tau_T \ll 1$ ) and weak neutron absorbers must be used as moderator, coolant and construction materials.

As can be seen from the neutron balance in Figure 2, at the end of a run the principal loss is due to neutron leakage. The remaining losses are attributable to absorption by structural materials.

In building the reactor of the first APS, a number of technical problems had to be solved, the most important of which was the construction of reliable fuel elements. Their reliability could be thoroughly studied in a small reactor with correspondingly low power. As for the use of steel as fragment-proof cladding, this problem could be solved only by successively replacing the steel with other materials such as zirconium, for example. Therefore, as can be seen from the neutron balance, for the first loading of the reactor the amount of plutonium produced in our case does not compensate the loss of  $U^{235}$  and the multiplication factor decreases with time.

In addition, during warm-up, as part of the water is forced from the fuel channels by thermal expansion, neutron leakage increases and the multiplication factor decreases, since resonance capture by  $U^{238}$  is augmented.

From an examination of the change of reactivity with increasing power in the APS reactor beginning at 20° C, the following observations may be made:\*

a) Decreased reactivity results from increased temperature of the medium (neutron gas) and simultaneous expulsion of a portion of the water. This change in the data of the table is called the temperature effect  $\Delta k_t$  which will be expressed in units of  $k_{eff}$ \*\* as follows:

$$\Delta k_t = (k_{eff} - 1)_{t=20^\circ C} - (k_{eff} - 1)_{t=t_{op}} \quad (27)$$

where  $t_{op}$  is the operating temperature of the reactor.

\* It will be recalled that reactor warmup requires much less time than that required to poison the reactor with  $Xe^{135}$ , and that the rise of the power begins when there is no  $Xe^{135}$  in the reactor.

\*\* By  $k_{eff}$  is usually meant the quantity

$$k_{eff} = \frac{k_{\infty} \mu_{inter}}{1 + \alpha^2 L^2 \tau e^{\alpha^2 \tau}} \quad (26)$$

b) Decreased reactivity results from poisoning by  $\text{Xe}^{135}$ :

$$\Delta k_{\text{pois}} = (k_{\text{eff}} - 1)_{t=t_{\text{op}}} - (k_{\text{eff}} - 1)_{t=t_{\text{op}} - \tau} \quad (28)$$

$\tau = 0$   $\tau = 2 \text{ days}$

where  $\tau$  is the time during which the reactor has operated at a certain power  $N$ .

It is easily shown that, other conditions being equal,

$$\frac{\partial^2 \Delta k_{\text{pois}}}{\partial N^2} < 0. \quad (29)$$

c) Continued operation at constant power level leads to a monotonic decrease of reactivity. The residue of the reactivity:

$$\Delta k_{\text{res}} = (k_{\text{eff}} - 1)_{t=t_{\text{op}}} - (k_{\text{eff}} - 1)_{t=T_r} \quad (30)$$

$\tau = 2 \text{ days}$   $\tau = T_r$

where  $T_r$  is the length of the run, compensates the decrease of reactivity resulting from loss of  $\text{U}^{235}$  (allowing for the accumulation of  $\text{Pu}^{239}$  and  $\text{Pu}^{241}$ ) and the accumulation of other fission products.

These two processes are customarily called "slagging" and depletion. The difference

$$\Delta k_{\text{tot}} = (k_{\text{eff}} - 1)_{t=20^\circ\text{C}} - (k_{\text{eff}} - 1)_{t=T_r} \quad (31)$$

$\tau = 0$   $\tau = T_r$

is called the total reactivity, which at the beginning of a run must be compensated either by introducing special absorbers into the reactor or by other means (for example, by artificially increasing neutron leakage).

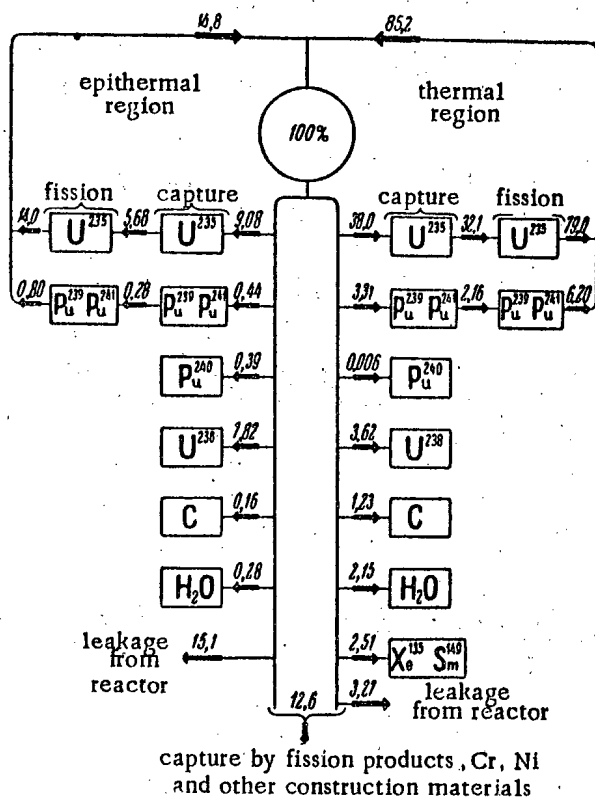


Figure 2. Neutron balance of the APS reactor at the end of a period of vibration.

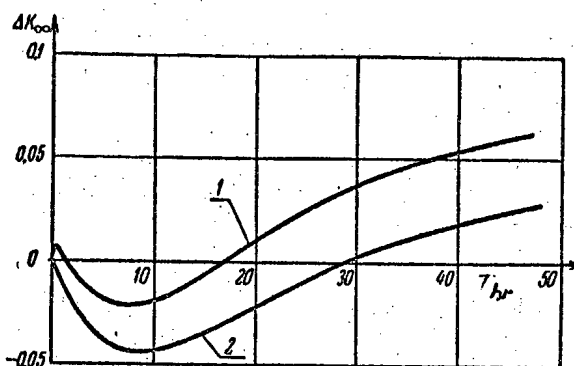


Figure 3. Reactivity change of reactor after shutdown (before shutdown the reactor was operated at rated power). 1) During cooling of the reactor from its operating temperature to  $20^\circ\text{C}$  for 48 hrs; 2) at the operating temperature of the reactor.

From an analysis of the data of Table I (page 30) it may be noted that the calculated value of  $\Delta k_{\text{tot}}$  does not include any compensation of the so-called "xenon buildup", i.e., the reactivity decrease which results from temporary excess of  $\text{Xe}^{135}$  density above its nominal rated amount after shutdown. This is due to the appreciable temperature effect  $\Delta k_t$  possessed by the reactor. Thus if toward the end of a run the reactor is shut down for some reason its rated operating conditions can

be reestablished only after a short period of operation at low power and low coolant temperature. Of course this method cannot be used in those steam power plants which have only one reactor and for which stoppages or operation at a low temperature cannot be permitted. The change of reactivity of the APS reactor due to the change in the quantity of  $\text{Xe}^{135}$  after shutdown is shown in Figure 3.

Boron carbide rods are used in the APS reactor as absorbers.

A calculation of the reactivity equivalent of the rods is, generally speaking, a problem in which it is not legitimate to make direct use of the diffusion approximation since the neutron density close to a strongly absorbing rod suffers a sharp change. However the size of the region in which the diffusion theory approximation cannot be used is small compared with the region of activity of the rod  $\sim (L_T^2 + \tau_T^2)^{1/2}$ . Therefore the diffusion approximation can be used if the boundary condition at the surface of the rod is correctly formulated. For this purpose in designing the APS reactor we used a theory developed by D. F. Zaretskii and D. D. Odintsov (1951) for "gray" rods [4]. On this basis E. Ya. Mikhlin (1952) developed a method of calculating the reactivity equivalent of the rods in a three-group approximation.

### THERMAL CALCULATIONS

The atomic power station operates at high thermal loads. The thermal power output reaches almost 450 kw/kg  $\text{U}^{235}$ . It was therefore necessary to carry out detailed calculations of the temperature conditions under which the individual parts of the reactor were to operate, above all the fuel elements (FE) and the graphite brickwork. These calculations were naturally carried out both for normal operation of the reactor at its nominally rated power and for various unstable conditions and emergencies.

#### Stable Operation

A calculation of FE temperatures during normal operation under stable conditions is not especially difficult and reduces to the solution of the equation for heat conduction with appropriate boundary conditions. The results are given in Figure 4.

In these calculations it was assumed that the generation of heat in the FE is proportional to the thermal neutron flux at a given point of the core. This simplification is entirely permissible since in the APS reactor the number of fissions induced by intermediate neutrons is about 15% of the total number of fissions.

An important characteristic of the heat generation in the reactor is the degree of nonuniformity of heat-source distribution in the core. The so-called nonuniformity coefficients of heat-source distribution along the radius and axis of the reactor are defined as the ratios

$$k_r = \frac{Q_{\max}(r, z_0)}{Q(r, z_0)} \quad \text{and} \quad k_z = \frac{Q_{\max}(r_0, z)}{Q(r_0, z)},$$

where  $Q(r, z)$  is the number of fissions per unit volume of the core, and  $r_0$  and  $z_0$  are fixed values of the coordinates. From these relations it follows that the maximum heat-source density is  $k_v = k_r \cdot k_z$  times greater than the mean heat-source density of the core. As has already been mentioned it was assumed for the APS reactor that

$$k_r = \frac{\Phi_{\max}(r, z_0)}{\Phi(r, z_0)} \quad \text{and} \quad k_z = \frac{\Phi_{\max}(r_0, z)}{\Phi(r_0, z)},$$

$\Phi(r, z)$  is the thermal neutron flux.

The calculations showed that if the control rods do not cause any artificial distortion of the heat source distribution of the core (see, for example, curve 1 in Figure 5) it may be stated that  $k_v \leq 1.6$ . Then the maximum thermal flux in the FE is  $\Phi_{\max} = 1.6 \cdot 10^6$  Cal / m<sup>2</sup> hr.



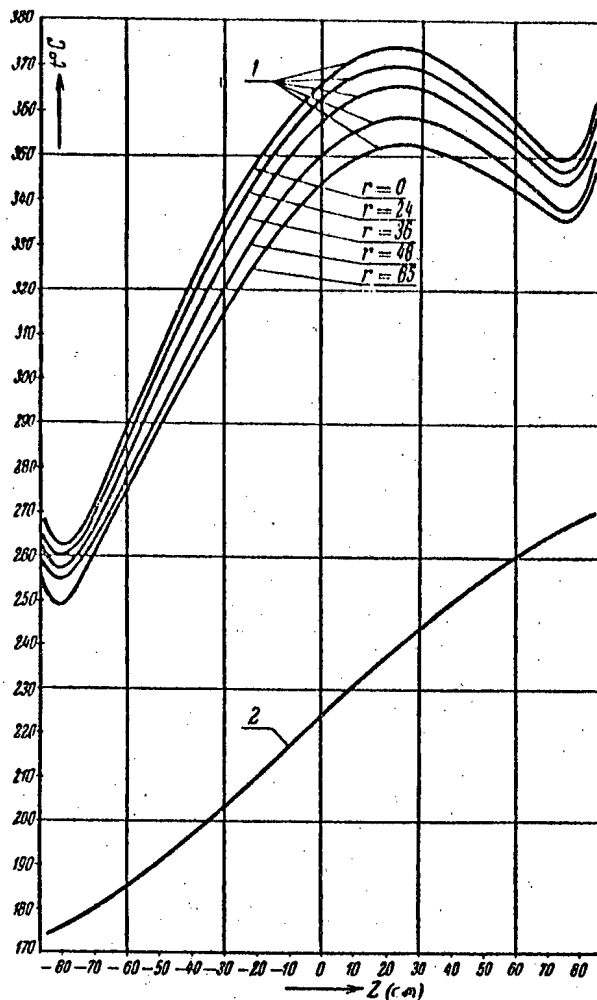


Figure 4. Variation of temperature of fuel elements with height in fuel-bearing channels at nominally rated reactor power ( $N_T = 30,000$  kw).  $r$ (cm) is the distance from the reactor axis to the channel; 1) temperature on outside surface of fuel element; 2) mean temperature of water in fuel elements.

Comparison of the calculated curves  $\Phi(r, z_0)$  and  $\Phi(r_0, z)$  with experimental results showed satisfactory agreement (Figures 5 and 6).

The curves of Figure 4 show that the temperature of the FE for stable operation of the APS reactor at its rated power does not exceed  $370^\circ\text{C}$ . The assumption that this temperature is absolutely safe was later confirmed by experiment and by the actual operation of the atomic power plant.

Another important problem requiring solution was the temperature of the graphite during operation at full power. It was necessary to determine the maximum graphite temperature, as it could limit the power of the reactor, and its average temperature, which was needed to obtain the average energy of thermal neutrons in the reactor.

It should be noted that at the very beginning of these calculations it was necessary to have a clear idea of the degree of accuracy with which it was possible to calculate the temperatures and temperature drops in the graphite blocks. The problem of the generation of heat in the graphite can be solved fairly simply in the first approximation if it is assumed that all energy of the penetrating radiations generated both in fission and in non-fission neutron capture, namely, neutron and gamma ray energy, is

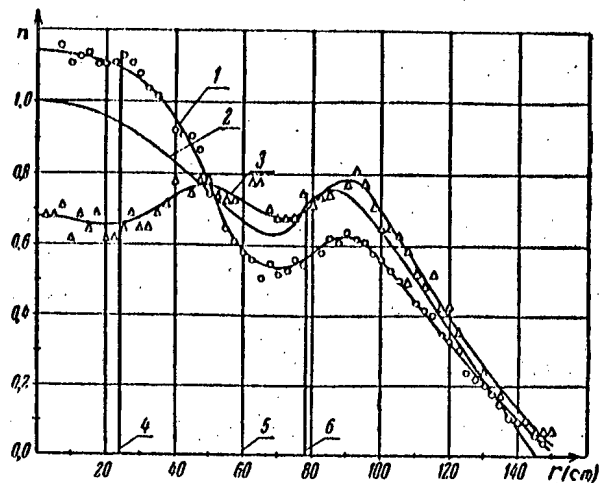


Figure 5. Thermal neutron density as a function of the reactor radius.

1) Experimental curve; control rods of inner ring raised, outer rods lowered; 2) theoretical curve calculated on the assumption that the materials of the control rods are uniformly "distributed"; 3) experimental curve; control rods of outer ring raised, inner rods lowered; 4) control rods (inner ring); 5) control rods (outer ring); 6) core boundary.

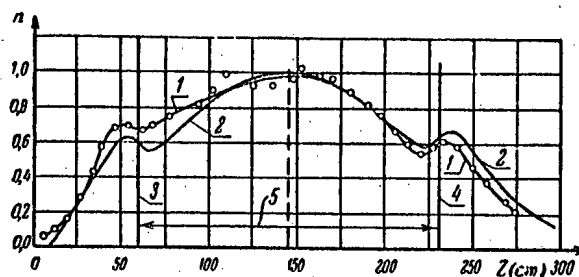


Figure 6. Thermal neutron density as a function of the reactor radius.

1) Experimental curve; control rods of inner ring lowered, outer rods raised inside upper reflector; 2) theoretical curve; materials of control rods uniformly "distributed" in core; 3) lower reflector; 4) upper reflector; 5) core.

released as heat in the same channel where the radiation originated. It will be shown below that such accuracy in determining heat release in the graphite is entirely permissible since there are factors which introduce a very large amount of indeterminacy in graphite temperature calculations.

Inside the fuel cell the fission neutron energy (averaging 5 Mev per fission) can be released both into the graphite and into the water. The energy released in the graphite is determined by the equation

$$\Delta E_b = A \int_{E_T}^{\infty} \frac{[V \xi \rho' \sigma_s(E)]_b q(E)}{[V \xi \rho \sigma_s(E)]_b + [V \xi \rho \sigma_s(E)]_{H_2O}} dE,$$

where  $\xi$  is the mean logarithmic decrement of neutron energy loss;  $V$  is the volume of graphite or water in the cell;  $\rho$  is the density of the nuclei;  $\sigma_s(E)$  is the scattering cross section;  $q(E)$  is the slowing down density;  $q(E)$  is proportional to the power of the reactor;  $A$  is a constant of proportionality; and  $E_T$  is the average thermal neutron energy.

These calculations gave

$$\Delta E_b = 0.85(\Delta E_b + \Delta E_{H_2O}).$$

The total fission neutron energy comprises about 2.5% of the energy released in fission. Thus into the graphite of the APS reactor there is released, due to slowing down of fission neutrons, about 2% of the total energy generated in the core.

In order to determine the fraction of the gamma-ray energy released in the graphite the gamma spectrum of the reactor was approximated by four groups of gamma rays with the energies 1 Mev, 1.5 Mev, 2.5 Mev and 8.0 Mev, corresponding respectively to 30%, 60%, 7% and 3% of the total. The calculations indicated that the energy released in the reactor in the form of gamma radiation comprises 8.5% of the total fission energy, of which about 7% is released in the graphite.

Thus altogether about 9% of the total fission energy is released in the graphite stack. The volume of the graphite per cell of the core lattice is  $0.023 \text{ m}^3$ ; consequently the volumetric heat-release rate in the graphite of the core is

$$q_{vb} = \frac{0.09 \cdot 860 N_F k_v}{0.023 \cdot n_p} \approx 1.3 \cdot 10^6 \text{ kcal/m}^3 \text{ hr},$$

where  $n_p$  is the number of fuel-bearing channels of the APS reactor and  $N_F$  is defined as the total energy which must be liberated per unit time through fission to provide the given thermal power  $N_T$ . The APS reactor was so designed that practically all the heat released in the graphite was utilized. Therefore the difference between  $N_F$  and  $N_T$  will be only the neutrino energy if we neglect leakage of neutrons and gamma radiation from the reactor, i.e.,  $\frac{N_T}{N_F} \approx 0.95$ .

More careful calculations indicated that only 7.5% of the heat was released in the core, and 1.5% outside the core in the reflector and shield due to neutrons and gamma rays escaping from the core; thus  $\frac{N_T}{N_F} \approx 0.93$ .\* However, the leakage of neutrons and gamma radiation takes place principally in the peripheral region of the core. Therefore in the center of the reactor the heat-release rate was changed very little by this correction and was  $q_{vb} = 1.2 \cdot 10^6 \text{ Cal/m}^3 \text{ hr}$ .

The heat source distribution in the graphite is shown in Figure 7 and Figure 8. The curves of  $\Phi(r, z_0)$  and  $\Phi(r_0, z)$  are shown for comparison. After determining the source distribution the graphite tem-

\*The relation  $\frac{N_T}{N_F}$  is a special kind of efficiency factor of the reactor. For the APS reactor the ratio is about 0.93. The ratio can decrease to 0.87 if the reactor does not utilize all the heat liberated in the moderator.

perature was determined directly by solution of the equations of heat conductivity.

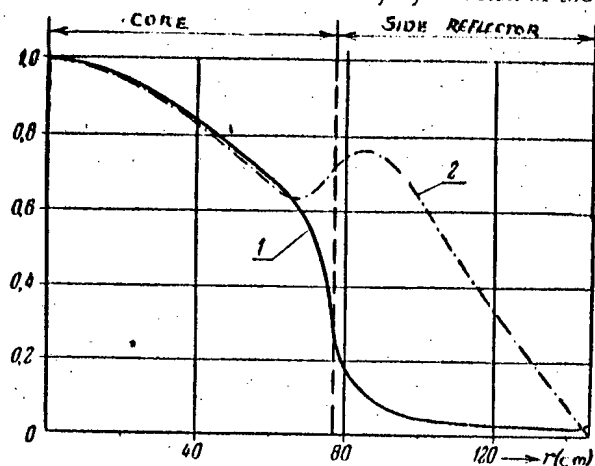


Figure 7. Heat-release rate in the graphite brickwork along the reactor radius.

1) Heat-release in graphite; 2) thermal neutron density.

In order to calculate the graphite temperature in the APS reactor it was quite sufficient to evaluate the heat-release by the above method, since two other factors were the source of a much larger error.

First, there is the gradual change of the properties of graphite in the reactor due to radiation [6], especially the change of thermal conductivity, which is very complicated and is difficult to estimate.

Second, about half of the entire temperature drop between the coolant and the graphite takes place in spaces lying in the path of the thermal flux. Thus, for example, the calculation showed that in the region with the highest heat-release rate about 220° C out of a total drop of 470° C takes place in the gaps. The magnitude of the drop in the spaces can be determined only approximately, since due to the nonconcentricity of the parts and

the allowances for their machining the size of the gaps can vary within wide limits. In addition the thermal conductivity of the helium which fills the gaps may differ from the value used in the calculations since air and water vapor may possibly get into the graphite brickwork.

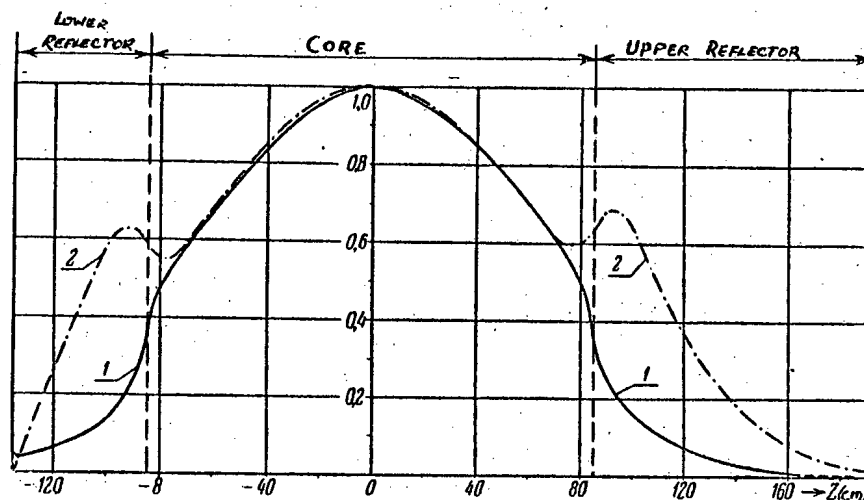


Figure 8. Heat-release rate in the graphite brickwork along the axis of the reactor.

1) Heat-release in graphite; 2) thermal neutron density.

Measurements of the graphite temperature during operation of the reactor showed that the greatest temperature drop between the coolant water and the graphite is 530° C. The difference of 60° C between the calculated and measured values of the temperature drop can be explained fully as being due to the above factors.

In this article we cannot describe in detail the thermal calculations carried out for stable operation of the APS reactor; therefore we now proceed to examine forms of unstable operation and emergency situations in the APS reactor.

### Unstable Operation and Emergency Situations

These questions occupied an important place in the physical and thermal calculations for the reactor. The solutions ensured normal operating conditions of the atomic power station. It was first necessary to clear up questions connected with the change of reactivity during safety action with the resultant change of reactor power, since it was very important to have an idea of the behavior of the APS reactor in all possible emergencies. These calculations were carried out on the basis of the equations of reactor kinetics involving five groups of slowing-down neutrons.\*

The mathematical problem reduced to the solution of a system of six differential equations with variation of coefficients depending on different assumptions regarding time dependence of the reactivity. Figure 9 gives as an example the curve of the drop in power during safety action as obtained theoretically compared with the experimental oscillographic curve recorded at startup of the APS reactor.

The greatest danger for the operation of the APS reactor is the boiling of water in the fuel channels, which could result in vapor lock with substantial reduction of heat removal from the FE as a result of which the FE might overheat and rupture.

In order to understand the behavior of the FE under such conditions we performed laboratory experiments on the hydraulic resistance of the FE as a function of the thermal load for given flow ( $\Delta p = f_1(q)$  with  $G = \text{constant}$ ) and separate experiments to determine the dependence of the resistance on the flow at a given thermal load ( $\Delta p = f_2(G)$  for  $q = \text{constant}$ ).

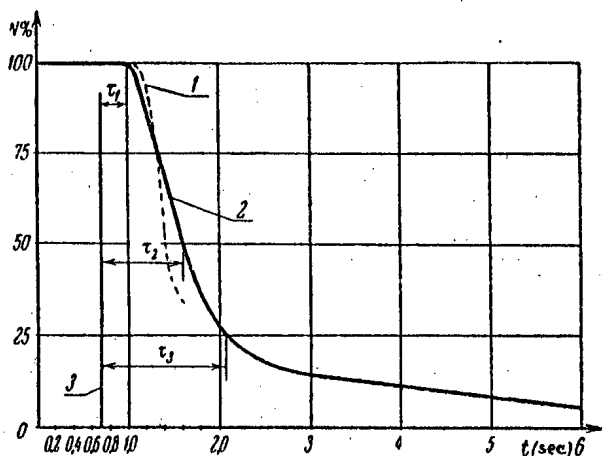


Figure 9. Reactor power as a function of time.

$N$ — power in %;  $\tau_1 = 0.26$  seconds;  $\tau_2 = 0.90$  seconds;  $\tau_3 = 1.36$  seconds.

1) Theoretical curve; 2) experimental curve; 3) danger signal.

water in the fuel channels. An increase of the heat content to  $i'$  or above may result from improper increase of the reactor power or from an interruption of the water circulation. In either case the safety devices will operate. But from the moment when the danger begins until diminished heat generation is established in the FE there is a period called the "period of safety action". This period may be sufficient to enable the FE temperature to exceed the permissible level because of low heat capacity.

As an example we shall determine the rise of FE temperature on the assumption that the reactor power increases by 50% with complete absence of heat removal from the FE and the coolant water. With the heat capacity of the FE material  $c \approx 0.05$  Cal/kg °C the power of the channel of highest capacity  $N = 300$  kw, nonuniformity index of heat release along the reactor axis  $k_2 = 1.25$  and channel weight  $g = 6$  kg,

These experiments showed that at water pressure of  $p = 100$  atm,  $\Delta p = BG^2$  practically, where  $B$  is the proportionality factor over a very wide range of changes in flow and thermal loads. However, this dependence holds only so long as the heat content of the water  $i$  inside the FE is lower than the heat content  $i'$  at saturation temperature. But as soon as the heat content of the water inside the FE reaches a value close to  $i'$  the resistance increases sharply, the circulation of water stops and the FE under thermal load may go out of order.

The rupture of FE must be considered a serious danger causing entrance of fission products into the reactor stack. The similar entrance of molten uranium can also lead to very serious consequences.

We therefore first performed calculations to determine the heat content of the coolant

\* See, for example, [1].

we find that in this channel the rate of temperature rise of the FE reaches

$$v = \frac{1.5 N \cdot 860 \cdot k_z}{3600 \cdot g \cdot c} = 450^\circ \text{C/second.}$$

Since the time required for safety action of the APS reactor is approximately 1 second we may conclude that if the conditions assumed in our example correspond to actuality the temperature of the FE will be inadmissibly high (of the order of  $800^\circ\text{C}$ ) even with safety action. It was therefore necessary to carry out more careful calculations in order to determine the actual operation of the reactor in case of an accident.

In this connection we shall first consider the case of accidental rise of the reactor power due to increased reactivity at constant water flow in the fuel channels, which may result from sudden entrance of a considerable quantity of water into the graphite stack.

The reactivity as a function of the quantity of water in the core of the APS reactor is graphically depicted in Figure 10. The operating point is seen on the left hand branch of the curve. Therefore, with the entrance of an additional quantity of water into the core the reactivity, and thus the power, of the reactor will increase. The change in the quantity of water in the core during warm-up and cooling of the reactor takes place comparatively slowly and does not lead to accidents, since in this case the reactor remains under control of the automatic and manual regulating system. The cause of rapid entrance of water into the stack, leading to rapid rise of reactor power, may be the rupture of a tube in a fuel channel or in a channel of the regulation and safety system.

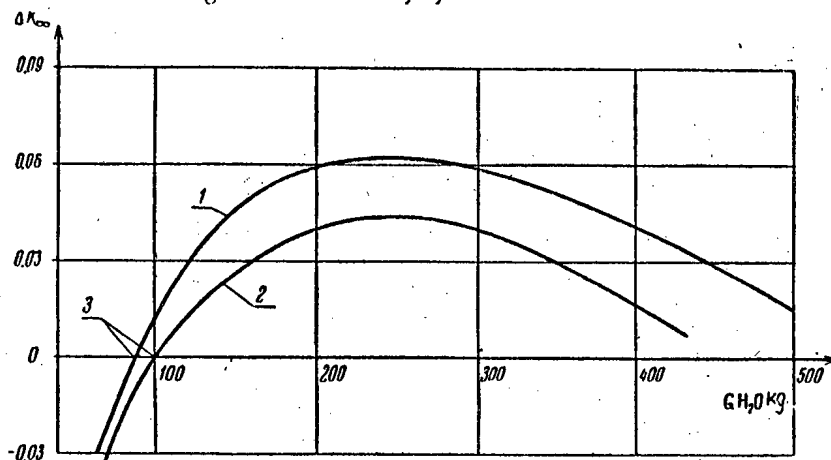


Figure 10. Change of reactivity as a function of the quantity of water in the core.

1) At operating temperature; 2) at  $20^\circ\text{C}$ ; 3) rated quantity of water in the reactor.

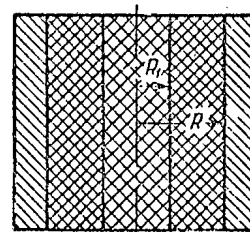


Figure 11. Calculated reactor type with water-filled graphite stack.

In calculating the change of reactivity induced by rapid entrance of water into the graphite stack we considered the most unfavorable case of filling of the gaps of the graphite stack with water, that is, the rupture of

a tube in the center of the core and the spreading of the water from the center to the periphery with no water in the reflector. This problem reduced to the calculation of the reactivity depicted in Figure 11, in which the radius  $R_1$  increases in correspondence with the rate at which the stack fills with water. The reactivity  $\Delta k(t)$  was determined by solution of the equations for nonequilibrium neutron diffusion.

As has been mentioned above it was assumed that the power of the reactor is directly proportional to the thermal neutron flux. The change of thermal neutron flux as the stack was filled with water, with simultaneous safety action, was obtained from the solution of the kinetic equations of the reactor with five groups of slowing-down neutrons. Figure 12 gives the calculated curves of the change of reactor power with the stack filling with water at rates from 5.0 to 10 liter/sec.

As the power of the reactor changed as a function of time with constant water flow  $G_c$  in the fuel channels, the heat content of the water in a channel at height  $z$  and time  $t$  was calculated from the

equation

$$i(z,t) = i(z, 0) + \frac{1}{G_c} \int_{z-Wt}^z q_l(x, 0) f(t') dx,$$

where  $q_l(x, 0)$  is the quantity of heat transferred to the water per unit length of the fuel channel at time  $t = 0$ ;  $f(t')$  is the function representing the change of power with time normalized to unit at  $t' = 0$ ;  $t' = t - \frac{z-x}{W}$

is the time required for transference of water in the channel from point  $(z - Wt)$  to point  $x$ ; and  $W$  is the rate of flow of water in the channel.

The water delivery  $G_c$  can be considered constant and equal to the flow through the corresponding channel under stable operation of the reactor, since the rupture of tubes in one channel has practically no effect on other channels. The formula given does not take into account the change of the heat content of the material of the FE, i.e., it gives the maximum possible increase of the heat content of the water.

The change with time of the heat content of the water at the outlet of the channel of highest thermal power (the central channel) at different rates of filling of the core with water is given in Figure 12.

In order to forestall the possibility of the entrance of a large quantity of water into the graphite stack each channel is provided with a device which cuts off the channel in case of rupture of any tube within it.

Laboratory experiments showed that the maximum rate of flow of water into the stack following the rupture of a FE tube did not exceed 2.0 l/sec even if the devices shutting off the water flow did not operate. Therefore on the basis of the data in Figure 12 it may be assumed that the rupture of a fuel channel tube does not result in boiling of the water in other channels and thus to the disruption of the heat-removal from the FE. For this reason, as indicated by the calculations, the temperature rise of the FE is insignificant and does not reach a dangerous level. It must be added that the calculated increase of reactivity due to water in the stack was somewhat too high in comparison with the results of experiments.

We now consider the case of decreased water flow in the fuel channels at constant reactor power. A drop in the flow rate can take place in all channels simultaneously with accidental switching off of the principal circulating pumps. When the pumps are shut off the water circulation in the fuel channels does not halt immediately, but continues for some time due to the inertia of the coupled pump and electric motor rotors as well as because of the inertia of the water itself. However, this circulation stops very soon, so that the cooling of the FE quickly stops if there is no provision for automatic switching of the pumps to an emergency source of electric power. At the same time the heat release of the FE cannot stop instantaneously even with the operation of emergency shielding since, firstly, fission due to slowing-down neutrons continues for some time and, secondly, there is a continuation of the release of energy from the decay of radioactive fission products. Therefore it would be necessary to determine the speed with which the pumps are switched to the emergency power source.

Considering the small thermal inertia of the FE in the APS reactor we may assert the following: If the relative change of flow rate  $\frac{G_0 - G(t)}{G_0}$  of the water through the fuel channels (at any instant after the pump power is cut off) does not become larger than the corresponding relative change in the power  $\frac{N_0 - N(t)}{N_0}$ , the heat removal from the FE is not disturbed. Actually in this case at any instant the heat transfer coefficient  $\alpha(t)$  (from the FE walls to the water) will depend practically only on the flow rate in the fuel channels, i.e., on the magnitude of the flow rate at time  $t$ , namely  $\alpha(t) \sim [G(t)]^{0.8}$ . Therefore, in order to answer the question as to just when, following the switching off of the pumps, the overheating of the FE begins, we compared the curves of  $\frac{G(t)}{G_0}$  and  $\frac{N(t)}{N_0}$  obtained theoretically.

The reactor power as a function of time under safety action was determined from the formula

$$N(t) = \frac{\Phi(t)}{\Phi_0} (N_0 - N_{0\text{frag.}}) + N_{\text{frag.}}(t),$$

where  $N_{0frag}(t)$  is the thermal power of the FE due to the decay of the radioactive fission products;  $N_{0frag} = N_{frag}(0)$ ;  $\Phi(t)$  is the thermal neutron flux,  $\Phi_0 = \Phi(0)$ . The change of flow rate as a function of time was determined from the equation of the conservation of energy of the circulating circuit with pump power shut off. This equation can be written as follows:

$$\frac{d}{dt} \left[ \frac{I \omega^2(t)}{2} \right] - \frac{dE(t)}{dt} - T \omega^3(t) - \frac{\Delta p(t) G(t)}{\gamma} = 0,$$

where the first term characterizes the change of kinetic energy of the motor and pump rotors as a function of time; the second term is the change of kinetic energy of the water in the circuit; the third term is the work dissipated in overcoming friction (in bearings, etc.) affecting the rotation of the motor and pump rotors; and finally, the fourth term is the work of circulating the water through the circuit. This equation was solved on the basis of the assumption that the kinetic energy of the water  $E(t)$  and the pressure losses  $\Delta p(t)$  are proportional to  $G^2(t)$ , i.e.,  $E(t) = A G^2$ ,  $\Delta p(t) = B G^2$ , and that  $G(t) = c \omega(t)$ , where  $\omega(t)$  is the rotational speed of the pumps.

In this case the solution is given by

$$\frac{G(t)}{G_0} = \frac{\exp \left[ -\frac{T}{I - 2Ac^3} t \right]}{1 + \frac{Bc^2}{T\gamma} G_0 \left[ 1 - \exp \left( -\frac{T}{I + 2Ac^3} t \right) \right]}$$

The automatic system was so designed that switching of the pumps to the emergency power supply took place within 4 seconds after cutting off of the main power supply. The calculations showed that this insures complete safety of operation. This is very clear from the comparison of the curves for  $\frac{N(t)}{N_0}$  and  $\frac{G(t)}{G_0}$  in Figure 13. For comparison, experimental curves are given for the change of water flow rate and rotational speed of the pump rotors following the cutting off of the electric power. It can be seen that the agreement of the calculation and experiment is quite satisfactory, especially immediately after the power supply is cut off.

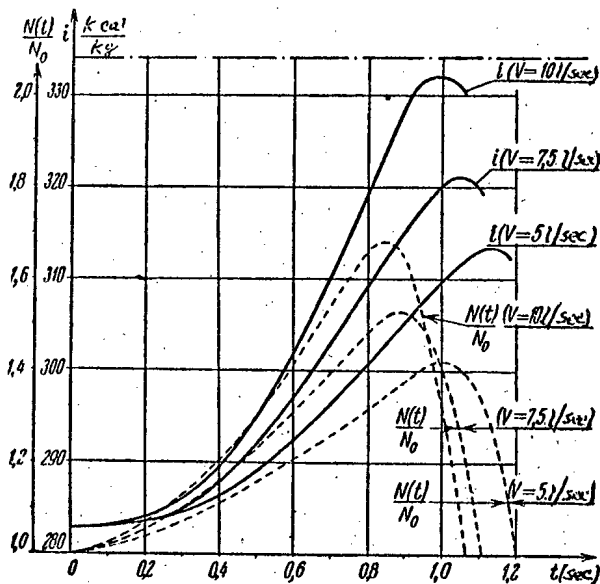


Figure 12. Relative change of reactor power  $\frac{N(t)}{N_0}$  and heat content of water  $i$  at outlet of central channel as the graphite stack was filled with water at rate  $V$  with simultaneous safety action.

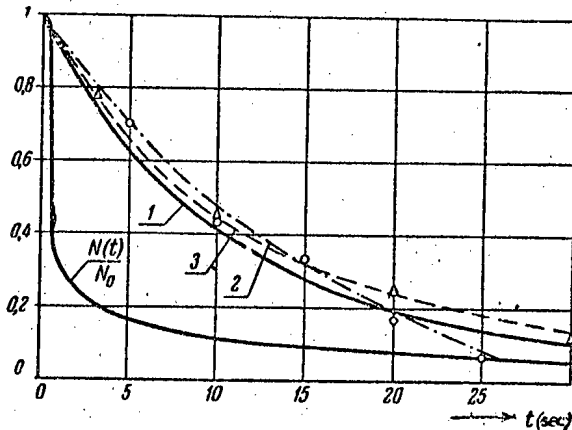


Figure 13. Change of water flow rate  $\frac{G(t)}{G_0}$ , pump rotation speed  $\frac{\omega(t)}{\omega_0}$  and reactor power  $\frac{N(t)}{N_0}$  following cutting off of circulating pump power supply.

- 1) Theoretical curve of change of flow rate and rotational speed of pump rotor  $\frac{G(t)}{G_0} = \frac{\omega(t)}{\omega_0}$ ;
- 2) experimental curve of change of flow rate  $\frac{G(t)}{G_0}$ ;
- 3) experimental curve of rotational speed of pump rotor  $\frac{\omega(t)}{\omega_0}$ .

We note in conclusion that the scope of the physical and thermal calculations is far from being exhausted by the problems touched upon in this article, as the final choice of the reactor type can be made only from a comparison of calculated results for many types which differ in the design of individual elements, and the design in turn is determined by the technological and chemical possibilities of developing fuel elements, etc.

The following participated in the physical and thermal calculations for the reactor of the Academy of Sciences atomic power station: P. I. Aleshchenkov, Yu. V. Arkhangel'skii, D.F. Zaretskii, G. I. Marchuk, P. E. Nemirovskii, S.M. Feinberg and others.

The greater part of the computations was performed by Z.M. Kurova, V.M. Skripova and S. I. Shagalina.

#### LITERATURE CITED

- [1] S. Glasstone and M. C. Edlund, The Elements of Nuclear Reactor Theory, For. Lit. Press, Moscow, 1954.
- [2] D. Hughes, Neutron Studies for Nuclear Reactors, For. Lit. Press, 1954.
- [3] K. D. Tolstov, F. L. Shapiro and I. V. Shtranikh, Average Neutron Velocities in Various Media. Report at the Conference of the Academy of Sciences of the USSR on the Peaceful Uses of Atomic Energy July 1-5, 1955. (Session of the Section of Physico-Mathematical Sciences). USSR Acad. Sci. Press, 1955.
- [4] D. F. Zaretskii and D. D. Odintsov, Effective Boundary Conditions for "Gray Bodies". Report of the Soviet Delegation at the International Conference on the Peaceful Uses of Atomic Energy on "Reactor Design and Theory". USSR Acad. Sci. Press, 1955, p. 279.
- [5] B. G. Erozolimskii, Measurements of the Effective Number of Secondary Neutrons from  $U^{235}$ ,  $U^{235}$  and  $Pu^{239}$  for Primary Neutrons in the Energy Range from 0.3 to 100 ev. Report at the Conference of the Academy of Sciences of the USSR on the Peaceful Uses of Atomic Energy. (Session of the Section of Physico-Mathematical Sciences). USSR Acad. Sci. Press, 1955, p. 369.
- [6] V. I. Klímenkov and Yu. N. Aleksenko, Change in the Properties of Graphite Irradiated by Neutrons. Report at the Conference of the Academy of Sciences of the USSR on the Peaceful Uses of Atomic Energy July 1-5, 1955 (Session of the Section of Physico - Mathematical Sciences). USSR Acad. Sci. Press, 1955, p. 322.



# A STUDY OF THE IODIDE PROCESS OF REFINING ZIRCONIUM

## FACTORS THAT AFFECT THE RAPIDITY OF THE REFINING PROCESS

V. S. Emel'yanov, N. D. Bystrov and A. I. Evstyukhin

### INTRODUCTION

During the time that the iodide method of refining zirconium has been in existence investigators have accumulated a considerable amount of experimental data. Nevertheless there has thus far been no reliable information about certain very important theoretical and practical aspects of the refining process. The data of different investigators are not always in agreement and sometimes are flatly contradictory.

At the same time it is quite obvious that further progress in the utilization of the iodide process depends to a considerable degree on the correctness of our understanding of the nature of the basic phenomena in the refining process. It is the purpose of the present work, which was carried out at the Moscow Institute of Engineering Physics from 1954 to 1955, to investigate certain practically important but still insufficiently studied aspects of the process. The basic problem, on the solution of which almost the entire investigation was essentially dependent, was a clarification of the effect of the temperature of the reaction apparatus on the rate of the process. For this purpose we obtained new experimental data concerning the dependence of the process rate on technological factors and also investigated the lower zirconium iodides. The data of this last investigation and the general conclusions of the entire investigation will be presented in another article.

### EXPERIMENTAL

All of the experiments were performed with a glass or quartz vessel of small size; this enabled us to establish sufficiently reliable thermostatic control, to measure the filament temperature with an optical pyrometer and to perform direct visual observation of the course of the process.

An overall view and representative dimensions of the reaction vessel are shown in Figure 1. As a rule three electrodes of 2 mm molybdenum wire were sealed in the tube. These enabled us to use two

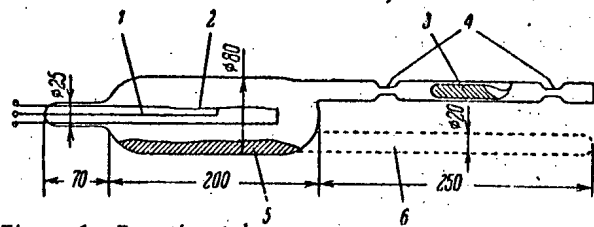


Figure 1. Reaction tube.

1) Molybdenum wire of 2 mm diameter; 2) tungsten wire filament (0.1 mm); 3) ampoule containing iodine; 4) seals; 5) raw metal; 6) auxiliary tube.

tungsten wires for deposition of zirconium and to carry out two experiments without reloading the tube. The zirconium was deposited on a tungsten wire of 0.1 mm. diameter and about 60 mm long. The final diameter usually did not exceed 1 mm since with a greater thickness of the heated wire its thermal radiation seriously affected the temperature aspect of the process.

The tube was heated in an electric resistance furnace supplied with a thermoregulator. The temperature of the vessel or of its individual parts was measured with a platinum-platinum rhodium thermocouple.

• Part I.

The filament temperature was measured with an OPPIR-09 optical pyrometer. The correction for absorption in the glass and in the tetraiodide vapor was found experimentally. For this purpose an additional wire was placed in the vessel and heated by a current (the platinum or zirconium wire was sealed in a glass ampoule to avoid oxidation). By measuring the temperature of this wire once inside the vessel and again at the end of the furnace, i.e., after passing out of the tube, we obtained a correction for absorption in the double thickness of glass and in a layer of tetraiodide vapor whose thickness was equal to the diameter of the tube. It was found that absorption in the tetraiodide vapor is low enough to be neglected. But absorption by the glass required corrections from 10 to 30–40° C, depending on the transparency of the vessel's walls.

The tube was evacuated to  $10^{-4}$  mm Hg while heated to a temperature which exceeded the maximum temperature during the experiment by 50–60° C.

Pure resublimed iodine (in some cases iodide) was introduced in a previously prepared sealed ampoule with a fine tip (see Figure 1). After the evacuation and sealing off of the vacuum system the tip of the ampoule could be broken by shaking the tube.

As raw metal we used calcined zirconium powder (–200 mesh) as well as the iodide (in the form of bars or chips).

### Dependence of the rate of the process on the filament temperature

De Boer and Fast [1] found that zirconium is deposited on the filament most rapidly when the latter is at a high filament temperature. A similar result was obtained by Doring and Mollere [2] who observed that the temperature dependence of the process rate up to 1500° C is expressed by

$$\log \alpha = \text{constant} - \frac{Q_A}{RT_D}$$

where  $T_D$  is the filament temperature;  $R$  is the gas constant; and  $Q_A$  is a certain parameter which the authors called the activation energy.

On the other hand Rainor [3] states that as low as 1200–1300° C the zirconium deposition rate becomes essentially constant.

The most valuable data from a practical point of view is that of Shapiro [4]. According to this data the process rate under industrial conditions depends to a considerable extent on the filament temperature up to 1400° C. Further temperature increase is accompanied by a smaller increase of the zirconium deposition rate and at about 1450° C the rate ceases to increase when the filament temperature is raised.

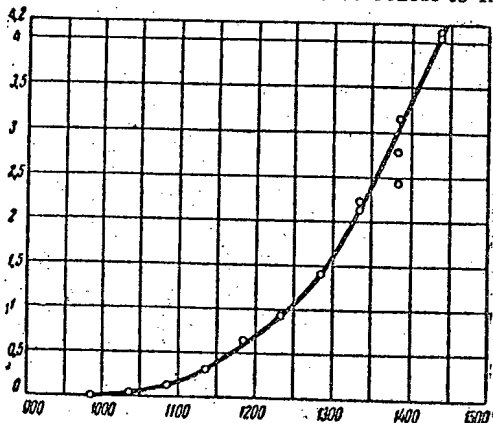


Figure 2. Dependence of the rate of the process on the temperature of the filament.

Ordinates: rate of filament growth  $\frac{\Delta d}{\Delta t} \cdot \frac{\text{mm}}{\text{hr}}$

Abscissas: filament temperature  $t^{\circ}\text{C}$

In order to investigate this temperature dependence we loaded the tube with 30 g of zirconium rods and 1–2 g of iodine. The temperature of the tube was maintained at a constant (260° C). The experimental curve in Figure 2 shows that under such conditions the rate of the process depends strongly on the filament temperature up to 1435° C.

Thus all the available data (with the exception of Rainor's) indicates that in the operating range (1200–1400° C) the rate of the process depends very strongly on the filament temperature.

For practical purposes this question may evidently be considered settled. But the theoretical explanation is still unsatisfactory. This refers in particular to Shapiro's explanation of the curve above 1400° C. Shapiro considers the bending of the curve to be caused by the fact that the iodine partial pressure near the filament ceases to rise with the temperature above 1450° C, which he explains by the fact that above

1400 °C the increase of the tetraiodide dissociation equilibrium constant becomes very slow. Indeed, at such temperatures the equilibrium constant of the tetraiodide increases very much more slowly than, let us say, at about 1200 °C. However, a calculation shows that its increase is still sufficiently rapid to ensure a considerable rise of the process rate even at temperatures above 1450 °C.

We consider the basic cause to be not the change of the equilibrium constant but the fact that the iodine pressure near the filament cannot increase without limit even when the equilibrium constant continues to change rapidly. In fact, the equilibrium pressures of iodine and zirconium tetraiodide near the filament must always satisfy the approximate relationship

$$P_I + P_{ZrI_4} = P_{tot.}$$

The total pressure in the tube is a function of the tube temperature alone and is independent of the filament temperature (since at the surface of the raw metal  $P_I \approx 0$ ). Thus no matter how large a value the equilibrium constant may assume the equilibrium pressure of the iodine cannot exceed  $P_{tot.}$

As the equilibrium constant changes the iodine pressure near the filament will change very rapidly only when it is of the same order of magnitude as the pressure of the tetraiodide.

After the iodine pressure becomes many times larger than the tetraiodide pressure, a further change of the equilibrium constant will indicate essentially only a change of the ratio of iodine and tetraiodide pressures. The absolute value of the iodine pressure will change extremely little. Consequently the process rate ceases to increase as the filament temperature rises independently of the rate of change of the equilibrium constant.

We note in conclusion that according to our experimental data at a tetraiodide pressure on the surface of the filament of about 0.35 mm the equilibrium pressure of iodine at 1300 °C would actually be very close to the tetraiodide pressure, with a value of about 0.4 mm. In full agreement with the above it was shown by experiment, as we have seen, that the process rate at this temperature is very sensitive to the change of the latter.

Rainor's data can be explained by the fact that he evidently conducted his investigation at a very low pressure of the tetraiodide. In this case according to the data of Holden and Kopelman [7] at 1300 °C almost every molecule of the tetraiodide which reaches the heated filament surface is decomposed. Any further increase of the filament temperature under these conditions could not be accompanied by a significant increase in the rate of zirconium deposition. Unfortunately the extreme indefiniteness of Rainor's data does not permit us to draw any more definite conclusions.

#### Dependence of the rate of the process on the quantity of iodine

Shapiro reports [4] that the rate of the refining process is independent of the amount of iodine in the reaction tube. However, according to his data for small amounts of iodine, after a small interval of time the process begins to slow down strongly. The greater the initial amount of iodine, the longer the process continues at its normal rate. Shapiro attributes this slowing down to the formation of nonvolatile lower iodides.

According to Rainor's data [3], however, the process rate depends on the amount of iodine; the optimum rate is observed with a very large amount of iodine— about 82.5 g per liter of tube volume or 53 g per kg. of sponge zirconium.

Both authors investigated this variation with large amounts of iodine as the most important practical case. But we have also paid special attention to the small quantity range.

The very first experiments showed that with very small quantities of iodine (3–5 mg per 50 g of Zr shavings) the process damps down rapidly, evidently as a result of the binding of the iodine in lower iodides. Therefore for this series of experiments we used as raw materials, not shavings, but iodide rods, which have a much smaller surface (rod diameter 2–3 mm and total weight about 100 g).

The process was conducted at a filament temperature of 1300 °C and tube temperature of 300 °C.

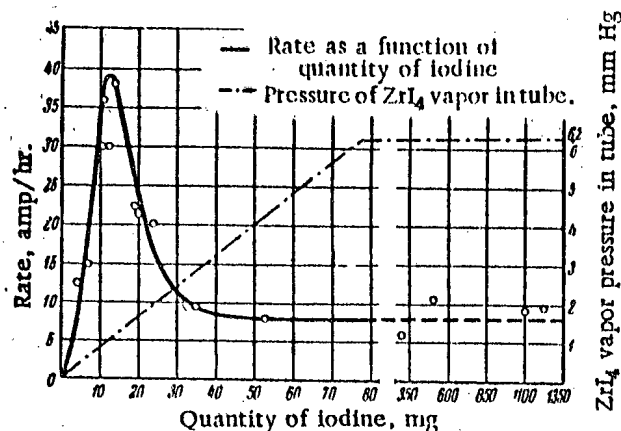


Figure 3. Dependence of process rate on quantity of iodine.

The data on the tetraiodide vapor pressure was calculated from the Clapeyron equation and is quite approximate (most likely too high) since the calculations did not take into account the presence of the heated filament nor the possibility of iodine binding in lower iodides.

The experiments showed that the rate of the process really depends on the quantity of iodine, and that the optimum rate is observed with negligibly small quantities of iodine—about 12 mg per liter of tube volume. The corresponding tetraiodide vapor pressure is much lower than the saturated vapor pressure at 300°C. It follows that the tetraiodide vapor pressure has a very great effect on the process rate.

With large quantities of iodine, when the pressure in the tube corresponds to the pressure of saturated tetraiodide vapor and thus is independent of the quantity of iodine, the process rate becomes constant. Comparatively small fluctuations are due to random fluctuations of other conditions of the experiment. This result is in complete agreement with Shapiro's data.

The only explanation of Rainor's data may be that almost all the iodine which he put into the reaction tube was bound in a nonvolatile lower iodide at the very start and could not participate in the transfer process. Consequently the actual amount of iodine in the gas phase was thousands of times smaller than the amount mentioned by the author in his article. The basis for such an assumption is the fact that Rainor carried out his experiments at a high tube temperature (460°C) and used sponge zirconium, i.e., a form of the metal with a very large surface. Under these conditions, as we shall see below, the formation of the lower iodide proceeds very rapidly.

As the most accurate verification of the above relationship, we carried out an experiment in which the tetraiodide pressure in the tube was produced by another method.

#### Process rate as a function of the tetraiodide vapor pressure in the reaction tube

For this run we used the same vessel as before but with an additional tubular section which served to produce the required tetraiodide pressure. In Figure 1 this additional section is represented by a dotted outline. The tube was loaded with 30 g of zirconium chips and 1 g of iodine. The tube was placed in a furnace in such a way that 70–80 mm of the added tubular section protruded. This latter was surrounded by a furnace which was regulated by a separate autotransformer.

In this run the tube was kept at a constant temperature of 300°C. The end of the added section was at a lower temperature, so that all excess tetraiodide condensed in it. By changing the temperature of the added section we were able to produce the required tetraiodide vapor pressure in the reaction tube. Figure 4 shows the curve obtained in this way for the process rate as a function of the tetraiodide vapor pressure. Actually the figure does not give the tetraiodide vapor pressure, but the temperature of the condensed tetraiodide. This was done in order to give the graphical representation of the relationship a form which is more conveniently compared with the results which follow below.

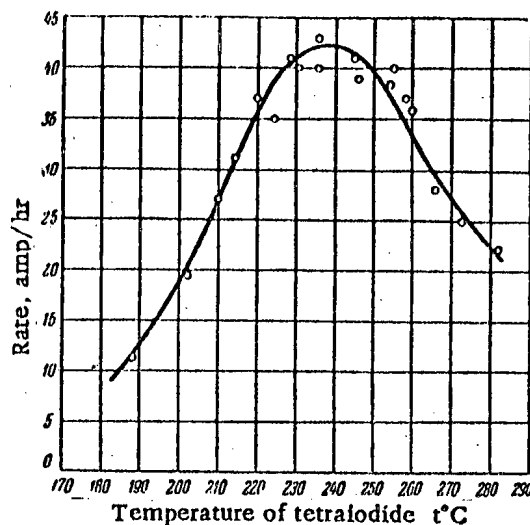


Figure 4. The process rate as a function of the tetraiodide vapor pressure.

The maximum rate of zirconium deposition is observed at the temperature 235–240 °C of the solid tetraiodide, which corresponds to a tetraiodide vapor pressure of about  $2-2.5 \cdot 10^{-1}$  mm Hg. But this is a very approximate value since it was calculated from the approximate equation for the zirconium tetraiodide vapor pressure given by Rahlfs and Fisher [5]:

$$\log P \text{ (mm)} = - \frac{29500}{4.57 \cdot T} + 12.05.$$

A comparison of our curve giving the process rate as a function of the tetraiodide vapor pressure with the curves showing the dependence on the tube temperature in the article of Doring and Moliere [2] shows the maximum rate in both instances appearing at the same temperature. This suggests that in the experiments of Doring and Moliere the decisive factor affecting the rate of the process was not the tube temperature (the temperature of the raw metal), as Doring and Moliere supposed, but the tetraiodide vapor pressure. In order to check this, we obtained the usual curve for the temperature dependence of the rate, as well as the dependence on the temperature of the raw metal at constant tube pressure.

#### Process rate as a function of the temperature in the reaction tube

The clarification of this relationship was a very difficult task which was further complicated by the fact that the data of different investigators on this problem were very contradictory and could not be generalized.

Fast [6] found that the rate increases rapidly as the temperature of the tube rises to 250 °C, reaches a maximum at approximately 300 °C and with further increase of the temperature to 500 °C declines very slowly. Fast relates this diminishing of the rate to the formation of lower zirconium iodides on the raw metal surface by the reactions



Doring and Moliere [2] found that this relationship has a sharp peak at tube temperature 230–250 °C. At higher temperatures the rate diminishes to very low values and then at about 420 °C begins to increase again. Doring and Moliere believe that the decline in the rate above 250 °C is due to the formation of the triiodide on the surface of the raw metal, as a result of which the zirconium is screened by a layer of the lower iodide and its iodization is impeded. As a result there is high partial pressure in the tube for the reaction



which blocks decomposition on the filament.

The further rise of the process rate above 420 °C is explained by the same authors as due to the decomposition of the triiodide, following which the raw metal again can be reached by iodine molecules.

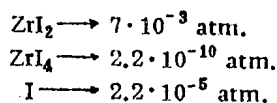
Rainor found that the optimum rate is observed at a raw metal temperature of about 560 °C. Moreover, it was found that the position of the maximum depends on the quantity of iodine used for the process; this provided a basis for the supposition that the pressure greatly influences the rate. In this connection Rainor assumes that the rate rises with increased tetraiodide pressure to a certain "critical dissociation pressure" after which, as the pressure increases, the rate drops rapidly due to increased pressure of free iodine, which inhibits decomposition on the filament.

Shapiro [4] reports that the maximum process rate under industrial conditions is observed at a reaction tube temperature of about 265 °C. On the basis of the fact that the raw metal in the tube has a temperature which is dependent on its proximity to the heated wires, Shapiro believes that the process rate is determined not by the temperature of the raw metal but by the pressure inside the tube.

On the basis of published thermodynamic data, Shapiro carried out some thermodynamic calculations which led him to conclude that at equilibrium the principal components of the gas phase is zirconium iodide and that the process rate is determined by the vapor pressure of this compound.

He notes, however, that his thermodynamic analysis does not explain the experimental curves for the dependence of the refining process rate on the tube temperature. In addition, Shapiro acknowledges that the diiodide really appears to play a much smaller part since the rate of transition of the zirconium tetraiodide to the diiodide is small (especially at low temperatures).

We consider it necessary to note that the special weakness of Shapiro's thermodynamic analysis does not appear to us to be the fact that he did not take into consideration the kinetics of the diiodide formation but that he used data which was too inaccurate. Thus Shapiro calculated in particular that under certain conditions the partial pressures of the components near the surface of the filament (at 1400°C) would be:



This result is in complete disagreement with the experimental data with which we are familiar.

Let us consider the following case: let the tube temperature be somewhat below 300°C so that the tetraiodide pressure in it is  $7 \cdot 10^{-3}$  atm (there is an excess of the solid tetraiodide). The filament is still fairly thin and its radiation is low; the metal temperature in this case will be practically the same as that of the tube. Under these conditions the pressure of the iodine and of the diiodide near the raw metal will be negligible and the vapor phase consists almost entirely of the tetraiodide at  $7 \cdot 10^{-3}$  atm. The vapor pressure near the filament would have to be the same. According to Shapiro the diiodide should predominate in the vapor phase at the filament surface at 1400°C. But this would mean that instead of growing, the filament would be dissolved. However, we know that under the above conditions the process operates normally. As will be shown in another article, we have observed this dissolving of the filament, but under entirely different conditions.

We investigated the above dependence in a glass tube (to 450°C) and in a quartz tube (above 450°C); the impure metal was in the form of shavings. The filament temperature was 1300°C. The different dimensions of the two tubes and the difference in the quantity of reacting material resulted, as can be seen from Figure 5, in some difference in the absolute rate. But we are interested in the overall dependence of the process rate on the tube temperature and not in the absolute magnitude. The low-temperature portion of our curve is in good agreement with the data of Doring and Molire. The high-temperature part differs strongly from the data of these investigators, to wit: in our experiments no rate increase was observed above 420°C. We shall return to a discussion of this fact below.

In order to prove that in the experiments described above the factor determining the process rate was the tetraiodide pressure and not the temperature of the impure metal, we ran an experiment in which we used a vessel with an added tubular section whose end was kept at 230°C throughout the experiment (this temperature corresponds, according to the above discussion, to close to the optimum tetraiodide vapor pressure). The temperature of the reaction tube (and consequently of the impure metal) varied from 235°C to 700°C.

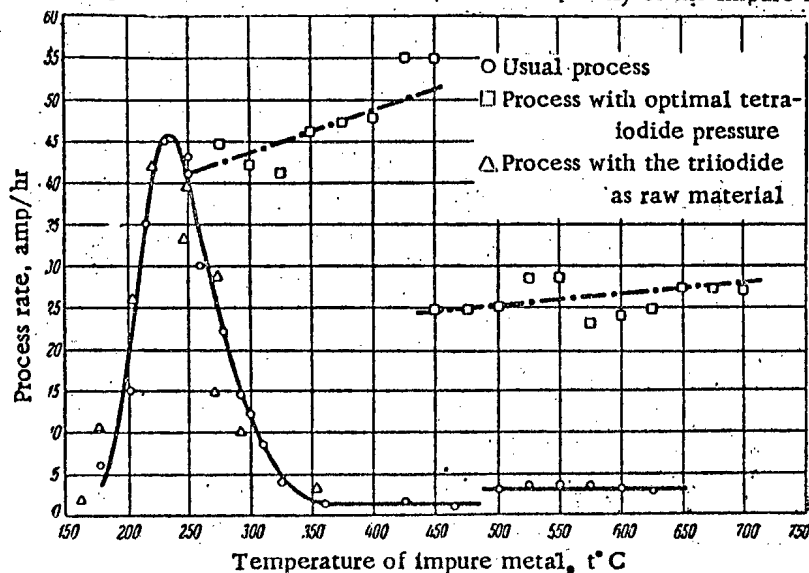


Figure 5. Process rate as a function of tube temperature. (The nature of the experiments using the triiodide as raw material will be explained in another article).

Above 450°C the experiment was again conducted in a quartz tube, which again resulted in a sharp change of the rate (see Figure 5).

These experiments led to a very interesting result: when the optimum pressure was maintained in the tube, the rate of zirconium deposition on the filament did not decrease as the temperature of the impure metal changed up to 700°C.

Thus we have shown very clearly and graphically that the factor which determines the rate of the refining process is not the temperature of the metal but the vapor pressure of the tetraiodide in the reaction tube.

This result may be of great practical value. In fact if it holds for large industrial apparatus we shall have a reliable means of ensuring and maintaining an optimum process. For this purpose it would only be necessary to equip the reaction apparatus with the necessary devices for producing and measuring the required pressure.

### Nature of the second maximum of the refining process rate

It was mentioned above that Doring and Moliere [2] observed a further increase in the process rate at tube temperatures above 420°C. Their experiments also suggested that the mechanism of zirconium transfer at high temperatures is the same as at the usual low temperatures. Doring and Moliere relate the second rise of the process rate to the destruction of the thick passivating film on the surface of the raw metal (in connection with the disappearance of the triiodide) and also with the increased number of tetraiodide molecules in the gas phase (due to dissociation of the lower iodides).

However, our experiments provide a basis for another explanation of this phenomenon. In fact, we have established that the process rate is determined by the tetraiodide vapor pressure in the tube. Accordingly, above 230 – 250 °C the process rate drops sharply as the pressure rises. This explains the first maximum of the rate.

With further increase of the tube temperature, two cases are possible:

1. If the raw metal has a large surface area and is present in a sufficiently large quantity (a powder in the experiments of Doring and Moliere), there will be a rapid conversion of the zirconium tetraiodide to a lower iodide, accompanied by a drop of the tetraiodide vapor pressure in the reaction tube. Under certain conditions (a large quantity of raw metal, high temperature, a fairly long period at the high temperature) the tetraiodide may be completely converted to the lower iodide. Then the tetraiodide vapor pressure in the tube will be determined by the dissociation pressure of the lower iodide. We should observe a new maximum process rate at the temperature at which the dissociation pressure of the lower iodide is equal to the optimum tetraiodide vapor pressure.

2. If the raw metal has small surface area and there is a small quantity of it (the zirconium shavings in our experiments), there cannot be a complete conversion of the tetraiodide during the course of the experiment, and, in addition to the lower iodide, the tube will contain a considerable amount of the tetraiodide. As a result, the pressure in the tube remains high and the process rate remains low. This is just what took place in our experiments.

Thus, according to the above, with regard to the mechanism of zirconium deposition both maxima of the process rate are identical. The only difference lies in the fact that at low temperatures the tetraiodide vapor pressure is determined by the temperature of the excess solid tetraiodide, whereas at high temperatures it is determined by the dissociation pressure of the lower iodide (i.e., essentially by the temperature of the raw metal).

We have obtained additional experimental confirmation of these hypotheses. The experiment was set up as follows. Into a quartz reaction tube (Figure 6) molybdenum leads were sealed, to the ends of which a tungsten filament was attached in the usual manner. Approximately 100 g of powdered zirconium was loaded into the tube (– 200 mesh). The tube was connected to a short U-shaped tin manometer. Between the manometer and the tube there was a section of tubing filled with zirconium filings. This served as a kind of filter to prevent the possible penetration of iodine to the surface of the tin. The manometer functioned as a null instrument; the vapor pressure inside the tube was balanced by the argon pressure, which was measured by the usual mercury manometer. The tube was surrounded by a short furnace which heated the tube and the

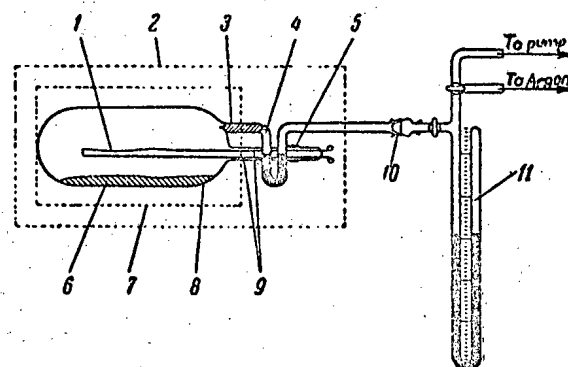


Figure 6. Reaction tube for the study of the high-temperature maximum of the process rate.

1) Tungsten filament; 2) general furnace; 3) zirconium "filter"; 4) tin manometer; 5) transition glass; 6) zirconium powder; 7) furnace for heating quartz tube; 8) quartz tube; 9) 2 mm molybdenum wire; 10) ground joint; 11) mercury manometer.

raw metal contained in it to 700° C. The entire apparatus was placed in a larger furnace which provided overall heating to 450 – 480° C.

Two experiments were performed: in the first experiment 0.8 g of the tetraiodide was introduced into the tube; in the second experiment 3 g was used. The results of the two experiments were identical.

When the general furnace was heated to 450° C the manometer showed no pressure. This indicates that the conversion of the tetraiodide to the lower iodide proceeds quite rapidly at low temperatures up to 270 – 275° C, i.e., before the tetraiodide pressure reaches 0.5 – 1.0 mm (in these experiments the manometer levels were read by eye with an error of about 0.5 mm Hg).

While the tube was being heated the filament was hot; then zirconium deposition was observed, which proceeded at a fairly rapid rate, although less rapidly than at the optimum tetraiodide pressure. At a tube temperature of 600° C the manometer began to show an increase of pressure inside the tube, which at about 650° C reached 30 mm Hg, whereupon the zirconium deposition was very much slowed and practically halted.

As the temperature dropped the tube pressure began to decrease. Below 600° C the decomposition of the zirconium on the filament was renewed.

These experiments, despite their qualitative character, enable us to draw two important conclusions:

1. There is a lower iodide whose dissociation pressure at a certain temperature in the 500 – 600° C range is equal to the optimum pressure.
2. With a large amount of the raw metal and a large surface area the formation of the lower iodide proceeds very rapidly, with the tetraiodide pressure dropping to low values. For this reason the deposition of zirconium on the filament takes place fairly rapidly.

We believe that this is the explanation of Fast's data [6] on the dependence of the process rate on the tube temperature. Additional confirmation is the fact that according to Fast himself the tube pressure in his experiments never exceeded 0.5 mm. Hg.

#### SUMMARY

The above experimental data show that the tetraiodide pressure in the reaction vessel strongly affects the course of the process. However, the data are still insufficient to reveal the exact nature of this influence. In a second article we shall give our ideas on this subject as well as the experimental results which serve as their basis.

#### LITERATURE CITED

- [1] J. H. De Boer and J. D. Fast, Z. anorg. allg. Chem., 153 (1926).
- [2] J. H. Doring and K. Mollere, Z. Elektrochem. Ber. der Bunsengesellschaft f. phys. Chem. 56, No. 4, 403 (1952).
- [3] W. M. Rainor, Symp. "Zirconium and Zirconium Alloys." Am. Soc. Metals, Cleveland, 71 (1953).
- [4] The Metallurgy of Zirconium. McGraw-Hill, USA (1955).
- [5] Rahlfs and Fisher, Z. anorg. allg. Chem, 211, 349 (1933).
- [6] J. D. Fast, Z. anorg. allg. Chem, 239, 145 (1938).
- [7] R. B. Holden and B. Kopelman, J. Electrochem. Soc., 100, No. 3 (1953).



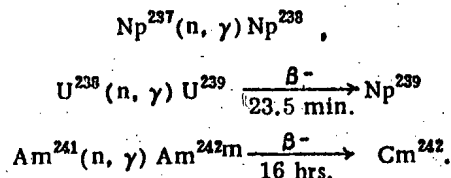
ENERGY LEVELS OF  $\text{Pu}^{238}$  AND  $\text{Pu}^{239}$  NUCLEI

S. A. Baranov, K. N. Shlyagin

I. Apparatus and Preparation of Radioactive Sources

In studying the decay of  $\text{Np}^{238}$ ,  $\text{Np}^{239}$  and  $\text{Cm}^{242}$ , the following apparatus was used: a magnetic  $\beta$ -spectrometer with double focusing [1], [2], a scintillation  $\gamma$ -spectrometer and proportional counter for the investigation of the soft  $\gamma$ -radiation, and other apparatus. The basic instrument was the  $\beta$ -spectrometer, which focused electrons at an angle of  $\pi\sqrt{2}$ . The resolving power was about 0.3% for a solid angle of about 0.45% of  $4\pi$ .

Specimens of  $\text{Np}^{238}$ ,  $\text{Np}^{239}$  and  $\text{Cm}^{242}$  were gotten by irradiating isotopes of  $\text{Np}^{237}$ ,  $\text{U}^{238}$ , and  $\text{Am}^{241}$  with thermal neutrons in the RFT reactor [3], according to the following reactions:



After careful chemical purification of the neptunium and curium samples to get rid of fission products and other impurities, the radiation sources for  $\beta$ - and  $\gamma$ -spectrometric investigation were prepared. The procedure for preparation of the sources is described in article [1]. The thickness of the active layer of the prepared sources for  $\beta$ -spectrometric investigation was a few micrograms per square centimeter. The sources used for  $\gamma$ -spectrometric investigation were not so thick.

II.  $\text{Np}^{238}$  - Decay Investigation

Some highly inconclusive works [4-9] have been devoted to the investigation of  $\text{Np}^{238}$ -decay. The first communication regarding some of the characteristics of the decay of this isotope was made in 1949 by Seaborg and others [4], who found the half-life of  $\text{Np}^{238}$ -decay to be about 2 days and at the same time, by use of an absorption method, determined the energy of the  $\beta$ - and  $\gamma$ -radiation. Freedman, Wagner, and Jaffey [6], by use of a double-lens spectrometer of 3 percent resolving power, found the electron spectrum of  $\text{Np}^{238}$  and proved that it consists of two  $\beta$ -spectra whose energies have upper limits of  $E_{01} = 0.258$  and  $E_{02} = 1.272$  Mev, and a few  $\gamma$ -transitions.

Measurements with the  $\beta$ -spectrometer. The  $\text{Np}^{238}$  electron spectrum that we got is shown in Figures 1 and 2. As is seen from the graphs, there are very many conversion lines and Auger-electron lines superimposed on the  $\beta$ -spectrum. A total of 38 conversion lines was discovered.

On the Kurie plot constructed from the experimental results, three partial  $\beta$ -spectra with limiting energies of  $E_{01} = (1236 \pm 5)$  kev,  $E_{02} = (280 \pm 10)$  kev, and  $E_{03} = (250 \pm 10)$  kev are clearly defined. There is possibly a fourth  $\beta$ -spectrum with limiting energy about 200 kev (Figure 3).

As will be shown below, measurement of the number of coincidences for  $\beta$ -particles of energies greater than 500 kev with conversion electrons ( $e_c$ ) from transitions with energies of 44 and 102 kev leads one to suggest that there is a  $\beta$ -spectrum with limiting energy  $E_{03} = 1139$  kev.

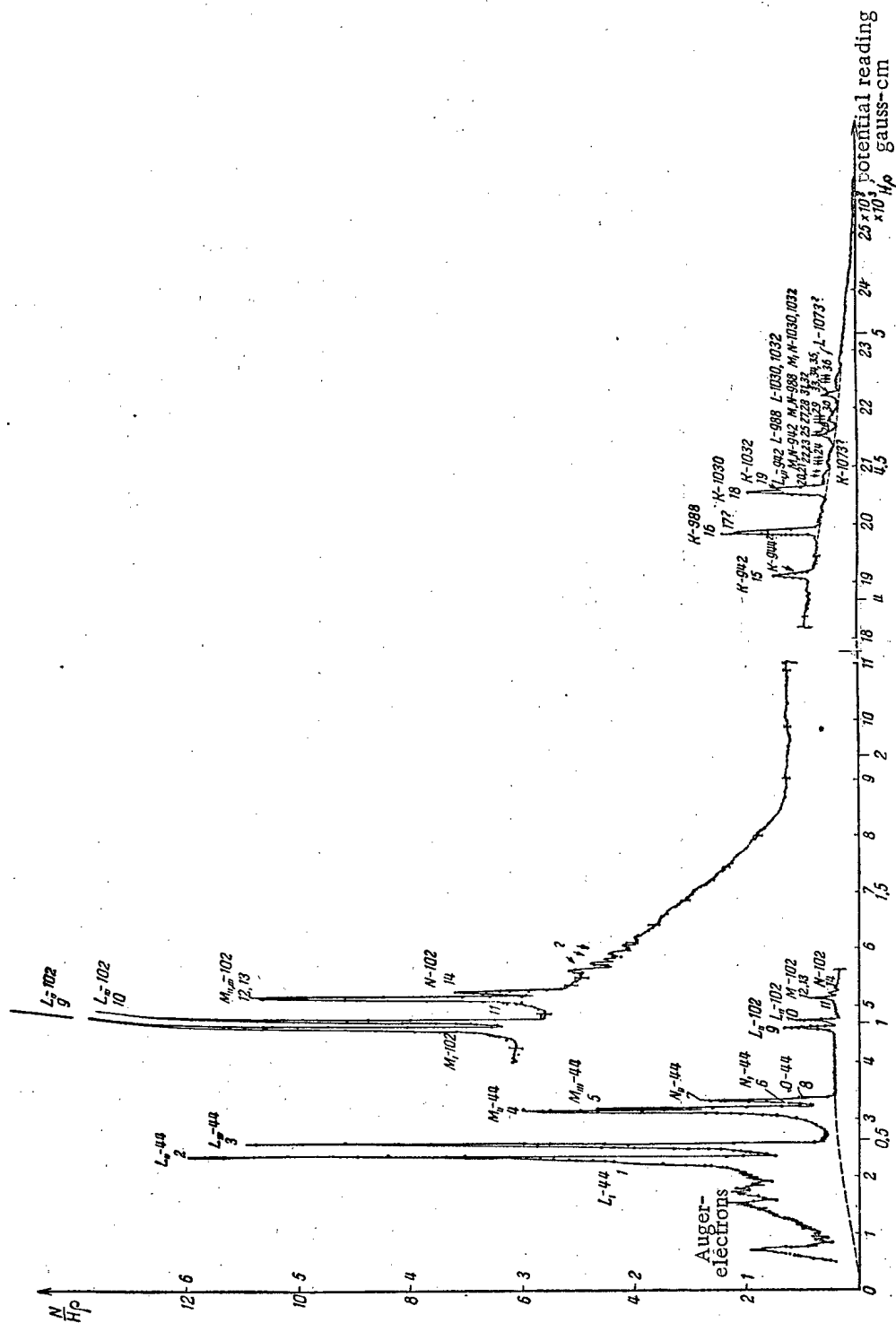
Figure 1. Electron spectrum of  $\text{Np}^{238}$

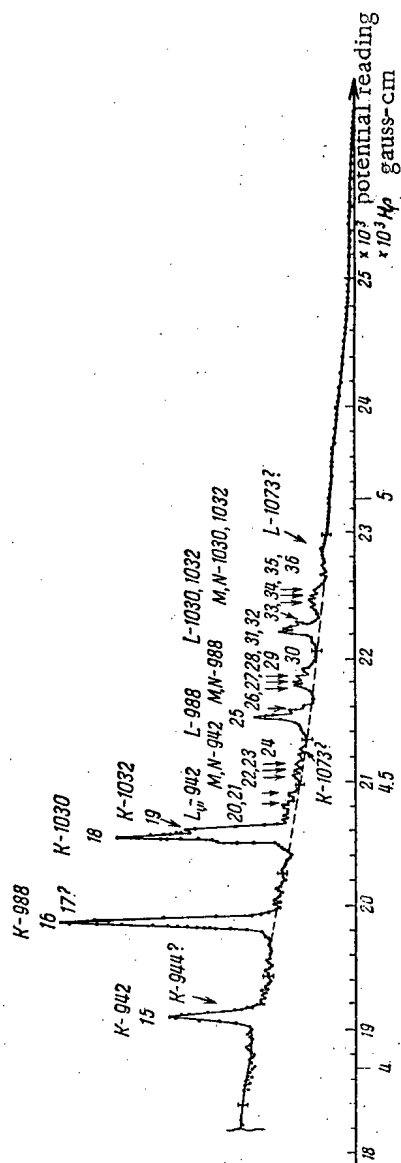
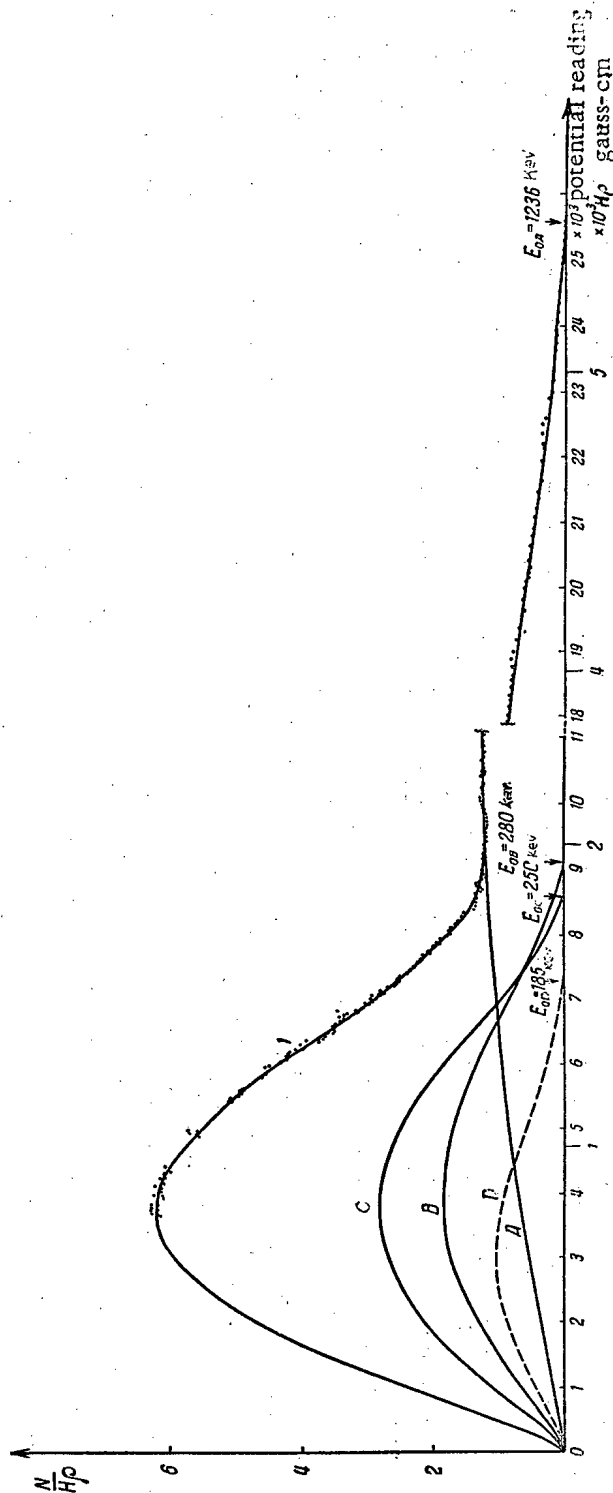
TABLE 1

Interpretation of the conversion lines occurring in  $\text{Np}^{238}$ -decay

Number of the electron line	Observed electron energy(kev)	Conversion shell	Transition energy (kev)	Conversion line intensity (arbitrary units)	Remarks
1	20.11	L <sub>I</sub>	43.22		
2	21.69	L <sub>II</sub>	43.94	2499	
3	25.79	L <sub>III</sub>	43.85	2280	
4	38.54	M <sub>II</sub>	44.10	1251	
5	39.43	M <sub>III</sub>	43.99	618	
6	42.55	N <sub>I</sub>	44.11	401	
7	42.72	N <sub>II</sub>	44.10		
8	43.94	O	44.20		
			average		
			44.03	$\Sigma = 7050$	
9	79.69	L <sub>II</sub>	101.94	131	
10	83.87	L <sub>III</sub>	101.93	69	
11	96.01	M <sub>I</sub>	101.94	—	
12	96.66	M <sub>II</sub>	102.22	43.2	
13	97.15	M <sub>III</sub>	107.72	38.5	
14	100.90	N <sub>II,III</sub>	102.15		
			average 101.98	$\Sigma = 290.7$	
15	819.92	K	941.67	9.7	
20	919.84	L <sub>II</sub>	942.09		
21	923.12	L <sub>III</sub>	941.18		
22	936.39	M <sub>II</sub>	941.94		
23	937.7	M <sub>IV</sub>	941.68		
24	940.05	N <sub>I</sub>	941.61		
			average		
			941.8*		
16	865.99	K	987.83	21.6	
25	966.16	L <sub>II</sub>	988.41	6.7	
26	968.97	L <sub>III</sub>	987.03		
27	981.35	M <sub>I</sub>	987.28		
28	982.48	M <sub>III</sub>	987.04		
29	983.6	M <sub>IV,V</sub>	987.48		
30	986.2	N <sub>I</sub>	987.7		
			average		
			987.7*	$\Sigma = 28.3$	
31	907.83	K	1030.0	~16.8**	} $\Sigma_K = 25.3$ $\Sigma_L = 6.2$
33	1008.1	L <sub>II</sub>	1030.35	~3.4**	
34	1024.0	L <sub>III</sub>	1029.26		
36	1024.0	M <sub>I</sub>	1029.93		
	1029.0	N <sub>I</sub>	1030.56		
			average 1030.0*		
19	910.0	K	1032.65	~8.5**	
32	1010.0	L <sub>II</sub>	1032.35	~2.8**	
35	1028.8	M	1032		
			average 1032.4*		

Total intensity of the  $\beta$ -spectrum— 9537Intensity of the partial  $\beta$ -spectrum with  $E_{01} = 1235$  and 1133 kev— 3911Intensity of the partial  $\beta$ -spectrum with  $E_{02} = 280$  kev— 1908Intensity of the partial  $\beta$ -spectrum with  $E_{03} = 250$  kev— 2957Intensity of the partial  $\beta$ -spectrum with  $E_{04} \sim 200$  kev— 762.

\*, \*\*, see following page.

Figure 2. Electron spectrum of  $\text{Np}^{238}$ .Figure 3. Beta-spectrum of  $\text{Np}^{238}$   
1) Experimental curve; A, B, C, D) partial  $\beta$ -spectra.

\* The average of two series of measurements.

\*\* Due to the poor separation of the conversion electrons, only the sum of intensities of the K- and L-peaks for  $E_\gamma = 1030$  and  $1032$  keV can be well determined.

The intensities of the partial spectra are distributed in the following way:

Limiting energy of the $\beta$ -spectrum (kev)	Intensity (%)	The value of $\log f \tau$
$E_{01} = 1236$	38	8.6
$E_{02} = 280$	20	6.6
$E_{03} = 250$	31	6.2
$E_{04} \approx 200$	8	—
$E_{05} \approx 1133$	2.8	9.0

Table 1 gives the interpretation of the conversion lines belonging to the  $\gamma$ -transitions of the  $\text{Pu}^{238}$  nucleus, as well as the intensities of these lines and of the partial spectra in arbitrary units.

The data of Table 1 establish the following  $\gamma$ -transitions of the  $\text{Pu}^{238}$  nucleus: 44, 102, 942, 988, 1030 and 1032 kev. The transition with energy  $E_{\gamma} = 927$  kev, detected in experiments of Rasmussen and others [10], was not clearly evident in our experiment.

Measurements with a scintillation spectrometer and proportional counter. For the measurement of the  $\gamma$ -spectrum on a scintillation spectrometer a crystal of  $\text{NaI(Tl)}$  was used. The instrument was calibrated in the interval 0.5-1.5 Mev with  $\text{Cs}^{137}$  and  $\text{Co}^{60}$   $\gamma$ -rays. Three maxima are clearly distinguished in the  $\text{Np}^{238}$   $\gamma$ -spectrum, corresponding to  $\gamma$ -rays with energies about equal to 940, 980 and 1030 kev. These values of energy agree well with the data gotten on the  $\beta$ -spectrometer. The intensity of these  $\gamma$ -rays coincided with the half-life of  $\text{Np}^{238}$ -decay.

In the experiments with a proportional counter filled with a mixture of heavy gases, maxima produced by 44 and 102 kev  $\gamma$ -rays were not clearly evident, which indicates a high conversion coefficient for these rays. By use of a photomultiplier with the  $\text{NaI(Tl)}$  crystal and of an end counter connected in coincidence (resolving power  $\tau = 2 \cdot 10^{-7}$  sec) and a multiple-channel differential pulse-height analyzer, the number of coincidences between  $\beta$ -particles of  $E_{\beta} > 500$  kev energies and conversion electrons from 44 to 102 kev transitions ( $e_{44}^-$ ,  $e_{102}^-$ ) was measured.

Figure 4 shows the electron conversion spectrum resulting from these experiments. Analysis of this spectrum establishes the fact that the  $(\beta, e_{44}^-)$ -coincidences make up about 33 percent of the total number of disintegrations, and the  $(\beta, e_{102}^-)$ -coincidences make up no more than 2.8 percent. In this way it can be seen that the partial spectrum A of Figure 3 consists of two  $\beta$ -spectra, whose limiting energies are 1133 and 1236 kev.

### III. $\text{Cm}^{242}$ -Decay Investigation

The  $\alpha$ -decay half-life of the isotope  $\text{Cm}^{242}$  is equal to 162.5 days. According to Asaro and others [11], it seems that the  $\alpha$ -spectrum consists of four monoenergetic groups of  $\alpha$ -particles. There exists no information in the literature on the electron spectrum of  $\text{Cm}^{242}$ .

TABLE 2

Interpretation of the electron lines occurring in  $\alpha$ -decay of  $\text{Cm}^{242}$

The number of the electron line	Observed electron energy (kev)	Conversion shell	Transition energy (kev)	Conversion line intensity (arbitrary units)
1	21.06	$L_I$	44.16	
2	21.73	$L_{II}$	43.98	49.5
3	26.03	$L_{III}$	44.09	42.0
4	37.18	$M_I$	44.11	
5	38.60	$M_{II}$	44.16	32.5
6	39.49	$M_{III}$	44.05	17.0
7	42.78	$N_{II}$	44.16	8.0
			average 44.10*	$\Sigma = 149$

\* The average of two series of measurements.

Figure 5 shows the electron spectrum of  $\text{Cm}^{242}$ . Analysis of this spectrum has shown that the observed electron lines correspond to 44-keV  $\gamma$ -rays. Table 2 gives the interpretation of the conversion lines, and shows their intensities.

If we compare the Auger-electron groups discovered in the electron spectra of  $\text{Np}^{238}$  and  $\text{Cm}^{242}$  (see Figures 1 and 5), then we see that in the interval 0-500 gauss-cm these groups are essentially different from each other. It would seem that the intense group of electrons of  $\text{Cm}^{242}$  with energies of 1.5-3.5 keV can be explained as the ionization of curium atoms by  $\alpha$ -particles. We have observed this phenomenon previously in the investigation of  $\text{Am}^{241}$   $\alpha$ -decay [1, Figure 1].

#### IV. The Level Scheme of the $\text{Pu}^{238}$ Nucleus

In constructing the level scheme of the  $\text{Pu}^{238}$  nucleus, we used the following experimental data:

1. In  $\beta$ -decay of  $\text{Np}^{238}$  it seems that there is no  $\beta$ -transition to the ground level of the  $\text{Pu}^{238}$  nucleus.
2. There exist at least five  $\beta$ -transitions to excited  $\text{Pu}^{238}$  levels; the energies of these transitions are, respectively,

$$E_{01} = (1236 \pm 5) \text{ keV}$$

$$E_{05} \approx (1133 \pm 10) \text{ keV}$$

$$E_{02} = (280 \pm 10) \text{ keV}$$

$$E_{03} = (250 \pm 10) \text{ keV}$$

$$\text{and } E_{04} \approx 200 \text{ keV.}$$

3. There are coincidences between hard  $\beta$ -particles ( $E_{\beta} > 500 \text{ keV}$ ) and conversion electrons from 44 and 102 keV transitions.

4. Seven  $\gamma$ -transitions are observed in the  $\text{Pu}^{238}$  nucleus with energies of 44, 102, 942, 988, 1030, and 1032 keV.

The proposed level scheme of the  $\text{Pu}^{238}$  nucleus is presented in Figure 6. There is no pretense that this scheme is final. The level corresponding to an excited state of 305 keV is borrowed from the work of Asaro and others [11].

As can be seen from the drawing, seven excited levels are detected in the  $\text{Pu}^{238}$  nucleus. The four lower levels, in agreement with the theory of A. Bohr [12-15], belong to the lowest rotation band of this nucleus. The spins and parities of these levels ( $E_{1e} = 0, 44, 146, \text{ and } 305 \text{ keV}$ ) are equal to  $0+, 2+, 4+, 6+$ .

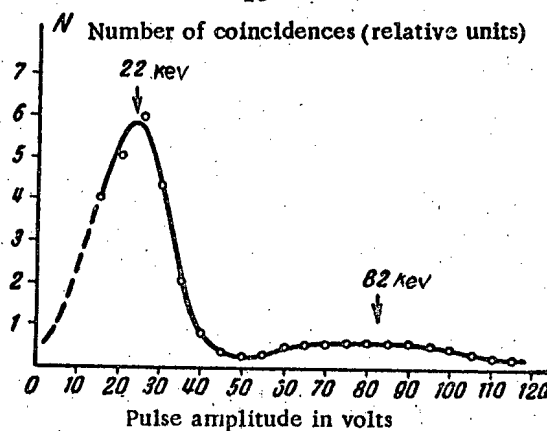


Figure 4. Spectrum of conversion electrons which are in coincidence with high-energy  $\beta$ -particles.

In order to clarify the multipole character of the high-energy  $\gamma$ -transitions ( $E_{\gamma} = 942; 988; 1030 \text{ and } 1032 \text{ keV}$ ), we extrapolated the tabulated data of Rouse [15] and got the theoretical values of the absolute conversion coefficients  $\Omega_K$  for the K-shell of the plutonium atom, taking into account the effect of screening. The accuracy of the values is about 15-20 percent. The resulting values of  $\Omega_K$  are presented in Table 3.

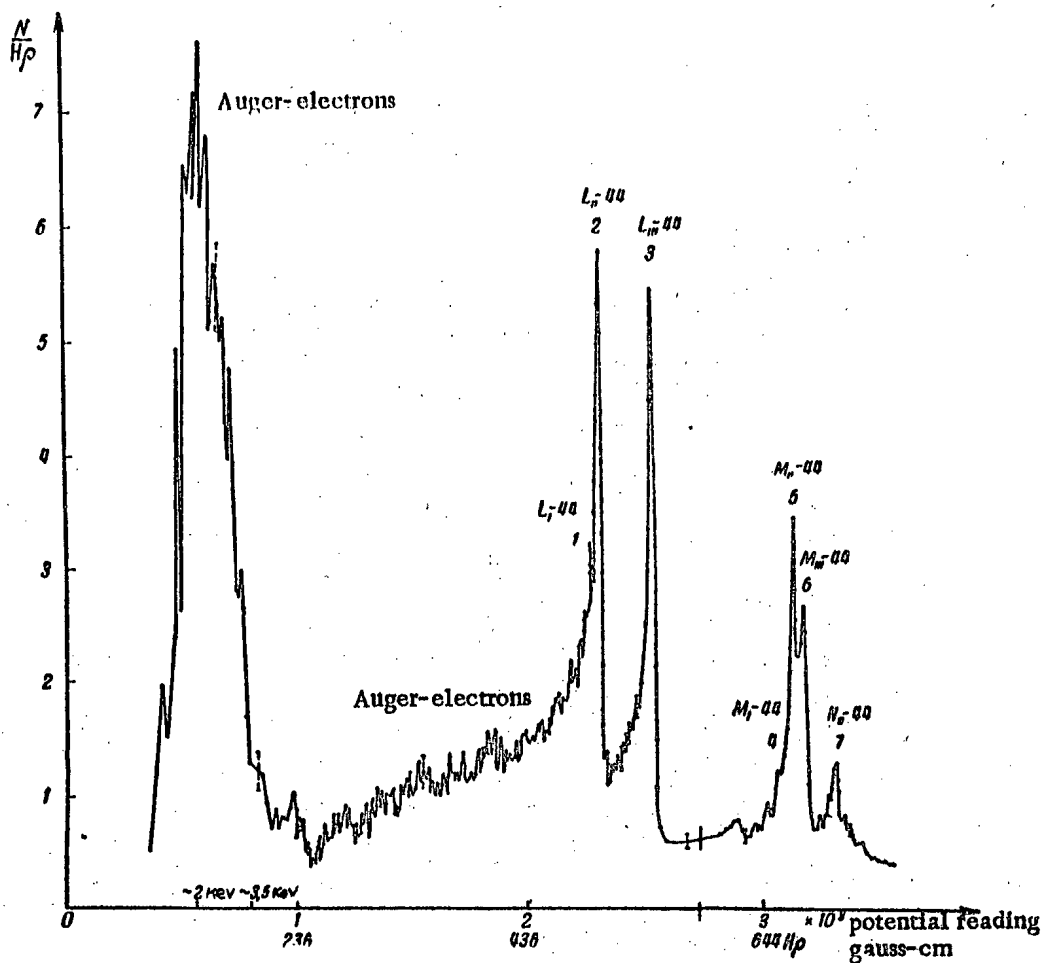
Figure 5.  $\text{Cm}^{242}$  electron spectrum.

TABLE 3

Multipole $E\gamma/m_0c^2$	E1	E2	E3	M1	M2	M3	$E\gamma$ kev
1.84	0.0036	0.0112	0.0235	0.091	0.137	0.189	942
1.93	0.0032	0.0105	0.0225	0.080	0.108	0.162	988
2.00	0.0030	0.0100	0.0203	0.072	0.070	0.137	1030

Based on the data of Table 1 and on the decay scheme (Figure 6), the following experimental values of  $\Omega_K$  for the K-shell of the plutonium atom were found:

$$\begin{aligned}\Omega_K^{942} &= 0.0102, & \Omega_K^{988} &= 0.0090, \\ \Omega_K^{988} &= 0.0087, & \Omega_K^{1030} &= 0.0100\end{aligned}$$

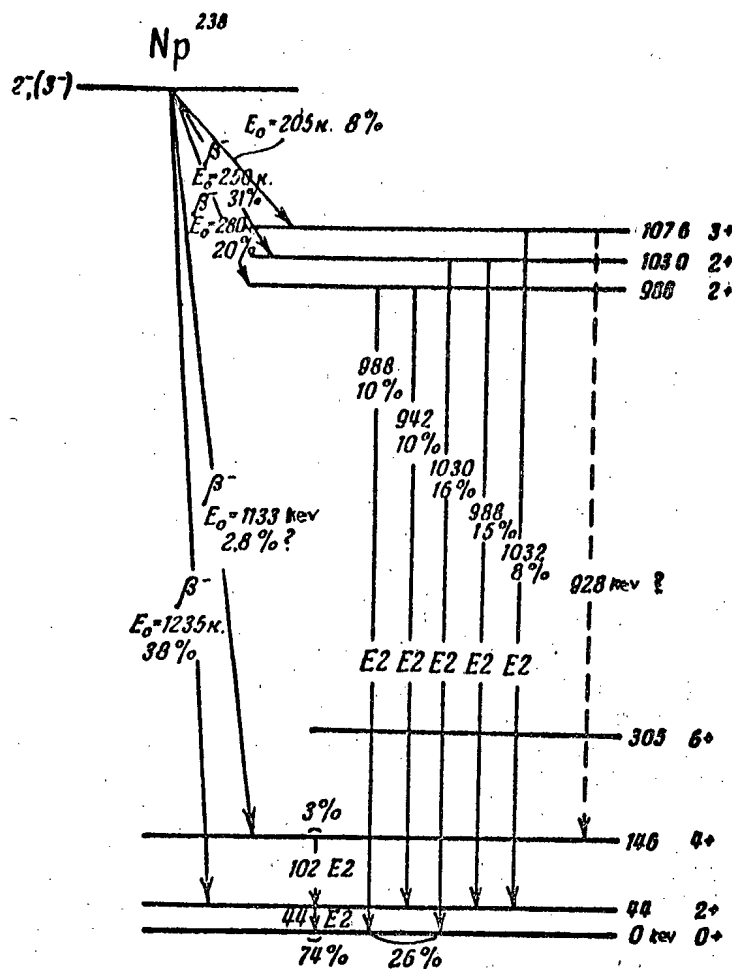
and

$$\Omega_K^{1032} = 0.0112,$$

where  $\Omega_K^{988}$  and  $\Omega_K^{988}$  are the conversion coefficients for the K-shell both with the same energy of 988 kev, but going respectively to the ground level and to the first excited level of the  $\text{Pu}^{238}$  nucleus.

By comparing the experimental and theoretical values of  $\Omega_K$ , we see that to all the high-energy  $\gamma$ -transitions of the  $\text{Pu}^{238}$  nucleus we may assign the multipole E2. This conclusion does not contradict the result of references [9] and [10]\* with regard to the multipole character of  $\gamma$ -transitions of energy  $E\gamma = 986$  and 1029 kev. Since all the high-energy transitions belong to the class E2, then the following spins and par-

\* The results of the cited article became known to us only after the completion of the present work.

Figure 6.  $\text{Pu}^{238}$  nuclear levels.

ties can be assigned to the detected 988, 1030, and 1076 keV levels:

$$I_{988} = 2+, I_{1030} = 2+, I_{1076} = 3+,$$

From the values of the spins and parities of the nuclear  $\text{Pu}^{238}$  levels, as well as from the value of  $\log ft$  for the  $\beta$ -spectra, it is possible to get two values for the spin of the ground state of  $\text{Np}^{239}$ :  $I_0 = 3-(2-)$ .

#### V. $\text{Np}^{239}$ Decay

Many works [16-20] have been devoted to study of decay of the  $\beta$ -active isotope  $\text{Np}^{239}$  ( $T_{1/2} = 2.3$  days). However, to the present time many of those elements of the level structure of the  $\text{Pu}^{239}$  nucleus remain unclear, which arise as a result of the  $\beta$ -decay of  $\text{Np}^{239}$  and the  $\alpha$ -decay of  $\text{Cm}^{243}$ . Thus, for instance, the spins of the  $\text{Pu}^{239}$  energy levels are not determined, there is no indication of the existence of rotational levels in this even-odd nucleus, and so on.

The  $\text{Np}^{239}$  electron spectrum, taken in the energy interval 1-750 keV with a magnetic  $\beta$ -spectrometer [2], is shown in Figure 7. The interpretation of the electron lines is given in Table 4.

As is seen in Figure 7, there are many Auger-electron lines superimposed on the soft part of the  $\text{Np}^{239}$   $\beta$ -spectrum. Some of them, in terms of their energy, could have been put down as conversion lines. For instance, lines 1, 2, 3, 4 can be assigned to the conversion peaks  $M_{I-12}$ ,  $M_{II-12}$ ,  $M_{III-12}$ ,  $M_{IV-12}$  corresponding to 12 keV  $\gamma$ -transitions. Analogously, the conversion lines and others can be taken for Auger-electrons. However, comparison of the soft part of this spectrum (1-20 keV) with the same part of the  $\text{Np}^{238}$  spectrum



shows that they are similar. This would seem to point to an invalid conclusion on the part of the authors of reference [18] with respect to the existence of  $\gamma$ -transitions with energies of 13 and 19 kev. Electron-line 30 (electron energy, 75-77 kev) is put down by us also as an Auger-electron ( $K - 2L \approx 75$  kev). In references [18] and [20] this seems to be taken as the conversion peaks N-77 ( $E_\gamma = 77$  kev) and L-98 ( $E_\gamma = 98$ ).

As follows from Table 4, the following  $\gamma$ -energies are determined in the present work: 44.4, 49.3, 57.2, 61.4, 67.9, 106.2, 210.3, 228.4, 278.1, and 334 kev. The existence of  $\gamma$ -rays,  $E_\gamma = 334$  kev, is established by measurement of the spectrum of photo-electrons knocked out of a lead target. The above values for the  $\gamma$ -ray energies are in agreement with published results of other investigators. Gamma-transitions with energies of 98.3, 103.3, 125.3, 181.8, 254.6, 273.1, 285.6, and 316.1, established in a short note [20]\*, were not discovered by us. If these  $\gamma$ -lines exist, then their intensity is small.

For the 44, 49, 57, 68, 210, 228, and 278 kev  $\gamma$ -transitions, experimental values of the relative conversion coefficients for the atomic subshells of plutonium were found; these are

$$\begin{aligned} \left(\frac{L_I}{L_{II}}\right)_{44} &= \left(\frac{L_I}{L_{III}}\right)_{44} \approx 1.5; \\ \left(\frac{L_{II}}{L_{III}}\right)_{49} &\approx 1.0; \quad \left(\frac{L_{II}}{L_{III}}\right)_{67} \approx 1.0; \\ \left(\frac{L_{II}}{L_{III}}\right)_{68} &\approx 1.0; \\ \left(\frac{K}{L}\right)_{210} &\approx 6; \quad \left(\frac{K}{L}\right)_{228} \approx 4.8; \\ \left(\frac{K}{L}\right)_{278} &\approx 4.7. \end{aligned}$$

Comparison of the experimental and theoretical values of the relative conversion coefficients establishes the following multipole assignments:

$$\begin{aligned} (M1)_{44}^{**}; \quad (0.2 M1 + 0.8 E2)_{49}; \\ (E2)_{67}; \quad (E2)_{68}; \\ (M1)_{210}; \quad (M1)_{228}; \quad (M1)_{278}. \end{aligned}$$

We must now investigate separately the  $\gamma$ -transitions with energies 61 and 106 kev. From Figure 7 it is seen that the lines

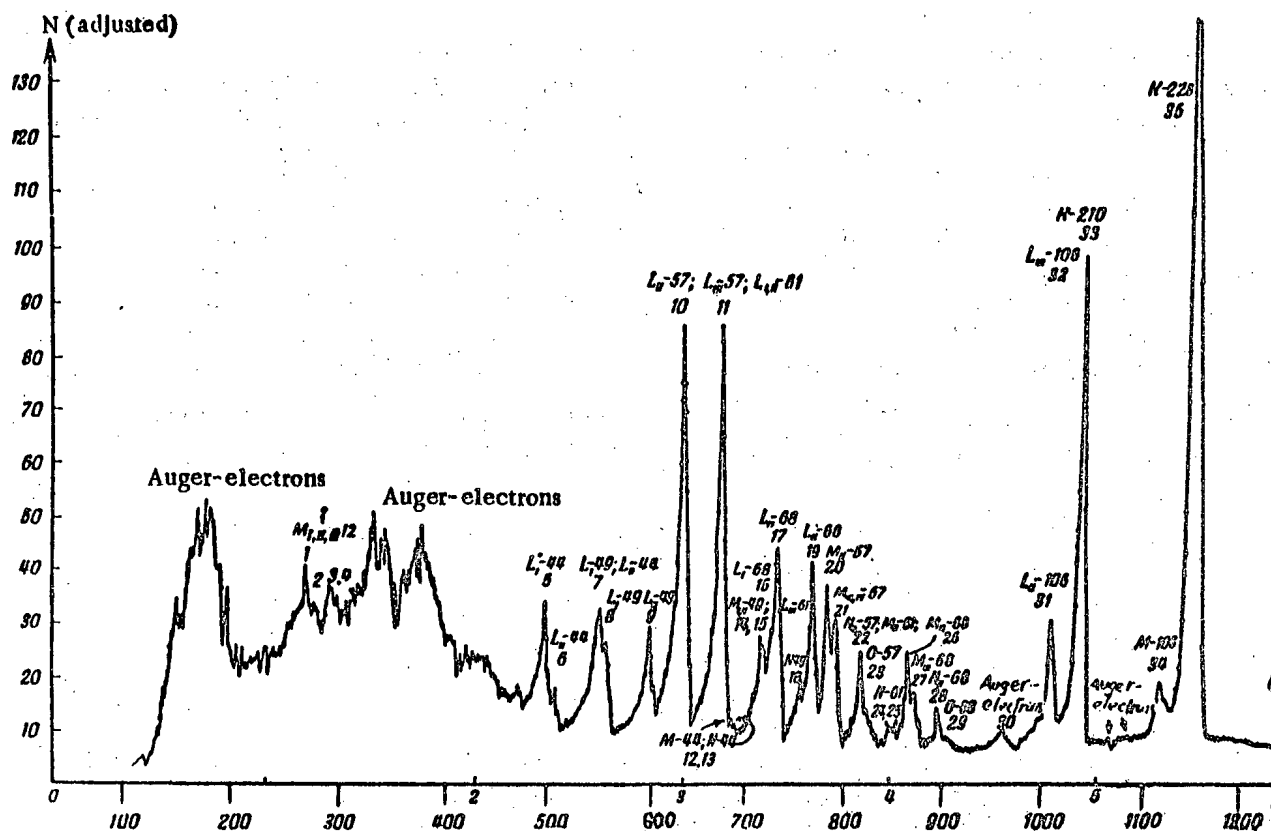
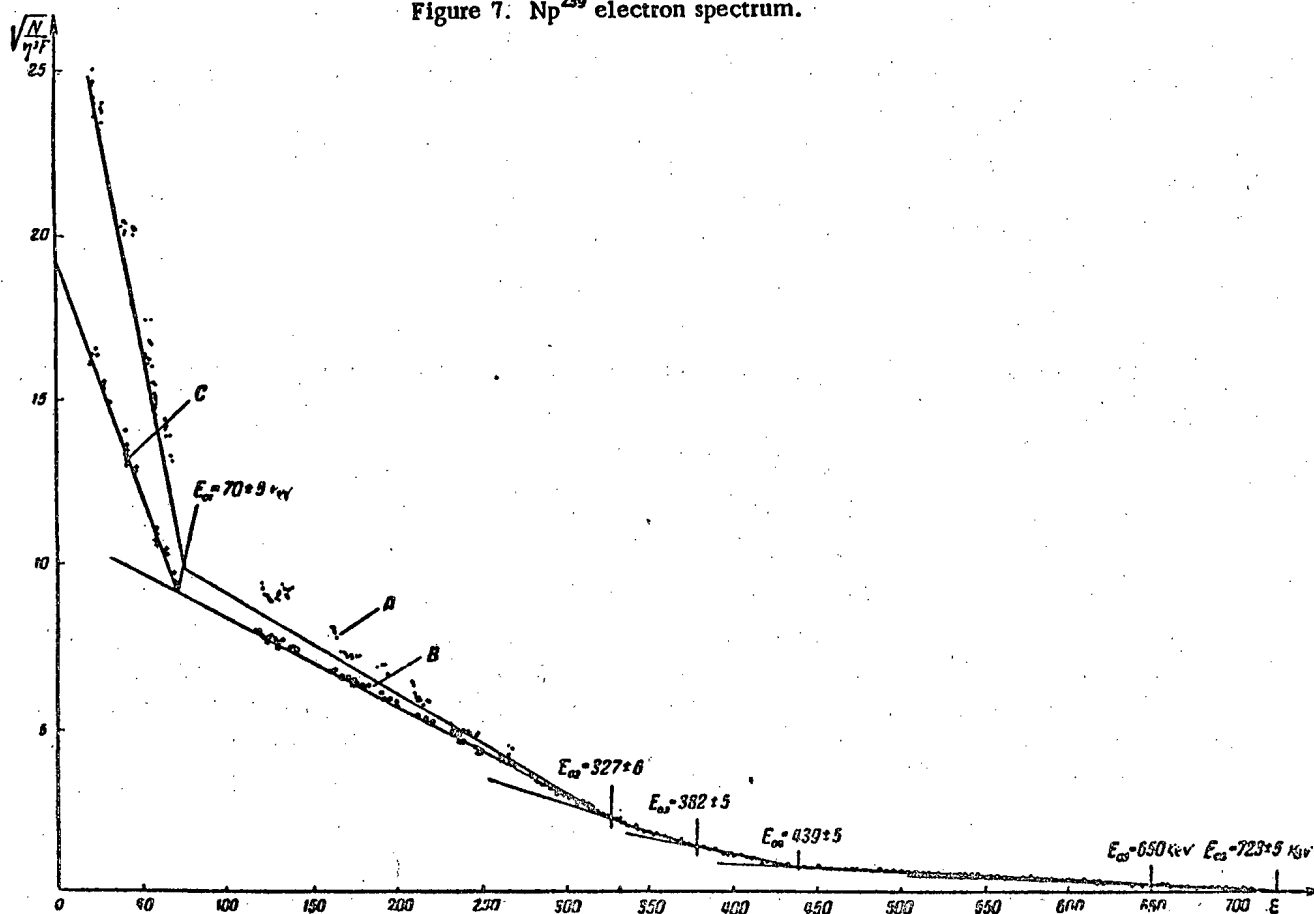
$$L_{I,II}-61, \quad L_{III}-61 \text{ and } M-61$$

coincide, respectively, with lines

$$L_{III}-57, \quad M-49 \text{ and } N_{I,O}-57.$$

Therefore, it is possible to decide about the existence of a 61 kev  $\gamma$ -transition only by the presence of the line  $N_{I,II} \dots -61$ , which is not masked by other conversion peaks. This situation necessitates careful treatment of the value for the conversion coefficient of 61 kev  $\gamma$ -rays on the atomic L-shell, which was presented in reference [19] ( $\alpha_L = 0.4 - 0.9$ ), and of the multipole E1 for this  $\gamma$ -transition, which was determined in references [19] and [20].

- \* The results of reference [20] became known to us after the completion of this investigation.
- \*\* The possible presence of E2 is not excluded.

Figure 7.  $\text{Np}^{239}$  electron spectrum.Figure 8. Kurie plot of the  $\text{Np}^{239}$   $\beta$ -spectrum.  
A, B, C are measured with sources of different intensities.

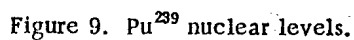
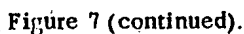


TABLE 4

Interpretation of the electron lines occurring in  $\beta$ -decay of  $\text{Np}^{239}$ 

Number of the electron line	Observed electron energy (kev)	Conversion shell	Transition energy (kev)	Line intensity (arbitrary units)	Multipole character of the transition	Remarks
(1)	(2)	(3)	(4)	(5)	(6)	(7)
1	6.38	$M_I$	12.31			
2	6.77	$M_{II}$	12.33			
3	7.52	$M_{III}$	12.08			
4	8.1	$L_I$	12.1			
			average 12.2 ?			
5	21.44	$L_I$	44.54	42		
6	22.2	$L_{II}$	44.45	8.3		
7	26.17	$L_{III}$	44.23	50		coincides with $L_I$ -49
12	40.04	$M_{III}$	44.56	3.6		
13	40.5	$M_{IV}$	44.48			
			average 44.45		$M1 + E2$	
7	26.17	$L_I$	49.27	50		coincides with $L_{III}$ -44
8	27.05	$L_{II}$	49.3	33.5		
9	31.28	$L_{III}$	49.34	34.4		
14	43.36	$M_I$	49.34			
15	43.94	$M_{II}$	49.5	58		coincides with $L_{III}$ -61
16	44.76	$M_{III}$	49.32			
18	48.3	$N_{III,IV}$	49.43			
			average 49.34		$0.2M1 + 0.8 E2$	
10	34.98	$L_{II}$	57.23	170.3		
11	39.15	$L_{III}$	57.21	164.6		coincides with $L_{II}$ -61
20	51.7	$M_{II}$	57.26	69.5		
21	52.9	$M_{III,IV}$	57.46			
22	55.9	$N_{II}$	57.28	34.1		coincides with M-61
23	56.9	O	57.35			
			average 57.26		E2	
11	39.15	$L_{II}$	61.4	164.6		coincides with $L_{III}$ -57
14	43.36	$L_{III}$	61.42	48		coincides with M-49
22	55.9	$M_{II}$	61.46	34		coincides with N-57
24	60.09	$N_{II}$	61.47			
25	60.63	$N_{IV}$	61.39	6.8		
			average 61.43		(E1) ?	
17	45.71	$L_{II}$	67.96	57		
19	49.83	$L_{III}$	67.89	51		
26	62.29	$M_{II}$	67.85			
27	63.25	$M_{III}$	67.81	34.2		
28	66.5	$N_{II}$	67.88			
29	67.82	O	68	12.4		
			average 67.88		E2	
30	75-77	K-LL				Auger-electrons
31	83.7	$L_{I,II}$	106	49.3		
32	88.1	$L_{III}$	106.2	15(calc.)		coincides with K-210
34	100.7	$M_{II,III}$	106.3	41		
35	$\approx 106$	N, O	$\approx 106$			coincides with K-228
			average 106.1		E1	

TABLE 4 (continued)

(1)	(2)	(3)	(4)	(5)	(6)	(7)
33	88.4	K	210.1	168		coincides with $L_{III}-106$
37	187.3	$L_I$	210.4	24.5		
38	188.4	$L_{II} ?$	210.6			
39	$\approx 206$	M, N	210			coincides with $L_{II}-228$
			average 210.2		M1	
35	106.7	K	228.5	388		
39	206	$L_{I,II}$	228.2	81		
40	222.8	$M_{II}$	228.4	14.4		
41	228	N, O	228.5	3.8		
			average 228.4		M1	
36	156.4	K	278.1	260		
42	255.9	$L_{I,II}$	278.1	55.4		
43	272.9	$M_{II}$	278.5			
44	273.3	$M_{III}$	277.9	12.3		
45	277.4	N	278.2			
46	278	O	278.4	3.8		
			average 278.1		M1	
	$\approx 246$	K	$\sim 334$			K-photo-electrons of lead.

In the case of the 106 kev  $\gamma$ -transition, the conversion peak  $L_{III}-106$  coincides with line K-210, and it is impossible to separate them. If we assume, however, that the 106 kev transition is an electric dipole, then we can calculate the height of the  $L_{III}-106$  peak and determine the value of the total conversion coefficient for these  $\gamma$ -rays at the L-shell. According to our semi-empirical calculation,  $\Omega_L = 0.09$ . This value agrees with the theoretical value  $\Omega_L = 0.1$  of reference [19]. Thus the 106 kev  $\gamma$ -transition seems to be an electric dipole (E1).

Figure 8 shows the Kurie plot of the  $Np^{239}$   $\beta$ -spectrum. The high-energy part of the spectrum ( $E_\beta > 300$  kev) was investigated with a highly active source, and the low energy part ( $E_\beta < 300$  kev) with weaker sources. It was noticed that with highly active sources (curve A of Figure 8) a higher intensity for the soft components of the spectrum was observed. It would seem that this is due to the influence of the thickness of the active layer. Measurements were therefore made with sources of various thicknesses. The determination of the intensity of the soft components of the spectrum was carried out on the basis of measurements with sources of thicknesses such that the relative intensity of the partial spectra remained constant. The analysis of the Kurie plot allowed us to distinguish six partial  $\beta$ -spectra with limiting energies

$$E_{01} = 70 \text{ kev} \qquad E_{02} = 327 \text{ kev}$$

$$E_{03} = 382 \text{ kev} \qquad E_{04} = 439 \text{ kev}$$

$$E_{05} = (655) \text{ kev} \qquad E_{06} = 723 \text{ kev}$$

The  $\beta$ -spectrum with limiting energy 70 kev is here observed for the first time.

Table 5 gives the values of the relative intensities of the partial  $\beta$ -spectra both with and without the  $\beta$ -spectrum  $E_{01}$  taken into account.

The minor break in the Kurie plot at an energy of about 655 kev would seem to indicate the presence of a low-intensity ( $\sim 2\%$ ) partial spectrum with limiting energy  $E_{05} \approx 655$  kev. In this work this spectrum was not very distinct, and its intensity was accounted for together with the hardest component ( $E_{06} = 723$  kev).

Measurements on the proportional and on the scintillation counter. Measurements on the proportional and on the scintillation counter show that the most intense  $\gamma$ -rays are those whose energies are (68), 106; 210 and 278 kev, and the less intense ones are 44, 49, 57, and 61 kev. It is verified that the 106 kev  $\gamma$ -rays go in cascade with gammas of higher energy ( $E_\gamma > 200$  kev).

TABLE 5

Partial  $\beta$ -spectra of  $\text{Np}^{239}$ 

Spectrum	Upper limit of the spectrum (kev)	Intensity (arbitrary units) *	Relative intensity in %	
			with the $\beta$ -spectrum $E_{01}$ taken into account	without the $\beta$ -spectrum $E_{01}$ taken into account
$E_{01}$	$70 \pm 5$	525	22	—
$E_{02}$	$327 \pm 5$	832	35	45
$E_{03}$	$382 \pm 5$	508	21	27
$E_{04}$	$439 \pm 5$	383	16	21
$E_{05}$	$655 \pm 5$	137	6	7
$E_{06}$	$723 \pm 5$			

\* The same units as the conversion line intensities.

VI. The Level Scheme of the  $\text{Pu}^{239}$  Nucleus

Our experimental results on the  $\beta$ - and  $\gamma$ -transitions are in agreement with the results of other published works. The results of the measurements allow for the verification of the previously suggested decay scheme of  $\text{Np}^{239}$ , the determination of the possible spin values of the  $\text{Pu}^{239}$  nuclear levels, and the establishment of a hypothesis as to the possibility of the existence of rotational levels for this even-odd nucleus.

According to the decay scheme of  $\text{Np}^{239}$  deduced in references [11] and [21], the intensity of the  $\gamma$ -transitions from the 49 kev level should be equal to the intensity of all the  $\gamma$ -transitions going to this level ( $E_\gamma = 228$  and 285 kev). However, measurements show that the 49 kev  $\gamma$ -transition is about one third as intense as the transition with  $E_\gamma = 228$  kev. In order to remove the contradiction, it would seem necessary to introduce an additional level with energy 228 kev (Figure 9).

The presence of the  $\beta$ -transition with limiting energy 70 kev allows the inclusion, in the level scheme of the  $\text{Pu}^{239}$  nucleus, of another additional level of 656 kev energy.

The suggested level scheme of the  $\text{Pu}^{239}$  nucleus is shown on Figure 9. The data on  $\alpha$ -decay of  $\text{Cm}^{243}$  is borrowed from Asaro, Thompson, and Perlman [11].

The spins and parities of the  $\text{Pu}^{239}$  nuclear energy levels, determined on the basis of the multipoles of the  $\gamma$ -transitions as presented above, are shown in Figure 9.

As can be seen from the figure, the 278 kev energy level has spin and parity  $\frac{3}{2} \pm$ . This level is favored for  $\alpha$ -decay of  $\text{Cm}^{243}$ , and if it is taken as the rotational ground level of the  $\text{Pu}^{239}$  nucleus, then the spin and parity of the ground state of  $\text{Cm}^{243}$  could be  $\frac{3}{2} \pm$ . In this case, the first and second rotational levels of the  $\text{Pu}^{239}$  nucleus should be, respectively, the levels with energies 322 and 384 kev, and spins  $I_{322} = \frac{5}{2} \pm$  and  $I_{384} = \frac{7}{2} \pm$ . It is easy to see that the ratio  $E_2 : E_1$  for these levels is equal to  $106:44 = 2.41$ , which is in surprisingly good agreement with the well-known formula of A. Bohr and B. Mottelson [15]. However, the above derived multipoles for the 44 and 106 kev  $\gamma$ -transitions, i.e., M1 and E1, are somewhat in contradiction with the previous assumptions with regard to the rotational levels of the  $\text{Pu}^{239}$  nucleus. In the given situation, the multipole type of these  $\gamma$ -transitions should be E2. This contradiction can be removed if we assume that the isomeric level of 384 kev [19], for which  $I_{384} = \frac{3}{2} \pm$ , has almost the same energy as the rotational level with  $I_{384} = \frac{7}{2} \pm$ . The 106 kev gamma-transition from the isomeric level is the more intense and would seem to mask the possible transition from the second rotational level. It may be expected that the latter level will be discovered in  $\alpha$ -decay of  $\text{Cm}^{243}$ . As was shown above, the 44 kev  $\gamma$ -transition is not just a magnetic dipole radiation (M1); the possibility of a mixture of some electric quadrupole is not excluded (E2). Thus the above-mentioned possible rotational levels in

the  $\text{Pu}^{239}$  nucleus may exist. It would therefore be very interesting to observe the monoenergetic group of  $\alpha$ -particles, which, presumably, should be observed in the decay of  $\text{Cm}^{243}$ , with energy  $E_{\alpha} = 5.67$  kev and intensity  $\lesssim 1\%$ .

We consider it a pleasant duty to express our gratitude to R. M. Polevoi and to Yu. F. Rodionov, who carried out the measurements of the  $\gamma$ -spectra on the scintillation spectrometer and proportional counter.

We also thank G. N. Yakovlev and V. A. Vorobyev for placing at our disposal chemically pure preparations of neptunium and curium, and P. E. Nemirovsky, Ya. A. Smorodinsky, and L. A. Sliv for participating in the considerations of the derived results. We are glad to express our acknowledgement to V. V. Beruchko, S. N. Belenky, and G. V. Shishkin for their help in measuring the electron spectra.

#### LITERATURE CITED

- [1] S. A. Baranov, K. N. Shlyagin, Proceedings of the Session of the Academy of Sciences USSR on the Peaceful Uses of Atomic Energy, July 1-5, 1955 (Meeting of the division of physico-mathematical sciences), page 251.
- [2] S. A. Baranov, A. F. Malov, K. N. Shlyagin, Apparatus and Experimental Techniques (in the press).
- [3] Construction and Theory of Reactors (Report of the Soviet delegation to the International Conference in Geneva on the Peaceful Uses of Atomic Energy). Acad. Sci. USSR Press, p. 49, 1955.
- [4] G. T. Seaborg, A. C. Wahl, J. W. Kennedy, NNES-PPR, 14B, 13 (1944).
- [5] A. H. Jaffey, L. B. Magnusson, NNES-PPR, 14B, 978 (1949).
- [6] M. S. Freedman, A. H. Jaffey, F. Wagner, Phys. Rev. 79, 410 (1950).
- [7] J. W. Mihelich, Phys. Rev. 87, 646 (1952).
- [8] H. Slätis, J. O. Rasmussen, H. Aterling, Phys. Rev. 93, 646 (1954).
- [9] H. Slätis, T. O. Passel, J. O. Rasmussen, Phys. Rev. 99, 42 (1955).
- [10] J. O. Rasmussen, F. S. Stephens, Jr., D. Strominger, B. Aström, Phys. Rev. 99, 47 (1955).
- [11] F. Asaro, S. G. Thomson, I. Perlman, Phys. Rev. 92, 694 (1953).
- [12] A. Bohr, R. Mottelson, Phys. Rev. 89, 1102 (1953).
- [13] A. Bohr, Kgl. Danske Videnskab. Selskab, Mat.-Fys. Medd. 14, 26 (1952).
- [14] A. Bohr, R. Mottelson, Phys. Rev. 90, 717 (1953).
- [15] A. Bohr, B. Mottelson, Beta- and Gamma-spectroscopy, 468 (1955).
- [16] E. P. Tomlinson, H. W. Fulbright, J. J. Howland, Phys. Rev. 83, 223 (1951).
- [17] R. L. Graham and R. E. Bell, Phys. Rev. 83, 222 (1951).
- [18] M. S. Freedman, F. Wagner, Jr., D. W. Engelkemeir, J. R. Huizenga and B. Magnusson editor G. T. Seaborg, Rev. Mod. Phys. 25, 469 (1953).
- [19] D. Engelkemeir and L. B. Magnusson, Phys. Rev. 99, 135 (1955).
- [20] J. M. Hollander, W. G. Smith and J. W. Mihelich, Bull. Am. Phys. Soc. 30, 7, 11 (1955).
- [21] Frank Asaro, S. G. Thompson and I. Perlman, cited by J. M. Hollander, I. Perlman and G. T. Seaborg, Rev. Mod. Phys. 25, 469 (1953).

## MEASUREMENT OF FAST-NEUTRON SPECTRA BY TIME OF FLIGHT

G. F. Bogdanov, A. A. Kurashov, B. V. Rybakov and V. A. Sidorov

## INTRODUCTION

Spectrometric investigations with fast neutrons have great scientific and practical significance. Existing methods of fast-neutron spectrometry are, however, far from satisfactory. Only for neutrons with energies up to 2-3 Mev are there a number of good spectrometric investigations. But even these have been carried out only because of the existence of sources of monochromatic neutrons with variable energy, and not because there exist good neutron spectrometers for this energy range.

The methods for determining energies of fast neutrons are, in most cases, based on the registration of protons or other recoil nuclei (photographic emulsions, Wilson chambers, ionization chambers, organic scintillation counters, telescopes of proportional or scintillation counters, and so on). But because the spectrum of recoil nuclei is continuous, for spectrometry, one must use only a few percent of the recoil nuclei. Besides this, the layers of material in which the recoil nuclei are produced (radiators) must, in most cases, be thin. Accordingly, the efficiency of neutron spectrometers is very low ( $\sim 10^{-5}$ ), even for poor resolving power ( $\sim 10\%$ ). All neutron spectrometric investigations conducted with such apparatus are rather crude, since existing neutron sources are insufficiently intense for them.

The spectrometric method with the highest efficiency of neutron registration is the time-of-flight method, which can use a highly efficient, although spectrally indifferent, neutron detector. This method has long been used in investigations with slow neutrons. The maximum neutron energy at which spectra have so far been successfully studied with the apparatus for time-of-flight spectrometry of slow neutrons (mechanical selectors, pulsed cyclotron) is about 1 kev [1]. The resolving power of such spectrometers is mainly limited by the duration of neutron pulses ( $1\mu$  sec). Application of the highly efficient scintillation counters in such apparatus gives the possibility of raising its resolving power only through increase of the distance of flight, and not through the small resolving time of the scintillation counters. By such means, the upper energy limit of the spectrometer can be raised only to 20 kev [2].

Contemporary scintillation counters, consisting of an organic phosphor and a photomultiplier, have resolving power  $\sim 1\mu$  sec ( $10^{-9}$  sec). With them one could measure a time of flight for a few meters for neutrons with energies of tens of millions of electron-volts. Spectrometers exist in which measurements are made on the time of flight of the neutron between two scintillation counters connected in a coincidence circuit [3-5]. The instant of emergence of the neutron is fixed by a counter placed close to the source of neutrons, by registering the radiation (usually  $\alpha$  or  $\gamma$ ) accompanying the production of the neutron. But such a scheme is not always possible, and in the case of registration of  $\gamma$ -rays, does not allow sufficiently high counting rates because of the large backgrounds of accidental coincidences.

The neutron spectrometer that seems most advantageous is one using a pulsed source of neutrons and one scintillation counter. In such a spectrometer, the efficiency of neutron registration can be brought up to some tens of percent and the counting rates can be sufficiently high with background not very large. The source of neutrons must give pulses of duration about  $1\mu$  sec (in agreement with the resolving time of the scintillation counter). The repetition period of the pulses must be near the time of flight to the counter of the slowest neutrons under investigation.

An apparatus of this type has been applied by Cranberg and Levine for the study of inelastic scattering of neutrons [6]. Pulses of neutrons of duration  $2\mu$  sec with repetition frequency  $7.4 \cdot 10^6$  per second are obtained from an electrostatic generator, whose beam is oscillated before reaching a tritium target by a sinusoidal deflecting voltage with frequency  $3.7 \cdot 10^6$  per second.



The present paper describes a neutron spectrometer used with a cyclotron, utilizing the natural modulation of the cyclotron beam.

### Principle and General Design of the Spectrometer

As is well known, the acceleration of particles in the cyclotron occurs only in a rather narrow phase interval of the high-frequency voltage (HF), while in the removal of the beam from the cyclotron by an electrostatic deflector, only part of this phase interval is utilized. Consequently, the particles arrive at the target in short pulses (less than  $1/20$ th the period of the HF) once per period. Information is available on the measurement of the duration of the pulses of a cyclotron beam and on the application of the natural modulation of the beam for time-of-flight measurement of the energy of primary particles [7-9].

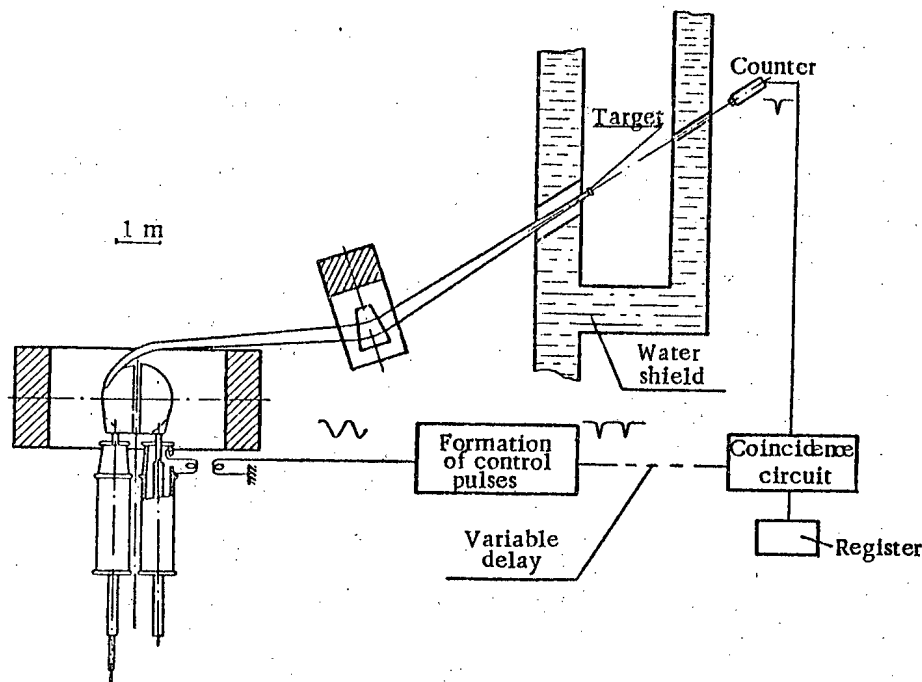


Figure 1. General scheme of the apparatus.

For example, Bloom [8], measuring the pulse width of an 18-inch cyclotron by a study of the coincidences of  $\gamma$ -rays with pulses synchronized with the HF, found that the pulse width was  $1-2 \text{ m}\mu$  seconds (period of HF  $54 \text{ m}\mu \text{ sec}$ ). Draper and McDaniel [10] used a cyclotron giving deuterons with energy 100 kev as a pulsed source of 14-Mev neutrons. The time of flight of these neutrons was measured for a distance of 60 cm. The instant of emergence of the neutrons from the target was fixed by the pulse of the deuteron current, increased by a broad-band amplifier.

The present work was done with a 150-cm cyclotron, whose beam was brought out of the vacuum chamber and was focussed by a magnetic prism at a distance of 12 m from the cyclotron. The general scheme of the apparatus is shown in Figure 1.

The repetition period of the pulses of particles was  $112 \text{ m}\mu$  seconds (the frequency of the accelerating voltage in the cyclotron was 8.9 megahertz). As will be shown below, the duration of the pulse on the target does not exceed  $5 \text{ m}\mu \text{ sec}$ . The neutrons and  $\gamma$ -rays emitted by the target are detected by a scintillation counter. The instant of detection of a particle by the counter is displaced from the moment of its emission by the target by its time of flight through the distance from target to counter. The pulses from the counter are delivered to the coincidence circuit, whose other arm receives pulses synchronized with the accelerating voltage of the cyclotron. By changing the amount of delay of these pulses, one can register pulses from the counter that have been produced at a time of any chosen phase of the accelerating voltage, i.e., register particles having one or another time of flight from target to counter. The instant of emergence of the par-

ticles from the target (the instant of impact of the primary particles on the target) is determined from the position of the  $\gamma$ -ray peak, produced by rays ordinarily resulting from various nuclear reactions in the target. This makes a special phase calibration unnecessary.

A monitor in the measurement of the coincidence counting rate is provided by a weak-current integrator [11], which measures the current of the primary beam on the target.

### Details of the Apparatus

The coincidence circuit. For time-of-flight measurement of neutron spectra, it would be extremely convenient to use a many-channel time analyzer, several varieties of which are already described in the literature [12-14]. But such analyzers require the use of amplifiers with distributed parameters for the preliminary amplification of the pulses from the photomultiplier, or of special tubes (for example, pentodes with secondary emission). The construction of such analyzers is in itself a major effort. Therefore, in the first stage of the development of a time-of-flight neutron spectrometer used with the cyclotron, for an experimental test of the fundamental principles of the method, we used the simplest possibility for measuring short times.

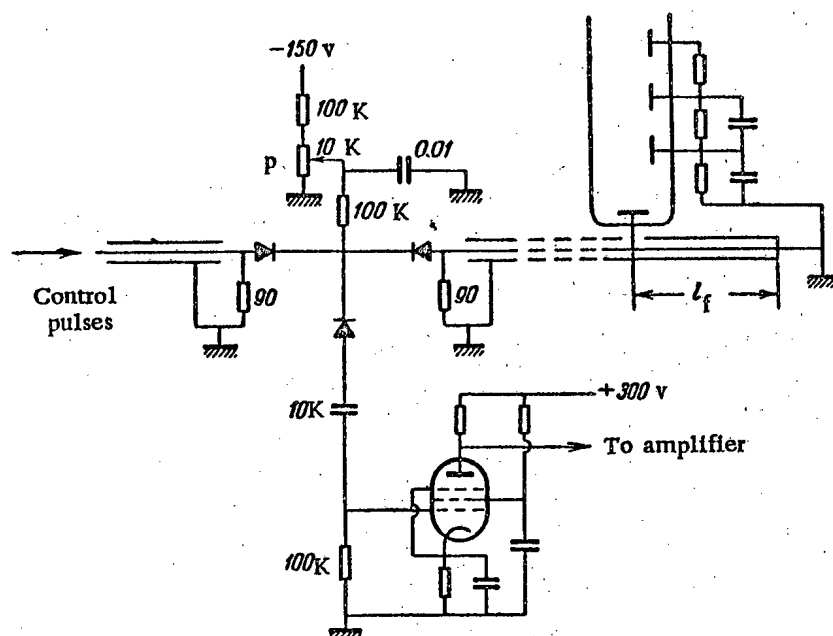


Figure 2. Coincidence circuit.

A coincidence circuit was used that does not require pre-amplification of the pulses (Figure 2). It is basically similar to the circuit described by De Benedetti and Richings [15], and is a parallel coincidence circuit using germanium diodes of type DGTs. After the circuit follows a linear amplifier (setting time  $0.2 \mu$  seconds, amplification coefficient  $\sim 20,000$ ) and an amplitude discriminator. Such a circuit has sufficiently high sensitivity and is simple to construct. By selection of the diodes and of their bias, given by the potentiometer P (Figure 2), it is easy to obtain a discrimination coefficient of about 50\*. At the same time the sensitivity of the circuit can be made at least such that coincidences of pulses of duration  $3 m\mu$  seconds and amplitude  $0.1 v$  are registered quite successfully.

Despite the fact that the characteristics of the diodes depend strongly on the temperature, to assure the necessary stability of the circuit parameters, it was sufficient to mount the germanium diodes on a separate chassis, thermally insulated from the amplifier chassis.

\*The discrimination coefficient is the ratio of the amplitude of the output pulse of the amplifier from a coincidence of similar pulses to the amplitude from an identical single pulse.

The resolving time of such a circuit is determined by the duration of the pulses delivered to it, right down to the input time constant ( $\sim 10^{-10}$  seconds).

The pulses were conducted to the coincidence circuit by a coaxial cable RK-2 with wave impedance 90 ohms.

The variable delay of the pulses in one of the arms of the coincidence circuit is accomplished by means of a commutator permitting change of the length of the conducting cable by steps of 0.2 m, which corresponds to delay of the pulse by 1 m  $\mu$  second.

The scintillation counter. The detector of neutrons is a scintillation counter, consisting of a plastic scintillator (a solid solution of terphenyl in polystyrene) and a photomultiplier. The pulse taken from the anode of the photomultiplier is formed by means of a shorted cable attached to the anode (cf. Figure 2). The conducting cable is matched to the end joined to the coincidence circuit.

The duration of the pulse after formation is  $\sim 3$  m  $\mu$  seconds. This value is near to the limit for the photomultiplier employed, and sets the main limitation on the resolving power of the spectrometer. In the spectrometer, we use a special photomultiplier, intended for fast coincidence circuits. Other available types of photomultipliers, in particular FEU-19, give poorer results.

The resolving time of a photomultiplier is determined by its construction. In the ideal photomultiplier, the pulse of anode current must repeat the form of the light pulse, i.e., rise instantly to maximum value and then fall according to the law of decay of luminescence of the scintillator. Then, as was shown by Post and Schiff [17, 18], the minimum resolving time of the scintillation counter is a statistical quantity, depending only on the decay time of the scintillator and the total number of photoelectrons in the pulse. In the case in question (neutron energy  $> 2$  Mev, decay time of scintillator luminescence  $\sim 3 \cdot 10^{-9}$  seconds), it is not greater than  $3 \cdot 10^{-10}$  seconds. But in a real photomultiplier, there is a broadening of the pulse basically due to inequality of length of the electron trajectories. Consequently, the anode current pulse takes some time to grow to its maximum value. If the time of growth of the pulse were close to zero, the pulse duration  $\tau'$  after its formation by the shorted cable of length  $l_f$  would be  $\tau_0 = \frac{l_f}{v}$ , where  $v$  is the speed of propagation of the pulse along the cable. In actual fact  $\tau' > \tau_0$ , and as  $\tau_0$  is decreased to zero,  $\tau'$  approaches some minimum value  $\tau_{\min}$  for the given photomultiplier, a value determined by the time of growth of the anode current pulse.

For the selection of a photomultiplier with optimal resolving time, we conducted measurements of  $\tau_{\min}$  for the available types of photomultipliers. For this purpose, the plastic scintillator, placed at the photoelectric cathode, was irradiated with  $\gamma$ -rays. The pulses were formed by a shorted cable attached to the anode of the photomultiplier, and were conducted to both inputs of the coincidence circuit. The counting rate of such artificial coincidences ("self-coincidences") was measured in its dependence on the delay of the pulses in one of the arms. Curves were taken for different lengths of the shorted cable. One of them is shown in Figure 3 (curve a). As the delay is increased, the counting rate of the self-coincidences falls, approaching zero for some value of the delay. The gradual fall of the counting rate is caused by the fact that the spectrum of pulses contains all amplitudes from zero to the maximum value, and the coincidences of pulses of small amplitude are registered only when the overlap is large enough. Coincidences of pulses of large amplitude (in comparison with the effective threshold of the circuit) cease to be registered only for delay of one of the pulses by a time  $\tau'$  equal to its width. Figure 4 shows the dependence of the pulse width  $\tau'$  so measured on  $\tau_0 = \frac{l_f}{v}$  for two types of photomultipliers (FEU-19 and the special type). Extrapolation of the curves obtained to  $\tau_0 = 0$  gives for FEU-19  $\tau_{\min} \sim 10^{-8}$  seconds, and for the special photomultiplier  $\tau_{\min} \sim 2 \cdot 10^{-9}$  seconds.

The rise time of the pulse thus determined does not fully characterize the resolving power of a photomultiplier, because the self-coincidence method excludes the statistical spread of the times taken by the pulse to travel from the photoelectric cathode to the anode. To estimate this spread we studied the coincidences in the registration of annihilation  $\gamma$ -quanta from a preparation of  $\text{Na}^{22}$  by two scintillation counters. The pulses were formed by shorted cables of such length that  $\tau_0 = \tau_{\min}$ , and the coincidence counting rate was measured as a function of the delay of one of the pulses. The curve of delayed coincidences for the special photomultiplier is shown in Figure 3 (curve b). The curve of delayed self-coincidences shown in the diagram (curve a) was taken with a forming cable of the same length. Comparison of the curves shows that the spread of travel times is of the same order as the time of growth of the pulse.

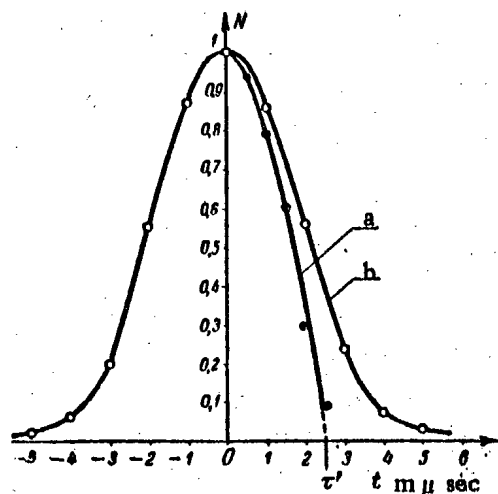


Figure 3. Coincidence counting rate as function of the delay of one of the pulses (special photomultiplier). a) "self-coincidences"; b) coincidences of pulses from two scintillation counters detecting annihilation  $\gamma$ -quanta from a preparation of  $\text{Na}^{22}$ . Both curves taken for length of forming cable  $l_f = 20$  cm, which corresponds to  $\tau_0 = 2 \cdot 10^{-9}$  sec.

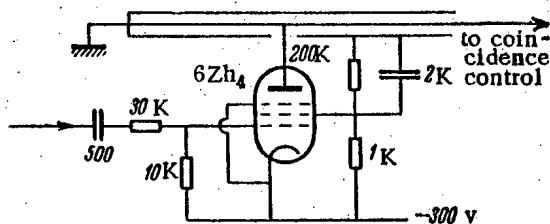


Figure 5. Forming circuit of the control pulses.

assembly and the individual parameters of the tube. The circuit does not work very stably and requires meticulous adjustment, in spite of its apparent simplicity.

In further work, it is proposed to form the control pulses by means of an electron-beam tube with deflected beam.

#### Time and Energy Resolving Power

The resolving time of the spectrometer is composed of the resolving time of the coincidence circuit and the duration of the pulse of primary particles on the target. It can be determined experimentally by studying the distribution in time of the  $\gamma$ -rays emitted by the target. For the adjustment of the spectrometer, we used the radiation from a tritium-zirconium target bombarded by protons. The counter was placed at a distance of 3 m from the target at angle  $0^\circ$  with the direction of the primary beam. Figure 6 shows the counting rate of the particles emitted by the target as function of their time of flight for the distance from target to counter. The upper curve was taken for proton energy 7.2 Mev, the lower for energy 4.8 Mev. Each curve shows two maxima. The first peak, at 10 m $\mu$  sec., corresponds to the detection by the counter of  $\gamma$ -rays produced in the interaction of the protons with zirconium. The second peak is formed by neutrons from the reaction  $T(p, n)\text{He}^3$ . The zero of the time scale was fixed after the identification of the  $\gamma$ -ray peak. The

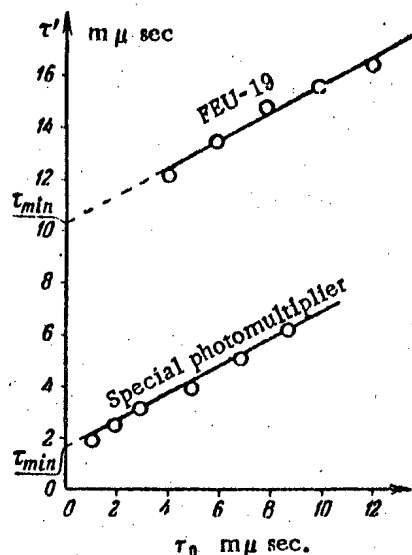


Figure 4. Dependence of the width  $\tau'$  of the shaped pulse on  $\tau_0 = \frac{2l_f}{v}$ , where  $l_f$  is the length of the forming cable and  $v$  is the speed of the pulse in the cable.

Formation of control pulses. The control pulses, synchronized with the HF of the cyclotron, are formed from the sinusoidal accelerating voltage by a circuit using a pentode 6Zh4, as shown in Figure 5. The HF voltage of amplitude 300 v is taken by a coupling loop from the resonance line of one of the dees. The length of the shorted cable corresponds to a duration of the formed pulse of 3 m $\mu$  sec. The choice of the resistances in the circuit and of the HF voltage was conducted empirically because of the strong dependence of the amplitude and shape of the pulse obtained on the

$\gamma$ -ray peak could be distinguished from a neutron peak either by replacing the target by a "flag" (zirconium without tritium on the same base as for the target), or by changing the distance from target to counter, or, finally, by changing the energy of the protons.

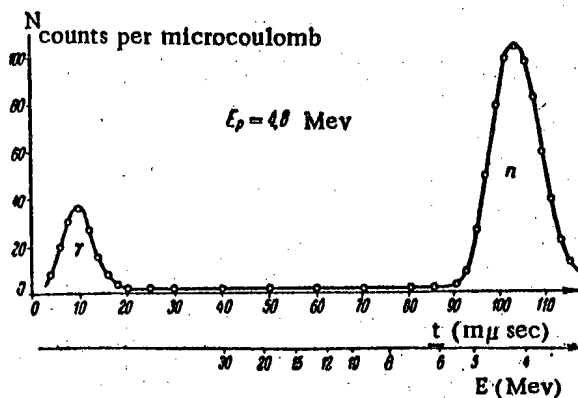
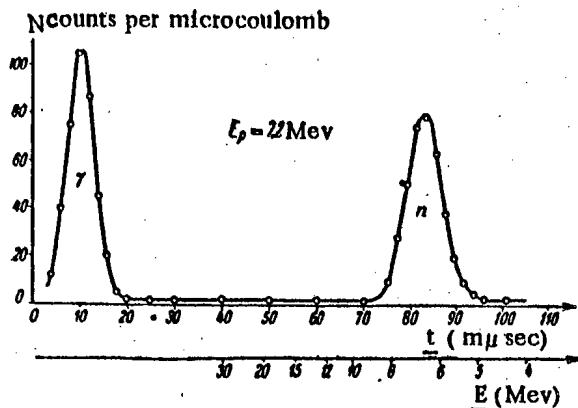


Figure 6. Counting rate of particles emitted by a tritium-zirconium target bombarded by protons, as function of their time of flight for the distance to the counter.

When the proton energy was reduced from 7.2 to 4.8 Mev, the neutron energy fell from 6.4 to 4.0 Mev, and the time of flight increased, so that the neutron peak was displaced to the right (Figure 6). With decreased proton energy, the sizes of the peaks were also changed. There were markedly fewer  $\gamma$ -rays, and the intensity of the neutrons grew to almost double the previous value, in agreement with the increase of the cross section for the reaction  $T(p, n)He^3$  (the sensitivity of the spectrometer for neutrons with energies 6.4 Mev and 4.0 Mev was roughly the same).

The half-value width of the  $\gamma$ -ray peak gives the resolving time of the spectrometer. As is seen from Figure 6, it is close to 7 mμ sec. From this it follows that the duration of the pulse of particles at the target does not exceed 5 mμ sec. The neutron peak is somewhat wider than the  $\gamma$ -ray peak because of the non-monochromaticity of the neutrons (the thickness of the target was 0.5 Mev for protons of energy 7 Mev).

The energetic resolving power of the spectrometer depends on both its resolving time and on the size of the base  $L$  (distance from target to counter). In the study of continuous neutron spectra, the size of the base is limited by the repetition frequency of the pulses of primary particles on the target.

The time of flight of a neutron with energy  $E$  for the distance  $L$  is

$$t_{\text{m}\mu\text{ sec.}} = \frac{72L(\text{m})}{\sqrt{E(\text{Mev})}} \quad (1)$$

If the repetition period of the pulses of particles on the target is denoted by  $T$  (in our case  $T = 112$  mμ sec) and the energy threshold of the counter by  $B$ , then the condition for the maximum value of  $L$  can be written

$$\frac{72L_{\text{max}}}{\sqrt{B}} = T + \frac{72L_{\text{max}}}{\sqrt{E_{\text{max}}}} \quad (2)$$

This condition means that the maximum length of the base is such that the slowest of the neutrons detected in the previous pulse arrive at the detector simultaneously with the fastest neutrons of the pulse in question. Then

$$L_{\text{max}} = \frac{T}{72 \left( \frac{1}{\sqrt{B}} - \frac{1}{\sqrt{E_{\text{max}}}} \right)} \quad (3)$$

and the limiting resolving power of the spectrometer is

$$\frac{\Delta E}{E} = \frac{2\pi}{t} = \frac{2\pi\sqrt{E}}{72L_{\text{max}}} = \frac{2\pi}{T} \sqrt{E} \left( \frac{1}{\sqrt{B}} - \frac{1}{\sqrt{E_{\text{max}}}} \right) \quad (4)$$

Here  $\tau = 7 \text{ nsec}$  is the resolving time of the spectrometer.

If the energy threshold of the counter is  $B = 2 \text{ Mev}$  (sufficiently low for most of the work with 14-Mev deuterons), and the maximum energy of the neutrons is  $E_{\text{max}} = 20 \text{ Mev}$ , then  $L_{\text{max}} = 3 \text{ m}$  and the limiting resolving power of the spectrometer for the investigation of the continuous neutron spectrum is

$$\frac{\Delta E}{E} = 0.061 \sqrt{E}.$$

$$\text{For } E = 3 \text{ Mev} \quad \Delta E/E = 10 \%.$$

$$\text{For } E = 7 \text{ Mev} \quad \Delta E/E = 16 \%.$$

$$\text{For } E = 15 \text{ Mev} \quad \Delta E/E = 24 \%.$$

If the neutron spectrum has a lower limit  $E_{\text{min}} > 2 \text{ Mev}$ , or if only the hard part of the spectrum is of interest and the energy threshold of the counter can be made higher than 2 Mev, the resolving power of the spectrometer can be raised correspondingly by increasing  $L$ . For example, for  $E_{\text{min}} = B = 5 \text{ Mev}$  and  $E_{\text{max}} = 20 \text{ Mev}$ ,  $L_{\text{max}} = 7 \text{ m}$  and the limiting resolving power of the spectrometer is  $\Delta E/E = 0.028 \sqrt{E}$ .

$$\text{For } E = 7 \text{ Mev} \quad \Delta E/E = 7 \%.$$

$$\text{For } E = 15 \text{ Mev} \quad \Delta E/E = 11 \%.$$

The energy threshold of the counter  $B$  should always be raised to  $E_{\text{min}}$  to reduce backgrounds.

In the investigation of neutron spectra consisting of one or several narrow energetic groups, the resolving power of the spectrometer can also be raised by taking  $L > L_{\text{max}}$  in such a way that the group being studied falls in an "open space" in the following period or after several periods.

In later work on the improvement of the resolving power of the spectrometer it is proposed to reduce artificially the repetition frequency of the pulses of particles on the target, and also to improve somewhat the resolving time of the spectrometer.

### Efficiency and Spectral Sensitivity

The efficiency of a scintillation counter for neutrons with energy 2 - 20 Mev amounts to several percent (the plastic scintillator used in the first work had diameter 3 cm and thickness 1.5 cm). Despite the small solid angle subtended by the counter (for  $L = 3 \text{ m}$ ,  $\omega \sim 10^{-4}$  steradian) the counting rate was high enough in all cases. With a proton current of 1 microampere on a thin tritium-zirconium target the maximum neutron counting rate was about  $5 \cdot 10^3$  counts per minute. In many cases (particularly in the work with deuterons) the neutron spectra could be studied with considerably smaller currents ( $\sim 0.01 \mu \text{ amp}$ ).

If necessary, the efficiency of the counter and the solid angle it subtends can be considerably increased by increasing the size of the scintillator.

For the comparison of intensities of different parts of spectra and for the determination of neutron production cross sections, it is necessary to know the spectral sensitivity of the apparatus. The intensity of a particular group of neutrons is proportional to the area under the corresponding peak in the spectrum. The variation with energy of the proportionality coefficient is determined by the energy dependence of the efficiency of the scintillation counter. In neutron detection, the flashes of light in the organic scintillator are produced by recoil nuclei of hydrogen and carbon. The scintillations from recoil carbon nuclei can be neglected, since their mean energy is less than that of the recoil protons, and the light yield per unit energy dissipated in the scintillator is much less for them than for the protons. The detection of events of inelastic reaction of neutrons with carbon (the reactions  $\text{C}^{12}(n, \alpha)\text{Be}^9$  and  $\text{C}^{12}(n, n')^3\alpha$ ) begins to make an appreciable contribution to the efficiency of the scintillator at neutron energies higher than 12 Mev [18]. Consequently the efficiency of the counter for neutrons with energy  $E$  (where  $E < 12 \text{ Mev}$ ) is proportional to the quantity  $\sigma(E) \left(1 - \frac{B}{E}\right)$ , where  $\sigma(E)$  is the known scattering cross sections of neutrons on protons and  $B$  is the energy threshold of the counter, which in the present case depends on many parameters of the circuit (in particular,

on the amplitude of the control impulses and the operation of the coincidence circuit).\*

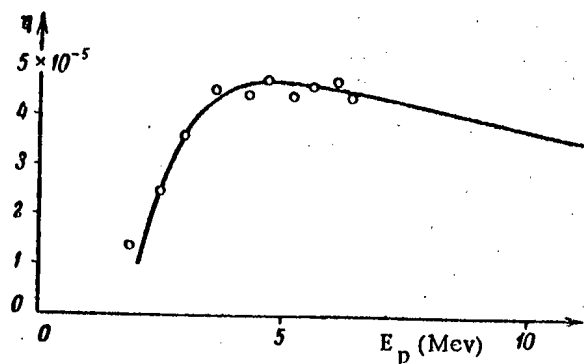


Figure 7. Energy dependence of the efficiency of the spectrometer. Division of the area of a neutron peak, expressed in units  $(\frac{1}{\text{sec.}} \cdot \text{m} \mu \text{ sec})$  by the quantity  $\eta$  corresponding to the neutron energy gives the neutron flux in units  $(\frac{1}{\text{sec} \cdot \text{steradian}})$ .

Thus the expression for the spectral sensitivity has the form

$$\eta(E) = A\sigma(E) \left(1 - \frac{B}{E}\right). \quad (5)$$

After each change of the circuit parameters, the spectrometer was calibrated with a known neutron flux produced in the reaction  $T(p, n)\text{He}^3$  [1], [19]. The calibration consisted of measurements of the sensitivity of the spectrometer for several neutron energies. On the basis of these measurements, the constants A and B were determined and the curve of spectral sensitivity was calculated. One of the calibration curves is shown in Figure 7 together with the experimental points obtained with  $L = 3 \text{ m}$ .

#### SUMMARY

The time-of-flight neutron spectrometer used with the cyclotron opens up broad new possibilities of use of the cyclotron for the study of nuclear reactions. We shall enumerate several of them. The efficiency of the spectrometer can be brought up to several tens of percent, which permits the study with existing neutron fluxes of secondary processes (for example, the spectra of scattered neutrons entirely free from the background of  $\gamma$ -rays produced in the target. The spectrometer gives the possibility of studying neutron spectra on a background of harder and more intense groups, thanks to which the first works on the study of neutron spectra [20,21] already gave new physical results. The use of several counters, connected in the spectrometer circuit and in coincidence circuits with each other, allows the study of neutron spectra accompanied by a definite secondary particle, and also of the angular correlations of particles emitted by the target (for example, the angular correlation of  $\gamma$ -quanta with neutrons of definite energy).

The difficulties encountered in the work are mostly connected with instability of the cyclotron. The taking of a spectrum with the existing one-channel circuit requires about an hour. During this time, the phase of ejection of the particles from the cyclotron may change relative to the HF phase because of a change of some of its parameters, and this seriously damages the accuracy of the measurements.

In work with deuterons, there are rather large backgrounds of neutrons and  $\gamma$ -rays produced outside the target. These may be taken into account by making difference measurements (target - "flag"), since the counting rate is sufficiently high. But the instability of the cyclotron makes the backgrounds variable, which decidedly decreases the reliability of the procedure.

To increase the accuracy of the results obtained with the spectrometer, we are now conducting work in two directions: stabilization of the cyclotron and construction of a multichannel circuit.

We are deeply grateful to N. A. Vlasov and S. P. Kalinin for their constant interest in the work and their great help in the solution of both theoretical and practical problems.

We also thank the collaborators of the cyclotron laboratory, who have aided in the carrying out of this work.

\* Consequently, the circuit will have a channel fixing the energy threshold of the counter.

## LITERATURE CITED

- [1] N. A. Vlasov, Neutrons, State Technical Press (1955).
- [2] L. Bollinger, G. Thomas, R. Palmer, Phys. Rev. 91, 452 (1953).
- [3] G. K. O'Neill, Phys. Rev. 92, 853 (1953).
- [4] A. Ward, Nature 173, 771 (1954).
- [5] D. B. James, P. B. Freacy, Proc. Phys. Soc. (London) 64(A), 847 (1951).
- [6] Cranberg, D. F. Levin, Phys. Rev. 100, No. 434 (1955).
- [7] J. H. Manley, M. J. Jakobson, Rev. Sci. Instr. 25, 368 (1954).
- [8] S. D. Bloom, Phys. Rev. 98, 233 (1955).
- [9] S. D. Bloom, C. O. Muchlhausen, H. E. Wegner, Phys. Rev. 99, 654 (1955).
- [10] J. E. Draper, B. D. McDaniel, Phys. Rev. 90, 362 (1955).
- [11] A. A. Kurashov, A. F. Linev, Apparatus and Experimental Technique (in press).
- [12] G. R. I. McLusky, N. F. Moody, Electronic Eng. 24, 330 (1952).
- [13] J. W. Keuffel, Rev. Sci. Instr. 20, 197 (1949).
- [14] N. F. Moody, Electronic Eng. 24, 289 (1952).
- [15] S. De Benedetti, H. J. Richings, Rev. Sci. Instr. 23, 37 (1952).
- [16] R. F. Post, L. I. Schiff, Phys. Rev. 80, 1113 (1950).
- [17] R. F. Post, Nucleonics 10, No. 6, 56 (1952).
- [18] G. M. Frye, J. L. Rosen, L. Stewart, Phys. Rev. 99, 1375 (1955).
- [19] N. A. Vlasov, S. P. Kalinin, A. A. Ogloblin, L. N. Samoilov, V. A. Sidorov, and B. I. Chyev, J. Exptl.-Theoret. Phys. (USSR) 28, No. 6 (1955).
- [20] G. F. Bogdanov, N. A. Vlasov, S. P. Kalinin, B. V. Rybakov, and V. A. Sidorov, J. Exptl.-Theoret. Phys. (USSR) 30, 185 (1956).
- [21] G. F. Bogdanov, N. A. Vlasov, S. P. Kalinin, B. V. Rybakov, and V. A. Sidorov, J. Exptl.-Theoret. Phys. (USSR) (in press).



## PRINCIPLES OF ACCELERATION OF CHARGED PARTICLES \*

V. A. Veksler

In the course of the last few years experimental physics has solved the problem of producing particles in the laboratory with energies of the order of a few billion electron volts. Such particles were previously observed only in cosmic rays, and then only in minute quantities. The artificial production of intense beams of particles with these energies, whose direct acceleration would require electric fields of several billion volts, gave the opportunity for discovering and studying many phenomena having basic significance for the understanding of the physics of the atomic nucleus and of elementary particles. There arose a new (and, perhaps, most comprehensive) field in modern nuclear physics, namely the physics of high energy particles, based on the new techniques of accelerating charged particles. The rate at which this new field has developed is indeed extraordinary. In the course of a few years discoveries followed one on the other.

The new accelerators not only gave the opportunity for achieving and studying the deep penetration of the atomic nucleus, but opened wide possibilities for the artificial synthesis of matter. One after another, atoms of the transuranic elements were created. With the help of accelerators it became possible to create various new particles artificially, to study their properties, and to get results of extremely great basic importance. All these various results were gotten owing to the rapid development of experimental methods, which allowed the acceleration of charged particles to tremendous energies.

Cockroft and Walton in 1932 were the first to succeed in achieving nuclear reactions with the help of protons accelerated in a constant electric field of a high-voltage tube. The Van de Graaff generator found wide application in nuclear investigations. However, with the aid of such linear methods it is not possible to accelerate particles to energies higher than 5-10 Mev, since for such high voltages it is difficult to achieve the insulation necessary for this purpose, and to prevent breakdown. Physicists chose to avoid the direct attack on this problem, and took the easy path. High voltages can be avoided if the accelerated particles are made to pass through the same relatively small potential difference many times, so that they store up the necessary energy gradually.

There are many means for the achievement of this idea. Some of them, for example linear accelerators, may in the future be widely used; however, up to the present time, the most basic are the so-called cyclic accelerators, in which the particle motion is performed along closed or almost closed trajectories.

In the following we will consider only cyclic accelerators.

The Cyclotron. As is well known, the famous Lawrence cyclotron is an instrument in which charged particles, moving in a magnetic field in almost closed orbits, and constantly returning (in their motion along semicircular trajectories) to the slit between dees with a relatively low voltage, pass many times through an electric field of always the same direction, and thus rapidly build up their energy.

As the particle velocity increases, so does the radius of the circle on which it moves in the uniform magnetic field (and, correspondingly, the length of its path between successive transitions through accelerating field).

The working principle of the cyclotron is based on the fact that until the particle accumulates a very large amount of energy, the time interval  $T$  during which it makes one revolution in the uniform magnetic field does not depend on the velocity  $v$  of the particle. This time interval is proportional to the ratio of the radius  $R$  of the circle on which the particle moves to its velocity  $v$ . Since the radius of

\*Lecture read at the international scientific-technical conference on the peaceful uses of atomic energy in Geneva in August, 1955.

this circle is itself proportional to the velocity,

$$R = \frac{mvc}{He} \quad (1)$$

the ratio  $R/v$  is independent of it. Therefore, if the frequency  $F_f$  of the alternating electric field which accelerates the particles is chosen so that it is equal to the frequency of rotation of the particles,

$$F = \frac{He}{mc} = F_f \quad (2)$$

then the particles will move in resonance with the electric field, and will be constantly increasing their energy; the "rhythm" of the particle motion and the "rhythm" of the accelerating electric field (which periodically changes direction) coincide in this case.

The successes achieved with the help of the cyclotron as well as with the new cyclic accelerators which appeared in 1940 — the betatrons — were accompanied by the improvement of these instruments and more thorough investigation of the mechanics of their operation. As for the betatrons, they are practically useless for the acceleration of heavy particles, and can be used only for the acceleration of electrons. In addition, for the study of nuclear forces physicists needed projectiles which would effectively interact with atomic nuclei, that is nuclear particles: protons, deuterons, and such. It is for this reason, of course, that the original hopes were based on the cyclotron. It was soon established, however, that charged particles cannot be given very high energies by the cyclotron. Indeed, Equation (2) shows that the frequency of rotation of the particles in the cyclotron depends on the particle mass. As the energy increases, the mass of the particle, which was assumed in Equation (2) to be constant, will, according to relativistic mechanics, also increase; as a result, the resonance between the rotational frequency and that of the alternating electric field  $F_f$  which accelerates the particles will be destroyed. As a result of such a destruction of resonance, the maximum energy which can be imparted, for example, to protons accelerated in a cyclotron is very close to 10-20 Mev.

Notwithstanding many attempts to solve the problem, the technique of accelerating particles with a cyclotron was arrested at the above mentioned level (in the sense of the maximum achievable energy) for more than ten years. It seemed that the "door" to significantly higher energies was shut tight. Wide acceptance was given to the point of view that the relativistic effect of mass increase quite generally limited the possibility of accelerating particles.

I and, somewhat later, MacMillan (Berkeley, California) succeeded in showing that this point of view was mistaken, and that the resonance method of acceleration still had enormous unrealized possibilities.

Let us describe here the entirely simple considerations which, 11 years ago, allowed us to move on from the impasse in the solution of this problem and then laid the basis for a new extremely complicated technique for acceleration of particles to very high relativistic energies. For this we will have to return to previous considerations. To a certain extent the reason for the skeptical attitude to the resonance method was explained by the fact that analysis of the mechanism of cyclotron acceleration actually always stopped half way through: only that part of the full cycle of the particle motion was considered for which the energy increases with time. No attention was paid to the fact that in the usual situation the energy change of particles in a cyclotron in no way resembles continuous increase along the energy scale, but much more nearly reflects the behavior of a pendulum, whose kinetic energy does not increase to a maximum, but falls to zero. I shall try now to clarify this perhaps at first paradoxical assertion.

Let us examine how the process of energy change of the particles takes place in the cyclotron. At first, as the energy increases, so does the velocity. As a result of the relativistic effect, the mass of the particles also increases. This causes the radius of the circle in which the particles move to increase faster than the velocity, and thus the time

$$T = \frac{2\pi (m_0 c^2 + W)}{He c} \quad (3)$$

that the particles spend in one revolution also gradually increases.

Lengthening of the period causes the particles to pass through the space between the dees at instants of time when the amount of energy transferred to these particles becomes gradually smaller and smaller. Finally, for some  $K$ -th revolution, the particles will pass through the slit in the dees at such a moment that, the electric field will be equal to zero. At this point, the acceleration cycle ends. For further revolutions the

electric field will no longer accelerate, but will slow up the particles, and they will be forced to give back the energy that they have stored up. The decelerating process will be exactly symmetric to the accelerating process, and therefore the particles will slow up to the same energy as that with which they started their motion in the accelerating cycle. After this (if we ignore the possibility that the particles may hit the ion source), the whole process repeats in its entirety. Thus the motion of particles in a cyclotron will actually be periodic: the particle will be alternately either on the crest of a wave of accelerating voltage, or in the zero "phase", passing between the dees at the instant when the accelerating voltage is zero, or in the "phase" of opposite sign, decelerating in the electric field of the dees. The change of phase will be periodic, and therefore in the following we shall speak of phase oscillations of the particles. At the same time the energy and radius of the particle trajectory will also be periodic, first increasing and then decreasing.

Of course, no one would think of using an actual cyclotron for such a senseless game, in which the energy gained in the first half is entirely lost in the second.

Naturally, physicists always tried to end the game after the first, and for them profitable, stage. Therefore particles were used immediately after the attainment of maximum energy. As will be shown below, however, the possibility of realizing phase oscillations in accelerators of similar type is of fundamental import, and promises a much higher gain than can be achieved by the cyclotron.

Self-phasing. Let us imagine that we succeeded in establishing conditions such that after each full cycle of phase oscillations the particle had a gain in energy. Clearly in this case it pays to prolong the game as much as possible. What must be done, then, to realize such a promising prospect? In order to answer this, let us remember that in a cyclotron the average energy gain per cycle of phase oscillations is equal to zero only because these oscillations are symmetric. The energy the particles gain in passing through the slit of the dees at those instants of time when the field is accelerating the particles, they lose in going through the decelerating field. The "equilibrium point" about which the phase oscillations vibrate is, therefore, that value of the electric field's phase for which the potential difference between the dees is equal to zero: the zero phase. Let us now attempt to displace the point about which the phase oscillations take place into the region of positive values of the phase. It is easy to prove that in this case, after completion of each cycle of phase oscillations, the particle has gained a decidedly significant amount of energy. Actually the phase oscillations will take place now as before, but in the course of these oscillations the particle either will never pass through the slit in the dees at those instants when the electric field decelerates the particles,\* or it will get energy during a large part, and lose it during a small part of the cycle.

The energy gained during the first part will be greater than the energy returned during the second part of the cycle. If we can succeed in maintaining this state of affairs sufficiently long, then the energy given to the particle can be made as large as desired. It turns out that the above state of affairs can be realized by some very simple methods.

The simplest way of doing this is slowly to vary any one of the parameters of the accelerator in time (in any given way); for instance, the magnetic field or the frequency of the accelerating electric field. Let us consider, for instance, an accelerator in which the frequency remains constant, and the field increases slowly in time (in comparison to the period of rotation). From Equation (3) it is seen that in this case such groups of particles can always be found which, in passing through the slit of the dees, will undergo an increase in energy and, in spite of this, will be displaced in phase in opposite directions toward each other. Actually the particles which undergo energy increases insufficient to compensate for the decrease in the length of the rotation, will descend in phase in the direction of increasing energy increments. Particles, on the other hand, receiving energy increments larger than is necessary for maintaining constant time of rotation will be displaced in the direction of smaller increments. In this way the phases of both groups of particles will clearly oscillate about the stable equilibrium point, remaining in that region of potential difference which will accelerate the particles.

Since the average rise in energy in one cycle of phase oscillations is equal to the product of the number of rotations per cycle and the "equilibrium" potential difference, the energy increase of the particles will be the same as that for particles which were in the "equilibrium phase" from the beginning (and therefore did not experience phase oscillations). Therefore, an "oscillating" particle will accumulate energy the same way. The process of accumulation of energy, that is, of acceleration of the particles, will continue as long as the point about which the oscillations take place lies above zero, that is, so long as the magnetic field is monotonically increasing or the frequency of the accelerating electric field is decreasing.

---

\* If the amplitude of these oscillations is less than the displacement of the point of equilibrium of the phase from the null point.

The state of affairs under consideration is called self-phasing. It is clear that self-phasing will take place only if the amplitude of the potential difference between the dees, which accelerates the particles, is greater than the voltage corresponding to the equilibrium point.

Self-phasing turned out to be a remarkably fruitful principle, leading to extremely fast rise in the energy range. Present resonance accelerators, based on the self-phasing principle, have increased the upper energy limit by a factor of thousands over that of a cyclotron, and allowed proton accelerations to energies of  $10^9 - 10^{10}$  ev, and perhaps even to energies of  $10^{11}$  ev. Resonance accelerators for electrons — synchrotrons — allow acceleration of these particles to billions of electron-volts, and it would seem that the limit has not yet been reached. Let us now consider very briefly, of course, the particular characteristics of the basic types of cyclic resonance accelerators.

The Synchrotron. The synchrotron is a resonance accelerator for electrons. The essential advantage of the synchrotron over the other cyclic electron accelerator, the betatron, of which we have already spoken, is the ability to drastically reduce the weight and strength of the electromagnet by constructing the pole pieces in the form of a narrow ring. This is because, for relativistic velocities, the accelerating mechanism automatically maintains the constancy of the electron orbit radius.

When electrons, as opposed to heavy particles such as protons, move under cyclic conditions, a significant role is played by the electromagnetic radiation emitted by the electrons.

The Soviet physicists Pomeranchuk, Ivanenko, and Artsimovich were the first to direct their attention to the fact that this radiation interferes with the mechanism of betatron operation, and establishes the maximum electron energy at a few hundred billions of electron-volts.

As opposed to the betatron, the resonance accelerator, or synchrotron, possesses the marvelous property that the occurrence of electromagnetic radiation does not interfere with the accelerating mechanism, as there is an automatic compensation for the radiation losses. This compensation occurs because the radiation losses reduce the electron energy and therefore reduce the duration of a rotation. Therefore the equilibrium phase is displaced in the direction of large accelerating voltages, and the particles receive some additional energy (in comparison to what they would get in the absence of radiation), which compensates for the losses.

In order to solve many problems of elementary particle physics, it is necessary to have electrons (and gamma-rays) of much larger energies, or of the order of several billion electron-volts. It seems to me that at the present time it is possible to construct a synchrotron designed for the production of 5-10 Bev electrons.

The Phasotron. The principle of phase stability led to particularly great successes in the acceleration of ions. There are two types of accelerators for heavy particles based on this principle. One of these is similar to the usual cyclotron (in the Soviet Union it is called a phasotron\*\*), and the other is a particular kind of combination of a synchrotron and a phasotron, which we call a synchrophasotron.

The phasotron differs from a cyclotron in that in a phasotron the frequency of the accelerating electric field is modulated in time. Just as in the cyclotron, the trajectory of the particles in a phasotron is an unwinding spiral. As opposed to the cyclotron, the difference in radius for each step of the spiral is very small, and for large energies it is only a few hundred microns. This caused by the fact that for frequency modulation rates close to 100 cycles, the uniform energy increase of the particles each time that they pass through the accelerating slit of the phasotron is a quantity of the order of  $10^4$  ev. The small change in radius for the spiral makes it difficult to extract the particles from the phasotron. Usually it is possible to remove about 0.1 percent of the particles. Effective beam extraction, realized by Dmitrievski and others on the Soviet phasotron, allowed the extraction of 5 percent of the beam of protons accelerated to 680 Mev.

At the present time there are 10 phasotrons operating in the world, giving particle beams with several hundred million electron-volts energy. In particular, in the Soviet Union the largest phasotron in the world is operating, constructed under the supervision of Meshcheryakov, Efremov, and Mintz, giving proton beams of 680 Mev. The magnet of this enormous accelerator weighs about 7000 tons. The diameter of the pole pieces of the electromagnet is 6 meters. The gap for the vacuum chamber of this phasotron is equal to 60 cm. The accelerator is able to operate at various pulse rates, and usually gives 80 pulses per second. The accelerated proton current attains  $0.3 \mu\text{a}$ .

\* Of course this compensation takes place within definite limits — until the radiation losses per rotation are as large as the maximum energy increase of the particles in the same time.

\*\* In England and America this accelerator is called a synchrocyclotron.

In spite of the great effectiveness of phasotrons when used basically as generators of  $\pi$ -mesons, it is not the phasotron, but another accelerator, a cross between a phasotron and a synchrotron called a synchrophasotron, which is most effective for the acceleration of ions to the highest energies.

The Synchrophasotron. In the Soviet Union, synchrophasotron is the name used to designate the accelerator in which an increasing magnetic field is used to regulate the trajectory of the particles, and the acceleration is accomplished by a varying electric field whose frequency increases in time. The accelerators constructed in America called the bevatron and the cosmotron and that in England called the proton synchrotron operate on the principle of the synchrophasotron. As far as the author knows, the first use of the synchrophasotron for the acceleration of heavy particles was suggested by Oliphant.

Crane was the first to direct his attention to the fact that the variation of the frequency of the electric field according to a formula depending on the magnetic field strength in the gap of the accelerator electromagnet allows the maintenance of a constant radius of curvature for all energies of the accelerated particles. In this case the pole pieces of the synchrophasotron electromagnet can be made in the form of a narrow ring. In all the large accelerators, for instance the bevatron, cosmotron, and others, the radial thickness of the ring is approximately 5-10 percent of the equilibrium orbit radius. Such construction allows the weight of the electromagnet and the power necessary for its operation to be some ten times smaller.

Present-day synchrophasotrons are enormous engineering jobs. To give an idea of the scale of the job undertaken in constructing these accelerators, I will present some data on the world's largest synchrophasotron, whose construction is being completed in the USSR. The magnet of the accelerator consists of four quadrants of average radius 28 meters, separated by straight sections, each 8 meters long. The weight of the magnet is about 36,000 tons, and the power consumption is 140,000 kilowatts. For simplification of the beam removal, the vacuum chamber is made in two parts with separate vacuums. Injection of protons will be accomplished by a linear accelerator at 9 Mev energy. The protons are accelerated in the chamber during 3.3 seconds, receiving an average energy of 2200 ev per revolution in two accelerating regions. The accelerating region is in the form of tubes through which the particles pass, with a maximum effective voltage of 5 kilovolts each.

The frequency of the accelerating field changes by a factor of 7.5, and its value corresponds to the instantaneous value of the magnetic field with an accuracy of 0.1 percent. Having performed 4.5 million orbital rotations and having gone a distance 2.5 times the distance from the Earth to the Moon, the protons will achieve a calculated energy of 10 Bev.

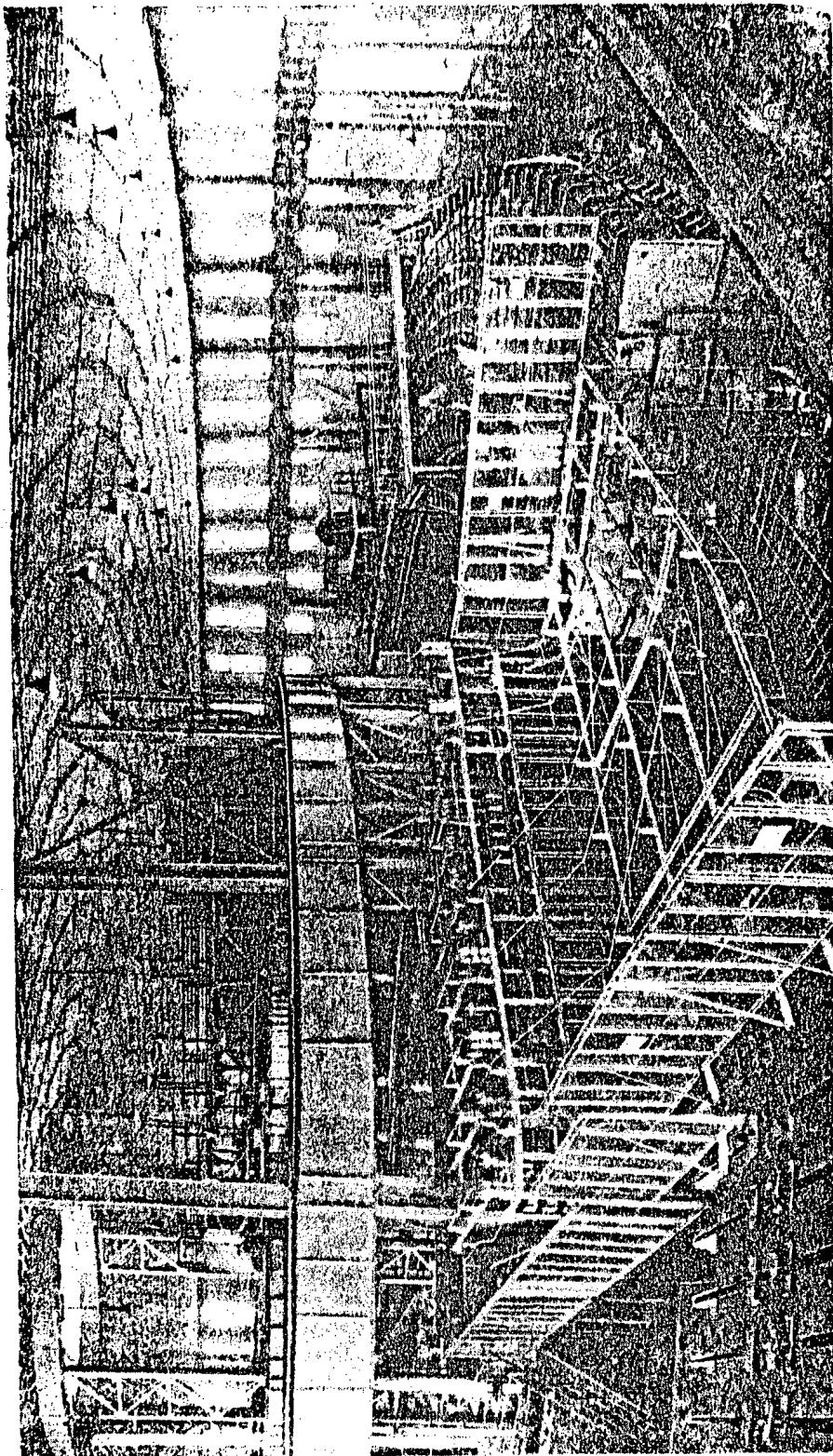
Some problems connected with the operation of this synchrophasotron (the problem of injection, resonance, noise and modulation of the magnetic and accelerating fields, observation of the beam, and others) were investigated, under the direction of Professor V. A. Petukhov, on an operating model giving protons of 180 Mev energy.

Accelerators have given us the opportunity of achieving great successes. Nevertheless, we are still very far from those extreme energies possessed by cosmic ray particles. In this connection I would like finally to discuss the problem of constructing those gigantic synchrophasotrons, calculated to give proton energies of the order of 50-100 Bev, which has received such widespread consideration in the course of the last few years.

Prospects for Accelerator Development. In the usual synchrophasotrons the magnetic forces, which so to speak bind the particles in their orbits and prevent their loss at the walls of the chamber, are actually very small. It is easy to show that these forces are determined by the gradient of the magnetic field in the gap of the electromagnet. In the usual synchrophasotron this gradient is in general insignificant, and therefore the quasi-elastic forces are small, whereas the amplitude of oscillations of the particles is large. This means that the dimensions of the pole gap must be relatively large. For larger dimensions of accelerators (which are necessary if we wish to increase the energy limit of the particles), it is necessary to increase the width and height of the gap between the magnetic poles correspondingly. Going on in this way, with present-day experimental accuracy and technical and industrial possibilities, it is hardly possible to reach energies larger than 10-20 Bev. To continue in this way seems not only senseless, but also wasteful.

In 1952, Livingston, Courant, and Snyder suggested a new and extremely clever method for solving the problem. Their idea was to increase substantially the forces holding the particles near their orbit.

For this purpose, it is necessary to make the gradient of the magnetic field in the radial and vertical directions very large in the pole gap of the synchrophasotron. Unfortunately, if the sign of the magnetic field gradient is chosen so as to insure strong vertical stability, then it turns out that the radial motion is completely unstable, and vice versa.



General view of the electromagnet of the 10 BeV synchrophasotron.

Livingston and his colleagues directed their attention to the fact that by alternating sections with opposite signs of the gradient, it is possible to obtain general stability of motion. Such a solution of the problem allows great increase in the magnetic forces which bind the particles, and reduces the necessary size of the gap of the electromagnet by a factor of 10 to 15. This method received the name of strong focusing. It seems, however, that nothing in this world is for free. Increasing the focusing forces by the strong-focusing method automatically increases the influence of all kinds of perturbations on the particles.

Furthermore, another difficulty arises. For a certain sufficiently large energy, usually called critical, the conditions of self-phasing disappear in accelerators with strong focusing. This threatens the loss of accelerated particles. It seems, however, that these difficulties can be overcome. By increasing accuracy in manufacture and assembly of electromagnets, it should be possible to avoid dangerous perturbations in the motion of the particles. Rabinovich and Kolomensky, as well as Vladimirsky and Tarasov, have proposed a clever method of avoiding the critical energy.

In 1953, the Soviet physicists Petukhov, Rabinovich, and Kolomensky suggested an interesting modification of the strong-focusing method, based on the use of a constant magnetic field. Very recently an analogous suggestion was published by Symon, Kerst, and others.

Thus at the present time in many countries, there is much very intense planning and investigation of accelerators calculated to give extremely high energies. For this it is necessary to realize a system which avoids the critical energy, makes use of a new method of controlling the frequency of the accelerating field (relation to the magnetic field gradient), and so on.

However, it is not really possible, with this type of accelerator, to move into the region of extremely high energies. As is well known, the radius of the magnet of any cyclic accelerator is simply related to the particle energy attainable in this type of apparatus; namely,  $W = 300 \text{ HR}$ .

Since modern magnetic materials will not give field strengths greater than 10,000-20,000 oersteds, for larger energies, the radius of the electromagnet must increase proportionally to the energy, which, as is obvious, leads to a practical limit of very high energies of the order of 50-100 Bev even for strong-focusing accelerators.

Since the potentialities of the usual and already developed methods seem to be exhausted, it has become necessary to look for some new direction. For instance, it would be possible to make a big step forward if we could succeed in finding some means of creating extra strong magnetic fields or of significantly increasing the upper limit of electric field strength in linear accelerators. Of course, even extra strong magnetic fields will not supply the possibility of sharply increasing the upper limit of electron energy, as in practice it is really the radiation that establishes this limit.

We may be sure, however, that experimental physics will be able to solve this problem and will learn to produce artificially particles with the enormous energies of  $10^{12}$  and  $10^{13}$  ev.

## METHODS OF URANIUM PROSPECTING

V. G. Melkov

At the present time three types of uranium deposits are known which are of practical interest: the magmatic (principally hydrothermal), the sedimentary and the sedimentary-metamorphic deposits. The laws of their formation and distribution still lack sufficient study although on the basis of the available data the most characteristic features of the favorable districts for each type and the structural features of the deposits have already been determined. This enables us to organize the search for uranium deposits on the basis of the geological division of the country and greatly facilitates direct reconnaissance within the favorable districts.

### 1. Geological Survey

The purpose of a geological survey is not only the distinguishing of favorable districts but also the establishing of their degree of likelihood in order to determine the order in which reconnaissance should be carried out. The general principles, methods and means of such a survey are well known. On the basis of a study of the geological structure of a country, an analysis of the history of its geological development and knowledge of the principal stages in the geological development of individual regions it is possible to distinguish the regions which are similar in their geological structure and history (tectogenesis, magmatism, sedimentation, paleogeography, etc.). After this the regions can be determined in the individual stages of whose geological history there was a combination of conditions favorable to the formation of some type of mineral deposit.

In a survey adapted to uranium prospecting we distinguish the territory which shows a likelihood of revealing magmatic deposits and basins in which sedimentary and sedimentary-metamorphic deposits are likely. In determining the favorable districts it must be kept in mind that uranium deposits and outcrops are found in regions built up of foldings from the Proterozoic, Caledonian, Varian and Laramian eras as well as in regions of considerable orogenic movements of the Alpine era. It must also be kept in mind that hydrothermal uranium deposits usually appear in epochs or stages of development of the earth's crust which are characterized by:

- a) The formation of large fractures accompanied by different and frequently repeated systems of numerous tectonic fissures of lower orders;
- b) The development of small igneous subsurface intrusions as well as surface eruptions of granitoid magma, which are usually successive differentiations of a single magma;
- c) The appearance of numerous dikes, especially of diabasic porphyrites.

In distinguishing the favorable portions of basins it must be kept in mind that sedimentary and sedimentary-metamorphic uranium deposits are found in strata of the Proterozoic, Paleozoic (especially the Ordovician, Carboniferous and Permian), Mesozoic (Triassic, Jurassic and Cretaceous) and Cenozoic (especially the Paleogene) eras. Moreover we must consider the possibility of finding sedimentary uranium ores

- a) In continental (lagoonal, lagoonal-lacustrine, etc.) facies, represented by coals and sandstones;
- b) In littoral shallow-water transgressive facies, represented by sandstones, oolitic limestones, phosphorites, clays, enriched in organic matter and frequently in phosphorus, not seldom vanadium, sulfur, fluorine, iron, molybdenum, barium, strontium, the rare earths, less frequently nickel, cobalt, zinc, lead, chromium, zirconium, hafnium and scandium.

These facies are uraniferous when formed near a dry area in a peneplaned or eroded surface under climatic conditions which favored considerable dominance of chemical weathering of the dry land minerals over physical weathering.



The geological conditions noted for the finding of sedimentary uranium ores are in complete agreement with its physico-chemical properties. Hexavalent uranium is quite soluble in acid and neutral natural waters as the uranyl ion ( $\text{UO}_2^{2+}$ ) and in alkaline waters as the uranyl-carbonate group. From waters of the first type directly and from waters of the second type evidently after breaking up of the group (with lower pH) the uranyl is easily removed by various sorbents (organic, carbonaceous, etc.) and possibly by phosphates. In addition, uranium is precipitated from alkaline waters by processes used for hexavalent uranium ( $\text{Fe}^{2+} \rightarrow \text{Fe}^{3+}$ ;  $\text{OH}^{1-} + \text{HS}^{1-} \rightarrow \text{S}^0 + \text{H}_2\text{O}$ , etc). By these processes and under the given conditions hexavalent uranium becomes quadrivalent.

In evaluating regions and basins it is necessary to consider not only the conditions favorable for the formation of commercial ores but also the subsequent processes which could lead to change or destruction of those deposits. We first estimate the possible extent of mineral erosion of the region and basin deposits. The most favorable districts are those subjected to weak erosion which has not destroyed the uraniferous formations. For sedimentary strata we also consider the character of the foldings and the degree of metamorphism. These processes lead to (a) changes of the stratification, (b) easily accomplished regrouping and redistribution of the uranium and (c) essential changes of the host rocks (recrystallization, shale-formation, etc.) and of their properties.

## 2. Geological Basis of Prospecting Methods

The search for commercial deposits in favorable districts and basins is accomplished in a number of steps which differ in the amount of work involved and in peculiarities of the methods and specific techniques.

The principal peculiarity of uranium prospecting is the wide utilization at all stages of various radio-metric methods. These methods are based on the radioactivity of uranium — the ability of uranium to disintegrate spontaneously and to transform successively into an entire series of other radioactive elements, with the emission of charged alpha and beta particles as well as gamma radiation. In some cases auxiliary use is made of another property of uranium — the ability of a number of uranyl compounds to luminesce under ultraviolet light.

In a large new area prospecting usually begins with air-radiometrical, surface car-radiometrical and radio-hydrogeological reconnaissance which in a short time finds the regions of the so-called radioactive anomalies, i.e., the regions characterized by high (compared with the surrounding territory) gamma radiation and concentrations of radioactive elements in subterranean waters.

This form of prospecting is based on the ability of uranium and its daughter radioactive elements (onium, radium, radon) to form around the upper oxidized parts of deposits and outcrops, the so-called "aureoles" which show high gamma radiation. In regions with dominant chemical weathering these "aureoles" are spread over a large area. Reconnaissance uses the tendency of the above-mentioned elements to be borne by subterranean waters to comparatively large distances from the deposits and outcroppings.

In districts with dominant mechanical weathering and also in case of primary uranium-quartz ores the same purpose is served by the ability of these ores to form fairly extensive mechanical "aureoles" (alluvial and eluvial deposits, principally pitchblende and uraninite).

In districts with radioactive anomalies as well as in the adjacent areas detailed prospecting and estimating work is carried on. Great importance is attached to the geological, geomorphological, hydrogeological, geomechanical and other peculiarities of the region containing the anomalies.

In the adjacent regions detailed prospecting is necessary because the anomalies may be somewhat shifted in position with respect to the original ores and also because not all ore-bearing zones or deposits are characterized by high surface radioactivity. This is characteristic, for example, of regions with hidden bodies of ore, districts covered with sediments, etc.

For efficient detailed prospecting and evaluation of radioactive anomalies and adjacent areas it is very important to understand and take into consideration the experientially established general geological laws of uranium distribution, the characteristics of familiar types of uranium deposits, the behavior of uranium in a weathered crust, etc.

These laws as applied to magmatic deposits are briefly as follows: \*

\* The infrequent deposits containing davidite (iron titanate containing 7% uranium) are not considered here.

1. Magmatic uranium deposits are formed predominantly in conjunction with the latest members of the magmatic differentiation of the granitoid magma, highly enriched with silicon and volatile components, somewhat less with alkalis and very poor in magnesium, iron and calcium.

2. Uranium deposits are found principally not in large extensive (regional) abruptions but in associated fractures. In these fractures, they conform to the branchings, bendings, and intersections with dikes of volcanic rocks, quartz and other veins or unmineralized fractures, and also to their intersections with certain host rocks which are usually comparatively enriched in iron oxides. The deposit of uranium ores is possible in regions near the branching of extensive fractures. Apparently a characteristic of the fractures in which uranium ores are formed is their frequent replacement.

3. Uranium has a tendency to form the largest ore bodies in fractures of predominantly "hard rocks": various metamorphic rocks (schists, gneisses, quartzites, hornstones, etc.) granites, granodiorites, acid effusive rocks, etc. Most favorable are strata of metamorphic or strongly metamorphosed rocks, among them those enriched with various minerals of divalent iron such as iron-bearing varieties of chlorites and amphiboles, magnetite, etc.

In intrusive masses within effusive and volcanic strata the largest bodies of uranium ore are formed preferably in hydrothermally altered zones containing clays and chlorites as well as talc and pyrophyllites and also in parts of dikes of basic volcanic rocks (diabasic porphyrites).

In strata of normal sedimentary rocks not subjected to regional metamorphism, at least not to a high degree, magmatic uranium deposits are not found except at times in those portions of these strata which are adjacent to the "hard rocks".

4. Mineralization of the uranium deposits did not take place at one stroke but passed through a few pulsational stages. There are deposits whose formation began with a pneumatolytic and ended with a hydrothermal period, passing through six or more stages of destruction and replacement. There are also deposits whose initial forming periods were marked by metasomatism (albites, etc.) and the formation of pores and caves.

The formation of uranium ores is usually associated with one of the latest stages. A characteristic of this uranium stage is the independence of its appearance not only in time but frequently even in space. This is most favorable, other conditions being equal, to the formation of the largest deposits. A characteristic of the uranium stage is also the comparatively small number of chemical elements accompanying the uranium. The principal permanent elements which appear together with the uranium are oxygen, silicon and iron. Not always but in large quantities are found carbon, calcium, fluorine; more seldom and in smaller quantities—magnesium, aluminum, sulfur, the rare earths; even more seldom and in extremely small quantities are found arsenic, lead, zinc and copper.

Under different conditions the above elements form different associations, such as pitchblende and silica (metacolloid); pitchblende-quartz-hematite; pitchblende-quartz-calcite or dolomite; pitchblende-chlorite (thuringite and daphnite), sometimes with quartz; pitchblende-fluorite-calcite and a few others. In addition to these principal minerals there appear at times small quantities of such minerals as pyrite, galenite, sphalerite, arsenopyrite, enargite, etc. The rare earths and sometimes lead, aluminum, silicon and a few more elements do not form independent minerals but are included in metacolloidal pitchblende systems.

In case of spatial shifting or the superposition of the uranium period of mineral formation on minerals formed in one or more preceding periods there appear regions with vein deposits characterized by complex many-mineral composition of the uranium ores and accompanied by considerable changes of different nature around the veins. Examples of many-ore bodies can also be given omitting the above-mentioned minerals of the uranium period and of the mineral composition of the host rocks: uranium ores with considerable amounts of iron, zinc and lead sulfides; with sulfides and sulfur salts of copper and bismuth, and barite; with copper, iron and molybdenum sulfides; with wolframite, iron, copper, lead and zinc sulfides, bismuth, sulfur salts and barite; with alkali (sodium) silicates and aluminosilicates, magnetite, hematite; with native silver, arsenic, bismuth, arsenides and diarsenides of cobalt and nickel, iron and copper sulfides; with iron sulfides, hydroaluminosilicates (hydromicas and montmorillonite, etc.), fluorite, etc.

The variety of the mineral composition of uranium deposits appears to be related to their size and the

richness of the ore. The following tendency has been noted: the largest deposits of rich ores usually contain a small amount of almost no sulfides. Uranium deposits with considerable amounts of sulfides are as a rule characterized by smaller size and leaner uranium ores.

5. The uranium period of mineral formation is accompanied by almost no change of the host rocks. It is possible to point definitely only to the formation of hematites (red coloration) and of chlorites (green coloration). The other most closely related formations are those of carbonates (dolomites, etc.), quartzes (jaspidean hornstonelike quartz), argillites (often a mixture of different quantities of hydromicas, montmorillonite, gilluassite, kaolinite), and fluorites.

6. In developing oxidation zones the behavior of the uranium and of its daughter radioactive elements (onium, radium, radon) differs considerably depending on the mineral composition of the primary ores and is in full agreement with the chemical properties mentioned above. In old ("worked through") oxidation zones with geologically long constant erosion base level the above differences are gradually effaced. This is due to the general tendency of compounds of hexavalent uranium (which in all cases are formed in the oxidation zone from pitchblende and uranium "blacks") to dissolve and thus leave the deposit.

In oxidation zones of essentially sulfide ores the uranium is more movable than in such zones containing uranium ores with little or no sulfides. In sufficiently young oxidation zones and lower erosion base levels the following differences are observed.

In sulfide deposits all of the uranium in the pitchblende dissolves. This favors the formation of well-developed secondary vertical zonality in the distribution of hypergenic uranium minerals characterized by a number of properties (from bottom to top).

In the cementation zone regenerated uranium pigments are found. In the subzone of active oxidation (recent oxidation subzone of the cementation zone) because of oxidation and dissolving of pitchblende there appear residual uranium pigments and solutions of  $U^{6+}$ . Still higher in the vertical profile of the oxidation zone a subzone is found which entirely lacks uranium minerals, and above this a subzone of uranium micas which are as a rule of the phosphor-calcium type. In this subzone when copper sulfides and arsenides are present in the primary ores arsenical and copper uranium micas are also formed. In this case the lower part of the subzone contains the arsenical and copper micas (zeunerite, torbernite and uranospinite) and above these the phosphor-calcium otenite. At the uppermost part are found the uranium silicates (uranophane) and minerals containing an admixture of uranium (uranium-bearing hyalite and calcite). Uranium-bearing limonite are found throughout the oxidation zone.

In deposits with little or none of the sulfides the pitchblende oxidation zone contains various uranium silicates and hydroxides, which are as a rule pseudomorphs of small or microcrystalline structure (gummities). The various uranium "blacks" and uranium micas are then very weakly developed. The quantity of the latter increases in the upper parts of the oxidation zone.

Thus even in this case vertical zonality is found in the distribution of secondary uranium minerals, although it is not so clear and not so well differentiated.

The following rules must be considered with respect to sedimentary deposits in detailed prospecting and evaluation of anomalies and adjacent areas;

1. The highest uranium content in oceanic deposits is found in a comparatively narrow (of the order of hundreds of meters) strip within a much wider stratigraphically favorable zone characterized by lower uranium contents. The richest uranium band, if it is found at all, is usually traced along a coastline at a comparatively small distance (from a few kilometers to a few tens of meters).

A similar tendency of high uranium concentrations in such districts is also observed in coal basins although the presence of uranium bodies in coal as in a number of other caustobiolites (asphaltites, etc) is apparently due frequently to epigenetic but not to syngenetic processes.

2. In normal sedimentary rocks uranium is usually found in mixed oxides and often in conjunction with organic matter (principally humic and the like), which can be found in phosphates (concretions of phosphorites, fossilized skeletons and integumentary parts of fish of phosphate composition, etc.), carbonates (shells, calcite oolites, etc.) and in a scattered state. In the form of independent minerals (pitchblende, "blacks") uranium is found seldom and in small quantities: such minerals are in small (often microscopic) deposits. Uranium is usually accompanied by pyrite (up to 30%) and frequently by large

quantities of sphalerite, galenite, sulfides of vanadium, barite, molybdenite(?), etc. Fluorine, the rare earths, scandium and a few other elements are usually found in the phosphatic rock components. The unoxidized sedimentary rocks enriched with uranium are not characterized by limonite and reddish ores. They are more frequently gray-green and gray.

3. With an increase in the degree of metamorphism and recrystallization of the limestone the link between organic matter and uranium is broken. There is first a transformation to hard highly carbonized compounds such as the anthraxolites and uranium is found in the form of pitchblende and other minerals characterized by epigenetic distribution in the seam of ore.

4. In the oxidation zone of sedimentary deposits poor in uranium secondary uranium minerals are almost entirely absent with the exception of uranium-bearing limonites and more infrequent separate laminae of otenite and torbernite. In the oxidation zone of sedimentary deposits that are richer in uranium considerable amounts of phosphates (alkali and alkali-earth micas) and sulfate-carbonates (Schroekingerites) usually are formed.

In uraniferous sedimentary strata enriched with vanadium, secondary vanadates are formed (tyuyamunite and carnotite). In all instances the secondary uranium minerals are accompanied by limonites, gypsum, iron sulfates and phosphates, magnesium, aluminum, etc.

### 3. Methods of Surveying

Airborne radioactivity surveying. The most rapid and therefore primary method of seeking out anomalies is the airborne radiometric survey.

This survey uses airplanes and helicopters equipped with automatic recording radiometric devices of high sensitivity, and small time lag (Geiger and scintillation counters), which record not only the total gamma activity of a field but also its spectral composition. The planes and helicopters are also equipped with devices for automatic altitude recording and for aerial photography.

Airborne radioactivity surveying is most efficient when conducted over a large area and is based on a thorough analysis of the geological structure of the area studied, with allowance for the geological peculiarities of the uranium deposits, and is conducted by geologists. The airborne survey, depending on the expected type of deposit, outcroppings, ground contour, degree of complexity and knowledge of the geological structure, etc., is conducted on various scales in equidistant parallel courses (corresponding to a given scale and height of flight) which are usually across the sought ore structures and levels.\* The length of a course is not usually more than 30-40 km. If the height is decreased the number of courses is increased.

Depending on the radiometric and aerial technique employed and also on the geography of the region the flights are conducted at a height of from 15-30 m to 100-150 m.

The results of the aerial radiometric survey together with the geological study are used to draw an aerial radiometric map showing isolines of gamma activity.

The radioactive anomalies discovered by air are expressed by totals of gamma activity which may be derived not only from uranium deposits and outcroppings but also from thorium deposits and areas of oxidized intrusive or effusive rocks, etc.

Regions with the requisite gamma activity are distinguished by aerial gamma spectrometry which takes into account the size, shape, intensity and position of the gamma anomalies with respect to geographical profile and basic elements of the geological structure.

Gamma anomalies, which are due to masses of igneous rocks, effusive strata, etc. have a size and shape corresponding to the areas of these rocks and characterized by almost identical levels of gamma radiation over the entire area (area anomalies).

Gamma anomalies due to deposits and outcroppings of uranium and thorium are characterized usually by a comparatively sharp gamma peak in local strips (local anomalies) and are not infrequently observable against the background of an area anomaly.

---

\* In very much disconnected regions the direction of the air courses must be chosen basically in accordance with the geographical profile of the region.

Carborne radioactivity surveying. This method serves to supplement the aerial method. It is used where the terrain permits, for a detailed study of the regions of high gamma activity detected from the air and for partial filling-in of the gaps in the aerial survey. In addition the automobile method is used for large-scale surveys in regions of comparatively small area.

Auto reconnaissance often cannot be planned as an area survey since the number of auto routes cannot be based only on the required scale but depends on the passability of the terrain and on the already available roads.

For auto surveys the most rugged recent models are used, equipped with radiometric devices similar to those used in the air.

Radiohydrogeological surveying. The principal advantage of this method is the possibility of discovering likely regions that are covered by considerable alluvial deposits which absorb gamma radiation as well as by the good possibility of finding hidden ore bodies.

The essence of this method is the determination in water samples from all natural and artificial bodies of water and from flowing water, of the concentration of radioelements, salts, redox potential, radioactive and non-radioactive gaseous products of the "decay" and "disintegration" of uranium atoms and a number of other quantities. Almost the entire analytical study of water samples is carried out directly under field conditions with equipment which has been especially developed for quick field analyses. As a result of radiohydrochemical studies accompanied by the usual hydrogeological observations suitable radiohydrochemical maps are drawn on a geological basis of the required scale.

Other methods. Areas in which aeroradiometrical and radiohydrochemical anomalies are found are subjected to the above-mentioned detailed geological, petrological, stratigraphical and mineralogical study utilizing various surface rocks and special methods developed to suit the properties of uranium and other radioactive elements.

Among these methods we may mention pedestrian and automobile gamma surveys as well as the beta-survey of favorable areas, the rapid emanation survey of regions covered by comparatively heavy deposits, the uranometrical survey, the luminescent mineral survey, the geobotanical survey, etc.

All of these surveys are quite simple. Autoborne gamma surveys were mentioned above. The other kinds of survey are based on general prospecting principles. According to the scale chosen from a consideration of the geological and geomorphological peculiarities of the region and the expected type of deposits, a network of parallel routes is established mainly along transverse lines. Along these routes continuous measurements are taken of gamma radiation and luminescence is observed, or at equal intervals (up to 5 m) samples are taken of rocks, soil, ground gases, and vegetation with corresponding beta and gamma readings.

Almost all the analytical investigations associated with the above surveys are carried out in the field. The results of all surveys are represented in appropriate profiles, maps and plans on a geological base.

Emanation survey. In carrying out an emanation survey which serves to determine the concentration of the gaseous radioactive elements radon and thoron which are formed in the radioactive decay of Ra and ThX (daughter elements of uranium and thorium), samples of ground air are usually taken at a depth of 0.8 to 1.0 meters with special sampling drills. When it is necessary to take air samples at greater depths special wells are dug. The radon and thoron content of a sample is found on the spot in a few minutes. The emanation survey is one of the depth prospecting methods.

Uranometrical survey. In this survey, which determines the uranium content in alluvial deposits associated with aureoles, the samples are taken at different depths by the use of drills as well as in pits and trenches. The uranium content of the samples is determined by a luminescence analysis because of the ability of uranium when dissolved in sodium fluoride to fluoresce under ultraviolet irradiation. The brightness of the fluorescence at low concentrations ( $1-5 \cdot 10^{-2} \%$ ) is proportional to the concentration.

Luminescent mineral survey. This survey, which is based on the ability of several secondary uranium and uraniferous minerals (certain uranium micas and uranium-bearing hyalite and calcite) to fluoresce in ultraviolet light, is carried out with continuous irradiation of the surface of outcroppings. This is done in darkness and continuously along the entire route. Points where the luminescence of uranium and uranium-bearing minerals appears are marked and later studied in daylight.

Geobotanical survey. This type of survey has two forms:

a) by the analysis of plant ash for radioactive (principally uranium) and other elements which, depending on the concentration of one kind or another of deposits in the region, is closely related to the deposits of radioactive ores.

b) by mapping of individual types of plants which in their growth or their chemical composition are affected by chemical elements found only in uranium deposits.

Both methods make it possible to discover hidden uranium deposits at a depth of from 20 to 25 m.

The above group of investigations usually enables us to determine the location and nature of radioactive anomalies.

After locating spots with evidence of leached out or partially preserved uranium mineralization an estimate of the size and extent of the mineralization is carried out by the usual methods. It is necessary to take into consideration the peculiarities of the structure of uranium deposits and of their oxidation zones, especially such as are due to the geographical and hypsometric position of the deposits as well as their surface profile. It is also necessary to keep in mind the possibility of considerable shifts of radioactive equilibrium, which follow rules for the different subzones of the hypergenetic zone, and which is very important for the correct development of the prospecting procedure.

#### LITERATURE CITED

[1] V. I. Baranov, Radiometry. USSR Acad. Sci. Press, 1955.

[2] Geological, Chemical and Metallurgical Studies (Reports of the Soviet Delegation to the International Conference on the Peaceful Uses of Atomic Energy). USSR Acad. Sci. Press, 1955, :

(a) V. I. Baranov, Prospecting for Uranium and Thorium Deposits by Aerial Radiometry and the Interpretation of Gamma Anomalies, pp. 11-20.

(b) A. I. Germanov, and A. A. Saukov, Prospecting for Uranium Deposits by Radiohydrogeological Methods, pp. 3-10.

[3] The Geology of Atomic Raw Materials (Reports of Foreign Scientists at the International Conference on the Peaceful Uses of Atomic Energy), State Geological Press, 1956, :

(a) H. L. Cannon and F. G. Kleinhemph, \* Botanical Methods used in Uranium Prospecting, pp. 461-472.

(b) R. Kavaka, Uranium Prospecting in Portugal and its African Provinces, pp. 284-296.

(c) P. F. Kerr, Wall Rock Changes Near Ores as Tests to be Used in Uranium Prospecting, pp. 451-460.

(d) P. F. Kerr, Uranium and Thorium Deposits, pp. 119-219.

\* Reference [3], parts a, b, c, d has been retranslated from Russian and may not coincide exactly with the original title as published by the United Nations.

## ISOTOPES IN THE STUDY OF THE PATHOGENESIS OF METABOLIC DISEASES

D. E. Grodzenski

Only as the natural sciences developed did medicine begin to acquire a firm scientific foundation.

The experimental method has become of primary significance for the progress of medicine as a scientific discipline.

At first, medical experimentation amounted to a crude interference in the normal activity of the organism, to the surgical removal or irritation of individual parts with observation of the ensuing results. In this way information was gathered concerning the functional purpose of the individual organs of the body.

As physics and chemistry developed, as the experimental methods of these sciences were developed and perfected, medicine constantly acquired new means of studying the vital processes.

Modern medicine in its experiments on animals and more directly at the sickbed uses all the resources and all the achievements of the exact sciences. X-rays, sensitive electrical measuring devices, multichannel oscillographs, electrical instruments for every conceivable purpose, complicated optical apparatus, the most precise methods of chemical analysis— all of these serve nowadays for the investigation of the mechanism by which an illness develops and for its diagnosis.

It is thus natural that the advances of nuclear physics during the past few decades were quickly incorporated into experimental medicine.

Biologists and physicians were mentally ready to make use of the newest discoveries in the formulation and solution of their scientific problems.

There were two special reasons for this fact.

At the beginning of the 20th century, principally as a result of the work of I. P. Pavlov, it became clear that physiological experiment can be most fruitful if it does not rudely disturb the vital activity of the organism. According to this principle, without changing the normal course of the studied process the experimenter must be able to interpret it, to reveal its relations to other processes and to discover the mechanisms which regulate it. This can be done only through the possession of a precise experimental technique. The isotopic method became an extraordinarily valuable addition to the methods previously at the disposal of the physiologist.

Of great significance for the rapid application of advances in nuclear physics to biology and medicine was the additional fact that the idea of labeling substances introduced into the bodily organism had occurred to biologists long before stable or radioactive isotopes were available. Moreover, the method had been used more than once in biological and physiological experiments.

However, until the fourth decade of the century, the possibilities of labeling compounds introduced into the organism were extremely limited. The principal labeling method was the association with the compound to be investigated of a substance foreign to the organism. Thus the investigator was not sure that his method did not alter the course of the processes in question.

It is therefore not at all surprising that the recently discovered radioactive isotopes were rapidly introduced into biological experimentation. It is sufficient to mention that the report of Fermi et al. [1] concerning the preparation of radioactive phosphorus ( $P^{32}$ ) from the reactions ( $H^1, \gamma$ ) and ( $d, p$ ) and the first note of Chievitz and Hevesy [2] on a biological experiment accomplished with the aid of this isotope appeared in the same year, 1935.

Thus 20 years have elapsed since artificially radioactive isotopes began to be used in biology. Approximately the same period has elapsed since a beginning was made of the use of stable isotopes, the first of which was deuterium, as labeled atoms.

During these two decades the contribution of the isotopic method to the development of biology and medicine has been so tremendous that it can hardly be calculated.

It can be said without exaggeration that, for example, the extremely rapid development of biochemistry and almost all its achievements in the last decade are due in large measure to the use of isotopes, especially in conjunction with other methods, in particular, all forms of chromatography.

For the investigation of metabolic processes and of the course of diseases in which metabolic disturbances are prominent, the use of isotopes has been extremely effective.

We shall endeavor to illustrate the significance of isotopes in medicine by choosing examples principally from the study of the pathogenesis of certain metabolic diseases.

But we must first make brief reference to the changes in general concepts concerning metabolism which have taken place due to discoveries resulting from the use of isotopes.

For some decades physiology had been dominated by Rubner and Folin's concept of two independent types of metabolism, the exogenous and the endogenous. According to this concept, food is regarded as fuel which supplies the energy needs of the organism. It was assumed that only a small portion of the food can serve as building material for the replacement of worn-out parts of the organism. The expression "exogenous metabolism" was understood to mean that in the adult organism of constant weight the food molecules are reduced to carbon dioxide and water while the nitrogen of the food is the direct source of excreted nitrogen. The structural parts of the organism were considered stable. In this view, nutrients supply replacements of worn-out parts and increase the size of bodily parts only during periods of growth and increase of weight.

To be sure, this metaphysical point of view was not shared by all physiologists. It was opposed, for example, by the Russian scientist A. Ia. Danilovskii, but a crushing blow was dealt to this hypothesis by the first isotopic experiments utilizing labeled deuterium and heavy nitrogen [3]. These were experiments on the metabolism of fats and albumins. Schoenheimer summarized his results as follows: "The large complicated molecules and the less complicated compounds which compose them: fatty acids, amino acids and nucleic acids, are continually participating in rapid chemical reactions. Ester, peptide and other bonds are broken, the fragments of complicated molecules which are thus liberated are mingled with those derived from other large molecules and with those which are absorbed from the alimentary canal, forming a 'metabolic background'.

"The molecules of any given compound are indistinguishable in origin. These molecules again become involved in innumerable processes. Fatty acids are dehydrogenated, hydrogenated, decomposed, built up and transformed into one another. While a few individual molecules of these acids decompose completely, other molecules of identical structures are being formed of the most various materials, especially out of carbohydrates. Similar reactions take place involving the products of the decomposition of albumins."

Thus the biological system on the basis of Schoenheimer's view is "one huge cycle of closely connected chemical reactions".

The idea of a continuous restoration of the "molecular regeneration" of the constituents of the organism — albumins, carbohydrates, fats, the crystalline structure of the bones and other parts — has been well established in modern biochemistry and physiology [4].

Thus far we still do not know the specific mechanisms of such restorative processes of the organism nor the way in which these processes are regulated in the sick as well as in the healthy organism. It is certain, however, that the isotopic method in conjunction with other experimental methods will enable us to solve this problem.

Great interest attaches, in particular, to the study of the synthesis and decomposition of albumins both in the entire organism and in its parts. The isotopic method plays the principal role in such studies.

The determination of the rate of entrance and departure of tracers from various biologically important compounds enables us, by the utilization of the quantitative methods of radiochemistry, to find the "average lifetime" of some parts of an organism.



"Mean lifetime" of various parts of organisms (data from different authors)

Object of study	Biological compound	Tracer	"Mean lifetime" of compound in days
Mouse	Cholesterol	D <sub>2</sub> O	15 - 25
Rat liver	Cholesterol	C <sup>14</sup> -acetate	8.5
Rat body	Cholesterol	C <sup>14</sup> -acetate	44.6
Human blood	Cholesterol	D <sub>2</sub> O	12
Rat	Saturated fatty acids of liver fat	C <sup>14</sup> -acetate	1
Rat	Unsaturated fatty acids of liver fat	C <sup>14</sup> -acetate	2
Rat	Saturated fatty acids of body fat	C <sup>14</sup> -acetate	23
Rat	Unsaturated fatty acids of body fat	C <sup>14</sup> -acetate	29
Dog	Fibrinogen (albumin of blood plasma)	Disappearance of S <sup>35</sup> from albumin	6
Human	Fibrinogen (albumin of blood plasma)	Disappearance of S <sup>35</sup> from albumin	16.2
Rat	Albumin of liver	Glycine-N <sup>15</sup>	11
Human	Plasma albumins	Glycine-N <sup>15</sup>	14
Healthy human	Erythrocytes	Glycine-N <sup>15</sup>	120
Pernicious anemia patient	Erythrocytes	Glycine-N <sup>15</sup>	85

Although the results of such studies in the adjoining table must be considered merely preliminary, they are evidence of the great instability of biological compounds in the living organism. It may be assumed that as there is improvement of the mathematical apparatus for the calculation of such data new laws will be discovered which govern the rates of synthesis and disintegration in the organism.

The most important result of isotopic investigations of metabolism was the establishment of the fact that the carbon dioxide formed through the oxidation of various compounds in the organism is partially used to build complicated organic molecules such as the glycogen of the liver.

With the aid of various compounds tagged with C<sup>14</sup>— intermediate products of the metabolism of glucose and other substances— detailed studies have been made of reactions and enzymatic systems that involve carbon dioxide in synthetic processes within animal organisms.

It must be considered a great achievement of organic chemistry and of the isotopic technique that methods have been developed for the synthesis of complicated organic compounds (such as the sugars, hormones, organic acids, etc.) with strictly determined positions of the singly or doubly labeled atoms of the molecule.

This makes it possible to trace the disintegration of labeled molecules in the organism and to follow their constituent atoms.

In addition, the introduction into the organism of comparatively simple labeled compounds and the analysis of naturally synthesized biologically important multiatomic molecules (such as cholesterol and hemoglobin) enable us to study the intermediate steps in the synthesis of such compounds.

We must note one additional theoretically important conclusion derived from isotopic studies of metabolism. This is the proof of the interconnection of different kinds of metabolism (of albumins, fats and carbohydrates) through the general intermediate products of metabolism with short carbon chains. The formation of certain ones of these intermediate products could only be proved by the isotopic method because of their rapid transformations within the body.

The new facts obtained through isotopes and relating to the fundamental problems of metabolism and to its individual details have influenced investigations of the pathogenesis of certain human diseases, especially those in which metabolic disturbances are most prominent.

One of the most widely used and effective methods of studying the pathogenesis of various diseases is the construction of their experimental models. This means that a disease is induced in animals which is similar in its symptoms to a human disease. It is much easier and more convenient to use the experimental model than the human being to study the changes of metabolism and other processes associated with the given disease.

For example, for the study of such a human disease as diabetes, it is an extremely valuable fact that the disease can be induced quite simply in animals (rats, rabbits, dogs, guinea pigs) by the use of alloxan, which is close in structure to certain constituents of complicated albumins — the nucleoproteins. Alloxan destroys the animal cells in which the hormone of the pancreas is produced, that is, insulin, which controls the metabolism of carbohydrates. This hormone was isolated a long time ago and has been used extensively for the treatment of diabetes, but the mode of operation of the hormone has not yet been fully explained.

In diabetes, the blood and urine contain an excess of glucose, and sugar appears. Some investigators attributed this to the decreased utilization of glucose, i.e., of its oxidation in the organism; others attributed it to increased glucose production in the liver. The dispute between the proponents of these two theories lasted for decades.

Experiments utilizing  $C^{14}$ -labeled glucose put an end to the dispute. Experiments on tissue sections from normal and diabetic rats, on whole animals and on healthy and ill humans led to the conclusion that in diabetes, the ability of the tissues of a sick organism to utilize glucose is diminished but that the production of glucose in the liver is augmented. It was also shown what disturbances of the intermediate reactions in the metabolism of glucose produce these changes, and to a certain extent there was clarification of the role of insulin in the regulation of metabolic reactions [5]. In addition, the very first isotopic studies of the pathogenesis of diabetes showed that it is accompanied by a disturbance of the production of fat: the liver loses its ability to synthesize fatty acids in long carbon chains [6].

It has already been mentioned that isotopic experiments proved that carbon dioxide is used to form various carbonaceous compounds such as glycogen.

B. N. Stepanenko and his collaborators have studied the effect of the hormone of the suprarenal glands, adrenalin, on the synthesis of glycogen in hungry rats and on the inclusion in newly formed glycogen of  $C^{14}O_2$  from subcutaneously injected radioactive sodium bicarbonate. It was found that in healthy, hungry rats adrenalin stimulated the synthesis of radioactive glycogen in the liver. In alloxanic diabetes in rats, the administration of adrenalin together with radioactive sodium bicarbonate did not result in the production of radioactive glycogen, which shows that in diabetes there is a disturbance of the synthesis of the carbon chain of glucose radicals [7].

Isotopic studies of metabolic disturbances in diabetes have still not resulted in complete understanding of the pathogenesis of this disease. However, it cannot be denied that these methods have considerably extended our knowledge of such disturbances.

The isotopic method will undoubtedly enable us to test the theories of Soviet researchers concerning the nature of these chemical changes in diabetes [8, 9].

D. L. Ferdman and V. A. Grigor'eva [10] in their studies of progressive muscular dystrophy used as their experimental model young rabbits from whose diet vitamin E had been eliminated. After such a vitamin-deficient diet for a month, the rabbits showed dystrophic changes in the skeletal muscles accompanied by a decrease in their size.

For a study of the rate of phosphorus metabolism in such functionally weakened muscles, radioactive

sodium phosphate was administered internally to the rabbits; after 2 hours they were killed and a study was made of the amount of radioactive phosphorus in various phosphoric compounds of the muscles which are involved in muscular contraction. It appeared that, other conditions remaining equal, there was more radioactive phosphorus in the phosphoric compounds of muscles in vitamin-starved rabbits than in healthy rabbits. Thus the amount of the phosphorus in the phosphocreatine of dystrophic muscles was about 4 times greater than in the control animals; in adenosine triphosphoric acid it was 3 times as great. The authors consider this a proof of the increased rate of replacement of phosphoric compounds in dystrophic muscles and note also that the total content of phosphoric compounds in the muscles of vitamin-starved rabbits was diminished. No intensification of phosphorus metabolism was observed in the muscles of hungry rabbits.

Such vitamin-starved animals were used to determine the rate of albumin replacement in muscles. For this purpose, the rabbits were given  $S^{35}$ -labeled methionine and measurements were taken of the radioactivity of nonalbuminous sulfur and of the sulfur of muscle albumin. It was found that in the skeletal muscles of sick rabbits the rate of replacement of albumin increases as compared with the control.

These authors postulate that the intensification of phosphorus and albumin metabolism in the muscles is the result of compensatory processes directed towards the preservation of the muscular functions.

Academician A. V. Palladin and N. B. Vertmäier have shown, by the same method, that the rate of albumin metabolism in various parts of the central nervous system of vitamin E-starved rabbits is diminished by approximately 50% [11].

Additional isotopic studies have bearing on the study of the pathogenesis of progressive muscular dystrophy in humans. These can be described essentially as follows. Creatine, which is found in the muscles combined with phosphoric acid (phosphocreatine) participates in the chemism of muscular contraction. The biological predecessors of creatine or methylguanidoacetic acid (the chemical term for creatine) have been shown through the introduction into the body of labeled amino acids to be glycine, arginine and methionine. The creatine molecule acquires the guanidine group from the arginine, the methyl group from the methionine, and the remainder of its composition from the glycine. This substance is synthesized principally in the liver and then enters the muscles. In the urine of a healthy organism only traces of creatine are detected, but creatinine is constantly found. Phosphocreatine is transformed into creatine in the organism by detachment of the phosphoric acid and closing of the ring. This process is irreversible. In a healthy human, about 2% of the muscular creatine is transformed into creatinine and excreted in the urine in one day, whereas in some diseases and especially in progressive muscular dystrophy, a very large quantity of creatine is found in the urine (creatinuria).

Where does this creatine come from? Does it enter the blood from pathologically affected muscles in order to be removed by the kidneys or is it synthesized in the liver, rejected by the unhealthy muscles and then eliminated from the body?

The answers to these questions were recently given in a report by Benedict et al. [12] of an investigation of the synthesis of creatin in sick persons who had taken glycine- $N^{15}$

One of the three nitrogen atoms in a molecule of creatine is derived from the nitrogen of glycine. Consequently when creatine is synthesized in the liver it should contain an excess of heavy nitrogen atoms. With normal passage of such labeled creatine to the muscles and the formation therefrom of creatinine, the latter should be excreted in the urine with its molecule containing the same excess of heavy nitrogen atoms as the molecule of creatine of the urine. But in three progressive muscular dystrophy patients, this was not observed. After the administration of labeled glycine, the creatine of the urine contained a large excess of heavy nitrogen, but the creatinine contained only an insignificant amount. In time the heavy nitrogen concentration of the creatine decreased rapidly, but very slowly in the creatinine. Hence it follows that creatinuria is not the result of the loss of creatine by the muscles; it is synthesized in the liver of the sick person in the same quantity as in the healthy individual, but is not utilized by the muscles due to their functional abnormality. The body's need of creatine has been reduced and the excess of creatine is eliminated in the urine.

These experiments with an experimental model as well as with human patients are, of course, still far from providing a solution of the problem of the pathogenesis of progressive muscular dystrophy, which is a serious human disease, but they give us an idea of the possibilities for the use of the isotopic method in determining the rates of pathological metabolic processes and the nature of the disturbances of metabolism in the body.

Gout is a peculiarly human disease. It is definitely linked with nutrition. Gout is characterized by a disturbance of the metabolism of the purine bases, constituents of the nucleic acids. The product of this metabolism (uric acid) is deposited in cartilage, tendon sheaths and joint capsules. In the finger and toe joints, and in the cartilage of the cochlea, the so-called gouty nodules are formed. Inflammation of the joints produces swelling, deformation and pain.

The isotopic method has made it possible to study the metabolism of uric acid in healthy persons and in gout patients [13].

Healthy individuals were given  $N^{15}$ -labeled uric acid internally and a measurement was taken of the excess of  $N^{15}$  in the uric acid separated from the urine. The secretion of labeled uric acid decreased exponentially. From the data, it was possible to calculate with what quantity of uric acid in the body the administered labeled acid was mixed, i.e., to determine the "metabolic background" of uric acid in the healthy and diseased body, and the rate of circulation of the uric acid and also to determine whether there is a breakdown of the uric acid molecule in the body.

The "metabolic background" of uric acid in the healthy human is approximately 1 g. The excess of  $N^{15}$  found in the urine not only in the uric acid, but also in ammonia and urea indicates that the uric acid produced in the tissues through oxidation of the purine bases is partly decomposed in healthy individuals into simpler nitrogenous compounds. In gout patients the "metabolic background" of uric acid increases sharply (by a factor of 15) in spite of the insignificant increase of uric acid in the blood. This indicates that the uric acid deposited in gouty nodules may to some extent be replaced by new uric acid molecules.

The cause of the increased formation of uric acid in gout was found through mouth feeding of healthy individuals and patients with  $N^{15}$ -labeled glycine [14]. The patients used the glycine for the synthesis of uric acid in quantities 3 to 4 times as great as in the case of healthy individuals.

Thus, in gout, the production of uric acid is increased and the rate of its decomposition is diminished; for the synthesis of the excess uric acid, the amino acids in food are used.

These facts make it possible to conduct research leading to a rational treatment of this disease, which would be a treatment aiming at a reduction of the synthesis of uric acid in the body. They may also serve as a scientific basis for the development of a system of therapeutic diet.

Although the technical procedures involving the use of stable isotopes are complicated and expensive, and the methods of determining the excess of the heavy isotope in an analyzed compound are comparatively insensitive, the safety of stable isotopes frequently forces us to use them on both healthy and diseased individuals.

Moreover, the study of nitrogen metabolism can be conducted only with the heavy isotope of this element since there is no other radioactive isotope of nitrogen suitable for biological purposes.

But in the study of the pathogenesis of certain diseases, especially on experimental models, even comparatively simple isotopic methods may be effective enough.

Thus, for a study of the cause of increased content of phospholipoids in human blood plasma during illnesses accompanied by yellow jaundice, the jaundice was induced in rabbits by cutting off of the bile duct. It was then found that the concentration of phospholipoids in the blood serum increases 4 to 5 times above normal. In order to learn how the absorption and utilization of phosphorus is affected by artificial jaundice, the control and "jaundiced" rabbits were given radioactive phosphorus after fasting, and the specific activity of the various phosphoric fractions of the blood serum was determined.

From this experiment, the authors concluded that the passage of inorganic phosphorus from the intestine into the blood in jaundice is enhanced and that the freshly synthesized phospholipoids quickly and in increased quantities pass into the blood [15].

These data may possibly have some practical significance and serve as a further explanation of the mechanism of metabolic disturbances, in particular of phosphorus metabolism in jaundices of various origins.

In diseases of the liver unaccompanied by jaundice, the blood content of all, inorganic and lipid, phosphorus remains normal.

The impression had been created that despite the fact that the liver was affected by disease, the metabolism of phosphorus and, in particular, the absorption and utilization of phosphorus were not disturbed. It was decided to test this theory by the isotopic method.

By various means, dogs were given a liver disease of the type of toxic hepatitis unaccompanied by jaundice. Then both healthy and diseased dogs were fed a solution of radioactive phosphorus and at different intervals measurements were taken of the specific activity of the total amount of phosphorus in the blood serum. The curves of specific activity in healthy and hepatic dogs differed sharply. In the latter, independently of the method of inducing the hepatitis, the curves were considerably lower and of different shape than for the healthy dogs.

These differences in the curves of specific activity versus time could result from a disturbance of the process of absorption or utilization of the phosphorus or from both factors. Control experiments by subcutaneous injection of radioactive phosphorus convinced these authors that in hepatitis without jaundice both absorption and utilization of phosphorus are disturbed [16].

In this instance also the isotopic method used on an experimental model enabled us to understand disturbances of physiological processes which could not be explained by any other means.

The isotopic studies of the pathogenesis of various diseases are far from being exhausted by those which have been reviewed in our short survey.

Thus, for example, a considerable portion of our knowledge of the pathogenesis of anemia has been obtained by using radioactive iron.

The isotopic method is also used to study the peculiarities of metabolism in cancerous tumors.

A persistent search is being conducted to detect the earliest changes of metabolism in radiation sickness.

Isotopes also enable us to understand the pathogenesis of arteriosclerosis, hypertension, certain vitamin deficiencies and diseases of the endocrine glands.

The very first years of the employment of isotopes for the solution of biological and medical problems revolutionized experimental techniques, enriched scientific knowledge with important information and forced us to reexamine many firmly rooted concepts of biology and medicine.

At present, radioactive isotopes are available not to tens, but to hundreds and thousands of researchers. But this is only a beginning. In isotopes, medicine has acquired such a powerful means of studying the vital processes of both man and animals and the pathogenesis of diseases that we may expect practically important results in the immediate future—new methods and means of preventing and curing the most serious diseases of mankind.

#### LITERATURE CITED

- [1] E. Amaldi, O. D'Agostino, E. Fermi, B. Pontecorvo, F. Rasetti, E. Segre, Proc. Roy. Soc. (London) A149, 522 (1935).
- [2] O. Chievitz, G. V. Hevesy, Nature 136, 754 (1935).
- [3] R. Schoenheimer, Dynamic State of Body Constituents, Harvard Press (1942).
- [4] V. A. Engel'gardt, Report at the Conference of the Academy of Sciences USSR on the Peaceful Uses of Atomic Energy, July 1-5, 1955 (Plenary Session). USSR Acad. Sci. Press, p. 80.
- [5] C. A. Villey, A. B. Hastings, J. Biol. Chem. 179, 673 (1949). A. E. Renold, A. B. Hastings, F. B. Nesbett, *ibid.* 209, 687 (1954). A. E. Renold, A. B. Hastings, F. B. Nesbett, J. Ashmore, *ibid.* 213, 135 (1955).
- [6] D. Stetten, G. E. Boxer, *ibid.* 156, 271 (1944).
- [7] B. N. Stepanenko, G. V. Zubrilina and L. P. Khaliurova, Proc. Acad. Sci. USSR 100, 521 (1955); also B. N. Stepanenko, Report at the Conference of the Academy of Sciences USSR on the Peaceful Uses of Atomic Energy, July 1-5, 1955 (Division of Biological Sciences). USSR Acad. Sci. Press, 1955, p. 305.
- [8] M. F. Gulyi, L. A. Mikhailovskaia and R. G. Degtiar, Problems of Medical Chemistry 1, No. 6, 426 (1955).

- [9] S. M. Leites and G. G. Pavlov, Problems of Medical Chemistry 1, No. 5, 54 (1955).
- [10] D. L. Ferdman and V. A. Grigor'eva, Proc. Acad. Sci. USSR 85, 863 (1952); also The Application of Isotopes in Technology, Biology and Agriculture, USSR Acad. Sci. Press, 1955, p. 214.
- [11] A. V. Palladin, N. V. Vertmaier, Proc. Acad. Sci. USSR 102, No. 2, 319 (1955).
- [12] J. D. Benedict, H. J. Kalinsky, L. A. Scarrone, A. R. Wertheim, D. Stetten, J. Clin. Invest. 34, 141 (1955).
- [13] D. Stetten, New York Acad. Med. 28, 664 (1952). J. D. Benedict, P. H. Forsham, D. Stetten, J. Biol. Chem. 181, 183 (1949). J. B. Wyngaarden, D. Ir. Stetten, J. Biol. Chem. 203, 9 (1953).
- [14] J. D. Benedict, M. Roshe, T. F. Gü, E. J. Bien, A. B. Gutman, D. Stetten, Metabolism 1, 3 (1952).
- [15] K. S. Zamyckina, D. E. Grodzenskiĭ and E. F. Panchenkova, Problems of Medical Chemistry 1, No. 3, 218 (1955).
- [16] K. S. Zamyckina and D. E. Grodzenskiĭ, The Application of Isotopes in Technology, Biology and Agriculture (Reports of the Soviet Delegation to the International Conference on the Peaceful Uses of Atomic Energy). USSR Acad. Sci. Press, 1955, p. 244.

## ATOMIC SCIENCE NOTES

### CONFERENCE ON THE PHYSICS OF NUCLEAR FISSION

A conference on the physics of fission was held at the Academy of Sciences from the 19th to the 21st of January 1956. More than 300 workers from various laboratories in Moscow, Leningrad, Kharkov and other cities took part. Some 15 papers, both original and survey, on basic problems in fission physics were presented and discussed.

In an introductory talk, which opened the conference, N. A. Vlasov listed and briefly described these problems.

The first paper, by B. T. Geilikman, which was devoted to a survey of the theory of fission, considered the numerous attempts to explain the height of the fission barrier. A consistent hydrodynamic treatment of the nucleus as a drop of charged liquid yields the lowest barrier to symmetric deformation. In order to explain asymmetric fission and in order to obtain a theoretical basis for a lower barrier, a model of the nucleus as a compressible and polarizeable liquid has also been considered. Although these approaches indicate a possible way to explain the predominance of asymmetric deformation, they are unreliable quantitatively.

Barrier calculations on the model due to A. Bohr require consideration of both the effect of non-sphericity of the nucleus and the modification of the energy levels of the various nucleons because of deformation. The work of Foster, Nelson and Nosov indicates that the contribution of various nucleons to that part of the energy of the nucleus which depends on deformation is comparable to the hydrodynamical energies calculated on the basis of the liquid-drop model. At present, however, these calculations are only qualitative in nature and can yield quantitative results only with a good deal of difficulty.

This same report contained a discussion of work devoted to calculation of the widths of nuclear levels with respect to fission. In particular, an explanation was offered of the non-monotonic behavior of the fission cross-section for fast neutrons with energies in the region 1-2 Mev above threshold which has been observed by Geilikman, Nemirovsky and Nosov. Analyzing the quasi-static properties of the fission process, the speaker indicated that excitation of the fragments could be explained by irreversible and non-quasi-static changes of the surface energy which accompany changes in the shape of the fragments in the period which follows the separation of the connecting section (neck). Instead of a shape which is elongated along the line of fission, the fragments tend to assume an oblate form, corresponding to the minimum energy for two nuclei at a distance comparable to their radii. If two nuclei come together in a reversible manner, they should have an oblate shape on contact; thus the barrier height is greater for colliding nuclei than for solid spheres and the interaction-potential curve for colliding fragments is not the same as the curve which is to be associated with fission.

Geilikman also discussed various attempts to explain asymmetric fission. The hypotheses as to sub-barrier fission, which tend to favor asymmetric fission because of the greater penetration in the asymmetric case (Frankel) or the instability to asymmetric deformations (Vladimirsky) are apparently not valid. The explanation of asymmetry as a consequence of the dependence of the fragment excitation energy on the degree of asymmetry (Fang) is not satisfactory because it is based on arbitrary assumptions. Attempts to explain asymmetric fission on the basis of nuclear shell effects, in particular the recent work of Kurie and Hill are not convincing since they are not formulated in a quantitative fashion and are also based on arbitrary assumptions. The most satisfactory work is that of Nosov, Businaro and Galone in which the asymmetry

of fission is explained by the instability of the liquid drop model to asymmetric deformation after the transition through the highest point of the barrier, i.e., after the transfer of mass from one part of the nucleus to the other immediately before the separation of the connecting section (neck).

V. I. Mostovoi presented a survey of foreign and Soviet work on the measurement of fission cross sections in the heavy nuclei for monochromatic slow neutrons. A large part of the report was devoted to an analysis of the results on partial widths obtained at the Brookhaven Laboratory (USA). The variation in neutron and radiation widths in going from level to level in  $U^{235}$  is found to be the same in fissioning and non-fissioning nuclei. The distribution of the number of levels by size of adjusted neutron widths is approximately exponential. The change in radiative widths between levels is very small. Presently available data on separation widths indicate that these change by roughly one order of magnitude in going from level to level. The separation width seems to fluctuate between the two most probable values (0.04 - 0.05 ev and 0.10 - 0.12 ev).

It would be of great interest and value to fission physics to carry out further research in the partial widths of fissioning nuclei, their distributions in different resonances and the relations between these distributions and the spin character of the levels.

A paper by Yu. S. Zamyatin was devoted to an analysis of the fission cross section for fast neutrons. The energy dependence for most cross sections in the region from 2 to 6 Mev exhibits a plateau; for energies greater than 6 Mev there is a gradual ascent to a new plateau. For several isotopes the values of the cross sections at the first plateau are in good agreement with the curve which gives the fission probability as a function of the stability parameter  $Z^2/A$ . Using this relation a formula for the magnitude of the cross section at the second plateau can be derived. Calculations made with this formula for several isotopes are in good agreement with the experimental data. The relation presented by Zamyatin should make it possible to predict the values of unknown cross sections for fission by fast neutrons.

The experimental data on the distribution of fission fragments by mass and charge was surveyed in a report by A. N. Murin. He considered results obtained by radiochemical, mass-spectrometer and various other techniques. The effect of nuclear shell structure on the mass distribution of fragments was noted; it appears in the so-called fine structure of the distribution. The absence of a fine structure in the fragment distribution from  $U^{235}$  was noted. The data on the distribution of fragments of a given mass by charge is fitted satisfactorily by a Gaussian distribution with a mean width of approximately 2 charge units.

In the report delivered by V. G. Nosov, an analysis was given of the stability of the nucleus to asymmetric deformation; this analysis is based on an ellipsoidal shape with complex symmetric and asymmetric deformations due to perturbations. It was shown that the nucleus becomes unstable against asymmetric deformations after transition through a critical shape. Rough estimates of the asymmetry yield a ratio of fragment masses which is not far from the experimental ratio.

The experimental data on the anisotropic distribution of fission fragments was considered in a report by I. M. Frank, who noted the growth of anisotropy with increasing deviation from unity in the ratio of fragment masses. The anisotropy is a non-monotonic function of the bombarding-particle energy, revealing, in  $U^{238}$ , for example, a maximum in the region of 10 Mev. The reduced anisotropy at high energies is easily explained by the preliminary emission of a neutron. Frank also called attention to the dependence of the fission asymmetry on the mass of the fissioning nucleus. With increasing mass of the fissioning nucleus there is virtually no change in the mass of the heavy fragment; in the high mass region only the distribution of light fragments shows any change.

A theoretical interpretation of fission anisotropy, based on general angular momentum conservation rules, was presented in a paper by V. M. Strutinsky. In the simplest case, that of spinless fragments, he has obtained an isotropy which is in agreement with the experimental data both for particle-induced fission and for photo-fission.

A survey of the experimental data on fission neutrons was given in a paper read by B. G. Erozolimsky. Experiments on the determination of the instant at which a neutron is emitted were considered; in this connection Zamyatin has established an experimental upper limit on the neutron emission time which is  $10^{-12}$  sec after fission. Attention was directed to the surprising asymmetry in the distribution of neutrons from fragments which has been observed by Frazer and Milton; these authors found that the number of neutrons emitted by the light fragment increases while the number emitted by the heavy fragment decreases according to how close to symmetry the fragment masses are; at symmetry these numbers are divergent instead of convergent. The



theoretical and experimental data on the variation in the number of neutrons emitted per fission event were compared with curves showing the energy dependence of this number presented in a report by Lichman at the Geneva Conference. Satisfactory agreement was found and is maintained when the curves are extrapolated to an energy of 14 Mev. A survey of the data of Soviet and foreign authors on neutron spectra indicates that these are consistent with the assumption of evaporation of neutrons by excited moving fragments.

N. A. Perfilov, N. S. Ivanova and V. P. Shamov reported on the results of a study of fission carried out with photographic emulsions at Perfilov's Laboratory (Leningrad Radiation Institute).

Ivanova reported on an investigation of uranium fission by protons with energies from 140 to 660 Mev. In this energy region the cross section varies smoothly between roughly 1.5 and 1 barns. The probability of fission after an inelastic collision of a proton with a uranium nucleus shows almost no variation over the entire energy interval, remaining in the neighborhood of 80%. It was noted that uranium fission through capture of slow  $\pi$ -mesons is markedly different from fission induced by protons with an energy of 140 Mev.

Shamov has established a connection between the mean excitation energy of the nucleus in collisions with fast protons and the number of emitted charged particles and set limits on the values of threshold for emissive fission of different nuclei.

The paper given by Perfilov was devoted to complex fission, particularly triple fission accompanied by the emission of  $\alpha$ -particles. On a diagram showing the angular distribution of  $\alpha$ -particles at different energies, it was indicated that while low-energy  $\alpha$ -particles (up to 10 Mev) are emitted preferentially at  $90^\circ$  to the line of flight of the fragments (actually slightly inclined toward the light fragment) the faster  $\alpha$ -particles reveal an angular distribution which is more or less isotropic.

A paper by T. A. Mostovoi was devoted to a study of triple fission (accompanied by  $\alpha$ -particles) using ionization chambers; this study revealed a variation in the relative probability for triple fission of  $U^{235}$  as a function of the energy of the slow neutrons, indicating that the probability for triple fission depends on the initial state of the fissioning nucleus.

A survey of the data on spontaneous fission was given in a paper by K. A. Petrzhak. He noted a discontinuous change of the spontaneous fission period as a function of the number of neutrons in the nucleus in going through the value 152, indicating the existence of a new magic number. Petrzhak also remarked on the deviation from a monotonic dependence exhibited by the spontaneous fission period as a function of the stability parameter for several even-even elements and also corroborated the sharp differences in the spontaneous fission periods for odd isotopes as compared with even isotopes.

The connection between the spontaneous fission period and the  $\alpha$ -decay period was pointed out in a paper by V. N. Mekhedov. The ratios of these periods for different isotopes exhibit a small spread in magnitude and fall off slowly with an increase in the number of neutrons in the nucleus, reaching unity for nuclei with  $N \approx 158-156$ .

In a report by L. E. Lazarev, a survey was given of the experimental data on photofission. The results of the measurements indicate that the fission cross sections show roughly the same dependence on the  $\gamma$ -energy as does the cross section for the photoneutron effect. The ratio between the photofission cross section and the cross section for the photoneutron effect in uranium is weakly dependent on energy. For an energy somewhat greater than 100 Mev the fission cross section increases sharply, reaching values equal to the cross section for the resonance maximum at an energy of approximately 15 Mev. The angular distribution of the fragments shows a maximum at an angle of  $90^\circ$  to the beam of incident  $\gamma$ -radiation. The anisotropy of the fragments in photofission as well as in particle-induced fission increases with an increase in the asymmetry of the fragment mass. The anisotropy is reduced at higher  $\gamma$ -energies. The data on the angular distribution of fragments in photofission obtained by Lazarev and co-workers indicates the important role played by quadrupole absorption of  $\gamma$ -radiation for energies below 10 Mev. The report also discussed the results of an investigation of the fragment mass in photofission which indicates a smaller asymmetry at higher  $\gamma$ -energies.

This conference was convened with several objectives in mind: to elucidate the present status of the basic problems of fission physics, to emphasize the most interesting problems, to call the attention of the participants to these problems, to help the conferees to make intelligent choices in mapping programs for future research and to expand personal contact between workers in different laboratories. It is felt that these objectives have been fulfilled most successfully.

N. A. Vlasov

## AN EXHIBITION ON THE USES OF ATOMIC ENERGY FOR PEACEFUL PURPOSES

A number of exhibitions devoted to the uses of atomic energy for peaceful purposes are being arranged at the present time. One of these is to open in Moscow in the near future.

Visitors to the exhibition will get a graphic idea of the variety of applications of atomic energy in the national economy and its many potentialities in industry, agriculture, science and medicine.

An operating atomic reactor will be demonstrated at the exhibition. The demonstration reactor is a heterogeneous reactor which uses thermal neutrons; the operating power of the reactor is 10 kw and can be increased to 100 kw. The reactor thermal fission elements are uranium rods 100 mm in length enclosed in aluminum jackets. Sixteen of these rods are placed in an aluminum container and the core of the reactor consists of twenty-four of these containers. The core is similar to that of the VVR reactor which is being furnished by the Soviet Union to a number of countries under the scientific-technical assistance program.

The fissioning element in the reactor is uranium, enriched with 10%  $U^{235}$ ; the total weight of uranium in the reactor, in terms of pure  $U^{235}$ , is 3 kg. Ordinary water is used to moderate and reflect the neutrons.

The reactor core is under water at the bottom of a tank 6 m in depth. The tank is open at the top; hence visitors will have an opportunity to become familiar with the details of its internal construction and operation. The 4-6 m layer of water which surrounds the core serves as a shield against radiation. When the reactor is in operation a characteristic glow is observed around the core (Cerenkov radiation).

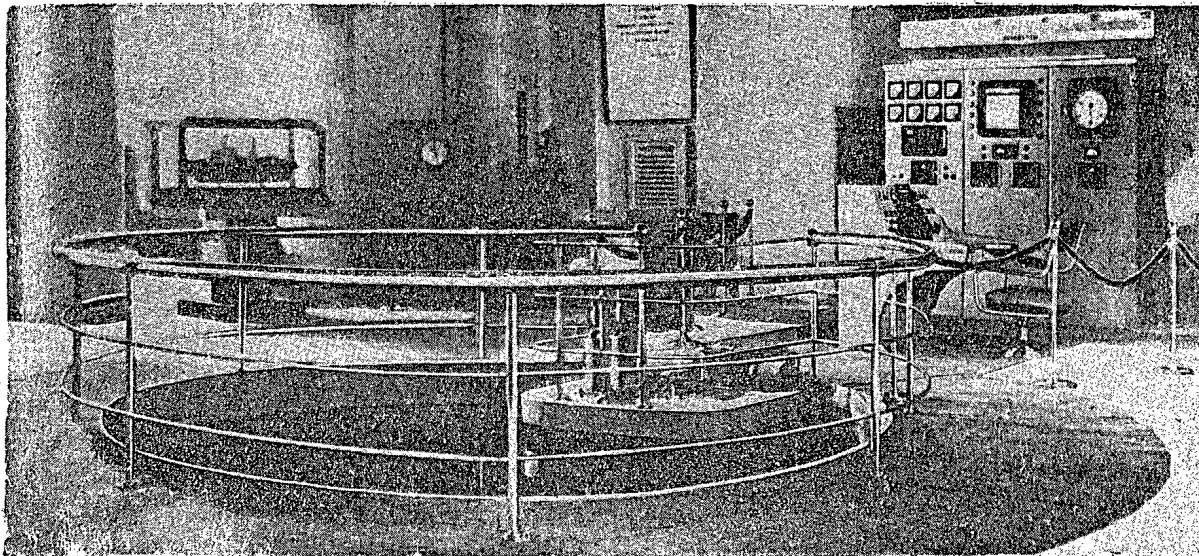


Figure 1. General view of the 10 kw thermal-neutron heterogeneous reactor.

The exhibition will have a model of the first atomic power station in the USSR, a model of the projected high-power stations which are to be built during the sixth Five Year Plan, and models of physics reactors for research purposes which are already completed or under construction. A large model ( $1/40$  th actual size) of an atomic electric power station with an aqueous water reactor, which is to operate at a

\* Aqueous water reactor.

power level of 200,000 kw, and detailed models of other power stations will give a good idea of the construction features of these new power sources which are being built by Soviet scientists and engineers. Visitors will also have an opportunity to become familiar with models of experimental atomic reactors which have been furnished to other countries by the USSR under the scientific-technical assistance program.

The exhibition will feature an atomic icebreaker built in the Soviet Union for operation under the difficult ice conditions in the Arctic. This powerful icebreaker has a displacement of 16,000 tons and an atomic power plant which can deliver 44,000 hp. Its speed is 18 knots and, since it uses an atomic power plant, this icebreaker can cruise 2-3 years without refueling.

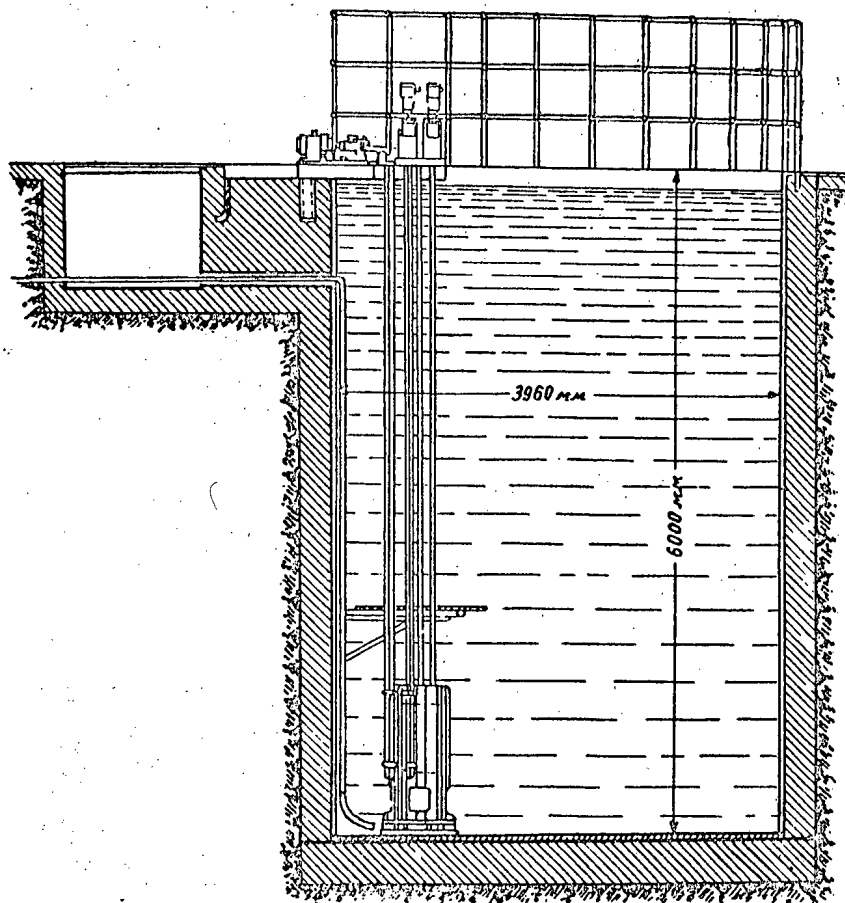


Figure 2. Sectional view of the heterogeneous demonstration reactor.

The counter has an exceedingly high resolving time (the order of  $10^{-10}$  sec) and has a transparent electrode which means that the point at which a particle is emitted can be located.

The exhibits in the section devoted to uranium geology, methods of prospecting and extracting uranium and thorium ores, and the chemistry of radioactive elements will be of great interest.

An especially interesting exhibit will be that in which the various materials used in the construction of atomic reactors will be shown.

A large section of the exhibition will be devoted to the uses of isotopes in the national economy. The exhibits in this section will deal with methods of obtaining radioactive and stable isotopes and their application in various branches of scientific research.

There will also be an especially comprehensive display on the application of radioactive isotopes and radiation for purposes of technological control and automation in manufacturing operations.

In the sections of the exhibition devoted to nuclear physics there will be a model of a Soviet synchrocyclotron which is the largest of its kind in the world and which accelerates protons to an energy of 680 Mev; there will also be photographs showing various stages of progress in the construction of the USSR 10 billion electron volt proton accelerator which is the largest accelerator of charged particles in the world. The construction work on this accelerator is completed and it is expected that start-up operations will get under way in the near future.

This section will also feature a large number of different kinds of instruments required for research in the realm of the atomic nucleus.

In particular, visitors will be able to become acquainted with a scintillation counter of new design which is intended for the detection and counting of nuclear particles,  $\gamma$ -rays, and x-rays.

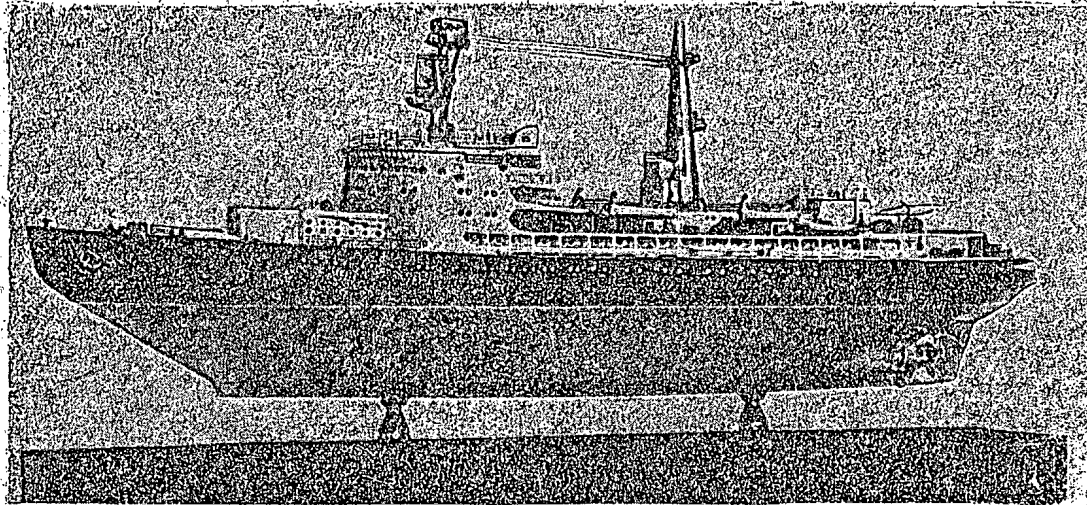


Figure 3. Model of the atomic icebreaker with a displacement of 16,000 tons and a power plant which can deliver 44,000 horsepower.

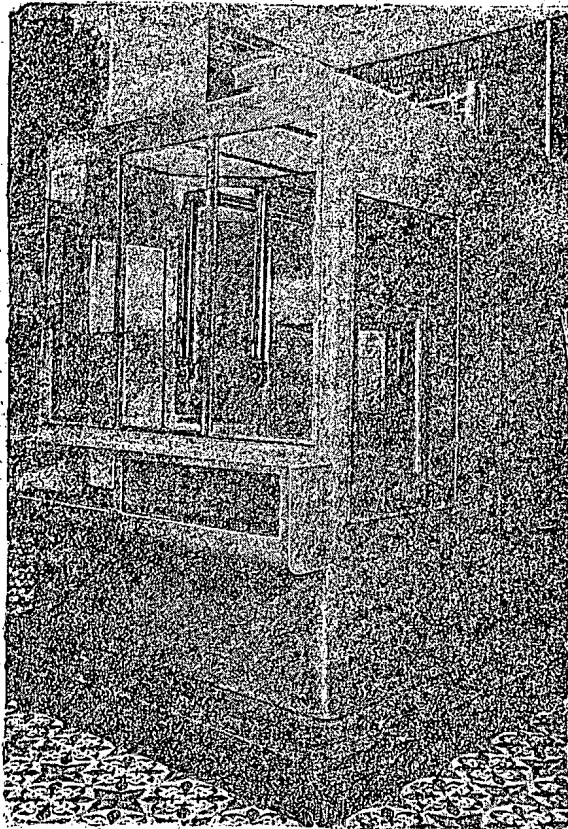


Figure 4. General view of the manipulator.

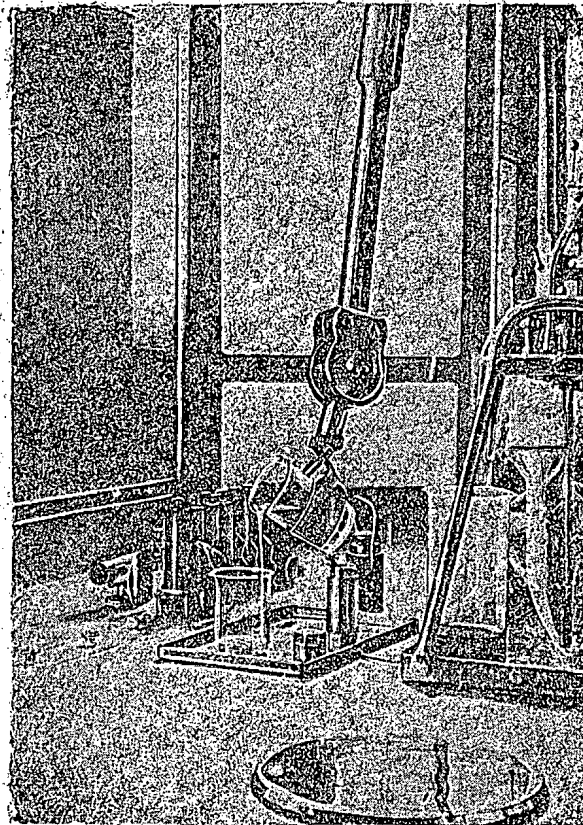


Figure 5. Details of the manipulator.

The great amount of equipment which will be shown is a convincing demonstration of the great value of these techniques and their widespread use.

There will be a separate exhibit on the uses of radioactive isotopes and radiation in medicine, especially for diagnosis of various diseases and malignant-tumor therapy.

There will also be a comprehensive display of dosimetry instruments and shielding techniques in connection with operations which involve radioactive materials; of special interest in this display is a large

manipulator which makes it possible to work on radioactive materials with adequate protection against the danger of exposure.

The things which will be shown at this exhibition, although representing only a part of the developments in the Soviet Union in the peaceful uses of atomic energy, still have great significance and scientific-technical value. Every visitor to the exhibition - specialist and non-specialist alike - will find much here that is interesting and instructive.

It is hoped that the dissemination of information at this exhibition will contribute to the further development of peaceful uses of atomic energy in the Soviet Union.

This interesting exhibition tends to invite comparison with the Soviet scientific-technical exhibition at the Geneva Conference on the Peaceful Uses of Atomic Energy in 1955. It is well known that the Soviet exhibition at Geneva enjoyed great popularity and received high praise. For example, the "Times", an English newspaper, in an article which appeared in the early days of the conference, wrote: "For the majority of the representatives of the press as well as for the delegates, the center of attraction was the Russian exhibition. . . . The exhibition indicates that extensive research in a number of fields has been carried out in the USSR . . . ."

Comparison of the two exhibitions shows the Soviet scientists and engineers have made a great deal of progress since the Geneva conference. The exhibition on peaceful uses of atomic energy is convincing evidence that the Soviet Union is making great strides in the direction of practical use of atomic energy.

I. I. Novikov

## News of Foreign Science and Technology

### CONSTRUCTION OF THE FIRST ATOMIC POWER STATION IN ENGLAND

Construction of the first English atomic power station, consisting of two uranium-graphite reactors with gas cooling, was commenced in May, 1953 at Calder Hall, Cumberland. The prospective power output of the station is 92 megawatts. The first reactor should begin to operate at the end of 1956, and by the end of 1957 the atomic power station will begin to produce electricity for general consumption [1, 2, 5].

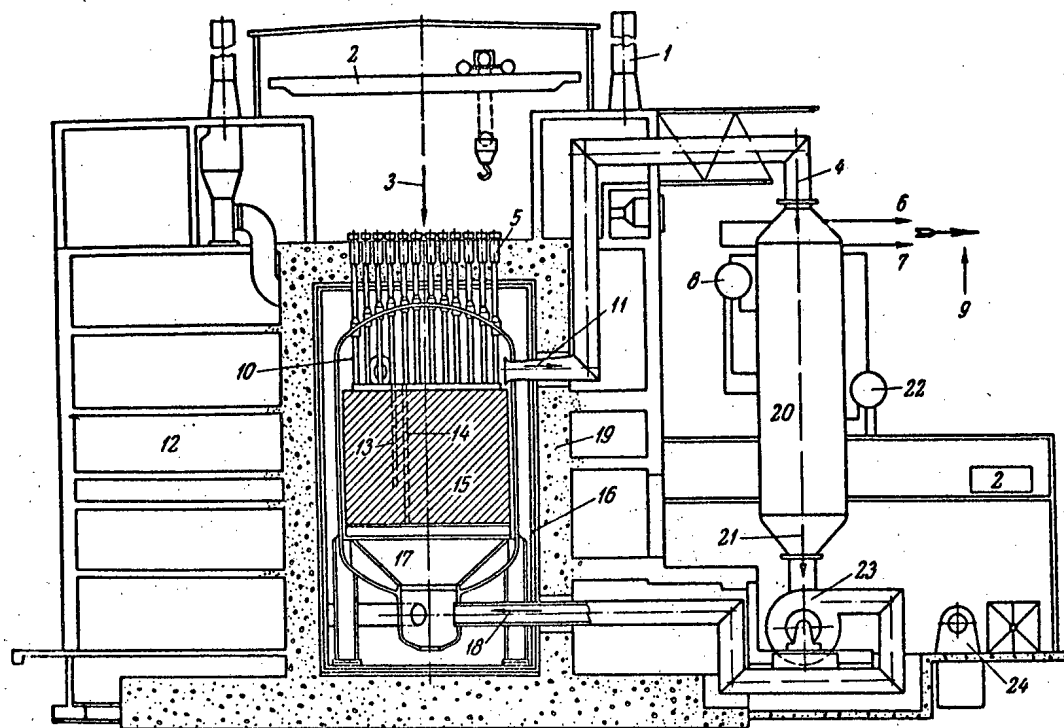


Figure 1. Schematic drawing of reactor [3].

1) Pipe for cooling air; 2) bridge crane; 3) channels for fuel elements and control rods; 4) hot gas; 5) charging tubes; 6) high pressure steam; 7) low pressure steam; 8) high pressure steam drum; 9) steam to turbogenerator assembly; 10) control rods; 11) hot gas outlet; 12) reversing and control unit; 13) control rod; 14) uranium rods; 15) graphite moderator; 16) heat shield; 17) hermetically sealed reactor casing; 18) cold gas inlet; 19) biological shield; 20) heat exchanger; 21) cold gas; 22) high pressure steam drum; 23) forced air circulatory cooling system with electric blower; 24) motor-generator.

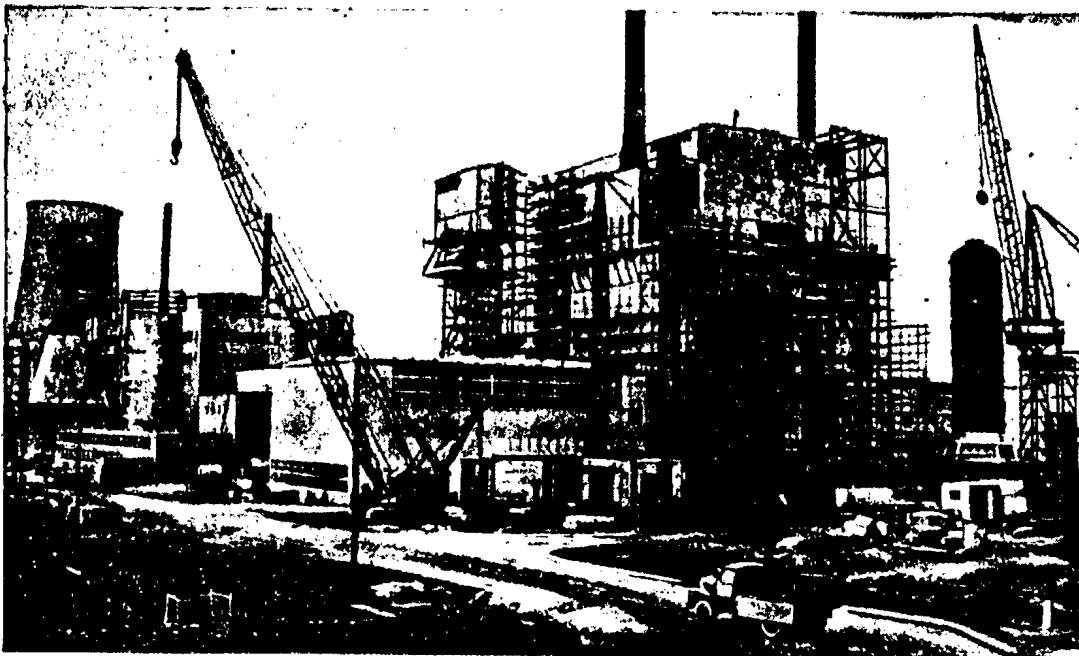


Figure 2. General view of atomic power station.

In the foreground – second reactor, on the left – first reactor. The administration buildings can be seen between the two reactors. Two cooling towers are visible behind the first reactor: the farther one fully completed, the nearer under construction [5].

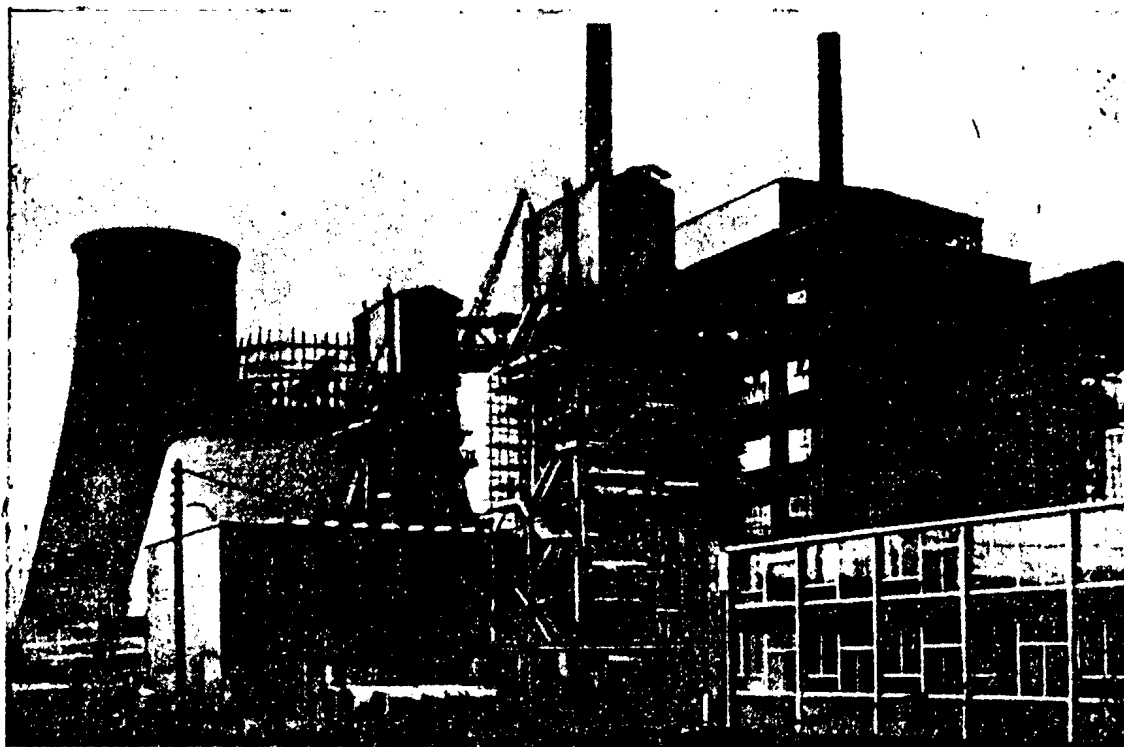


Figure 3. The building housing the first reactor. The heat exchanger is in the center, and the cooling towers to the left.



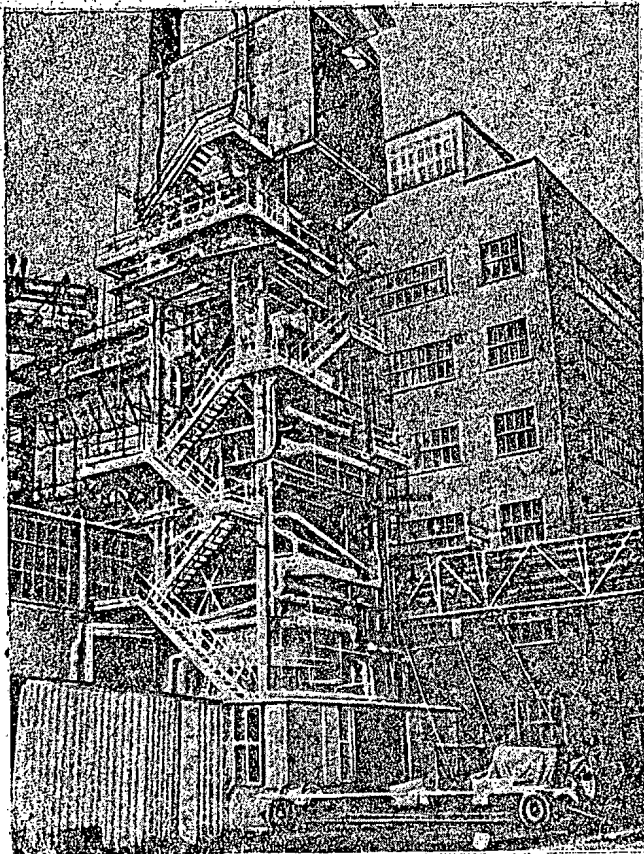
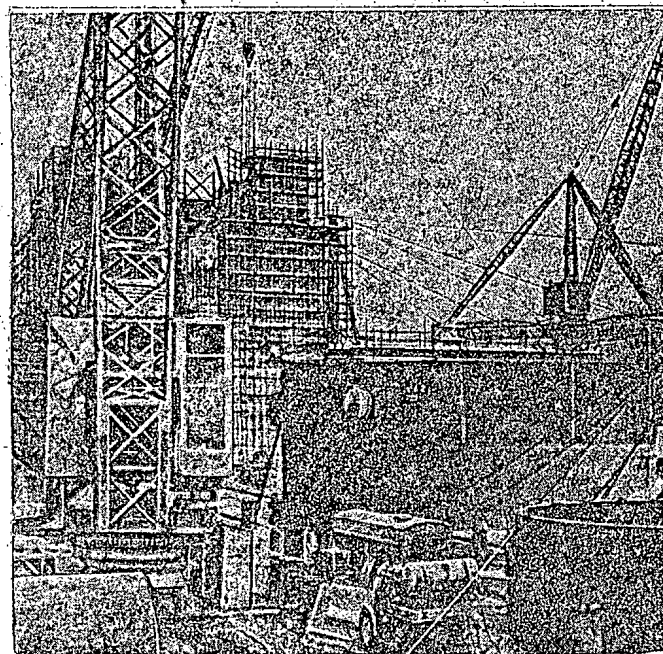


Figure 4. One of the four heat exchangers (the heat exchanger is hidden by boards, pipes and stairs) consisting of a steel cylinder 24.4 m high, 5.5 m in diameter, weighing 200 tons. The heat exchanger was transported to Calder Hall, disassembled (9 sections), and welded on the spot [5]. The heat exchanger pipes are supplied with fins. Water and steam flow through the pipes; hot carbon dioxide gas is in contact with the outside of the clusters of pipes.

Figure 5. Construction of one of the two reactors. In the foreground is a completed hermetically sealed reactor casing which will be set up in the reactor building to a height of 36.6 m [2].





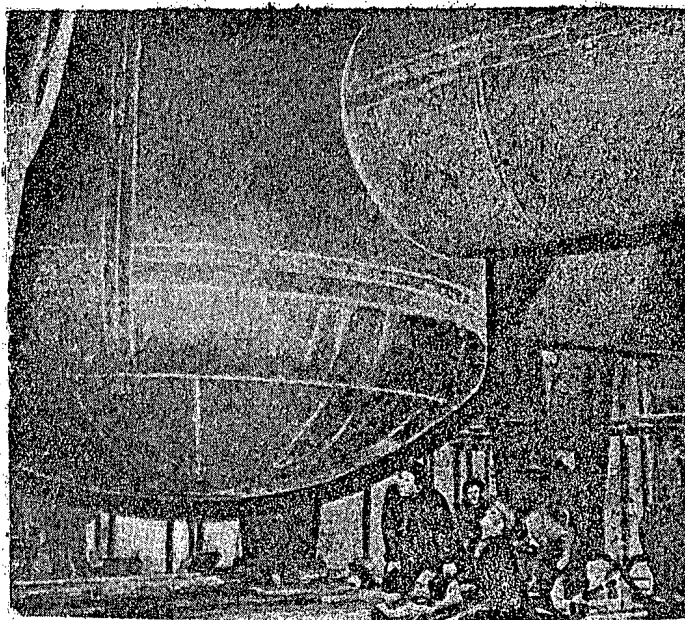


Figure 6. Bottom of the hermetically sealed reactor casing. On the left is the pipe through which carbon dioxide is returned from the heat exchanger to the reactor [2].

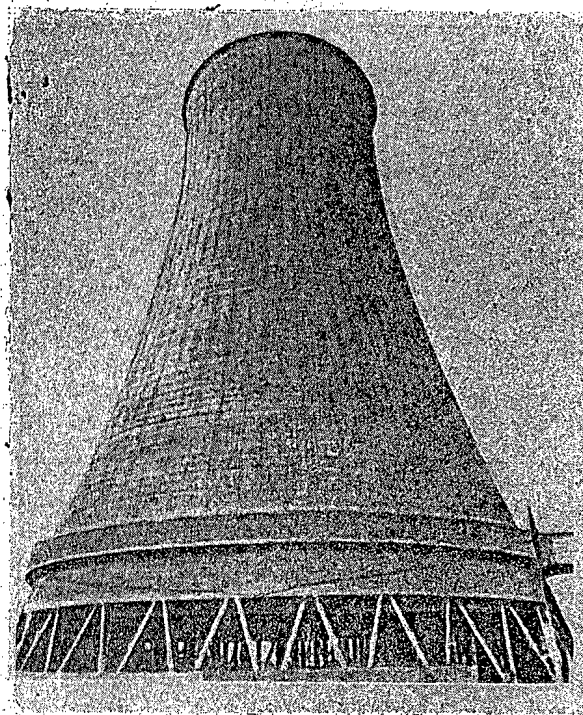
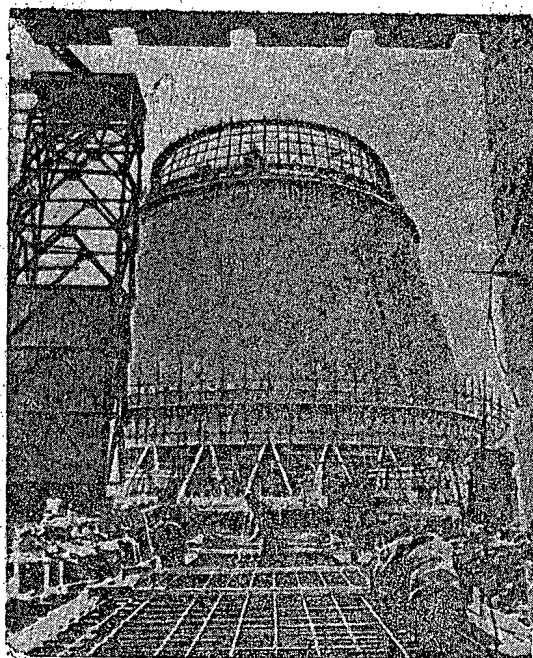


Figure 7. Two cooling towers. Construction of tower No. 2 on the left, completed tower No. 1 on the right. Two towers 88.4 m high and 61 m in diameter (at the base) are provided for each reactor. Each tower can cool  $13,500 \text{ m}^3$  of water an hour [5].

The active zone of the reactor is composed of several thousand graphite blocks, which serve as moderator, and is enclosed in a hermetically sealed steel casing 12.2 m in diameter and 18.3 m high, welded together from steel plates 60 mm thick. In the graphite there is a large number of vertical channels for fuel elements and control rods.

Natural uranium rods with metallic cladding are used for fuel. Control and safety rods consist of stainless steel tubes filled with boron steel blocks.

The core is surrounded by a concrete biological shield. To reduce heating of the concrete, the inner surface of the concrete is lined with steel sheets 100 mm thick.

Extraction of heat from the reactor is accomplished by carbon dioxide gas at seven atmospheres pressure, which circulates through the core and four heat exchangers located at the corners of the reactor building. More than 20 tons of carbon dioxide is required to fill the entire system. In the secondary loop of the heat exchanger is formed the steam which feeds four turbogenerators [3], [4].

The first Calder Hall unit will be included in the electric power system in October, 1956. The second reactor is scheduled to commence operation six months after the first, i.e., in April, 1957.

Of six reactors of the Calder Hall type, two will be built at Calder Hall and four near Annan (Dumfries county). [6].

V. V.

#### LITERATURE CITED

- [1] Engineering 180, No. 4674, 265 (1955).
- [2] Industrial Chemist 31, No. 371, 599-601 (1955).
- [3] A Programme of Nuclear Power, Her Majesty's Stationary Office, London, 1955.
- [4] C. Hinton, The Graphite-moderated Gas-cooled Pile and its Place in Power Production, Report No. 406 at the International Conference on the Peaceful Uses of Atomic Energy.
- [5] Sphere 223, No. 2911, 378-379 (1955).
- [6] Engineering 181, No. 4698, 143 (1956).

### PROJECTED DUAL CYCLE BOILING-WATER REACTOR

The projected reactor described here has been designed for an atomic power station of 180,000 kw capacity, and is to be built in the USA near Chicago. The choice of a boiling-water reactor without heat exchanger was made in an attempt to lower the operating pressure inside the core. Ordinary boiling-water reactors have comparatively low specific power output. Possible heat extraction is limited by the fact that the reactor becomes difficult to control when the steam content in the steam-water mixture within the core exceeds 10% by volume. When this happens, it is difficult to compensate for the rapid fluctuations of reactivity as a result of fluctuations in the effective density of the moderator. In the reactor under consideration here, this shortcoming is eliminated since steam is formed not only within the core, but also in a special tank (flash tank), which receives part of the water heated to boiling point at 42 atmospheres pressure in the core. Pressure in that tank is maintained at 24.5 atmospheres. Superheated water vaporizes in the flash tank, and 8% of it changes to steam while the temperature of the remaining water decreases to the boiling point of water at 24.5 atmospheres. The high pressure steam from the core and low pressure

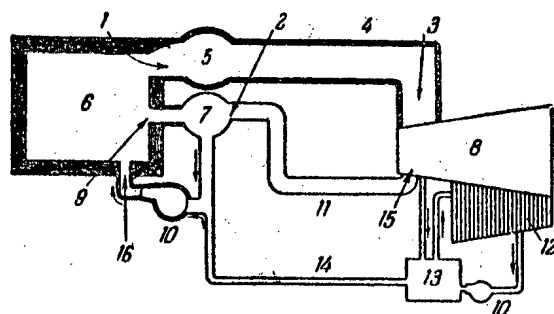


Figure 1. Flow sheet of the reactor.

1) Half of the heat output of the reactor is carried away by high pressure steam; 2) in the flash tank part of the water changes to steam; 3) turbine high pressure stage inlet; 4) steam at 42 atmospheres; 5) steam dome; 6) reactor, 42 atmospheres; 7) flash tank; 8) turbine; 9) half of the heat output of the reactor is carried away by superheated water; 10) pump; 11) steam at 24.5 atmospheres; 12) condenser; 13) feed-water preheater; 14) water; 15) turbine low pressure stage inlet; 16) cooled water returns to the reactor.

steam from the flash tank are conveyed to the respective stages of the turbogenerator, and the water cooled in the flash tank together with the condensate from the spent steam are conveyed back to the reactor. Because of this, steam is formed in the core mainly in its upper part. Apart from the fact that this system has several times greater specific power output than the usual boiling-water reactor, it has superior automatic control of power output with fluctuating load. The turbine governor regulates basically the input of low pressure steam (24.5 atmospheres).

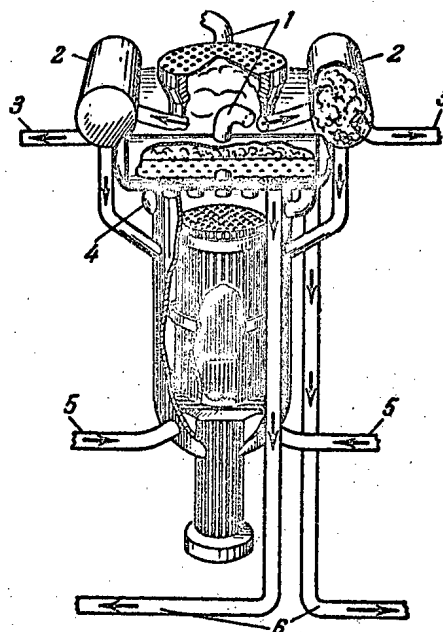


Figure 2. Reactor design.

1) Steam at a pressure of 24.5 atmospheres; 2) steam domes; 3) steam at a pressure of 42 atmospheres; 4) flash tank; 5) water from the flash tank and from the condenser, pumped into the reactor; 6) water from the flash tank.

Increased flow of steam causes increased rate of water circulation in the system because of the increased flow of superheated water from the core to the flash tank. The corresponding increase in density of the steam-water mixture causes an increase in reactivity of the reactor, raising its thermal power in proportion to the load. The negative temperature coefficient of reactivity which is characteristic of boiling water reactors under all emergency conditions guarantees complete safety of operation.

Figure 1 shows how the reactor operates. Figure 2 gives an idea of its construction.

G. B-v

#### LITERATURE CITED

- [1] Electrical World 143, No. 24, 71-74 (1955).
- [2] Electrical Engineering 74, No. 7, 625 (1955).

## THE ATOMIC SUBMARINE "NAUTILUS"

In 1954 there was placed in service in the war fleet of the U. S. A. the first submarine with an atomic power plant, which received the name "Nautilus". The displacement of the ship is 2700 tons.

The source of energy for the "Nautilus" is a thermal-neutron nuclear reactor. Ordinary water under high pressure serves as moderator and primary heat transfer medium. The specified pressure is maintained under any conditions of operation by means of a compensation tank with a steam space. A special centrifugal pump circulates the water in the primary circuit through the active zone of the reactor and the heat exchanger. The water in the secondary circuit of the heat exchanger is heated to boiling and converted into steam, which is used to drive steam turbines.

To assure greater buoyancy of the "Nautilus" in case of damage to its hull, the power installations of the submarine are located in two compartments. The reactor and the heat exchanger are installed in the reactor compartment. In the engine room there are two steam turbines, which can be operated either in parallel or independently. Here are also located the turbogenerators that supply the submarine with electrical energy, and the main control desk for all the machinery in both engine and reactor compartments. In case of emergency the motor of the submarine can run on a storage battery or a diesel driven generator.

A special light-weight shield assures the safety of the crew during operation of the reactor. This shield lowers the intensity of radiation to such a level that if the submarine were to cruise continuously for the lifetime of the reactor, members of the crew would receive a smaller dose of radiation than they receive during their lives by the action of cosmic rays, natural radioactivity of the earth's surface, periodic chest X-rays, and other "natural" causes.

The "Nautilus" has a system of control for radioactivity. It includes dosimeters to check the radioactivity of the air and  $\gamma$ -ray detectors installed in various sections of the submarine. Special apparatus indicates any damage to the tubes in the heat exchanger, giving warning of the penetration of the radioactive heat transfer medium from the primary circuit into the unprotected steam system. The radioactivity indicators assure the prevention of discharge of radioactive water while in dock or in other places where it could be dangerous to human beings.

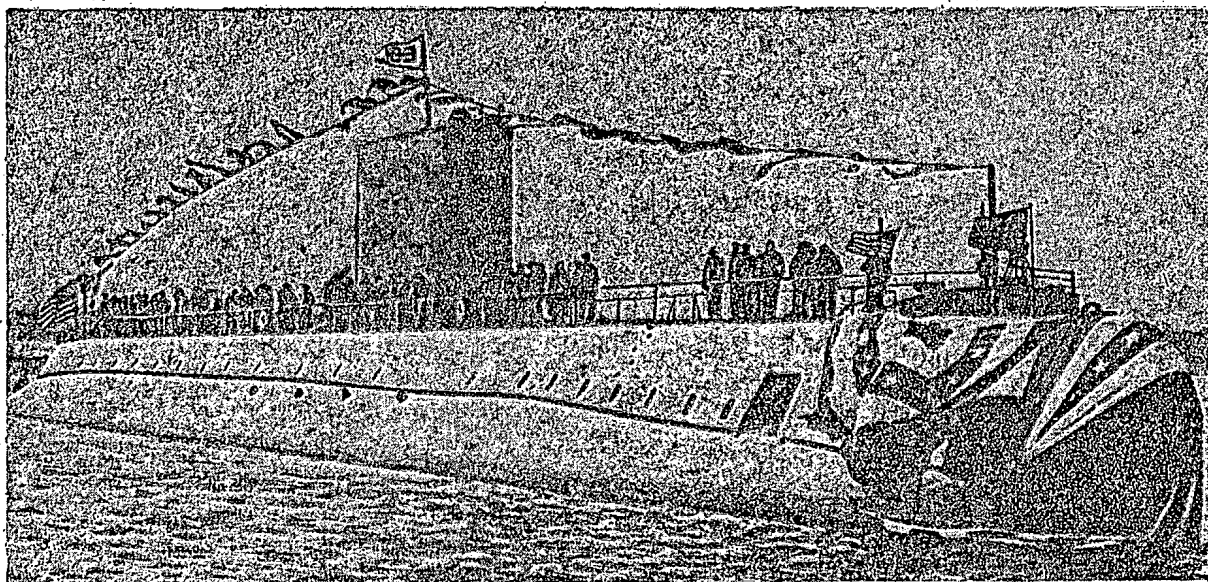


Figure 1. The atomic submarine "Nautilus" (SSN-571) after launching.

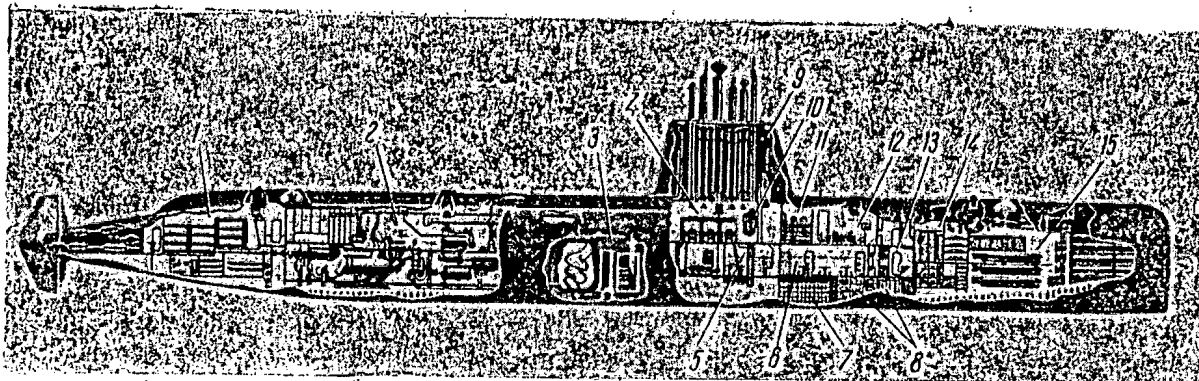


Figure 2. Longitudinal section of the "Nautilus".

1) Crew's quarters; 2) engine room; 3) reactor; 4) conning tower; 5) control room; 6) mess room for the crew; 7) battery room; 8) store rooms; 9) bridge; 10) periscope compartment; 11) commander's cabin; 12) officers' ward-room; 13) galley; 14) crew's quarters; 15) torpedo compartment.

During the design of the reactor for the submarine, a prototype was constructed, called STR-1\*. The power plant STR-2, installed in the "Nautilus", is essentially a copy of its prototype constructed on shore. Tests of the reactor STR-1 in June 1953 were conducted under conditions simulating an underwater voyage of the atomic submarine across the Atlantic ocean. During the tests careful measurements were made on the reactivity of the reactor for various pressures and temperatures of the heat-exchange medium in the primary circuit. There was a thorough investigation of the ability of the reactor to function under conditions of rapidly changing load on the submarine's propeller shaft. Practical tests were conducted on the possibility of making repairs by interchanging parts.

Recently there was put into service in the U.S.A. a second atomic submarine, named the "Sea Wolf". Seven more atomically driven submarines are being built.

Ven. S.

#### LITERATURE CITED

- [1] L. H. Roddis, J. W. Simpson, Marine Engineering 60, No. 2, 69-73, 83 (1955).
- [2] Science News Letter 68, No. 26, 405 (1955).
- [3] Science News Letter 67, No. 3, 66 (1955).
- [4] Navy Time 5, No. 3, 6 (1955).

\*Submarine Thermal Reactor

## DESIGN OF A PORTABLE POWER REACTOR

At the beginning of 1953 a group of engineers and physicists of the Oak Ridge National Laboratory (U.S.A.) was given the problem of designing a reliable and economical electrical station for use in remote regions to which access is difficult.

The installation as designed has a two-circuit heat-exchange system. The water circulating in the primary circuit removes heat from the active zone and, through the heat exchanger, heats the water of the secondary circuit and converts it into steam, which drives a turbogenerator and also serves to heat the building.

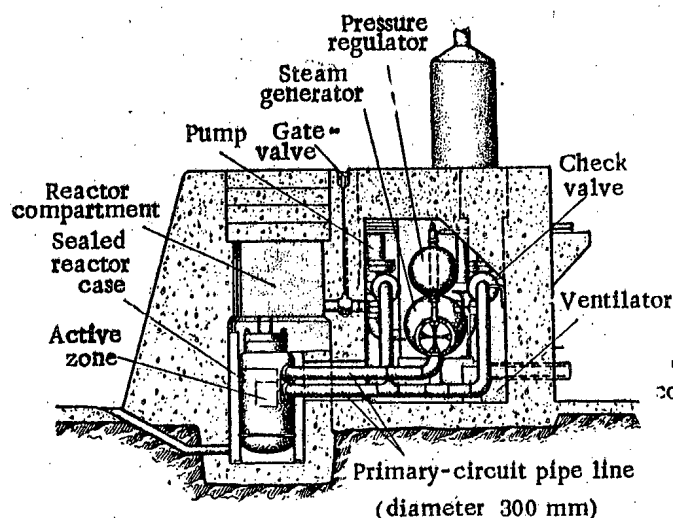


Figure 1. Primary cooling system. Location of components (vertical section).

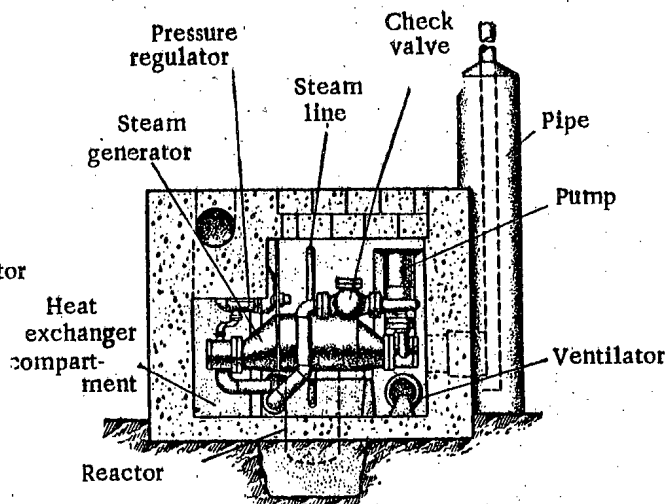


Figure 2. Primary cooling system. Showing the heat exchanger compartment.

The primary circuit consists of the sealed case of the reactor, a volume compensator, two circulating pumps, and a tubular heat exchanger, whose jacket forms part of the secondary circuit.

To avoid high concentrations of corrosion products the water in the primary circuit is continuously renewed by condensate from the secondary circuit. Therefore the primary circuit also includes a storage tank for the entering water, a demineralizer and two filters. Water is used in the primary circuit at the rate of 15.2 cubic meters per minute. The temperature of the water entering the active zone of the reactor is 222°C, and its temperature on leaving the active zone is 232°C. The pressure in the primary circuit is 84 atmospheres.

The secondary circuit consists of the turbogenerator with its condensers and cooling system, an arrangement for returning water from the heating system, a deaerator, and the heat exchanger.

The planned thermal power of the reactor is 10,000 kw, the total electric power is 1300 kw, and the useful electric power is 1000 kw.

The heat-developing elements of the reactor are prepared from highly enriched uranium. One charging is calculated to give 15 megawatt-years and requires about 25 kilograms of highly enriched uranium.

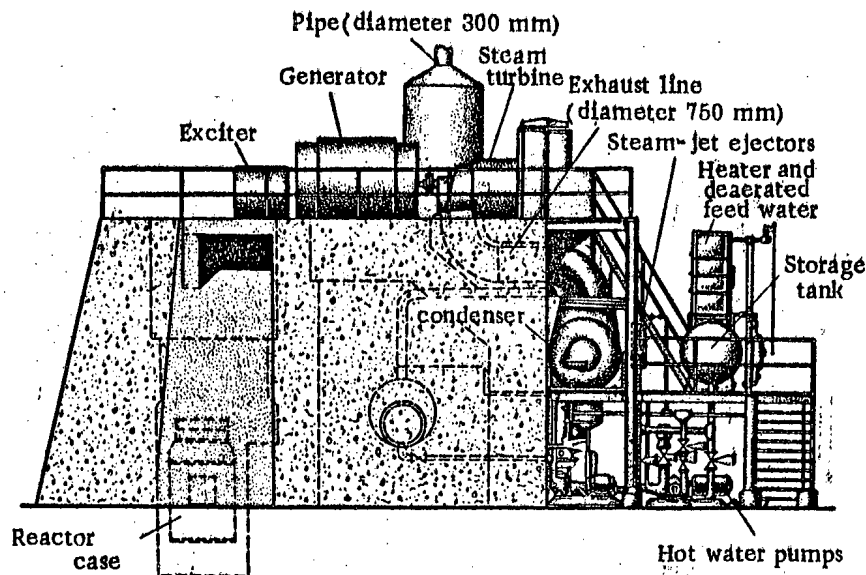


Figure 3. Steam and auxiliary equipment of the portable reactor.

The main steam generator consists of a one-passage tubular heat exchanger. The normal pressure in the steam generator is 13.5 atmospheres. In the absence of load the pressure rises to 29.6 atmospheres. The reactor power corresponds to the load if the temperature of the water leaving the active zone remains constant (232°C). The control system assures displacement of the control rods when the temperature of the water changes.

The concrete shield of the reactor consists of two sections, with the reactor located in one and the steam generator in the other. The shielding is calculated on the basis of 10 megawatts reactor power and allowable radiation dose 5.36 milliroentgens per hour. The walls and flat roof of the reactor building are assembled with plates consisting of a layer of insulation 3.7 cm thick, made of fiber glass, enclosed between two steel sheets.

According to preliminary estimates the cost of the installation amounts to 1,703,000 dollars.

For a study of the characteristics of the installation it was decided to build a full-scale electric station based on this reactor.

V. R.

#### LITERATURE CITED

- [1] Mechanical Engineering 77, No. 11, 967-970.



## ATOMIC BATTERIES\*

The discovery of the possibility of the direct transformation of atomic into electric energy has aroused great interest not only from a purely scientific, but also from a practical point of view. Atomic batteries may be divided into four types, depending on the method of changing atomic into electric energy.

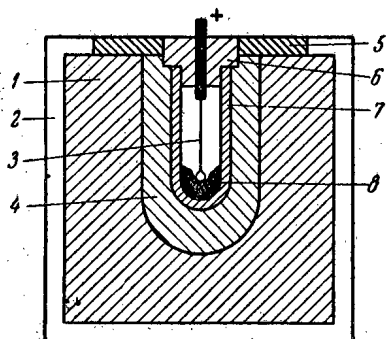


Figure 1. Battery with collector of primary current and solid dielectric.

1) Lead shield; 2) case; 3) contact wire; 4) aluminum collector; 5) plate; 6) bushing; 7) capsule (5, 6, 7 are of polystyrene); 8) radioactive substance.

Atomic batteries of the first type are modifications of a charging device (described by Moseley [1] as early as 1913), in which a metal sphere was charged by the  $\alpha$ -radiation of a radioactive source placed at its center on an insulating lead. Thus there was produced a difference of potential between source and sphere of more than 150 kV. Sources of this type are now prepared in three varieties:

- a) a conducting surface is charged by radioactive radiation ( $\alpha$  or  $\beta$ ) through a vacuum [2, 3];
- b) a conducting surface is charged by radioactive radiation ( $\alpha$  or  $\beta$ ) through a solid dielectric [4-6]; and
- c) a conducting surface is charged by means of secondary emission of charged particles produced by primary radioactive radiation [7].

Sources of electric energy of this type as a rule have small current strength (of the order of  $10^{-10}$ - $10^{-12}$  ampere) and are used either for anode supply in electron-ray tubes, or as devices for accelerating individual charged particles. The coefficient of current utilization of devices of this type is about 1 - 1.5%. If a mixture of  $\text{Sr}^{90}$  -  $\text{Y}^{90}$  of intensity 10 millicuries is used as the radioactive source, then with a device with polystyrene dielectric one can obtain a current of the order of  $10^{-12}$  ampere and an emf of the order of 10 kV. A battery with such a radioactive source can work without recharging for about 25 years (under the condition that the dielectric does not change its properties).



Figure 2. Battery with collector of primary current and solid dielectric.

\* W. Shorr, Report No. 171 at the International Conference on the Peaceful Uses of Atomic Energy (1955).

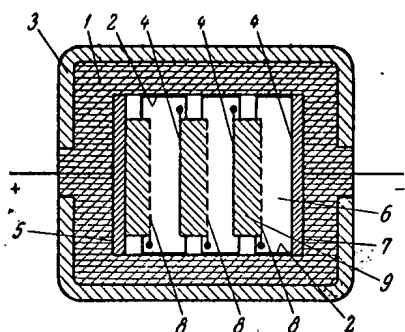


Figure 3. Battery with collector of secondary current:  
1) Dielectric; 2) spacer; 3) case; 4) collector; 5) source of radiation; 6) vacuum space; 7) end collector; 8) secondary electron emitter; 9) polystyrene disk with openings for terminals.

Besides  $\text{Sr}^{90}$ - $\text{Y}^{90}$ , it is also possible to use in batteries of this type tritium or other radioactive elements emitting  $\beta$ -particles of not too high energies.

The second type of atomic batteries includes those in which the radioactive radiation does not simply charge a conducting surface, but ionizes the atoms of a gas, so that under the action of the contact potential difference between the electrodes a current is produced inside the battery. This current can be used in the external circuit. The usual coefficient of current utilization in batteries of this type (including those with many elements) is about 1% [8-14].

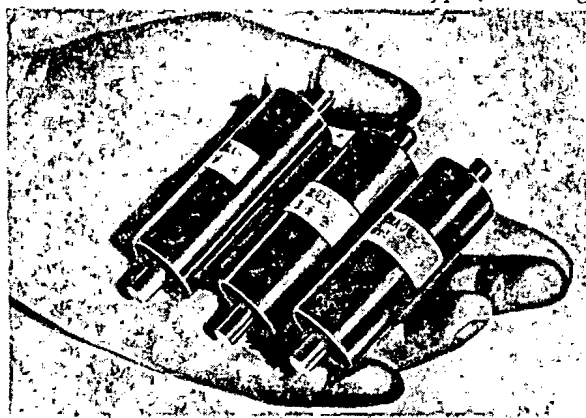


Figure 5. Experimental models of batteries with ionization of gas and use of the contact potential difference.

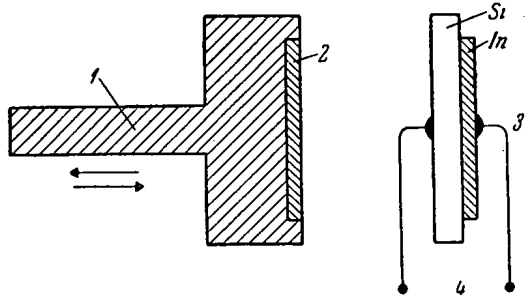


Figure 6. Battery with amplification of current at semiconductive  $p$ - $n$  junction.  
1) Metal support (movable); 2) source; 3)  $p$ - $n$  junction; 4) terminals.

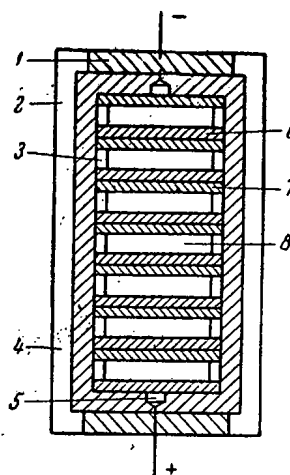


Figure 4. Battery with ionization of gas by radiation and use of the contact potential difference.

1) Ceramic disk; 2) insulating cartridge; 3) insulating ring; 4) sealed insulated case; 5) contact; 6) electrode with large work function; 7) electrode with small work function; 8) filling gas; mixture of argon, hydrogen, and tritium.

The third and most promising type of atomic battery is that with amplification of the current at a semiconductive  $p$ - $n$  junction [15]. Semiconducting alloy junctions of the  $p$ - $n$  type, when irradiated with  $\beta$ -rays, for example  $\beta$ -rays emitted by a  $\text{Sr}^{90}$ - $\text{Y}^{90}$  mixture, act as sources of voltage and current.

Rappaport [16] conducted measurements on alloy  $p$ - $n$  junctions of silicon and germanium of area about  $0.25 \text{ cm}^2$ . The source of radioactive radiation was a mixture of  $\text{Sr}^{90}$  and  $\text{Y}^{90}$  with 90 millicuries activity. An atomic battery with a silicon  $p$ - $n$  junction gave a voltage of the order of 0.25 v and short-circuit current  $10^{-5}$  amp; the corresponding values for a battery with a germanium  $p$ - $n$  junction were 0.03 v and  $2.5 \cdot 10^{-5}$  amp. The overall efficiency for both batteries was about the same, 0.4 %. The theoretical overall efficiency of a battery of this type is  $\sim 2\%$ .

Atomic batteries of the fourth type use the thermal energy of radioactive radiation. An example is a thermoelectric battery with  $\text{Po}^{210}$  [17] as heat source. The working principle of such a battery is no different from that of an ordinary thermopile. The battery contains several junctions of two different metals at different temperatures (some of the junctions are heated by the source of radioactive

radiation). The difference of temperature gives rise to a thermoelectric emf, which can then be used. The overall efficiency of such batteries amounts to 0.1 - 0.2 %.

The appearance of atomic batteries is a demonstration of the possibility of direct transformation of atomic energy into electric energy, and has undoubted scientific interest. But atomic batteries can so far not be used as sources of electric energy to supply any actual devices.

There is no doubt that the further development of the construction of atomic batteries, their perfection, and the discovery of new types of batteries will in the near future make possible the production of atomic batteries with a long term of service, useful as sources for all sorts of electronic devices.

VI. S.

#### LITERATURE CITED

- [1] H. J. G. Moseley, Proc. Roy. Soc. (London) A88, 471 (1913).
- [2] P. H. Miller, Phys. Rev. 69, 666 (1946).
- [3] S. M. Christian, E. G. Linder, J. Appl. Phys. 23, 1213 (1952).
- [4] J. H. Coleman, et al., Nuclear Batteries Radiation Research Corporation, West Palm Beach, Fla., Contract No. DA36 - 039SC - 42564.
- [5] P. Rappaport, E. G. Linder, J. Appl. Phys. 24, 9 (1953).
- [6] J. H. Coleman, Nucleonics 11, No. 12 (1953).
- [7] E. Schwarz, Secondary Emission Nuclear Battery, U. S. Pat. Application, Serial No. 434,095, June 2, 1954.
- [8] Millman and Seely, Electronics, McGraw Hill, 1951, p. 93 ff.
- [9] H. B. Michaelson, J. Appl. Phys. 21, 536 (1950).
- [10] Lord Kelvin, Mathem. and Phys. Papers, VI, Cambridge, 1911.
- [11] J. B. Kramer, The Electrician 93, 497 (1924).
- [12] P. E. Ohmart, J. H. Hutchinson, E. H. Daggett, J. W. Heyd, J. S. Stanton, The Radioelectric Effect, U. S. AEC, MLM-629, 1951.
- [13] P. E. Ohmart, J. Appl. Phys. 22, 1504 (1951).
- [14] R. R. Annis, Radioactive Battery, Signal Corps. Eng. Labs. Tech. Manual 1456, 1952.
- [15] G. J. Dienes, Radiation Effects in Solids, Annual Review of Nuclear Science, Vol. 2, 1953.
- [16] P. Rappaport, Phys. Rev. 93, 246 (1954).
- [17] K. C. Jorden, J. H. Birden, Batteries Using Polonium-210, Mound Lab., AEC Report MLM-984 (1954).

## ON WORK CONDUCTED IN THE U.S.A. TOWARD THE REALIZATION OF A CONTROLLED THERMONUCLEAR REACTION

In the third decade of this century, when the mass defect of the nucleus  $\text{He}^4$  was measured, it became clear that a reaction transforming hydrogen into helium has enormous interest for energy purposes. But only in the last few years, as a result of the careful measurements of cross sections for the reactions  $\text{D}(\text{d}, \text{n}) \text{He}^3$ ,  $\text{D}(\text{d}, \text{p}) \text{T}$ ,  $\text{T}(\text{d}, \text{n}) \text{He}^4$  and for a number of other reactions of nuclear synthesis, has it been established that the materials most advantageous for synthesis are the isotopes of hydrogen, deuterium and tritium. Only after these measurements was there a serious scientific basis for projects for reactors in which hydrogen is burned and heavier nuclei are formed. The cross sections of these reactions at small energies of the relative motion of the nuclei of hydrogen are very small; they become sufficiently large only at energies of some tens of kilo-electron-volts. Thus the reactions must occur in hydrogen heated to hundreds of millions of degrees.

To excite these reactions of synthesis, which have received the name of thermonuclear reactions, it is necessary in the first place to solve two problems: 1) to heat the hydrogen to the temperature in question, and 2) to maintain this temperature for a sufficient time for an appreciable part of the hydrogen to react.

As the temperature required exceeds the temperature of the interiors of stars, there arises the extraordinarily difficult problem of the thermal insulation of the gas, heated to the very high temperature, from the container in which the gas was held before heating. As is well known, the impulsive heating of a large quantity of hydrogen, by means of an atomic bomb explosion which initiates a thermonuclear reaction, produces the explosion of the hydrogen bomb. The use of a thermonuclear reaction for industrial energy purposes requires that one learn to heat a small quantity of hydrogen by using some other initiating agent.

Various suggestions about the production of a controlled thermonuclear reaction began to appear in many countries already in the nineteen forties. But the first official statement about allegedly successful experiments was made in 1951 by the then President of Argentina, Peron, who declared that on February 16, 1951 the German physicist Richter, in his laboratory on the island of Huemul (Argentina), succeeded in realizing a controlled thermonuclear reaction.

Since that time there have begun to appear in the American press notices about the fact that in a number of laboratories in the U.S.A. work is being conducted on the problem of a controlled thermonuclear reaction.

In 1952, there was a note in the popular journal "Science News Letter", stating that experiments were being conducted at the California Institute of Technology under the direction of Fowler on the initiation of the reaction, and that theoretical problems of initiating and controlling it for industrial purposes had already been solved [1]. In 1953, the same journal stated that the results of work on controlled thermonuclear reactions were being held strictly secret, but that such reactions had not yet been realized [2]. Only in the second half of 1955 did there appear three notes [3-5] giving more detailed information on the organization of the work on controlled thermonuclear reactions. From these notes it appears that the work was begun after the astrophysicist Spitzer suggested, in 1951, an idea for a means of thermal isolation and control of thermonuclear reactions. The main centers of the investigative work in this field are the laboratory of Princeton University (50 m from New York) and the Livermore Laboratory under the administration of the University of California. Some investigations are also conducted in the Los Alamos and Oak Ridge Laboratories and at New York University. Participants in the work are Edward Teller, L. Szilard, H. Grad, D. Kerst, W. Allis, and a number of other physicists and mathematicians.

Since the summer of 1955, many theorists have been attracted to work in this field, among them R. Landshoff, the astrophysicist Chandrasekhar, and others. It is stated that six more laboratories and universities are taking part in the work and that the total number of scientists engaged in the work is very great.

The technical and physical developments are kept strictly secret. It is indicated only that there have been investigations with a special apparatus on gas discharges compressed into a thin tube. There are general discussions about the possibility that the energy released in thermonuclear reactions might be converted directly into electric energy without the use of steam-driven generators. There is talk of the possibility of obtaining thermonuclear reactions of brief duration by heating a gas with an intense shock wave, and of the possibility of initiating the reaction by rapid heating of a filament by a very large pulse of electric current.

In a note in the journal "Nucleonics" it is said, in particular, that the problem of producing controlled thermonuclear reactions is not connected with the danger of producing a destructive explosion. [5]. A difficult problem is the obtaining of a mode of operation in which the energy released as a result of the reaction is greater than that expended in the initial heating of the gas.

The realization of a controlled thermonuclear reaction and its use for industrial purposes will eliminate the problem of obtaining mineral fuels, since the deuterium obtained in the water of the oceans is equally accessible to all countries and assures humanity of energy for billions of years.

The joint efforts of physicists of all countries of the world would help in the most rapid solution of this problem, which is directed toward increasing the well-being of all peoples.

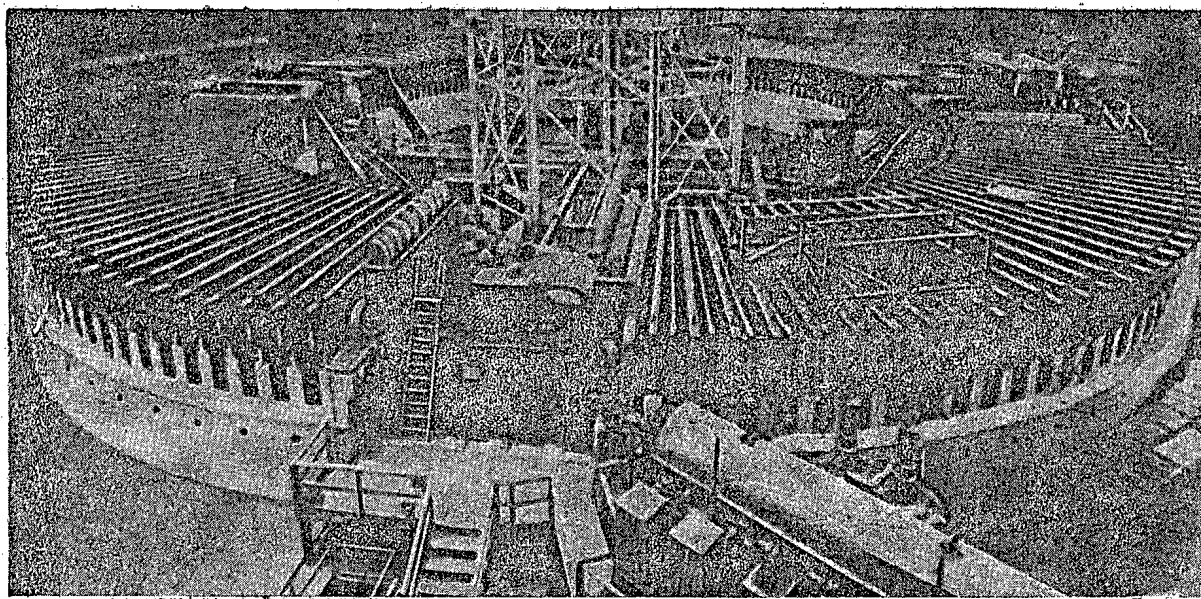
I. G.

#### LITERATURE CITED

- [1] Science News Letter 62, 18 (1952).
- [2] Ibid. 64, 229 (1953).
- [3] Time 66, 50 (1955).
- [4] Scientific American (1955).
- [5] Nucleonics Nos. 11, 12 (1955).

### DISCOVERY OF THE ANTIPROTON

One of the most important consequences of Dirac's theory is the existence of the positron — a particle having all the properties of the electron, but positively charged. The existence of the positron was "foretold" long before its experimental observation. In theoretical works concerned with nucleons it is commonly assumed that these particles, having spin  $\frac{1}{2}$  like the electron, are described by an equation like that of Dirac. If this assumption is correct, then there must exist an antiproton and an antineutron. But before the experimental demonstration of the existence of antinucleons the question of the applicability of Dirac's theory in this case remained open, especially since the magnetic moment of nucleons is not equal to the nuclear magneton, as would follow from the Dirac theory. In recent years, there have appeared several announcements of the observation in cosmic rays of events which could be regarded as antinucleons, but no certain conclusions were drawn on this question.



The Bevatron at the Radiation Laboratory of the University of California (Berkeley, U.S. A.)

In the laboratory coordinate system the minimum proton energy necessary for the production of a nucleon-antinucleon pair in impact with a free nucleon is 5.6 Bev. When account is taken of the momenta of nucleons inside the nucleus, it can be shown that the threshold for production of antinucleons must be about 4.3 Bev. The construction of a powerful synchronous-phase accelerator, called the bevatron, in Berkeley (U.S.A.) and the obtaining from it of protons with energy above 6 Bev offered the possibility of artificial production of antinucleons. Work on the observation of antiprotons, produced in bombardment of a copper target by the proton beam from the bevatron, was successfully carried out in September and October of 1955 by the American physicists Chamberlain, Segre, Wiegand, and Ypsilantis.

The search for antiprotons had to be conducted against an enormous background of negative  $\pi$ -mesons, whose probability for production is hundreds of thousands of times greater than that for antinucleons. For this purpose a system was constructed for analyzing particles as to their charge and mass. By means of two magnets and a concrete collimator about 3 m long, negative singly charged particles of momentum 1.19 Bev/c

were separated from the beam. The singly charged character of the particles was verified by the size of the pulses in scintillation counters.

Having been analyzed as to momentum, the beam of particles was analyzed as to velocity, and consequently as to mass, by two methods: the time of flight of the particles over a distance of 12.2 m between two scintillation counters was measured with accuracy of  $1 \text{ m } \mu \text{ second}$ , and by means of two Cerenkov counters particles were selected having a definite value of  $\beta (\underline{v/c})$ .

The adjustment and checking of the analyzing system were conducted with protons, which required only reversal of the direction of the current in the magnet windings.

It was established that a proton beam with energy higher than 5 Bev produces singly charged negative particles, with mass not differing from the proton mass by more than 5%, and lifetime sufficiently long for them to be registered by a system, to traverse which  $10^{-8}$  seconds was required. No doubt is aroused by the assertion that the observed particles are antiprotons.

Work is now going on on the observation of the annihilation of antiprotons in photographic films, in the Wilson chamber, and by electronic detection methods.

V. S.

#### LITERATURE CITED

- [1] O. Chamberlain, E. Segre, C. Wiegand, Th. Ypsilantis, Phys. Rev. 100, No. 3, 947 (1955).
- [2] Science 122, No. 3182, 1222 (1955).
- [3] Science News Letter 68, No. 18, 275 (1955)

## EXPERIMENTAL PORTABLE EQUIPMENT FOR THE IRRADIATION OF POTATOES

Irradiation of potatoes with a suitable dose of ionizing radiation can retard their sprouting [1-5], and also reduce to a minimum such undesirable changes as withering and loss of weight [2, 3].

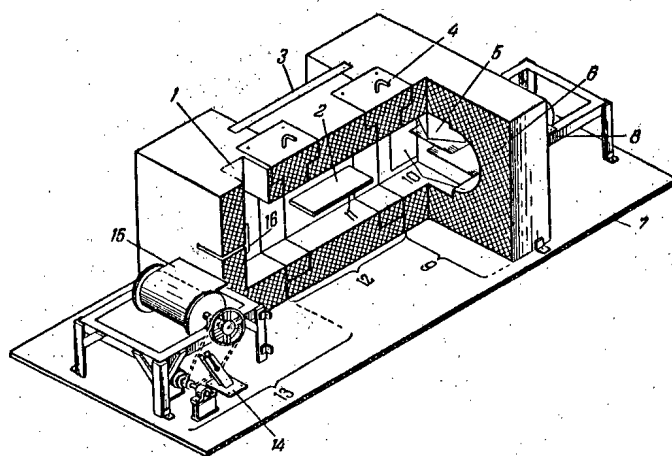


Figure 1. Experimental outfit for irradiation of potatoes and other vegetables, and also various products and materials.

1) Loading channel; 2) source container; 3) supplementary shield; 4) hatch for inserting source; 5) flange; 6) lead shield; 7) supporting plate; 8) idling drum; 9) return section; 10) return channels; 11) sources of radiation; 12) irradiation chamber; 13) section for loading and output of materials; 14) drive; 15) conveyor (web belt); 16) output channel.

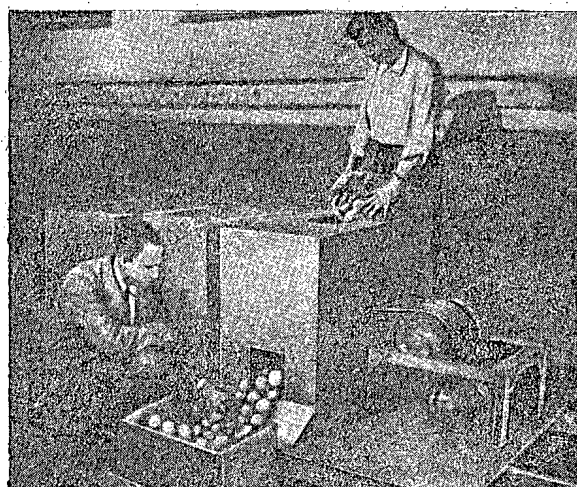


Figure 2. Model of the equipment (actual size)

In this connection the necessity arose of developing an experimental outfit for the irradiation of large quantities of potatoes, which would then be suitable for introduction into industrial use. If equipment were available for irradiation, it would be possible to irradiate annually 40-50 million bushels (1 bushel = 0.035 m<sup>3</sup>) of potatoes, which is more than 10% of the entire potato harvest of the U. S. A.

The experimental equipment described in a recent report [1] has high productivity — irradiation of up to 15 tons of potatoes per day with dosage 12,000 REP — and is sufficiently portable.

The total cost of the outfit is 50,000 dollars, including 20,000 dollars for the source of radiation.

The potatoes being irradiated fall from the loading channel (Figure 1) onto the web belt conveyor and pass over the source of radiation. The source consists of six plates of Co<sup>60</sup>, each of dimensions about 5.6 × 35 cm. The intensity of the source is 4 kilocuries, and the radiating surface is 0.09 m<sup>2</sup>. A special flange guides the potatoes into two return channels, from which they fall onto the inner side of the conveyor belt, whereupon they move under the source in the reverse direction. A second flange directs the potatoes into the output channel, and the cycle of irradiation is complete. The whole outfit (Figure 2) can be mounted on a trailer truck. The conveyor belt can be driven by a small gasoline engine or by an electric motor. Since the equipment does not have complicated moving parts, its whole interior can be washed out easily with a stream from a hose. The mechanism is solidly joined to heavy steel plates, so that in case of accident there is little chance of breaking the shielding. The lead shield



of weight 14 tons forms a box of dimensions 1.4 x 0.8 x 1.1 m, faced with steel plates.

Besides irradiating potatoes, this equipment can also be used for irradiating other vegetables, and also products and various materials, for example meat, pharmaceutical goods, and plastics; it is also useful for experimental work.

G. B-v.

#### LITERATURE CITED

- [1] O. A. Kuhl, A. H. Sparrow, B. Manowitz, Nucleonics 13, No. 11, 128 (1955).
- [2] A. H. Sparrow, E. Christensen, Nucleonics 12, No. 8, 16 (1954).
- [3] L. E. Brownell, J. V. Nehemias, J. J. Bulmer, Mich. Project, 1943; 7-23-P, U. S. AEC, 1954.
- [4] R. L. Sawyer, S. L. Dallyn, Am. Potato J. 32, No. 4, 141 (1955).
- [5] A. H. Sparrow, J. Schairer, E. J. Lawton, Unpublished results.
- [6] Nucleonics 13, No. 7, 15 (1955).

## A PHYSICAL METHOD FOR SEPARATING URANIUM FROM FISSION FRAGMENTS\*

As is well known, in the fission of a uranium nucleus two radioactive fragments are formed, which because of recoil fly off in opposite directions. If the fission occurs in a grain of "fuel" material whose dimensions do not exceed the free path of the radioactive fission fragments (amounting to 1.9 cm in air and 8  $\mu$  in uranium oxide), then the fragments fly out beyond the limits of the grain of fuel.

This property of the fragments can obviously be utilized for the separation of uranium from the radioactive fission fragments. Thus, at the Brookhaven National Laboratory (U. S. A.) the following experiments were conducted. Uranium oxide, ground up so that the size of the particles did not exceed 1  $\mu$ , was introduced in the form of a suspension into a 3% solution of gelatin. The cooled gelatin solution was irradiated in the active zone of a reactor, after which it was liquefied and freed from particles of uranium oxide. It was found that all the radioactive fragments remained in the gelatin, and the grains of fuel had only the activity caused by the radioactive decay of  $U^{239}$  and  $Np^{239}$ .

Such a method, however, obviously cannot provide complete separation of uranium from radioactive fragments, because of the relatively low melting temperature of the gelatin, which liquefies in the reactor, causing precipitation of the suspension. This method, which merits further development, has not yet received any practical application.

Yu. T.

---

\*Nucleonics 13, No. 12, 77 (1955).

## Bibliography

### BOOKS ON QUESTIONS OF THE PEACEFUL APPLICATION OF ATOMIC ENERGY

(PUBLISHED 1955-1956)

#### 1. Atomic Physics

Session of the Academy of Sciences of the USSR on the Peaceful Uses of Atomic Energy, July 1-5, 1955. Plenary Meeting. Academy of Sciences of the USSR Press, 1955, 106 pages, 6 rubles.

Session of the Academy of Sciences of the USSR on the Peaceful Uses of Atomic Energy, July 1-5, 1955. Meeting of the Division of Physical-Mathematical Sciences. Academy of Sciences of the USSR Press, 1955, 376 pages, 14 rubles 25 kopecks.

Physical Investigations, Reports of the Soviet delegation to the International Conference on the Peaceful Uses of Atomic Energy, Geneva, 1955. Academy of Sciences of the USSR Press, 1955, 332 pages, 14 rubles 25 kopecks.

Experimental Reactors and Physics of Reactors. Reports presented by foreign delegations at the International Conference on the Peaceful Uses of Atomic Energy, Geneva, 1955. State Technical Press, 1956, 756 pages, 24 rubles 75 kopecks.

Neutron Physics. Problems of contemporary physics. Collections of translations and surveys of foreign periodical literature, Foreign Literature Press, 1955, 199 pages, 10 rubles 50 kopecks.

Generalized Model of the Nucleus, Problems of contemporary physics. Collections of translations and surveys of foreign periodical literature. Foreign Literature Press. Part I, 1955, 145 pages, 10 rubles 50 kopecks; Part II, 1955, 212 pages, 10 rubles, 50 kopecks.

Electronics of Semiconductors. Problems of contemporary physics. Collections of translations and surveys of foreign periodical literature. Foreign Literature Press, 1955, 196 pages, 10 rubles 50 kopecks.

Polarization of Particles in Nuclear Reactions. Problems of contemporary physics. Collections of translations and surveys of foreign periodical literature. Foreign Literature Press, 1955, 213 pages, 10 rubles 50 kopecks.

Radioactivity. Problems of contemporary physics. Collections of translations and surveys of foreign periodical literature. Foreign Literature Press, 1955, 179 pages, 10 rubles 50 kopecks.

Experimental Methods of Nuclear Physics. Problems of contemporary physics. Collections of translations and surveys of foreign periodical literature. Foreign Literature Press, 1955, 204 pages, 10 rubles 50 kopecks.

Azimov, S. A., Investigation of Electron-Nuclear Showers and of the Absorption of Nuclearly Active Particles in Air and in Dense Absorbers of Various Atomic Weights. Dissertation. Physical Institute of the Academy of Sciences of the USSR, Physical-Technical Institute of the Academy of Sciences of the Uzbek SSR, 1955, 12 pages.

English-Russian Dictionary in Nuclear Physics and Technology. E. V. Shpolsky, Editor. Institute of Scientific Information of the Academy of Sciences of the USSR, 1955, 288 pages, 20 rubles.

Atlas of Effective Neutron Cross sections of the Elements, Academy of Sciences of the USSR Press, 1955, 260 sheets, 95 rubles.

Birks, G., Scintillation Counters. Translated from the English by A. S. Belousov and E. I. Tamm, P. A. Cerenkov, Editor. Foreign Literature Press, 1955, 151 pages, 8 rubles 15 kopecks.

Vlasov, N. A., Neutrons, edited by P. I. Lukirsky. State Technical Press, 1955, 427 pages, 16 rubles 30 kopecks.

Goldansky, V. I., New Elements in the Periodic System of D. I. Mendeleev. Second edition, revised and enlarged. State Technical press, 1955, 168 pages, 2 rubles 85 kopecks.

Lavrukhina, A. K., Radiochemical Investigations of Nuclear Transformations Occurring through the Action of High-Energy Particles. Dissertation. V. I. Vernadsky Institute of Geochemistry and Analytical Chemistry, Academy of Sciences of the USSR, 1955, 28 pages.

Landau, L. D., and Smorodinsky, Ya. A., Lectures on the Theory of the Atomic Nucleus. State Technical Press, 1955, 140 pages, 5 rubles 70 kopecks.

Mironov, V. D., and Stefani, E. P., Automatic Electronic Regulators for Thermal Processes. State Energetics Press, 1955, 224 pages, 7 rubles 20 kopecks.

Murin, A. N., Introduction to Radioactivity. Leningrad University Press, 1955, 251 pages, 8 rubles 45 kopecks.

Application of Betatrons for Technical X-ray Detection of Defects. Collection of data from material in the foreign press. Institute of Scientific Information, Academy of Sciences of the USSR, 1955, 20 pages, no price.

Scintillation Counters. Collection of data from foreign journals. Institute of Scientific Information of the Academy of Sciences of the USSR, 1955, 32 pages, no price.

Fursov, V. S., Uranium-Graphite Nuclear Reactors. Academy of Sciences of the USSR Press, 1956, 40 pages, 65 kopecks.

Experimental Nuclear Physics, E. Segre, Editor. Translated from the English. Foreign Literature Press, 1955, vol. I, 662 pages, 41 rubles; 1956, vol. II, 493 pages, 31 rubles 20 kopecks.

Hughes, D., Neutron Optics. Translated from the English by E. L. Burshtein, M. I. Pevzner, Editor. Foreign Literature Press, 1955, 156 pages, 7 rubles 50 kopecks.

## 2. Atomic Energetics.

Session of the Academy of Sciences of the USSR on the Peaceful Uses of Atomic Energy, July 1-5, 1955. Meeting of the Division of Technical Sciences. Academy of Sciences of the USSR Press, 1955, 337 pages, 14 rubles 65 kopecks.

Reactor Construction and the Theory of Reactors. Reports of the Soviet delegation at the International Conference on the Peaceful Uses of Atomic Energy, Geneva, 1955. Academy of Sciences of the USSR Press, 1955, 305 pages, 13 rubles 40 kopecks.

The Metallurgy of Nuclear Energetics and the Action of Radiation on Materials. Reports presented by foreign delegations at the International Conference on the Peaceful Uses of Atomic Energy, Geneva, 1955. Metallurgy Press, 1956, 714 pages, 22 rubles 10 kopecks.

Atomic Energetics. Reports presented by foreign delegations at the International Conference on the Peaceful Uses of Atomic Energy, Geneva, 1955. State Energetics Press, 1956, 726 pages, 24 rubles 35 kopecks.

Kirensky, L. V., and Drokin, A. I., Atomic Energy and its Application. Krasnoyarsk, Book Press, 48 pages, 85 kopecks.

Leshkovtsev, V. A., Atomic Energy. Scientific-popular Library, No. 72, 2nd edition. State Technical Press, 1955, 64 pages, 1 ruble 10 kopecks.

Lapp, R. E. and Andrews, G. D., Physics of Nuclear Radiation. Translated from the English, under the direction of Prof. K. V. Astakhov and others. Military Press, 1956, 436 pages, 11 rubles.

Murray, R., Introduction to Nuclear Technology. Translation from the English, P. E. Stepanov, Editor. Foreign Literature Press, 1955, 408 pages, 20 rubles 40 kopecks.

Namias, M., Nuclear Energy. Liberation and Use. Translated from the French. Foreign Literature Press, 1955, 296 pages, 11 rubles 80 kopecks.

Application of Atomic Energy to Peaceful Purposes. I. T. Aladyev, Editor. Academy of Sciences of the USSR Press, 1956, 157 pages, 2 rubles 20 kopecks.

Problems of the Utilization of Atomic Energy. Collection of reports. Military Press, 1955, 320 pages, 4 rubles 10 kopecks.

Energetic Nuclear Reactors and the Utilization of Fission Products. Collection of reports. Translated from the English. Foreign Literature Press, 1955, 188 pages, 10 rubles.

### 3. Atomic Ores and Materials.

Investigations in the Fields of Geology, Chemistry, and Metallurgy. Reports of the Soviet delegation at the International Conference on the Peaceful Uses of Atomic Energy, Geneva, 1955. Academy of Sciences of the USSR Press, 1955, 367 pages, 15 rubles 60 kopecks.

Chemistry of Nuclear Fuel. Reports presented by foreign delegations at the International Conference on the Peaceful Uses of Atomic Energy, Geneva, 1955. State Chemical Press, 1956, 552 pages, 18 rubles.

Geology of Atomic Raw Materials. Reports presented by foreign delegations at the International Conference on the Peaceful Uses of Atomic Energy, Geneva, 1955. State Geological-Technical Press, 1956, 506 pages, 23 rubles 15 kopecks.

Actinides, edited by G. Seaborg and G. Katz. Translated from the English by Yu. V. Gagarinsky and E. M. Tsenter, edited by Prof. and Director of Chemical Sciences A. V. Nikolaev. Foreign Literature Press, 1955, 702 pages, 45 rubles 20 kopecks.

Baranov, V. I., Radiometry. Academy of Sciences of the USSR Press, 1955, 328 pages, 20 rubles 20 kopecks.

Meerson, G. A., and Zelikman, A. N., Metallurgy of Rare Metals (Teaching Aid for metallurgical training centers). Metallurgy Press, 1955, 608 pages, 14 rubles 85 kopecks.

Miller, G. L., Zirconium. Translated from the English, under the direction of S. G. Glazunov and A. A. Kiselev. Foreign Literature Press, 1955, 392 pages, 18 rubles 50 kopecks.

Production of Beryllium by Methods of Powder Metallurgy. Powder Metallurgy of Heat-Stable Alloys. Reviews of papers in foreign journals. Institute of Scientific Information, Academy of Sciences of the USSR, 12 pages, 5 rubles.

Samuelson, O., On the Application of Ion Exchange in Analytical Chemistry. Translated from the English by A. P. Kubantsev, edited by K. V. Chmutov. Foreign Literature Press, 1955, 286 pages, 14 rubles 60 kopecks.

Collection of Works on Radiochemistry. Academy of Sciences of the USSR Press, 1955, 262 pages, 14 rubles 25 kopecks.

Songina, O. A., Rare Metals, 2nd edition revised and enlarged. Metallurgy Press, 1955, 384 pages, 13 rubles 30 kopecks.

Chemistry of Rare Elements, Collection of reports; editorial board: I. V. Tananaev (responsible editor) and others. No. 2. Academy of Sciences of the USSR Press, 1955, 164 pages, 8 rubles 75 kopecks.

Zirconium. Collection of translated reports from foreign periodical literature. Foreign Literature Press, Part I, 1954, 174 pages, 9 rubles 65 kopecks; Part II, 1955, 186 pages, 10 rubles 55 kopecks.

### 4. Application of Radioactive Isotopes.

Session of the Academy of Sciences of the USSR on Peaceful Uses of Atomic Energy, July 1-5, 1955. Meeting of the Division of Biological Sciences. Academy of Sciences of the USSR Press, 1955, 339 pages, 13 rubles 70 kopecks.

Session of the Academy of Sciences of the USSR on the Peaceful Uses of Atomic Energy, July 1-5, 1955. Meeting of the Division of Chemical Sciences. Academy of Sciences of the USSR Press, 1955, 375 pages, 14 rubles 75 kopecks.

Application of Isotopes in Technology, Biology, and Agriculture. Reports of the Soviet delegation at the International Conference on the Peaceful Uses of Atomic Energy, Geneva, 1955. Academy of Sciences of the USSR Press, 1956, 467 pages, 19 rubles 60 kopecks.

Application of Radioactive Isotopes in Industry, Medicine, and Agriculture. Reports presented by foreign delegations at the International Conference on the Peaceful Uses of Atomic Energy, Geneva, 1955. Academy of Sciences of the USSR Press, 1956, 725 pages, 23 rubles 80 kopecks.

Verkhovskaya and others, Methods of Marked Atoms in Biology, under the general editorial direction of A. M. Kuzin. Moscow University Press, 1955, 452 pages, 12 rubles 15 kopecks.

Vinokur, Ya. G., Experiment on the Use of Radioactive Isotopes for the Investigation of Processes inside Boilers. Dissertation. The G. M. Krzhizhanovsky Institute of Energetics, Academy of Sciences of the USSR, 1955, 12 pages.

Gamma-ray Inspection of Metals. Collection of reports, edited by S. T. Nazarov. Academy of Sciences of the USSR Press, 1955, 143 pages, 5 rubles 65 kopecks.

Grodzensky, D. E., Radioactive Isotopes in Biology and Medicine. Moscow, "Science", 1955, 40 pages, 60 kopecks.

Zelinsky, O. V., and others, Methods of Application of Radioactive Carbon<sup>14</sup> for the Study of Photosynthesis. Moscow-Leningrad, Academy of Sciences of the USSR Press, 1955, 90 pages, 4 rubles 95 kopecks.

Ivanov, I. I., and others, Radioactive Isotopes in Medicine and Biology, Practical Procedure. Medical Press, 1955, 232 pages, 11 rubles 25 kopecks.

Isotopes in Microbiology. Reports of the conference on the application of marked atoms in microbiology, edited by A. A. Imshenetsky. Academy of Sciences of the USSR Press, 1955, 240 pages, 15 rubles 25 kopecks.

Kalinachenko, V. R., Investigation of Hydrogen Isotope Exchange of Aromatic Compounds in a Medium of Liquid Hydrogen Bromide. Dissertation. The L. Ya. Karpov Physical-Chemical Institute, Moscow, 1955, 16 pages.

Working Methods for Use of Radioactive Indicators. Academy of Sciences of the USSR Press, 1955, 288 pages, 13 rubles 20 kopecks.

Marked Atoms in Investigations of Plant Nourishment and the Use of Fertilizers. Reports of a conference. Academy of Sciences of the USSR Press, 1955, 175 pages, 12 rubles 50 kopecks.

Nadeinskaya, E. P., Investigation of the Wear of a Cutting Instrument by Means of Radioactive Isotopes. Machinery Press, 1955, 134 pages, 4 rubles 60 kopecks.

Nichiporovich, A. A., Light and Carbon Nourishment of Plants (Photosynthesis). Academy of Sciences of the USSR Press, 1955, 287 pages, 4 rubles 60 kopecks.

Application of Isotopes in Agronomic and Soil Investigations. Collections of reports. Academy of Sciences of the USSR Press, 1955, 334 pages, 13 rubles 50 kopecks.

Application of the Method of Marked Atoms in Physics and Technology. Collection of reports, edited by Candidate in Chemical Sciences V. G. Vasilyev. Foreign Literature Press, 1955, 372 pages, 17 rubles 60 kopecks.

Application of Marked Atoms in Analytical Chemistry. Reports at a conference, A. P. Vinogradov, Editor. Academy of Sciences of the USSR Press, 1955, 235 pages, 14 rubles 50 kopecks.

Use of Radioactive Phosphorus for the Treatment of Skin Diseases. Collection of papers, M. N. Pobedinsky, Editor. Medical Press, 1955, 172 pages, 7 rubles 20 kopecks.

Application of Radioactive Isotopes in Metallurgy. Collection of papers, I. N. Kidin, Editor. Metallurgy Press, 1955, 359 pages, 16 rubles 70 kopecks.

Industrial Application of Radioactive Isotopes. Selection of data from materials in the foreign press. Institute of Scientific Information, Academy of Sciences of the USSR, 1955, 30 pages, no price.

Radiobiology. Basic Features of the Action of Radiation on Living Organisms. Translated from the English, G. M. Frank, Editor. Foreign Literature Press, 1955, 496 pages, 24 rubles 65 kopecks.

Sakharov, M. M., Study of the Catalytic Cracking Reaction of Hydrocarbons by the Use of Radioactive Carbon<sup>14</sup>. Dissertation. Institute of Physical Chemistry, Academy of Sciences of the USSR, 13 pages.

Collection of Works on Radiation Chemistry, N. A. Bakh, Editor. Academy of Sciences of the USSR Press, 1955, 263 pages, 14 rubles 25 kopecks.

Collection of Works on Radiobiology, edited by N. I. Nuzhdin. Academy of Sciences of the USSR Press, 1955, 159 pages, 11 rubles, 20 kopecks.

Tatochenko, L. K., and Medvedev, S. V., Industrial Gamma-ray Inspection. Metallurgy Press, 1955, 151 pages, 6 rubles.

Works of the Scientific Session Devoted to the Achievements and Problems of Soviet Biophysics in Agriculture, edited by A. M. Kuzin. Academy of Sciences of USSR Press, 1955, 292 pages, 17 rubles 75 kopecks.

Works on the Application of Radioactive Isotopes in Medicine, A. Ignatyev, general editor. 2nd edition. Medical Press, 1955, 264 pages, 12 rubles 40 kopecks.

Shatalina, G. A., Investigation of some Questions of Analytical Chemistry by Means of a Radioactive Isotope of Cerium. Dissertation. Gorky State University, Department of Analytical Chemistry, 1955, 6 pages.

## 5. Atomic Safety Technology

Action of Radiation on the Organism. Reports of the Soviet delegation at the International Conference on the Peaceful Uses of Atomic Energy, Geneva, 1955, 173 pages, 9 rubles.

Dosimetry of Ionizing Radiations. Reports presented by foreign delegations at the International Conference on the Peaceful Uses of Atomic Energy, Geneva, 1955. State Technical Press, 1956, 604 pages, 21 rubles 15 kopecks.

Aglintsev, K. K., Principles of Dosimetry of Ionizing Radiations. Medical Press, Leningrad Section, 1955, 288 pages, 11 rubles 90 kopecks.

Aleksandrova, E. A., On the Functional Diagnostics of Sicknesses of the Thyroid Gland by the Radioactive Iodine Method. Dissertation. Ministry of Health of the USSR, Central Institute of Higher Instruction of Physicians, 1955, 14 pages.

Borisov, E. V., Safety Technique in Work with Radioactive Isotopes, edited by P. L. Gruzin. Trade Union Press, 1955, 116 pages, 2 rubles 85 kopecks.

Bochkarev, V., and others, Measurement of the Activity of Sources of Beta and Gamma Radiations. Academy of Sciences of the USSR Press, 1955, 249 pages, 10 rubles 30 kopecks.

Bydin, Yu. F., Destruction of Negative Halogen Ions in Collisions with Inert Gas Atoms and Hydrogen Molecules. Dissertation. Leningrad Physical-Technical Institute of the Academy of Sciences of the USSR, 1955, 11 pages.

Temporary Sanitary Regulations for Construction and Equipment of a Cabinet for Gamma-ray Therapy. Medical Press, 1955, 12 pages, 25 kopecks.

Gorodinsky, S. M., and Parkhomenko, G. M., Labor Hygiene in Work with Radioactive Isotopes. Materials for sanitary-educational work. Edited by A. A. Letavet. Medical Press, 1955, 40 pages, 90 kopecks.

Grodzinsky, D. M., Effect of Small Doses of Ionizing Radiation on Vegetation. Dissertation. Botanical Institute of the Academy of Sciences of the Ukrainian SSR, Kiev, 1955, 15 pages.

Deactivation. Removal of Radioactive Contaminations. Collection of data from foreign journals. Institute of Scientific Information, Academy of Sciences of the USSR, 1955, 56 pages, no price.

Egorov, A. P. and Bochkarev, V. V., Blood Generation and Ionizing Radiation. 3rd edition. Medical Press, 1955, 256 pages, 9 rubles 20 kopecks.

Krongauz, A. N. and others, Condenser Dosimeter for X and Gamma Radiations. From the Reporter for Roentgenology and Radiobiology, 1955, no. 6. Medical Press, 1955, 7 pages, no price.

Pelman, S. G., The Role of Intratissue Radiation Therapy in the Combined Treatment of Cancer of the Lower Lip. Dissertation. Ministry of Health of the USSR, Central Institute of Higher Instruction of Physicians, 1955, 10 pages.

Sanitary Regulations and Standards for Work with Radioactive Isotopes. Announcement of the head of the State Sanitary Inspection, Ministry of Health of the USSR. Medical Press, 1955, 18 pages, 45 kopecks.

Sviridov, V. V., Investigation of the Influence of Preliminary Irradiation on the Thermal Disintegration of Solid Substances. Dissertation. V. I. Lenin Belorussian State Institute, Minsk, 1955, 12 pages.

Spesivtseva, V. G., Investigation of the Functional Conditions of the Thyroid Gland by Means of Radioactive Iodine-131 in some Pathological Conditions. Dissertation. First Moscow Medical Institute of the Order of Lenin, 1955, 9 pages.

Tarusov, B. N., Principles of Biological Action of Radioactive Radiations. Medical Press, 1955, 140 pages, 5 rubles 60 kopecks.

Yu. S.